Envelope glycoproteins of vesiculoviruses: characteristics of antibody interactions and immunogenicity

Altar Mert Munis

Thesis submitted to University College London

for the degree of Doctor of Philosophy

2018

Division of Infection and Immunity

University College London

Declaration

I, Altar Mert Munis, confirm that the work presented in this thesis is my own. Where information has been derived from other sources, I confirm that this has been indicated in the thesis.

Abstract

Vesicular stomatitis virus Indiana strain is the prototype envelope glycoprotein for the genus Vesiculovirus. While the wild-type virus, VSVind, has developed into a potent and versatile oncolytic virotherapy and vaccine vector delivery platform, the G protein (VSVind.G) is ubiquitously used to pseudotype lentiviral vectors (LVs) for experimental and clinical applications. Recently, G proteins derived from other vesiculoviruses (VesG), for example, Cocal, Piry, and Chandipura viruses have been proposed as alternative LV envelopes with possible advantages compared to VSVind.G. However, vesiculovirus research has not developed extensively, and there is a gap in knowledge regarding the antigenic and immunogenic characteristic of VesG. In this work, I investigated two anti-VSVind.G monoclonal antibodies for their ability to cross-react with other VesG, identified the epitopes they recognise, and explored the mechanisms behind their neutralisation activity. Furthermore, these G proteins were characterised for their sensitivity to inactivation by fresh mammalian sera. Using some mix-and-match constructs, I identified that the hypervariable PH domain of VSVind.G confers sensitivity to otherwise serum resistant Cocal G. I further examined VesG regarding their immunogenicity, explored the humoral immune response triggered by systemic administration of LVs and investigated the inhibitory effects of the induced anti-G neutralising response on subsequent LV administrations. However, this could be alleviated using a heterogeneous panel of envelopes sequentially. Taken together, this work will broaden the use of VesG pseudotyped lentiviral vectors in clinical gene therapy by providing the proof-of-concept to circumvent anti-envelope immunity where repeated systemic vector administration is necessary and the opportunity to modify the VesG and improve G protein-containing advanced therapy medicinal products and vaccine vectors.

Impact Statement

Vesiculovirus research is expanding rapidly following their adaptation to oncolytic virotherapy and clinical gene therapy. Therefore, well-characterised antibodies that recognise these G proteins are useful for vesiculovirus research, development of G protein-containing advanced therapy medicinal products (ATMP), and VSVind-based vaccine vectors. Here I have identified antibodies that can cross-react with a variety of the VesG and cross-neutralise VesG-LV. I further characterised the commercially available monoclonal anti-VSVind.G antibodies in-depth including their affinities towards VSVind.G, VesG-LV neutralisation strengths, epitopes, and the key amino acid residues that dictate G protein-antibody interactions. Furthermore, despite recent successes of LV-mediated gene therapy in clinical trials and approvals of ATMP using this technology, repetition of systemic administration of LVs remains to be a problem due to the humoral immune response induced by the primary administration. To overcome this problem, I explored immunogenic properties of VesG and demonstrated that anti-envelope immune response can be evaded by utilising a heterogeneous panel of envelopes allowing repetitive LV administration. This method will serve as a proof-of-principle and may help achieve higher levels of therapeutic transgene expression and anti-tumour effect in LV-based gene therapy and oncolytic virotherapy.

Acknowledgements

I would like to thank my supervisors, Mary Collins, Yasuhiro Takeuchi, and Giada Mattiuzzo for supervising this PhD and their guidance throughout my time in the lab. I am especially grateful to Mary for finding the means for this research and all her support, insights, and encouragement have been sincerely appreciated. I am indebted to Yasu, his friendly advice, vision, and motivation have been great assets. I am also sincerely thankful to Giada, her inspiration and dedication to my development have been invaluable.

I would like to express my deep gratitude to James Eyles. His dynamism, invaluable advice, sincerity, and support have encouraged me to widen my research.

It has been a privilege to be part of the Collins/Takeuchi group and I wish to express my thanks to all past and present members. Especially a special thanks to Maha Tijani for training me during the early stages of my PhD and her critical advice during the past three years. I owe many thanks to dear colleagues with whom I enjoyed working: Kam, Chris, Ilaria, and Joanne.

I want to acknowledge the Biological Services Division at the National Institute of Biological Standards and Control (NIBSC) for their expertise and help in parts of this study. I also gratefully acknowledge the funding from NIBSC which made this PhD possible.

Finally, I am eternally indebted to my parents for their unwavering support, unending inspiration, and unconditional love. I sincerely appreciate all their hard work to provide the opportunities that enabled me to pursue my passions, goals, and attempt this PhD without hesitation. My sister and grandmother have been there all along and I am grateful for their humour, support, and friendship.

Table of Contents

List of Figures

List of Tables

Abbreviations

aa	Amino acid
AAV	Adeno-associated virus
Ab	Antibody
ADA	Adenosine deaminase deficiency
ADCC	Antibody-dependent cell-mediated cytotoxicity
ADE	Antibody-dependent enhancement
AIDS	Acquired immune deficiency syndrome
ALD	Adrenoleukodystrophy
APC	Antigen presenting cell
APOBEC-3G	Apolipoprotein B mRNA editing enzyme catalytic polypeptide-like-3G
ARSA	Arylsulfatase A
ATMP	Advanced therapy medicinal products
BET	Bromodomain and extraterminal
bGHpA	Bovine growth hormone poly A
bGLOB	Beta-globin
BLT	Bone marrow, liver, thymus
BSA	Bovine serum albumin
CA	Capsid
CAR	Chimeric antigen receptor
CCR5	C-C chemokine receptor type 5
CGD	Chronic granulomatous disorder
CHAV	Chandipura virus
CHAV.G	Chandipura virus G protein
CJSV	Carajas virus
CMV	Cytomegalovirus

COCV	Cocal virus
COCV.G	Cocal virus G protein
CPM	Counts per minute
cPPT	Central polypurine tract
CR	Cysteine-rich
CTL	Cytotoxic T lymphocyte
CXCR4	C-X-C chemokine receptor type 4
CypA	Cyclophilin A
DC	Dendritic cell
DI / DII / DIII / DIV	Domain I / Domain II / Domain III / Domain IV
DMEM	Dulbecco's modified eagle medium
DNA	Deoxyribose nucleic acid
dNTP	Deoxyribonucleotide triphosphate
dsDNA	Double-stranded DNA
DTT	Dithiothreitol
EDTA	Ethylenediaminetetraacetic acid
eGFP	Enhanced green fluorescent protein
EIAV	Equine infectious anaemia virus
ELISA	Enzyme-linked immunosorbent assay
ESCRT	Endosomal sorting complexes required for transport
FACS	Fluorescence-activated cell sorting
Fc	Constant fragment
FITC	Fluorescein isothiocyanate
FIV	Feline immunodeficiency virus
Fluc	Firefly luciferase
FLV	Feline leukaemia virus
FSC	Forward scattered light
Fv	Variable fragment

G	Glycoprotein
Gapdh	Glyceraldehyde-3-phosphate dehydrogenase
gDNA	Genomic DNA
GFP	Green fluorescent protein
gRNA	Genomic RNA
GRV	Gammaretroviral vector
GVHD	Graft-versus-host disease
HA	Haemagglutinin
HEK	Human embryonic kidney
HF	High-fidelity
HI	Heat-inactivated
HIV	Human immunodeficiency virus
HIV-1	Human immunodeficiency virus type-1
HLA	Human leukocyte antigen
HSC	Haematopoietic stem cells
HSCT	Haematopoietic stem cell transplantation
IFN	Interferon
Igs	Immunoglobulins
IL-2	Interleukin 2
IN	Integrase
ISFV	Isfahan virus
IV	Intravenous
IVIS	In vivo imaging system
Kd	Dissociation constant
L	Viral polymerase
LB	Luria Bertani
LDLR	Low-density lipoprotein receptor
LEDGF/p75	Lens epithelium-derived growth factor
LTR	Long terminal repeat

LV	Lentiviral vector
M	Matrix protein
MA	Matrix
mAb	Monoclonal antibody
MAC	Membrane attack complex
MARAV	Maraba virus
MARAV.G	Maraba virus G protein
MBL	Mannose-binding lectin
MEM	Minimum essential medium
MESF	Molecular equivalent soluble fluorophores
MFI	Median fluorescence intensity
MHC	Major histocompatibility complex
miRNA	Micro RNA
MLD	Metachromatic leukodystrophy
MLV	Murine leukaemia virus
MOI	Multiplicity of infection
Mo-MLV	Moloney murine leukaemia virus
MW	Molecular weight
MX2	Myxovirus resistance 2 protein
N	Nucleoprotein
nAb	Neutralising antibody
NADPH	Nicotinamide adenine dinucleotide phosphate
NC	Nucleocapsid
NK	Natural killer
p75	Low-affinity nerve growth factor receptor
p75NTR	Neurotrophin receptor
PAMP	Pathogen associated molecular pattern
PBS	Phosphate-buffered saline
PCL	Packaging cell line

PCR	Polymerase chain reaction
PEGylation	Polyethylene glycosylation
PFA	Paraformaldehyde
PH	Pleckstrin homology
PIC	Pre-integration complex
PIRYV	Piry virus
PIRYV.G	Piry virus G protein
polyA	Polyadenylation
PP	Phosphoprotein
PPT	Polypurine tract
PR	Protease
qPCR	Quantitative PCR
RABV	Rabies virus
RABV.G	Rabies virus G protein
RAP	Receptor-associated protein
RLU	Relative light units
RNA	Ribonucleic acid
RNase H	Ribonuclease H
ROI	Region of interest
RRE	Rev response element
RT	Reverse transcriptase
RU	Response units
RV	Retroviral vector
SAMHD1	Sterile α motif domain – and histidine-aspartate domain-containing protein 1
SC	Subcutaneous
SCID	Severe combined immune deficiency
SD	Standard deviation
SDM	Site-directed mutagenesis

SDS	Sodium dodecyl sulphate
SEM	Standard error of mean
SERINC	Serine incorporator
SFFV	Spleen focus-forming virus
SIN	Self-inactivating
SIV	Simian immunodeficiency virus
sLDLR	Soluble LDLR
SOC	Super-optimal broth with catabolite repression
SPR	Surface plasmon resonance
SSC	Side scattered light
SU	Surface unit
SV40	Simian virus 40
TBE	Tris/Borate/EDTA
TCR	T cell receptor
TLR	Toll-like receptor
TM	Transmembrane unit
TNFα	Tumour necrosis factor α
TRIM	Tripartite motif
tRNA	Transfer RNA
TU	Transduction units
UV	Ultraviolet
VCM	Vector containing media
VesG	Vesiculovirus G proteins
VLCFA	Very long chain fatty acids
VSV	Vesicular stomatitis virus
VSVala	Vesicular stomatitis Alagoas virus
VSVala.G	Vesicular stomatitis Alagoas virus G protein
VSVind	Vesicular stomatitis Indiana virus

VSVind.G	Vesicular stomatitis Indiana virus G protein
VSVnj	Vesicular stomatitis New Jersey virus
VSVnj.G	Vesicular stomatitis New Jersey virus G protein
WAS	Wiskott-Aldrich syndrome
WPRE	Woodchuck post-transcriptional regulatory element
wt	Wild-type
YWTD	Tyrosine-tryptophan-threonine-aspartate domain
αGal	Galactosyl(α1-3)galactosyl
(+)	Positive

1 Introduction

1.1.Gene Therapy

Gene therapy is the introduction of exogenous genes into the cells of patients in order to treat diseases via gene editing, addition or deletion (1). This method of treatment originated from the identification of genetic causes for several disorders and developed the strategy that possible curative clinical benefits could be achievable with a single treatment following the expression of the correct genes in patients (2). Application of gene therapy required a vehicle for delivering the exogenous genomic material into the nucleus of patients' cells, and as viruses can transform mammalian cells through transferring parts of their genetic material, the idea of using viruses as vectors was born (3).

By the late 20th century, the causes of many primary immunodeficiencies were identified, and many preclinical studies were underway using the gene transfer approach. Following the subsequent development of gene delivery vectors

including replication-defective retroviruses, adenoviral and adeno-associated virus (AAV) vectors encouraging results were obtained in preclinical disease models (2). The use of viral vectors and the growing biological knowledge of retroviruses led to the first clinical trial of gene transfer into humans in late 1990s (4, 5). However, the early gene therapy trials raised issues regarding the toxicity of vectors and vector-mediated insertional mutagenesis leading to activation of proto-oncogenes (2). This led to more research into the biology of the vectors to improve their safety and efficacy. The unique ability of lentiviruses to infect both dividing and nondividing cells, combined with the possible self-inactivating (SIN), safe vector designs helped translation of successful gene therapies into the clinic.

Thus far several clinical trials have targeted haematopoietic stem cells (HSC) as well as T cells for a range of disorders (6). Notably, adoptive T cell therapy has been a promising approach targeting tumour–associated antigens. Furthermore, autologous HSC-based clinical trials have led to curative benefits in several primary immunodeficiencies, metabolic, and storage disorders (2). However, there are still several obstacles remain, and further work is needed to improve the efficacy and manufacture of vectors, prevent potential genotoxicity, and limit off-target effects of these promising approaches (7-12).

Several recent clinical trials utilising retroviral vectors are summarised in *Table 1-1.*

Table 1-1: List of Selected RV-mediated Gene Therapy Clinical Trials. ADA-SCID, adenosine deaminase deficiency; X-SCID, X-linked severe combined immunodeficiency; X-CGD, X-linked chronic granulomatous disorder; WAS, Wiskott Aldrich syndrome; WASP, WAS protein; ALD, adrenoleukodystrophy; MLD, metachromatic leukodystrophy; IL2RG, interleukin-2 receptor common gamma chain; ARSA, arylsulfatase-A; LV, lentiviral vector; GRV, gammaretroviral vector; MLV-A, amphotropic murine leukaemia virus; GALV, gibbon ape leukaemia virus; TAR; transactivation response element; CAR, chimeric antigen receptor.

Target Cells	Disease Group	Disease/Transgene	Vector	Envelope	References
Hematopoietic Stem Cells (CD34+)	Primary Immunodeficiencies	ADA-SCID; ADA	GRV	MLV-A	(13)
			GRV	GALV	(14)
			GRV	GALV	(15)
		X-SCID:IL2RG	GRV	MLV-A	(16)
			GRV	GALV	(17)
			GRV	GALV	(18)
		X-CGD: gp^{phox91}	GRV	GALV	(19, 20)
			GRV	GALV	(21)
			GRV	MLV-A	(22, 23)
		WAS: WASP	GRV	GALV	(24)
			LV	VSVind.G	(25)
			LV	VSVind.G	(26)
	Hereditary Anaemias	β-thalassemia: $\beta^{A(T87Q)}$	LV	VSVind.G	(27)
	Storage Disorders	ALD: ABCD1	LV	VSVind.G	(28)

		MLD: ARSA	LV	VSVind.G	(29)
	HIV Infection	AIDS; Tat/Rev shRNA, TAR decoy and CCR5 ribozyme	LV	VSVind.G	(30)
T Cells	Cancer	Neuroblastoma; αGD2-CAR	GRV	GALV	(31, 32)
		Lymphoma/Leukaemia; αCD19-CAR	GRV	RD114	(33-35)
			GRV	GALV	(36)
			GRV	GALV	(37, 38)
			GRV	RD114	(39)
			LV	VSVind.G	(40, 41)
			LV	VSVind.G	(42-44)
		Melanoma; αMART-1, αgp100, αNY-ESO-1, and αgp53 T-cell receptors	GRV	GALV	(45)
			GRV	GALV	(46)
		Synovial Sarcoma; αNY-ESO-1 T-cell receptor	GRV	GALV	(47)
		Colorectal Cancer; αCarcinoembroyonic antigen T-cell receptor	GRV	RD114	(7)
	HIV Infection	AIDS; αgp120 RNA	LV	VSVind.G	(48, 49)
Neurons	Neurodegenerative Disorders	Parkinson's Disease; tyrosine hydroxylase, aromatic L-amino acid decarboxylase and GTP cyclohydrolase-1	LV	VSVind.G	(50)

1.2.Retroviral Biology

The retrovirus family comprise of many enveloped RNA viruses that contain two copies of positive (+) sense, linear, single-stranded RNA genome (51). Retrovirus family is divided into two main subfamilies: Orthoretroviridae and Spumaretroviridae. Orthoretroviridae is further divided into simple and complex viruses which include gammaretroviruses and lentiviruses within them respectively. The replication method of retroviruses is considered the hallmark of this family as they use the reverse transcriptase enzyme encoded by the *pol* gene to transcribe the single-stranded viral RNA into double-stranded DNA (dsDNA) which integrates into the target cell genome (52-55).

1.2.1.Retrovirus Structure

Most retroviruses have similar structural morphology which is made up of the virion core housing the genomic materials: two copies of genomic RNA associated with the nucleocapsid (NC) protein and a tRNA which is involved in the initiation of the reverse transcription. The capsid (CA) surrounds the core and contains the three enzymes pivotal for retroviral infection: protease (PR), reverse transcriptase (RT), and integrase (IN) (56). Matrix (MA) lies right below the viral envelope which is acquired from the host cell membrane. The envelope glycoprotein of retroviruses forms spikes protruding from the viral surface and is composed of a surface unit (SU) and a transmembrane domain (TM) (57).

1.2.2.Retroviral Genome

All retroviruses encode *gag-pol* and *env* genes. These are necessary for the formation of the structural components described above. *Gag* encodes for all internal structural proteins of the virus. Precursor Gag polyprotein gets proteolytically cleaved into MA, CA, and NC. Furthermore, the *Pro-Pol* from the *Gag-Pro-Pol* precursor goes through similar modifications to form the enzymatic components PR, RT, and IN (58). *Env* encodes the glycoprotein which after post-translational glycosylation and cleavage forms the viral envelope (56). In simple retroviruses, like murine leukaemia virus (MLV),

these are the only genes encoded by the viral genome (*Figure 1-1*). However, complex retroviruses encode several other regulatory and accesorry genes. For example, in the HIV-1 lentivirus genome there are regulatory genes *tat* and *rev,* in addition to accessory genes *nef, vif, vpr* and *vpu* (53, 56).

These essential, regulatory, and accessory genes are flanked by long-terminal repeats (LTRs) (51). LTRs are generated during the reverse transcription process, comprised of identical sequences, and contain the same three regions (i.e. U3, R, and U5). The motifs housed in the LTRs, promoters, enhancers, and polyadenylation signals, drive viral transcription and control post-transcriptional modifications (58).

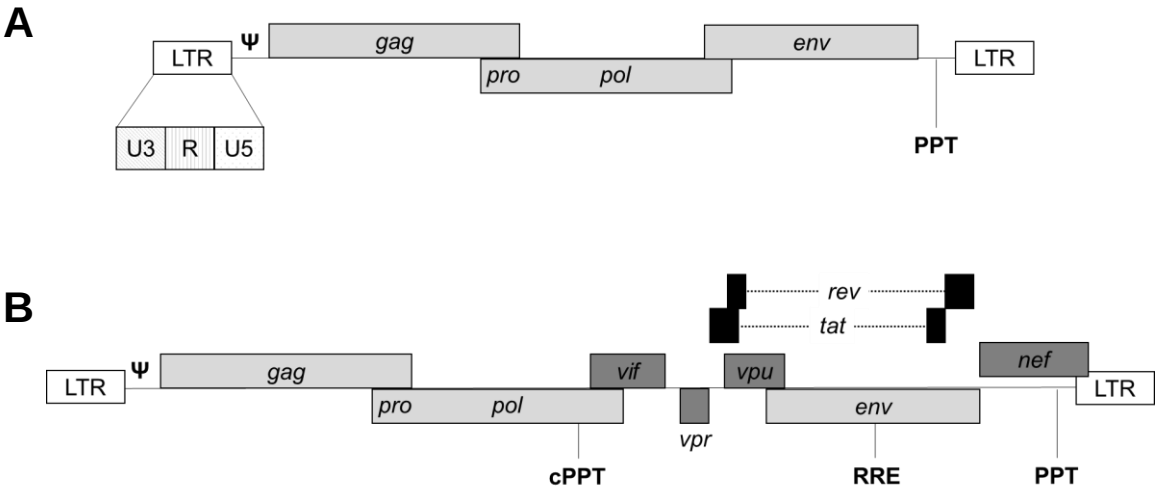

Figure 1-1: Retroviral Genomes. Genomes of **(A)** Mo-MLV (simple retrovirus) and **(B)** HIV-1 (lentivirus). The essential genes encoding structural and enzymatic components of the virus, *gag*, *pol*, and *env* are shown in light grey. The regulatory genes, *tat* and *rev*, are coloured black and the accessory genes, *vif*, *vpr*, *vpu*, and *nef*, are depicted in dark grey. LTR: long-terminal repeats; U3: LTR element derived from sequences unique to 3' end of the RNA genome; R: LTR element derived from sequences repeated in both LTRs; U5: LTR element derived from sequences unique to 5' end of the RNA genome; Ψ: packaging signal; PPT: polypurine tract; cPPT: central polypurine tract; RRE: rev response element.

1.2.3.Principles of Retroviral Life Cycle

Retroviruses infect the host cell by receptor-mediated fusion of viral envelope with the cellular membrane and release of the virion core in the cytoplasm. The attachment of virions to the target cells are mediated by the interactions between the Env and cellular receptors. Several receptors utilised by the major retroviral subgroups have been identified (57), however, gammaretroviral and lentiviral receptors have been more extensively studied. Most GRVs use multiple membrane spanning transporter proteins such as CAT-1 (cationic amino acid transporter), Pit2 (sodium/phosphate co-transporter), XPR1 (inorganic phosphate transporter) (59, 60). These receptors are responsible for both attachment and fusion of GRVs. On the other hand, some lentiviruses, such as human and simian immunodeficiency viruses (HIV and SIV), use two receptors: one for attachment and the other for cell entry. Namely, the CD4 antigen on T helper cells is the high-affinity receptor involved in virus-cell recognition whereas the chemokine co-receptors, CCR5 or CXCR4, are involved in endocytosis of the viral particles (61-68). However, binding of the viral glycoprotein to its specific receptor is not sufficient to trigger viral entry. The attachment of the viral surface protein to the cellular receptor leads to conformational changes that expose a fusion peptide followed by fusion (52, 57, 69, 70). The site of fusion for viruses is either the plasma membrane or the endosomes following endocytosis. If the virus carries out fusion in the endosome, the changes in the pH within the endocytic vehicle triggers conformational changes which lead to membrane fusion. However, not all retroviruses are pH dependent (e.g. ecotropic MLV) (71, 72).

After cell entry, reverse transcription occurs, followed by the dsDNA entering the nucleus and integrating into the host cell genome using the viral integrase. Following viral fusion, genomic RNA in complex with NC is delivered to the cytoplasm where it is reverse transcribed (57). Reverse transcription begins from a tRNA bound to the genomic RNA and carried out by the RT. Specifics of lentiviral reverse transcription are discussed in section 1.3.4. In simple retroviruses, such as GRVs, nuclear entry of the dsDNA occurs only when the cell is going through mitosis when the nuclear envelope dissociates which

renders them unable to infect non-dividing cells (73, 74) . However, in lentiviruses nucleoprotein complex can enter the nucleus during interphase via active transport allowing infection of non-dividing cells (75-77).

The viral IN mediates the interactions between the viral DNA and host cell DNA. The integration is completed via the cellular enzymes which ligate the viral and host DNA, correct nucleotide mismatches, and repair gaps and breaks (78). The unique characteristic of retroviral infection is that the reverse transcription and integration of the viral genome into the host cells make the infection permanent and it is passed onto the daughter cells.

With integration, the provirus becomes a part of the cellular genome and, like other viruses, can employ the cellular systems such as RNA polymerase II and ribosomes to express viral genes and proteins (52, 53). The structural proteins of retroviruses are translated as *gag* and *gag-pol-pro* precursors (approximately in a 10:1 ratio) to ensure correct amounts of proteins are packaged into each virion (56, 79). Viral assembly occurs in the host cell plasma membrane; the *gag-pro-pol* core and gRNA migrate to the assembly site directed by the MA domain. The packaging signal, Ψ, in the retroviral RNA interacts with *gag* to ensure encapsidation of the particle (80). It acquires its envelope and subgenomic RNA during the budding process, and then the virus is released from the plasma membrane.

The late stages of the life cycle involve maturation of the viral particle which in most cases occur at late assembly or quickly after budding. *The gag-pro-pol* precursor is cleaved by viral proteases to initiate maturation of the particle following which the virion detaches from the membrane (58).

1.2.4.HIV-1 Life Cycle

HIV-1 is a lentivirus which is a part of the complex retrovirus subfamily. It is characterised by a long incubation, latent, period during which the virus pathogenicity is at low levels. In its two copies of (+) sense RNA genome wild-type (wt) HIV-1 encodes nine genes: *gag, pol, env, rev, tat, vpr, vpu, vif,* and *nef* (53, 56). Its replication cycle often can be divided into an early and a late stage (81). In the early phase, viral attachment and entry to cell occur, and

this phase ends in proviral integration. Late phase is characterised by viral gene expression, particle assembly, budding, release, and maturation (70) (*Figure 1-2)*.

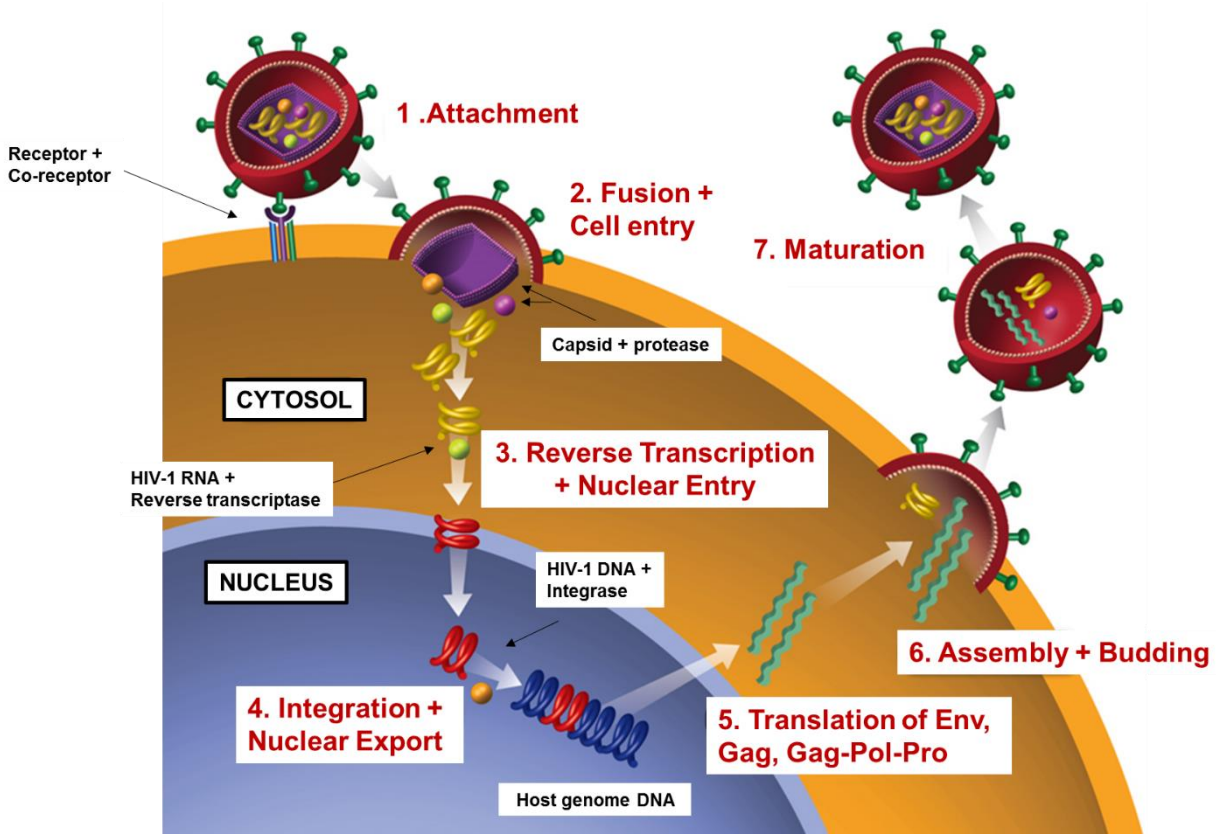

Figure 1-2: Simple Schematic of HIV-1 Life Cycle. The major steps of the human immunodeficiency virus type-1 life cycle are shown. The lentiviral proteins are only shown where relevant, and some are not shown at all (e.g. accessory proteins). The relevant cellular components are labelled in the diagram. Adapted from (82).

The envelope of HIV-1 is a homotrimer with each monomer consisting of gp120, the receptor-binding unit, and gp41, the fusogenic transmembrane unit. In the early phase of the HIV-1 replication cycle, gp120 binds to the CD4 receptor which is followed by conformational changes in both envelope subunits. The changes in the gp120 subunit result in its attachment to co-receptors CCR5 or CXCR4 while the changes in gp41 enable the insertion of the fusion peptide into the target cell membrane (83, 84). In studies performed with patients with HIV-1 infection, it has been elucidated that the co-receptor

CCR5 usage is predominant in the asymptomatic early phase of the infection and following disease progression, in many patients, HIV-1 utilises CXCR4 for cellular entry (85-87). The interactions between the gp41 and the co-receptors lead to membrane fusion and releases the nucleocapsid into the cytosol (88). It was assumed that HIV-1 fusion takes place at the plasma membrane as it follows pH-independent pathways and expression of the envelope glycoprotein on cell surface leads to syncytia formation in cells expressing the receptors (71, 89, 90) However, a recent study utilising live cell imaging suggested that HIV-1 fuses with endosomal membrane (91).

Reverse transcription of viral RNA follows viral fusion (*Figure 1-3)*. This is initiated when tRNA binds to the primer binding site (PBS). $tRNA^{lys3}$ is the main transfer RNA utilised by HIV-1 while others (e.g. $tRNA^{pro}$ and $tRNA^{trp}$) have been identified in other retroviruses (92). Using $tRNA^{lys3}$ as a primer the synthesis of the negative strand DNA begins, which later hybridises with the 3' end of gRNA using the identical R sequences in the LTRs (93-95). Following this, the extension of the negative DNA strand continues towards the 5' end of the genomic RNA. Simultaneously, gRNA is degraded by RNase H except for the highly resistant PPT and cPPT regions. These two regions are later exploited as primers in the synthesis of the positive strand DNA. The extension is halted when RT reaches the tRNA primer sequence at which time HIV-1 RNase H cleaves the primer one nucleic acid from the 3' end (96, 97). A second strand transfer occurs; this time the complementary PBS sequences lead to annealing of both DNA strands which form the circular intermediate. Upon completion of extension, a double-stranded provirus is produced with identical LTRs on each side (98).

The reverse transcription process is the main contributor to the HIV-1 genomic diversity which poses an essential issue during development of vaccines and drugs to treat AIDS (99, 100). This genomic diversity is due to two main reasons: the infidelity of the RT and the complex steps of reverse transcription (101). The lack of proof-reading activity of RT leads to high rates of mutation (102). In addition, the two strand transfers, tRNA transfer to 3' end of positive-strand and PBS transfer to 5' end on negative strand, leads to recombination events contributing to the divergence of the viral sequences.

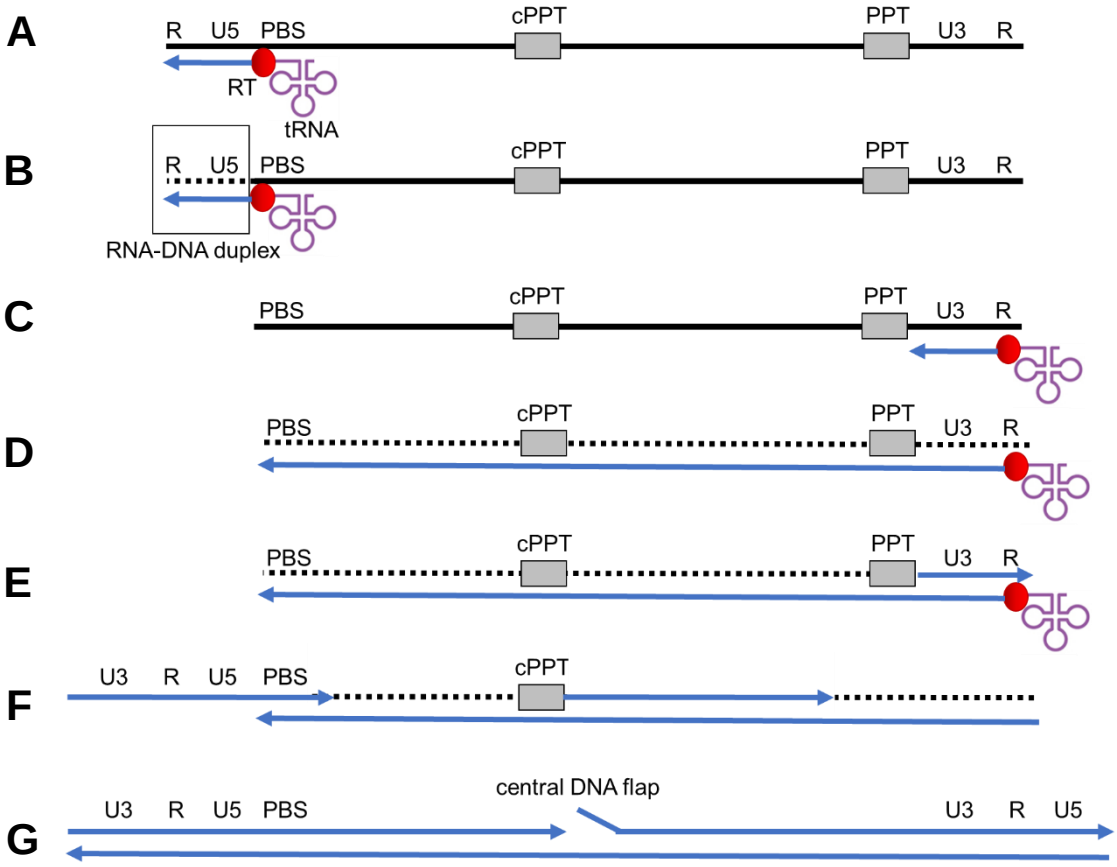

Figure 1-3: Steps of Reverse Transcription. Schematic of HIV-1 reverse transcription depicting the conversion of ssRNA genome into double stranded DNA. RNA is shown in black and DNA in blue. **(A)** Reverse transcription is initiated using the RT following base painting of tRNA with the primer binding site. **(B)** Minus-strand synthesis starts from the U5 and R sequences in the 5' end of the genome. The RNase H activity of RT degrades the viral RNA as an RNA-DNA duplex is created at this stage (dotted line). **(C)** The minus strand is transferred to the 3' end of the viral RNA utilising the identical R sequences. **(D)** DNA synthesis continues while viral RNA gets degraded except for RNase H resistant cPPT and PPT sequences. **(E)** cPPT and PPT sequences act as primers for the plus strand DNA synthesis. **(F)** The tRNA primer is cleaved by RNAse H domain and plus strand DNA elongated from the PPT sequence is transferred to the 3' side of the minus strand DNA. DNA synthesis of the plus strand is resumed from the cPPT. **(G)** Following elongation of both strands of DNA, a double stranded provirus is produced with a central DNA flap caused by the cPPT. Adapted from (103).

The processes in HIV-1 life cycle after cell entry and reverse transcription is still unclear. Viral uncoating is the next crucial step which enables

translocation of the reverse transcribed viral genome into the target cell nucleus (104). It has been established that the uncoating occurs in the early stages of the infection and contributes to the transition between the reverse transcription complex and the pre-integration complex (105).

The dsDNA-viral integrase interaction forms the pre-integration complex (PIC) which later enters the nucleus and integrates into the host cell DNA (106, 107). Currently there is no consensus on how HIV-1 enters the nucleus, but it is agreed that it involves active transfer as unlike most retroviruses it is not dependent on the dissolution of the nuclear membrane to enter the nucleus (108). There are several theories regarding the mechanism behind HIV-1 nuclear import including the binding of importins to nuclear localisation signals in all PIC components aiding in the transport of the complex through interactions with nucleoporins (76, 109-111). Another theory involves the interaction of HIV-1 capsid in the nucleoprotein complex with the nuclear pore protein NUP358 for import to a transcription-active region (112).

The integration happens in a non-random manner with a high preference towards active transcription units. This is believed to ensure efficient viral gene expression after integration (113, 114). Viral integrase coordinates the integration process which happens in three steps. First, 3' end of the proviral DNA is cleaved by IN. After, this recessed 3' end attacks the phosphodiester bonds in the chromosomal host cell DNA to initiate strand transfer. Integration is completed by DNA repair by the host cell mechanisms (115). The IN and LTRs of retroviruses promote preferential interactions with active host cell promoters and enhancers, specifically MLVs with bromodomain and extraterminal (BET) family proteins and HIV with lens epithelium-derived growth factor (LEDGF/p75) (116-120). N-terminal nuclear localisation signal and chromatin binding elements on LEDGF/p75 strongly bind to the IN and guide the PIC to the target site (121). It has been shown that depletion of LEDGF/p75 reduces HIV-1 infectivity and alters the integration sites (115, 122, 123). Studies have demonstrated that the states of target cell chromatin during viral infection as well as different host proteins utilised to guide the PIC to the target genome sites determine the integration profile differences between MLV and HIV-1 (107, 124).

The integration is followed by the commencement of the late phase during which the viral genome is transcribed under the control of the U3 segment in viral 5'-LTR by the cellular RNA polymerase II complex. The two NF-κB sites in the enhancer region of HIV-1 LTR play an essential role in the initiation of the two-phase transcription (125). The expression of multiply-spliced regulatory genes characterises the first phase and the later phase involves the expression of singly-spliced and unspliced RNAs.

Following post-transcriptional processing, both spliced and unspliced viral RNAs are exported to the cytosol. Adaptor complex TREX associates with the central nuclear transport receptor TAP to ensure the export of mature mRNAs only (126). However, HIV-1 also requires the export of unspliced RNAs. The Rev protein encoded by the genome interacts with RRE and ensures nuclear export of unspliced RNAs (127). This mechanism is exploited in lentiviral vector production as the packaging cells encode Rev and the vector genome contains RRE.

The first proteins to be translated, Tat and Rev, play critical roles in regulating the transcriptional and post-transcriptional gene expression levels. While Tat is responsible for the recruitment of the cellular RNA polymerase II, Rev promotes nuclear export of the viral RNAs (128, 129). Gag and Pol are translated in the cytoplasm. Env is translated in the rough endoplasmic reticulum and localises in the cell membrane (130). During post-translational glycosylation and modifications, Env is cleaved in the Golgi apparatus to produce the mature units of the envelope glycoprotein: surface unit (SU) and the transmembrane unit (TM).

After these units are transported to the cell membrane, viral assembly, budding, and release of immature virions occur. In most retroviruses, including HIV-1, these three processes occur simultaneously. Expression of Gag alone among other viral proteins is sufficient for viral budding to occur, however, in HIV-1 it accumulates at the cell membrane where it initiates RNA encapsidation (131). Viral assembly and budding follow this as previously explained. As the last step in the HIV-1 life cycle, viral protease triggers viral maturation, and mature infectious HIV-1 virions are formed (132).

Some accessory proteins are also packaged into the HIV-1 particles. Vpr, Nef, and Vif have vital roles in host-pathogen interactions. Consequently, p6 in Gag recruits Vpr, Vif is packaged dependent on its interactions with the viral RNA, and Nef is incorporated passively (133, 134). Membrane fission allows the release of the assembled viral proteins as virions. For this HIV-1 exploits cellular endosomal sorting complexes required for transport (ESCRTs) which are naturally involved in vesicle formation and membrane scission. Two peptide motifs in p6 interact with ESCRTs and mediate viral release. Mutations in these motifs have been shown to significantly reduce HIV-1 release from infected cells (133). Lastly, immediately after virion release particle maturation occurs. This process involves cleavage of Gag into MA, CA, NC, and p6, and Gag-Pro-Pol into PR, RT, IN, and the Gag cleavage products above (135, 136). Following maturation, the virus particle is ready to infect a new target cell.

1.3.Retroviral Vectors

As obligate parasites, viruses have evolved to exploit cellular machineries to deliver their genomes into the cells of higher organisms. Manipulation of the genomes of several viruses have enabled their conversion into viral vectors. The permanent integration of the viral genome allowed long-term gene expression and the genome could be further manipulated to make them replication-defective and less pathogenic. Owing to these characteristics, they are attractive tools for the efficient delivery of therapeutic genes into target cells.

Retroviral vectors were amongst the earliest vectors to be developed. They were initially derived from gamma-retroviruses such as the Moloney murine leukaemia virus (Mo-MLV) (137). In addition, replication defective vectors derived from avian and bovine retroviruses as well as alphaviruses have been reported (138-142) Later lentiviral vectors (LVs) were developed based on HIV-1 (143). There are also other LVs based on simian immunodeficiency virus (SIV), equine infectious anaemia virus (EIAV), and feline immunodeficiency virus (FIV) (144).

1.3.1.Principles of Retroviral Vector Design

These vectors are produced from producer cells expressing the structural and enzymatic components of the particle (envelope and packaging constructs) as well as the vector genome carrying the transgene of interest (transfer vector construct). The efficient transduction and integration of these vectors are ensured via the inclusion of several *cis*-acting viral sequences. LTRs are vital for transcription initiation and carry out essential functions throughout reverse transcription. Therefore, they are indispensable to achieving functional vectors. Promoter, viral enhancer, and polyadenylation sequences within LTRs ensure full-length transcription of the vector genome (137, 145). Moreover, incorporation of the transgene into the vector particles requires a packaging signal. In HIV-1 this signal, Ψ, is made up of a stem-loop in *gag.* Therefore, a modified version of this loop is included in the vector to ensure packaging (146, 147). Lastly, inclusion of primer binding site (PBS) and polypurine tract (PPT) are essential for initiation of the first- and second-strand DNA synthesis (148). Utilising these viral elements the first replication-competent retroviral vectors based on rous sarcoma virus, MLV, HIV-1, and human foamy virus were generated (149-153).

However, for most research and gene therapy applications safer, non-replicating vectors are necessary. This was achieved by replacement of retroviral coding regions with transfer genes so that the vectors were incapable of synthesising the viral proteins required for additional rounds of replication (148). The viral enzymes and structural proteins necessary for the initial infection were provided *in trans* by cells transfected with packaging plasmids (i.e. cells expressing *gag-pol* and *env*). LTRs were manipulated for safer vector designs. 5' LTR drives transcription of the vector genome and thus needs to be intact, yet, most of the transcription binding sites can be removed from the U3 region of the 3' LTR. Vectors carrying these deletions are referred to as self-inactivating (SIN). During reverse transcription, the deleted U3 (ΔU3) is transferred to the 5' LTR resulting in an integrated provirus with two ΔU3s. Therefore, when SIN vectors transduce cells, they are defective in production of vector RNA genomes (154).

Currently transient production is the most efficient mode of retroviral vector production (155). This is achieved by three plasmid co-transfection of the packaging plasmid (encoding *gag-pol*), envelope plasmid (encoding the envelope glycoprotein), and the vector plasmid (encoding the transgene of interest and the *cis*-acting elements). Transient production of vectors yields high-titres for a short amount of time and is advantageous for research where production of various vectors is needed in small amounts. However, GRV's success in clinical trials (discussed in section 1.2.1) required production of large amounts of vectors with batch-to-batch consistency. This has led to the development of stable GRV production through packaging cell lines (156, 157). Thus far generation of packaging cell lines producing LVs suitable for widespread clinical use has proven to be challenging. Throughout this thesis transient LV production was utilised for all experiments (LV production methods discussed in detail in section 1.5.1).

1.3.2. Other Elements in Vector Design

Several modifications have been made to the vector design to drive and increase the specificity, level, and longevity of the transgene expression. As SIN vectors have transcriptionally inactive LTRs, they are incapable of driving gene expression. Therefore, internal promoters have been utilised to drive high levels of transgene expression. Promoters derived from human cytomegalovirus (CMV), gammaretroviral LTRs, simian virus 40, and spleen-focus forming virus (SFFV) are commonly used (158). In addition, vector packaging and expression were made Tat-independent by replacing the 5' promoter and enhancer sequences in the U3 region with another heterologous promoter (159).

Furthermore, advances in the vector design have led to the investigation of several *cis*-acting accessory factors which enhanced transgene expression. The main two were the inclusion of Woodchuck post-transcriptional regulatory element (WPRE) (160) and polyadenylation (polyA) enhancers (161). WPRE is derived from Woodchuck hepatitis virus and is now frequently included in retroviral vector design (162). A study in the late 1990s by Zufferey and colleagues demonstrated that inclusion of this regulatory sequence increased

gammaretroviral and lentiviral vector titres by approximately ten-folds (163, 164). On the other hand, polyA sequences were inserted in vectors to decrease transcriptional readthrough of the 3'LTR which is associated with the changes made to achieve SIN designs (165). Addition of 3' polyA enhancer sites aided with transcriptional termination and increased vector titres and transgene expression (161). Moreover, further addition of cPPT has been demonstrated to improve transduction efficiency and titres, hence, is now incorporated into the vector design (166, 167).

1.3.3.Safety of Retroviral Vectors

Despite their several advantageous characteristics (e.g. ability carry large genetic payloads, decreased immunogenicity compared to some other vectors, ability to integrate into the host genome), there are a number of safety concerns associated with the use of retroviral vectors in clinical applications. A major one is the rise of replication competent retroviruses through recombination between the vector and packaging constructs expressed in producer cells. To prevent this packaging constructs are provided in separate plasmids with reduced homology between the vector and helper constructs. There have been no reported cases of identification of replication-competent retroviruses in any clinical trials or preclinical studies that utilised HIV-1-based LVs to date.

Furthermore, the permanent integration achieved through retroviral infection which makes them attractive tools for gene delivery has the potential to lead to insertional mutagenesis. Integration of retroviral genome into regions with enriched transcription factor binding sites has caused transcriptional activation of nearby proto-oncogenes resulting in myelodysplasia or lymphoid leukaemia in gene therapy trials for X-linked SCID (16, 168), WAS (169, 170), and CGD (171).

1.4.Lentiviral Vectors

The major drawback of utilising GRVs is that they are unable to transduce non-dividing cells. This becomes a concern when targeting non-dividing or slow-

dividing cells such as haematopoietic stem cells, the main target of immunodeficiency disorder trials; quiescent lymphocytes, targeted in cancer trials; hepatocytes; neurons; and muscle fibres. However, since lentivirus PIC can cross nuclear membranes (see section 1.3.4), they can transduce these cells more efficiently (50, 146, 172-175). Their efficiency can be further increased following stimulation of cells into the G_0/G_1 phase (176-178).

Furthermore, as discussed above, insertional mutagenesis is caused due to retroviral integration to transcriptional hotspots. In contrast to GRVs' tendency to integrate preferentially around transcriptional start sites enriched in proto-oncogenes and genes regulating cell growth and proliferation (179, 180), it has been reported that LVs target transcriptionally active sites of the host genome and integrate more widely throughout the genome (114, 179-181). Therefore, LVs' integration pattern suggests lower oncogenic potential and thus better vector safety (182-184).

For lentiviral vectors, the packaging components underwent various iterative developments leading to the latest vectors typically using a four-plasmid system (i.e. two packaging plasmids encoding *gag-pol* and *rev, env* encoding plasmid, and vector plasmid encoding transgene of interest) (144, 159). In these vectors, the necessary *trans*-acting components are split into three plasmids to increase the safety (*Figure 1-4)*. All HIV-1 accessory genes are excluded from the packaging plasmids. The first plasmid encodes the *gag-pol* genes which are responsible for the structural and enzymatic components of the particles. The second plasmid expresses the *rev* gene that enables the export of the viral RNA from the nucleus. Lastly, the envelope is provided by the third plasmid; this is usually a heterologous glycoprotein most commonly that of vesicular stomatitis virus Indiana strain (VSVind.G) (185).

In LVs, the interaction between the viral Rev and RRE encoded in the vector plasmid is required for the successful nuclear export of the genome (186). This interaction is required for the expression of both the transgene encoded by the vector and *gag-pol* encoded by the packaging construct. As discussed in section 1.3.4 Rev is required for the nuclear export of unspliced lentiviral RNA. Although the constructs used in LV production are not identical to wild-type

(wt) HIV *gag-pol,* Rev is still required for correct expression and stabilisation of the *gag-pol* RNA (187, 188). To circumvent this problem, there have been attempts to codon-optimise *gag-pol* constructs to make the expression of the

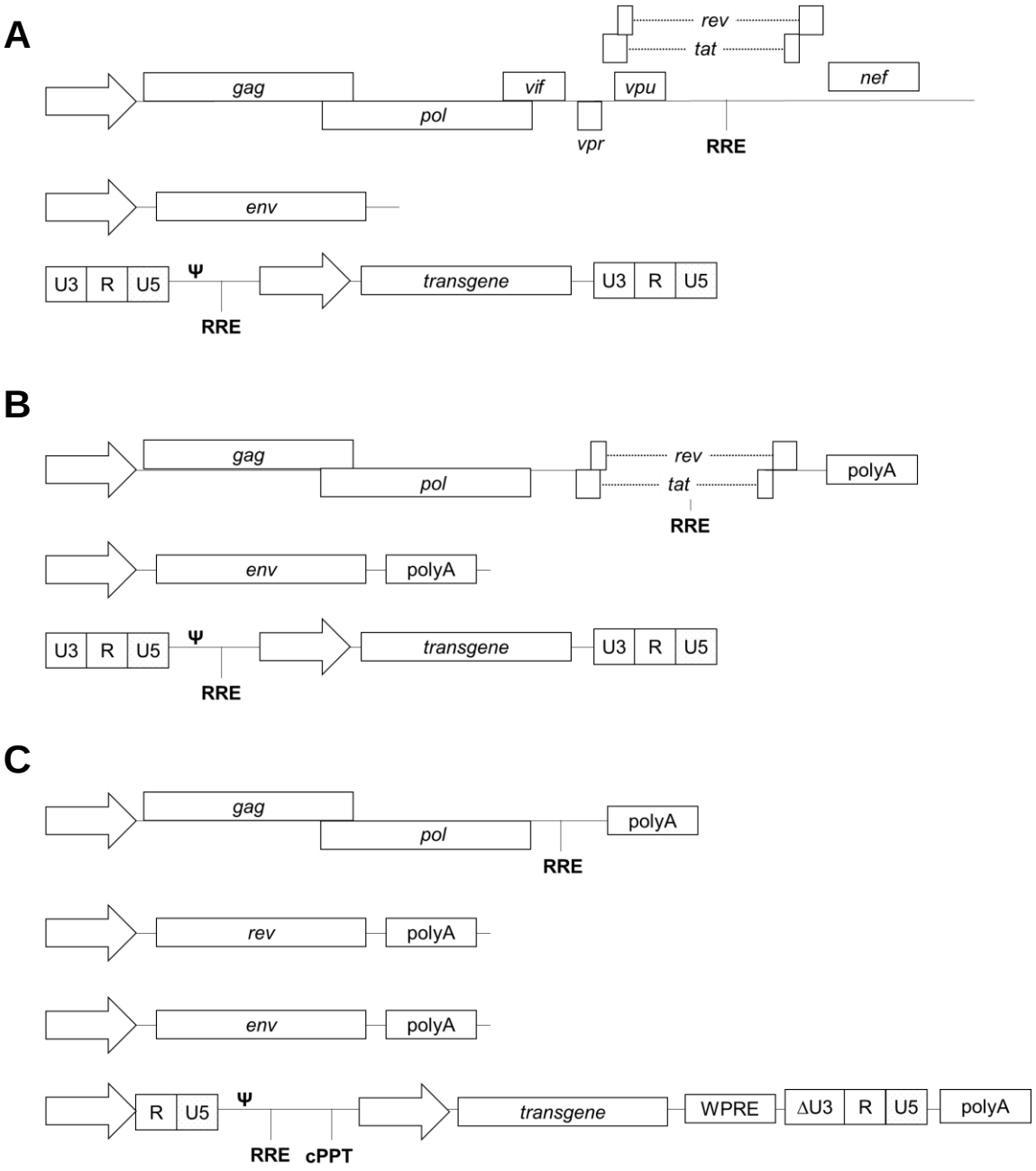

proteins Rev-independent. However, this was soon abandoned as vectors produced using the codon-optimised sequences yielded substantially lower titres in the presence and absence of Rev (187).

Figure 1-4: Engineering of Lentiviral Vector Systems to Improve Biosafety and Performance. **(A)** First generation lentiviral vectors. All HIV-1 proteins except the Env are provided in a packaging plasmid. Heterologous envelope (usually VSVind.G) is provided separately in a second plasmid, and notably, the vector construct has intact LTRs. Both packaging and envelope plasmids contain strong constitutive promoters (e.g. CMV). **(B)** The second generation system still consists of three plasmids. All HIV-1 accessory genes are removed, but the system is Rev and Tat dependent. **(C)** In the third generation vector system, the packaging plasmid encodes *gag* and *pol*, while *rev* is provided in a separate plasmid. The system is Tat-independent as 5' U3 in the transfer vector is replaced with a promoter, and it is SIN following deletions in the 3' U3 enhancer region. Addition of cPPT and WPRE elements have aided in increasing titres. U3: LTR element derived from sequences unique to 3' end of the RNA genome; R: LTR element derived from sequences repeated in both LTRs; U5: LTR element derived from sequences unique to 5' end of the RNA genome; Ψ: packaging signal; cPPT: central polypurine tract; RRE: rev response element. Arrows signify locations of the heterologous promoters.

1.4.1.Production of Lentiviral Vectors

Currently, the most efficient method to produce LVs is by transient transfection of human embryonic kidney (HEK) 293T cells (189, 190). Following transfection of plasmids, the supernatant containing the produced vectors is collected, filtered to clear out cell debris, and if desired, concentrated by ultracentrifugation. In this method, the vector production duration is usually two to three days, and there is relative batch-to-batch viral vector titre variation (191). This method is ideal for preclinical research where low amounts of vectors encoding different transgenes or different pseudotypes are needed. However, clinical trials require large amounts of the same vector with minimal discrepancies in characteristics between each batch (192). In clinical trials where gammaretroviral vectors were utilised production of the vectors from stable packaging cell lines has been preferred.

Stable production is achieved by transfecting the plasmids into the producer cells followed by selection for the viral gene expression. This production method reduces the risk of DNA recombination between different plasmids

which in return helps to reduce the possibility of generating replication-competent vectors. In addition, stable production enables the production of large batches with minimal variations in titre levels as well as reducing production costs.

However, development of such stable packaging cells lines has proven challenging. Notably, the constitutive expression of the gold-standard VSVind.G envelope is reported to be toxic to cells leading to syncytia formation and cell death (193). This has led to the construction of LV producer cell lines with inducible VSVind.G expression (194, 195). Another approach has been to use alternative envelopes such as that of the feline endogenous virus RD114 with a modified cytoplasmic tail to allow LV incorporation (RDpro) (196-199) and the G protein of Cocal virus, a vesiculovirus phylogenetically related to VSVind (200). While producer cell clones for clinical use have been developed using these envelopes, they have not progressed to clinical trials (201, 202).

The work presented in this thesis focuses on characterisation of VSVind.G and several other G proteins from the vesiculovirus genus for their use in preclinical research and clinical gene therapy.

1.5.Viral Membrane Fusion Proteins

Viral membrane fusion proteins can be classified into several distinct groups based on their structural similarities, fusion mechanisms, and viral fusion proteins (203). Despite such diversity these viral fusion proteins are responsible for both viral-cell and cell-cell fusion which dictate viral spread, pathogenicity, and persistence of infection (84, 204, 205). Virus-cell fusion is mediated by one (e.g. retroviruses) or more (e.g. herpesviruses) glycoproteins found on the viral membrane and it follows several environmental or physical triggers including low pH and receptor binding (206-208). Viral membrane fusion proteins are generally grouped into three based on their key structural features: class I, class II, and class III.

1.5.1.Class I

Class I proteins form homotrimers in both their pre- and post-fusion forms and are typified by the α-helical coiled coil structure (209). The unique characteristics of class I proteins are illustrated by influenza virus haemagglutinin: while the viral attachment is dictated by one subunit, another is responsible for fusion (210). Sendai virus HN/F proteins function similarly whereby F protein drives membrane fusion following its unmasking via receptor-recognition by HN (211).

1.5.2.Class II

The fusion domain of class II proteins mainly consists of β-sheets (203). In addition, the fusion protein on these viruses, such as Dengue (212) and West Nile viruses (213), associate with a chaperone protein which triggers fusion in response to low pH. When activated these proteins assemble into homotrimers (from homodimers – flaviviruses or heterodimers –alphaviruses) which is critical for the fusion process (214). Fusion proceeds through extensive domain rearrangement resulting in the connection of the viral and cell membranes (215).

1.5.3.Class III

Class III proteins are a relatively novel group with the structural confirmation of a combination of both class I and class II. VSVind.G is the only class III protein of which the structures of both pre- and post-fusion conformations are elucidated (214, 216). Rabies virus G protein, herpes simplex virus 1 glycoprotein B, baculovirus gp64, and G proteins from other vesiculoviruses are considered to be all class III proteins (217-219). In addition to structural difference, the key feature of class III proteins is the reversibility of the low-pH-induced conformational changes during membrane fusion (220).

1.6.Rhabdoviruses

Rhabdoviruses are a biologically diverse group of viruses which can infect vertebrates, invertebrates, and plants (221). The natural host for the majority of rhabdoviruses are arthropods which they exploit to infect vertebrate or plant

hosts. There are several exceptions: lyssaviruses (e.g. rabies virus (RABV)) have evolved to infect vertebrates without using other organisms as vectors and sigmaviruses (e.g. Drosophila melanogaster sigma virus) are congenitally transmitted in fruit flies (222).

The name rhabdovirus is based on its characteristic shape and is derived from the Greek word “rhabdos” meaning rod or wand. The rhabdovirus shape is epitomised by the bullet or cone-shaped form characteristics of vesicular stomatitis virus (VSV) (223). The replication mechanism of their non-segmented, negative sense, single-stranded RNA genome is almost universal across the family. Their replication cycle involves cell entry, facilitated by clathrin or receptor binding-mediated endocytosis, uncoating, transcription and translation, genome replication and assembly, and budding (221, 224).

The classical vertebrate rhabdoviruses are composed of the two genera vesiculoviruses and lyssaviruses which are represented by the prototype species VSV and RABV. Vesiculoviruses have a broad host range including mammals and are transmitted by insects while lyssaviruses utilise bats as their principal reservoir hosts (221, 222, 225, 226). Structurally they share the enveloped bullet shape packaging a genome consisting of five genes (3’-N-PP-M-G-L-5’) (227, 228). Reverse genetics of the prototype viruses allowed exploration of rhabdovirus evolution, investigation of gene expression and pathogenesis, and led to their development as vaccine vectors and oncolytic viruses (229, 230). These prototype viruses, VSV and RABV, have been studied extensively for decades and serve as model systems for investigating rhabdovirus life cycle, infectivity, and antigenic properties (221).

1.6.1.Rabies Virus

RABV, similar to the vesiculovirus Chandipura virus, is closely associated with fatal diseases in humans. RABV is the model virus of the genus Lyssavirus. The glycoprotein of rabies virus is comprised of four domains: signal peptide, ectodomain, transmembrane and cytoplasmic domain (231). The native RABV.G is located in the viral envelope and homotrimerises on viral surface (232, 233). It is the only antigen on the viral surface that is responsible for entry of the viral particle into the cell. It is a special protein that combines the

characteristics of class I and II virus fusion peptides (234). It is able to bind at least three different receptors, allowing virus endocytosis: the neurotrophin receptor (p75NTR), the nicotinic acetylcholine receptor, and the neural cell adhesion molecule (235-240). Following virus endocytosis, the fusion between the virus and the cell membrane is mediated by RABV.G through hydrophobic interactions occurring in low pH environment of the endocytic compartments (241, 242). Beyond its utilisation for virus infection studies and vaccination, RABV.G has also been used for studies of the nervous system. It has been used for mapping or tracing neuronal connections for better understanding nervous system processes (243).

1.6.2.Vesiculoviruses

Vesiculoviruses are a genus of the Rhabdoviridae that can infect mammals, insects, and fish. Taxonomically classified using host range, serological relatedness, and genome organisation, the genus has sixteen viruses assigned to it (225, 244). Most ubiquitously studied members of the genus can cause diseases in farm animals, while other vesiculoviruses can also infect humans causing diseases ranging from febrile syndromes to fatal encephalitis (244-246).

The first vesiculovirus described is the vesicular stomatitis virus (VSV). With its four serotypes, VSV Indiana (VSVind), VSV New Jersey (VSVnj), Cocal virus (COCV), and VSV Alagoas (VSVala), it is one of the most studied viruses. In fact, its serotype VSVind is regarded as the prototype virus for all vesiculoviruses (244, 247-250). It infects domestic farm animals such as cattle, swine, and horses causing lesions in oral tissue, udders, and hooves (251). First described in 1927, VSV infections were seen in livestock as early as the 1810s in the USA while the infections in South America date back to 1930s. VSV infection is mainly endemic in South and Central America while several outbreaks have been reported in central-northern Mexico and the southwestern United States over the past five decades (252-255). The only two VSV cases seen outside the Americas were in France during World War I and South Africa in 1897 as single cases of isolated infections (250, 256).

Two other major vesiculovirus serotypes are Chandipura virus (CHAV) and Piry virus (PIRYV). Isolated in northern Brazil, PIRYV has only 5 cases of human infection all of which were non-fatal lab accidents (251). On the other hand, CHAV is becoming a health concern in India and is classified as an emerging human pathogen. First isolated in 1966 as the cause of febrile diseases, more recently it has been associated with outbreaks of fatal encephalitis in children in India (257-259). It is very likely that there are many more vesiculoviruses yet to be discovered that exist in nature circulating in animals, humans, and insects without any visible symptoms.

1.6.2.1.Use of Vesiculoviruses in Pseudotyping Viral Particles

Pseudotyping is producing virus particles or viral vectors using the surface glycoprotein of a foreign virus. The result is called a pseudotyped virus particle. This method was first used in cells infected with two different viruses resulting in phenotypically mixed particles or pseudotypes (260-263). The choice of envelope used to pseudotype virus particles can alter cell tropism, increase or decrease the stability and infectivity of the virus particle, or change sensitivity to serum complement proteins.

The glycoprotein of VSVind (VSVind.G) is commonly used as a model envelope in many studies (146, 264, 265). VSVind.G pseudotyped retroviral particles can produce high titres, are physically stable during ultracentrifugation, and have a wide range of cell tropism. However, viral vectors that bear the VSVind envelope are hypersensitive to human serum which may limit their potential for *in vivo* applications (266). Furthermore, the glycoprotein is reported to be cytotoxic (267).

This led some investigators to look for new substitute envelopes to replace VSVind.G. Another VSV serotype, COCV, has been reported to share VSVind.G's advantages while lacking some of the drawbacks such as cytotoxicity and inactivation by human serum complement (200, 202). This indicates that the envelopes of some vesiculovirus subfamily members might be more suitable to high titre viral vector production than VSVind.G.

1.6.2.2.Vesiculovirus Classification, Genome Organisation, and Viral Proteins

Vesiculoviruses have a genome that is a single-stranded RNA molecule with negative polarity (268-270). This negative sense RNA codes for five structural proteins: nucleoprotein (N), viral polymerase (L), phosphoprotein (PP), matrix protein (M), and glycoprotein (G) (269, 271, 272).

The interactions between N, PP, and L make up the transcription and replication complex which modulates the RNA-dependent RNA polymerase activity (273, 274). The most abundant protein, M, interacts with the G protein monomers and drives their trimerisation on the viral surface (275). G protein is a class I membrane-associated glycoprotein with a small transmembrane and C-terminal domain. More than 90% of its N-terminal region protrudes from the viral surface forming spikes on viral envelope. It plays a critical role in the viral life cycle as G is both involved in receptor recognition and the fusion of viral and cellular membranes (246, 268, 270, 275).

When comparing full-length genomes of VSVind, VSVnj, and COCV, although the length of noncoding regions varies significantly, the five structural protein lengths are within six amino acid residues of each other. The structural proteins N, M, and L are the most conserved ones on both nucleotide and amino acid levels while G and PP have much more variance (247). The analyses of these structural proteins highlight that although VSVnj and COCV viruses are genetically closely related to VSVind strain, all three are serologically distinct (249, 276).

1.6.2.3.Vesiculovirus Glycoprotein Structure

In natural vesiculovirus infection, the G protein plays a critical role during the initial steps. The trimers of the envelope protein anchored to the viral cell membrane mediate both receptor recognition and membrane fusion (264, 268, 269). The attachment of virus onto the target receptor initiates the endocytotic pathway mediated by the glycoprotein followed by pH-dependent viral fusion (268). The decrease of pH in the early endosomal compartments of the target cell induces conformational changes in the viral G protein which then trigger

the fusion of the viral envelope with the cell membrane (224, 269, 277-280). The pH-dependent fusion is a shared characteristic amongst vesiculoviruses which occurs around pH 6 (269, 281-283).

Furthermore, its central role in receptor attachment and viral penetration into the target cell makes the G protein the principal target of neutralising antibodies generated by the humoral immune response (251). Therefore, exploration of the functional domains and immunogenic determinants of the vesiculovirus glycoproteins is essential to understanding the structure-function relationship of antigenicity, host range determination, and infectivity (264).

1.6.2.3.1.Vesiculovirus glycoprotein comparison and phylogenetic analysis

The glycoproteins of VSVind (prototype for vesiculoviruses), VSVnj, and CHAV have been relatively well studied. However, there is little known about the other VesG, namely Maraba virus G protein (MARAV.G), COCV.G, VSVala.G or PIRYV.G. The G proteins of these seven vesiculoviruses have been sequenced. While CHAV.G and PIRYV.G have a similar number of amino acid residues, 530 and 529 respectively, other five G proteins are shorter, around 511-517 amino acid residues long (248, 264, 284-286).

The phylogenetic analysis of the amino acid sequences of the G proteins indicates that both MARAV and COCV are closely related to VSVind (*Figure 1-5)* (264). On the other hand, it is evident that CHAV and PIRYV are closely related to each other as well (245). These lineage distinctions seen at glycoprotein level fit the vesiculovirus clusters identified after full-length genome analysis (244).

A

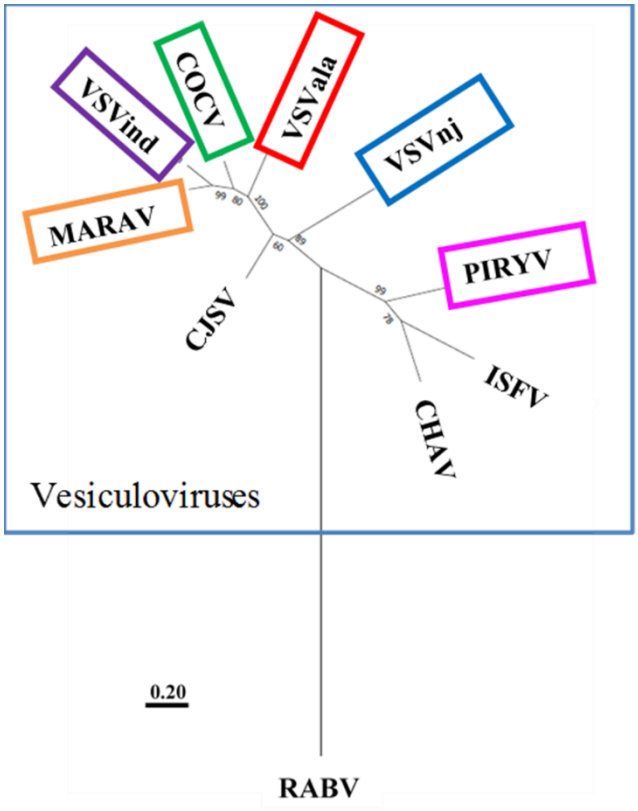

B

Virus	%aa Identity
VSVindiana	100%
Maraba	78%
Cocal	72%
VSValagoas	64%
VSVnew jersey	50%
Piry	40%

Figure 1-5: Phylogenetic Relationship of Vesiculoviruses Based on G Protein Amino Acid Sequences. **(A)** G proteins of the major vesiculoviruses, as well as the G protein of the rabies virus (another prototype rhabdovirus, utilised as the base for the phylogenetic tree), were included in the analysis. The amino acid sequences were aligned using ClustalOmega online multiple sequence alignment tool (EMBL-EPI) (see *Table 2-16)*. The evolutionary analyses were conducted in MEGA7 (287). The evolutionary history was inferred by using the maximum likelihood method based on the Jones-Taylor-Thornton matrix-based model (288). The tree with the highest likelihood is shown with the bootstrap confidence values (out of 100) indicated at the nodes. The tree is drawn to scale, with branch lengths measured in the number of substitutions per site, depicted in the linear scale. CJSV: Carajas Virus, ISFV: Isfahan Virus. Vesiculoviruses that this thesis focuses on are highlighted in coloured boxes. **(B)** The percent amino acid identities of the G proteins compared to VSVind.G are summarised in the table.

Deduced amino acid sequences show that vesiculovirus G proteins (VesG) are typical class I membrane-associated glycoproteins with long extracellular regions at the N-terminal ends, a hydrophobic transmembrane domain anchoring the protein to the cell membrane, and a C-terminal domain that projects into the cell (244, 289). Results of amino acid sequence analyses show a high degree of structural and functional similarity between the seven glycoproteins (234, 246, 289-291). The G protein alignment demonstrates that there are a large number of blocks of amino acid residues conserved amongst the different vesiculovirus strains (*Figure 1-6)* (289). With approximately 78% and 72% sequence homology respectively, MARAV.G and COCV.G are the most similar G proteins to the prototype VSVind.G. VSVala.G follows with 64%, while VSVnj.G has 50% homology. PIRYV.G has the most variance amongst six VesG with just 40% sequence homology on amino acid level (*Figure 1-5)*.

The signal sequences of the seven strains show a number of differences in length and amino acid composition (264, 289). However, in the four VSV serotypes, the nature of the signal peptides, precisely, the presence of a charged residue near the N-terminal end, the hydrophobic central region and decreased hydrophobicity at the C-terminal end is maintained (292, 293). On the other hand, the predicted signal sequences of CHAV.G and PIRYV.G are larger than that of VSV serotypes and MARAV.G (21 residues compared to 16 for VSVind.G/VSVnj.G/VSVala.G/MARAV.G and 17 for COCV.G). They do not show the homologous nature seen between VSV serotypes and CHAV.G has no lysine residue near the expected cleavage site (264, 285, 289).

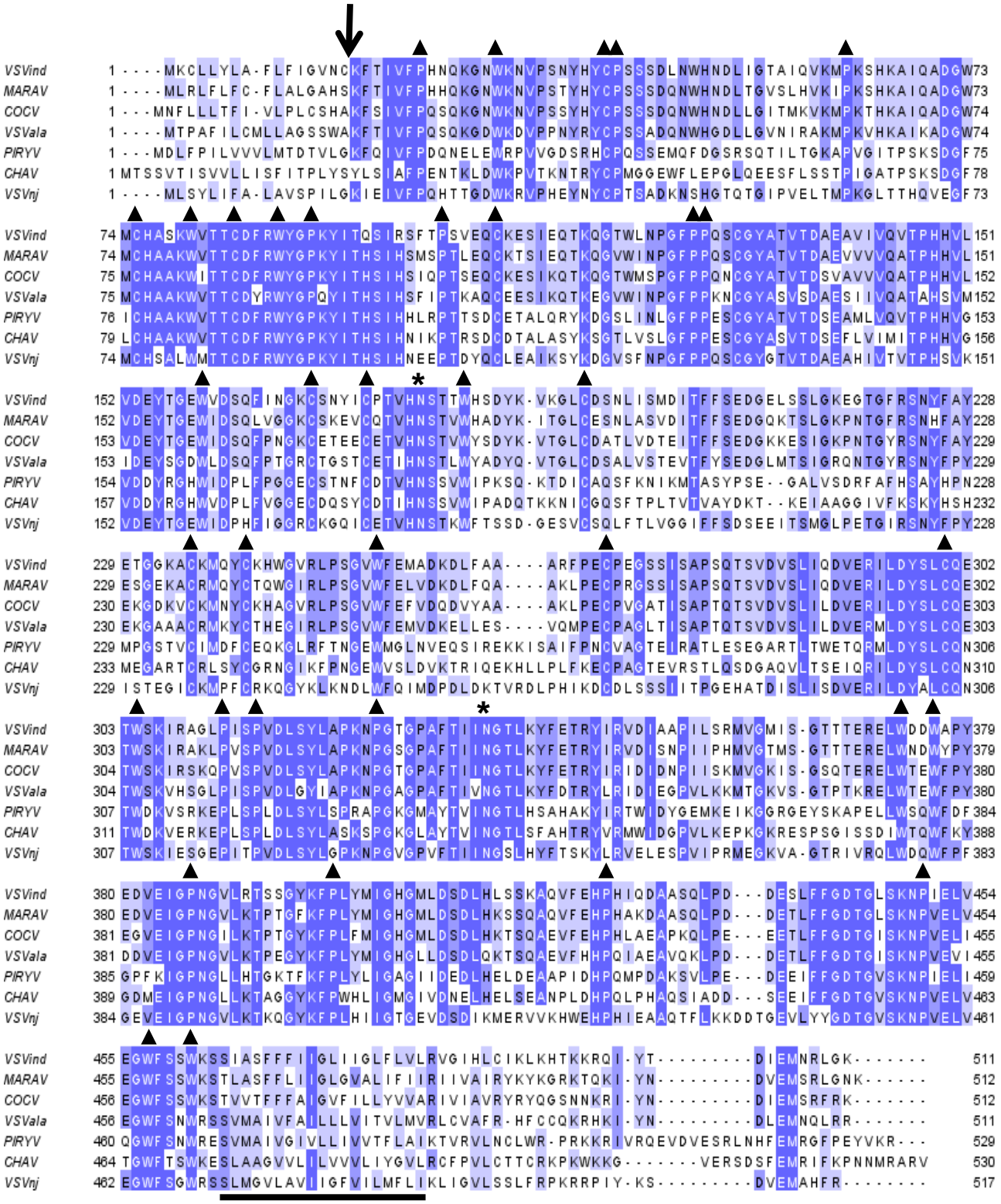

Figure 1-6: Multiple Amino Acid Sequence Alignment of the G proteins of Major Vesiculoviruses. The sequences of major vesiculoviruses were aligned using ClustalOmega online multiple sequence alignment tool (EMBL-EPI) (see *Table 2-16)*, and the alignments were visualised using JalView software (294). Dashed lines represent gaps introduced to maximise matching of amino acid residues. Blue shading indicates percent identity; dark blue:

80-100%, medium blue: 60-80% light blue: 40-60%, and no colour indicating <40% identity. The arrow indicates the signal peptide cleavage sites. The asterisks indicate the two conserved sites for N-linked glycosylation. The hydrophobic membrane-anchoring domains are underlined. The conserved W, P, C residues are annotated with triangles.

Furthermore, the N-linked glycosylations occur at identical positions on all seven G proteins since there are only two sites in each glycoprotein that contain the potential glycosylation sequences of asparagine-X-serine/threonine (248, 295). The two sites are precisely aligned within highly conserved regions. Similarly, most of the tryptophan (W), proline (P), and cysteine (C) residues occur in non-variant positions in all seven VesG. It is hypothesised that while P residues might be defining domains, C residues are possibly involved in disulphide bond formation which is essential for the protein to assume its functional folding (264).

On the other hand, the membrane anchoring sequences of the virus G proteins do not have a similar level of homology. For COCV.G this is located at amino acid residues 465-483 and shows approximately 50% identity to that of VSVind.G (264). Like the signal sequences, the transmembrane domains of the glycoproteins are amongst the least conserved regions at the amino acid level. However, in all seven, the hydrophobicity of the region is maintained which implies that the exact amino acid may be insignificant as long as the hydrophobicity is conserved (248). A similar trend can be observed in the cytoplasmic domains of the G proteins as there is minimal identity. Although the amino acid homology is not shared, the overall charge distribution is conserved (248, 264). Since the cytoplasmic sequence is shown to have a critical role in virus assembly by providing an essential scaffold for the matrix protein and the nucleocapsid to bind, it can be concluded that the amino acid character of the domain drives this process (248, 296).

A couple of the conserved blocks of amino acid residues amongst the G proteins can be matched to VSVind.G's functional domains. Two of the largest conserved blocks, located at aa residues 74-90 and 123-136 of VSVind.G, lie

in its fusogenic domain[1] (297). Thus, these two conserved regions may represent the fusion peptide of vesiculoviruses and may play an essential role in controlling the low-pH-induced conformational changes of the glycoproteins (298-302).

Moreover, covalent modification of VSVind.G at the cytoplasmic domain is a known characteristic of the protein (289). The covalent attachment of fatty acids, such as the palmitic acid, to cysteine or less frequently to serine or threonine residues via thioester bonds is a well-observed occurrence that VSVind.G shares with CHAV.G and PIRYV.G. However, it has been demonstrated by biochemical and genetic means that COCV.G and VSVnj.G do not share this characteristic (244, 285).

1.6.2.3.2.G protein conformational states, domains, and structure

Based on fusion kinetics analysis of VSVind.G and other rhabdovirus G proteins, it has been elucidated that the G protein assumes three key conformational states which have distinct biochemical and biophysical characteristics (241, 269, 270, 281, 300, 301, 303-306). The native, pre-fusion state is detected at the viral surface above pH 7. When activated by low pH, the active, hydrophobic state drives interactions with the target membrane as the first step of viral fusion (300). The post-fusion state is antigenically distinct from both native and active states and is fusion-inactive (307). There is a pH-dependent equilibrium between all three states of the G protein which shifts towards the post-fusion state at low pH. Unique to rhabdoviruses, this low-pH-induced structural change of the G protein is reversible and is essential to allow transportation of the mature G protein through the acidic compartments of the Golgi apparatus and for it to assume its infectious, pre-fusion, state when it is on the viral surface (301, 303, 306, 307).

Both pre- and post-fusion (i.e. native and inactive) states of VSVind.G, as well as possible monomeric intermediates in the active state and several conformations of the fusion complex, have been identified by X-ray

[1] In this thesis, the amino acid residue numbers of VesG are indicated, unless otherwise specified, with regards to the precursor G proteins containing their respective signal peptides.

crystallography (269, 270, 297, 307). Though it shares some features with well-known class I and class II fusion proteins, VSVind.G has been classified in a novel class of fusion proteins, class III, due to the reversibility of its structural changes (269, 308). In both structures, four distinct domains were identified within the N-terminal extracellular domain of the G protein (*Figure 1-7)* (270, 297).

The domains can be summarised:

a. Domain I

Also called the lateral domain, is a β-sheet rich domain made out of approximately 90 amino acids in two discontinuous segments.

b. Domain II

Domain II, the trimerisation domain, is involved in forming the six-helix-bundle in the trimeric pre-fusion conformation. The four α-helices making up this domain dictate trimerisation of the G proteins via hydrophobic interactions.

c. Domain III

Domain III is organised into two α-helices and two β-sheets and contains the fold of pleckstrin homology (PH) domain. This is the most exposed domain of VSVind.G in the pre-fusion conformation. Domain III, inserted into domain II, is located at the top of the G protein. Thus, it is hypothesised that it might be involved in receptor recognition.

d. Domain IV

Domain IV is the only domain made up of a single continuous segment. It is inserted into domain III and contains two hydrophobic fusion loops that are capable of interacting with the target membrane. The structure contains six β-sheets with highly conserved amino acid residues. Multiple disulphide bonds in this domain help to stabilise the structure of the G protein.

The conformational changes from pre- to post-fusion structure of VSVind.G entails a dramatic reorganisation of the entire molecule. During these changes domains I, III, and IV retain their tertiary conformation. However, they undergo rearrangements in their relative orientation. This is mediated by the structural

changes in the hinge regions and the major refolding of domain II (269, 270, 297).

The post-fusion structure looks like the flipped version of the pre-fusion conformation relative to the rigid block of domain I (269). Therefore it is postulated that these changes might not be topologically possible without the transient dissociation of the trimer of the G protein (270, 309). There has been some evidence suggesting that monomeric intermediates are involved in the structural transition of VSVind.G (269, 290). One intermediate in the fusion pathway is found to expose the fusion domain at the top of the molecule allowing the interaction of the fusion loops with the target membrane (269).

Although the structural organisations of the two separate conformations of VSVind.G are very different to other classified fusion proteins, namely class I and class II, the amino acid alignment of the VesG shows that all these glycoproteins should have similar folds (269). In support of this, recently the low-pH conformation of CHAV.G has been elucidated, and striking similarities to VSVind.G have been observed (246). The high structural similarity expected from the primary structure of the peptides is also evident in the protein's tertiary structure. The overall structure of CHAV.G is very similar to the post-fusion conformation of VSVind.G and the three identified domains, central domain, fusion domain, and pleckstrin homology domain, are more conserved than expected from the sequence divergence of the molecules (246, 297, 310, 311). While the central and upper parts of the fusion domain are almost superimposable, PH domain appears to have the most divergence. This is expected since, along with DI, VSVind.G's DIII which contains the PH domain is thought to be the major target of the neutralising antibodies with multiple epitopes reported in these two domains (312). PH domain remains to be the most divergent domain amongst the vesiculoviruses which might be reflecting the effects of host-pathogen interactions or immune-system driven evolutions (246).

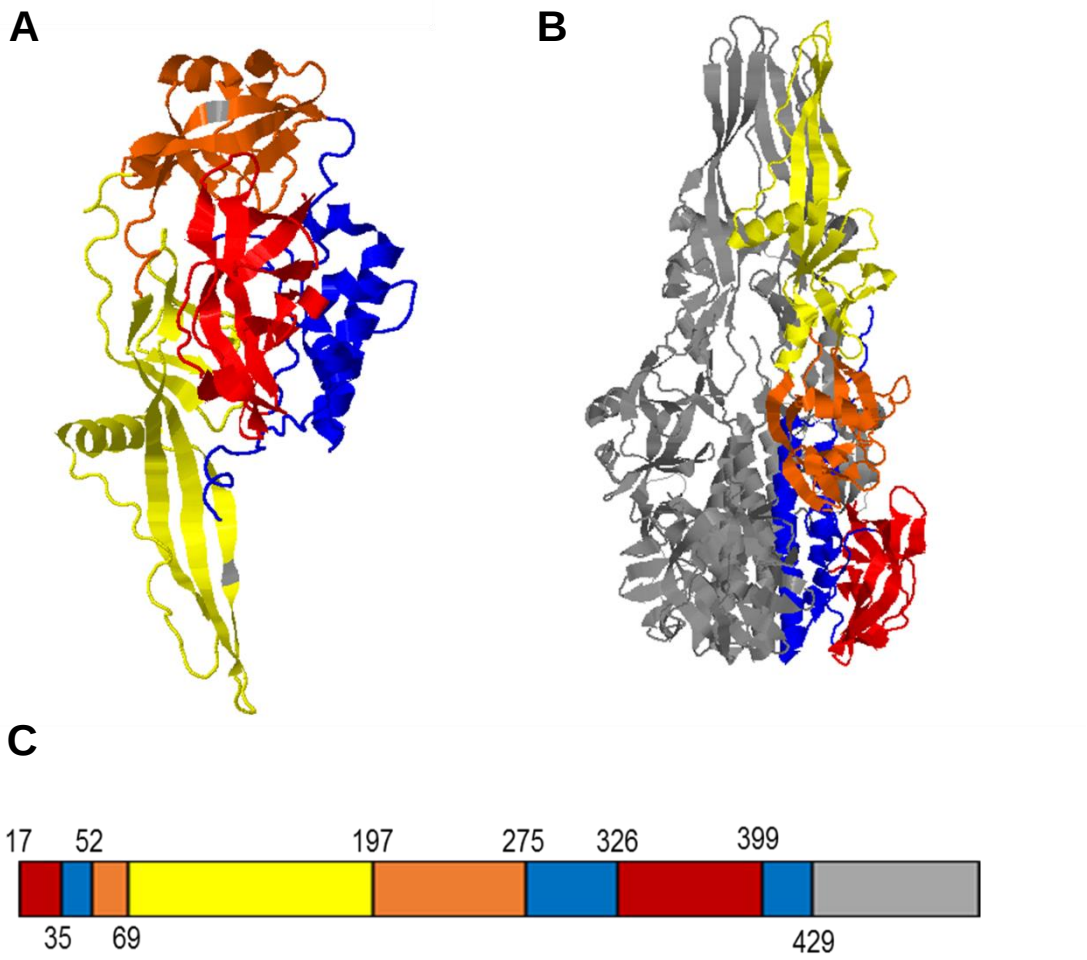

Figure 1-7: Overall Structure and Domain Organisation of VSVind.G in Pre- and Post-Fusion Conformations. Mature VSVind.G protein (aa 17-429) generated by thermolysin-mediated limited proteolysis of virions (i.e. Gth (270, 297)) in **(A)** pre- and **(B)** post-fusion monomeric and homotrimeric conformations respectively (PBD IDs: 5I2S and 5I2M respectively). VSVind.G monomers are coloured by domain (red: DI, lateral domain; blue: DII, trimerisation domain; orange: DIII, PH domain, yellow: DIV, fusion domain; grey: transmembrane and C-terminal domains). 3D structures were retrieved from RCSB Protein Data Bank, visualised, and coloured using JalView software. **(C)** Domain architecture of VSVind.G depicted in a linear diagram. Domain boundaries are numbered according to the G protein precursor (i.e. including the signal peptide). Figure adapted from (297).

1.6.2.4.Vesiculovirus Glycoprotein Function

1.6.2.4.1.Cellular receptors for vesiculovirus cell entry

Receptors are critical to understanding the mechanism of viral disassemblies. Envelope-receptor interactions either directly trigger the conformational changes that lead to fusion or they help to guide the virus-receptor complex to cellular locations where environmental cues such as pH trigger fusion and lead to infection (313). Viral surface units, such as membrane glycoproteins or viral capsid, attach to factors (e.g. heparan sulphate proteoglycans) located on the target cell surface during the initial interactions between a virus and a host cell (89, 314, 315). These first interactions may lack specificity and are often mediated by electrostatic forces. They help the virus to recruit specific receptors which triggers the processes leading to cell entry. Some receptors can efficiently aid virus endocytosis. Alternatively, for others, receptor binding may activate signalling pathways that facilitate viral entry by directly promoting viral fusion or aiding pH-induced conformational changes within endocytic compartments of the target cell (313).

Many viruses exploit the intrinsic properties of endocytic vesicles to pass through the cell membrane. They require exposure to low pH or lysosomal enzymes to initiate fusion (313). Recently it has been elucidated that viruses can exploit several different endocytic mechanisms which are either constitutively active or can be induced in host cells (316).

Like other endocytic cargoes, most of the endocytosed viruses are transported to the endosomes. In these intracellular compartments, viruses use environmental cues, primarily low pH, to initiate the membrane fusion that allows them to translocate their genome into the host cell cytoplasm (317, 318). There are several advantages to viral fusion from endosomes. Endosomes lack the actin-myosin cytoskeleton barrier that limits receptor mobility (319). Furthermore, in the case of enveloped viruses, it limits the display of viral proteins on the cell surface where the innate and adaptive immune systems may target them, and in the case of viruses which enter cells through membrane lysis, for example adenoviruses, it limits the membrane damage to just endocytic components (313). However, there are several obstacles

invading viruses need to avoid. While endosomes can return the virus-receptor complex to the cell surface through their sorting function, maturation of the vesicle to late endosomes and lysosomes generates a potentially hazardous environment for the virus (320). Thus, many viruses fuse at mildly acidic pH 6.0 while others exploit the changing environment to control the timing or cellular location of fusion (313).

The entry of the vesiculoviruses into the host cells is dictated only by their glycoprotein that protrudes from the viral surface (234). The G protein first mediates the viral attachment by interacting with the cellular receptor. In the case of VSVind.G, the low-density lipoprotein receptor (LDLR) and its family members have been demonstrated to be the cellular receptors responsible for viral entry (321-323). It is shown that LDLR is the primary entryway for VSVind.G pseudotyped particles in various cell lines which include a human epithelial cell line. Furthermore, this viral infection could be successfully inhibited in a dose-dependent manner via soluble LDLR molecules and was entirely blocked by the addition of receptor-associated protein (RAP) which is known to bind to other LDLR family members [74]. Similar dose-dependent partial inhibition of COCV.G pseudotyped LV (COCV.G-LV) infection has also been demonstrated (200).

Recently, the crystal structures of the interactions between VSVind.G and two cysteine-rich domains of LDLR, CR2 and CR3, have been elucidated (323) (*Figure 1-8)*. These complexes highlighted that both domains of LDLR interact with the same residues on the G protein in its pre-fusion conformation and the interactions are blocked following pH-induced conformational changes. This is due to the fact that the residues which mediate the interactions are pulled apart in the post-fusion conformation.

The basic residues H24 and K63 on VSVind.G dictate CR domain and G protein interactions by interacting with acidic residues on the CR domains, D69/73/79, E80 and D108/112/118, E119 respectively on CR2 and CR3. These interactions allow docking and coordination of Ca^{2+} ions which are essential for LDLR functionality (321, 322, 324-326). In addition, R370 on VSVind.G interacts with the carbonyl groups in the LDLR main chain forming

the key residue-residue interactions between the two proteins (323). This mode of binding which involves calcium cage-mediated protein-protein interaction that VSVind.G exploits is identical to that of LDLR and its endogenous ligands (324, 327-329). However, the key residues on VSVind.G that are involved in receptor binding are not conserved amongst the genus. For example, CHAV.G does not have basic residues in the positions corresponding to 63 and 370 (I68 and S379 respectively) and does not bind to LDLR CR domains (323). Therefore, neither the use of this epitope nor the receptor can be generalised to all vesiculoviruses.

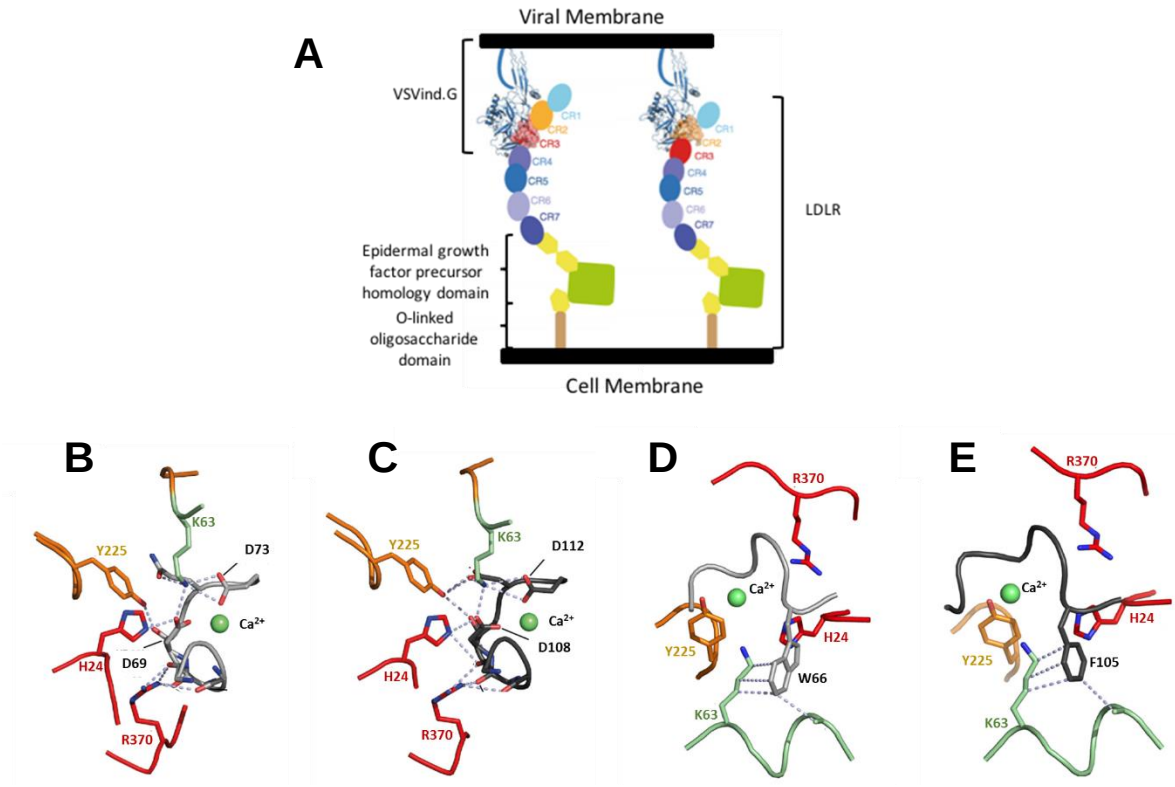

Figure 1-8: Crystal Structures of Interactions Between VSVind.G and CR2-CR3 Domains of LDLR. **(A)** Diagram demonstrating the bound structure of VSVind.G to both CR2 and CR3 on LDLR at neutral pH while both proteins are anchored to the viral and cell membranes respectively. Detailed structure of basic VSVind.G residues H24, K63, Y225, and R370 interacting with the acidic residues on **(B)** CR2 and **(C)** CR3. Detailed struture of the hydrophobic interactions betweeen the aromatic residues of **(D)** CR2 and **(E)** CR3 with VSVind.G. The lateral domain of VSVind.G is in red, the pleckstrin homology domain (PHD). The S2 domain within PHD that dictates VSVind.G-CR interactions is coloured green. LDLR residues are in black. The calcium ion is depicted as a green sphere. Adapted from (323).

1.6.2.4.2.pH sensing mechanism

In the pre-fusion structure of VSVind.G, three histidine residues, H76, H178, and H423, cluster together and act as the pH sensing molecular switches for the glycoprotein (270, 297, 305). Although counterparts of this switch have not been identified in other vesiculoviruses' pre-fusion structures, the histidine residues are conserved between all seven vesiculovirus strains analysed (see *Figure 1-6)*. It is postulated that low pH triggers conformational changes allowing the fusion domain to move away from the viral surface and towards the target membrane. This is mediated by the protonation of the histidine residues leading to the destabilisation of the interaction between the C-terminal end of the ectodomain and the fusion domain (269, 270).

In contrast, in the post-fusion structure of VSVind.G, four acidic residues, D284, D290, D409, and D411, are brought closer which has been demonstrated to play the role of the pH sensing switches for the transition back to pre-fusion conformation from the post-fusion conformation (246, 330). The acidic character of the residues corresponding to D290, D409, and D411 of VSVind.G is conserved throughout the vesiculoviruses. However, this is not the case for D284. Although these residues are critical for VSVind.G, local amino acid differences suggest that other vesiculoviruses such as CHAV have evolved alternate structural solutions. For CHAV.G the cluster formed by D290, E255, and H230 act as the pH sensing switch. The deprotonation of these residues at high pH levels results in the destabilising effect that triggers the conformational change back to the pre-fusion structure. It is thought that these three amino acid residues compensate the switch of D284 with A292 for the correct function of the G protein (246).

Comparison of the 3D structures of CHAV.G and VSVind.G revealed substantial divergence between vesiculoviruses (e.g. location of pH sensing residues), however, preservation of key functional and structural aspects (246, 270, 297). Most strikingly the orientation difference between fusion and PH domains between the two G proteins demonstrated strict structural constraints. However, despite these malleable local conformations, overall structure and function of the G protein with regards to the pH-dependent fusion of homotrimers are retained throughout the genus (246, 331, 332).

1.6.2.4.3.Fusogenic activity

The first step of a successful infection is the translocation of the viral genome across the cell membrane into the host cell (333). For enveloped viruses, such as vesiculoviruses, this step is mediated by the glycoproteins on the viral surface that promote both receptor recognition and membrane fusion. As mentioned in the previous sections, the activation of the fusogenic pathway involves major structural rearrangements and refolding of the glycoprotein. This is triggered by molecular cues involving receptor recognition and low pH. After endocytosis, upon reaching the acidic endosomal compartments, VesG undergo low-pH-induced structural changes from their trimeric pre-fusion conformations to post-fusion conformations. These changes lead to the exposure of the fusion peptide or loops which then drive the merger between viral and endosomal membranes (269, 270, 277, 290, 300, 303, 304, 334).

To identify the critical sequences for this fusogenic activity, investigators have used mutational analysis. It is known that VSVind.G is sensitive to even mildly acidic pHs and its levels of infection are at their highest around the physiological pH (i.e. pH 7.2) (246, 280). In support of this, researchers have observed a thirty-fold drop in the titres of wt VSVind when the infections were carried out at pH 7.0 compared to infection rates at pH 7.2 and a further thirty-fold drop at pH 6.8 (251). Through pH-driven adaptations and mutations, four amino acid replacements, F18L, Q301R, K462R, and H65R, were identified in low-pH adapted versions of VSVind.G. F18L and Q301R were identified as the major contributors to pH adaptation. In addition, the fact that three out of the four changes were to arginine residues suggests that these positive charges are essential for modulating pH-induced conformational changes in the G protein.

While VSVind.G is extremely sensitive to mildly acidic pHs, it is reported that both VSVnj.G and CHAV.G have lower pH thresholds for their fusogenic activity (246, 251). While VSVind replication is completely hindered at acidic pH, cell-to-cell fusion assays demonstrated that CHAV and VSVnj were able to replicate in infected cells and cause syncytia formations under the same conditions. This viral vigour and resilience in mildly acidic pHs are postulated

to be the reason behind why VSVnj outbreaks in animals and CHAV outbreaks in humans are more severe than VSVind infections (251). When the glycoprotein alignment is carefully analysed, it can be seen that VSVnj.G already contains the K462R amino acid switch while CHAV.G has the F18L switch. This suggests that PIRYV.G which also has the amino acid replacement K462R might also have a lower pH threshold compared to VSVind.G.

The pH-dependent fusion of two lipid bilayers involves a hemifusion state facilitated by VSVind.G (220). In this state, conformational changes that expose the fusion peptide pull the bilayers closer and accelerate the merging of the two membranes. The merger is modulated by the equilibrium between the pre-fusion trimers and extended monomers in the active state. pH-induced attachment of VSVind.G occurs even in the absence of specific receptor interactions explaining the observation of syncytia formation following its expression in cells (335). At neutral pHs (i.e. pH 7-8), only a low number of fusion loops are exposed, but as the pH decreases, attachment becomes progressively tighter and stronger. The fact that the fusion loops extended by the monomeric G can withdraw from the membrane after raising the pH highlights the reversibility of this fusion process (220). Lowering the pH below 6.6 facilitates fusion loops to cluster as trimers pulling the lipid bilayer and the G protein much closer, provided that a critical number of post-fusion trimers can form within the contact zone of the virion and the lipid bilayer. Depending on the number of G in the pre-fusion trimeric and monomeric conformations on the virion surface, the equilibrium requires pH to drop to 6.2 or lower to ensure the dissociation of enough number of trimers and extension of fusion loops from monomers before the critical number of post-fusion trimers will be present within the contact zone for membrane fusion to ensue.

This shows that although receptor recognition is important for binding and entry into target cells, for VSVind.G, and therefore other VesG, pH or protonation is the trigger that initiates conformational transitions in the fusion proteins (220). The antiparallel interactions between the fusion domains and transiently stable monomeric intermediates during virion fusion is the hallmark characteristic that differentiates VSVind.G and other class III fusion proteins

from class I and II. In addition, the mechanism through which VSVind.G fuses also opens up the possibility that, depending on the local environment (pH, viral membrane curvature, local glycoprotein density), the G proteins can be shuttled onto the path of the post-fusion trimer network leading to spontaneous fusion (277, 336).

1.6.3.Vesiculoviruses as Oncolytic and Vaccine Vectors

Many naturally occurring and laboratory produced strains of viruses are utilised as clinical tools to fight human diseases (337). Most notably, VSVind, has become a clinically significant vaccine vector and in recent years is being investigated as a potent oncolytic virus.

1.6.3.1.Oncolytic Virotherapy

VSVind's oncolytic ability stems from its sensitivity to type I interferon (IFN)-based antiviral responses (338). As tumours progress they become unresponsive to IFN signalling, lose expression of IFN stimulated genes (e.g. major histocompatibility complex), and accumulate defects in genes that promote apoptosis and halt cell growth (339-342). While VSVind replication is robustly suppressed in normal tissue via IFN signalling, it flourishes in non-responsive cancer tissue.

Due to the defects in the IFN pathway, *in vitro,* VSVind preferentially infects, replicates in, and lyses tumour cells while healthy cells with intact IFN pathways remain unaffected (343). Mixed culture infection and viral propagation assays have elucidated that tumour cells with protein kinase receptor deficiencies and defects in *p53, ras,* and *myc* are extremely susceptible to VSVind-induced apoptosis (344, 345).

Furthermore, VSVind's oncolytic capacity on several human cancer cell lines derived from lungs, ovary, prostate, colon, breast, and brain (e.g. A549, Lewis lung carcinomas, LNCaP human prostate carcinomas) have been demonstrated in detail (342, 344, 346, 347). This lytic efficiency also could be translated to *in vivo* applications where both human xenografts and immunocompetent syngeneic cancers have been eradicated in several animal

models (342, 346, 348, 349). VSVind also efficiently targets leukaemic cells in primary multi myeloma patients and purges bone marrow while having no effect on normal bone marrow progenitor cells or peripheral blood leukocytes (350, 351).

Following the advent of virus cloning and plaque rescue (352), researchers have produced modified VSVind mutants (e.g. A1 and A2) (338, 347) which displayed enhanced tumour selectivity and less dependence on IFN signalling (342). Another approach undertaken to improve safety and enhance therapeutic efficacy is to ensure tumour selectivity via virus targeting. Most notably replacement of VSVind.G with the envelope of Sindbis virus conjugated to a monoclonal antibody successfully retargeted the virus against Her2/neu receptor expressing breast cancers (353-355). Currently, incorporation of immunotherapeutic and suicide genes into the virus is being investigated (338).

All in all, VSVind has demonstrated substantial tumour selectivity and efficient oncolytic activity *in vitro* and potent anti-tumour activity in numerous *in vivo* models. However, although *in vitro* the viral infection remains potent and spreads, several studies have highlighted the need of administration of several therapeutic virus doses to elicit the desired oncolytic response *in vivo* implying that barriers regarding virus delivery and host immune response remain to be overcome for the establishment of a clinical therapy (356).

1.6.3.2.VSVind as a Vaccine Vector

Vaccine vectors expressing foreign proteins aim to elicit a robust and specific immune response exploiting the inflammatory properties of viruses. For these purposes attenuated or modified strains of animal viruses are ubiquitously utilised which also help to avoid problems associated with pre-existing immunity (357). These vectors can not only be delivered via injections but also administered intranasally through the mucosal route making them versatile and effective vaccines. Particularly, single intranasal administration of recombinant VSVind expressing influenza haemagglutinin (HA) and measles virus hemagglutinin has been shown to confer full protection to mice and rats against lethal challenges (358-360). A similar vaccine developed using the

Ebola virus (Zaire strain) envelope (rVSV-ZEBOV) was able to induce a neutralising response against the wt virus and demonstrated high levels of protection during the 2016 Guinea and 2017 Congo outbreaks (361-364). To date numerous recombinant VSVind-based vaccines have been reported against antigens from HIV-1, influenza, hepatitis C, and measles virus (360, 365-368).

1.7.Immunity

Infection of immunocompetent hosts by viruses or viral vectors triggers both innate and adaptive branches of the immune system. The innate immune response mainly controlled by the activation of type I interferon responses while adaptive immune response is responsible for production of specific antibodies and governing cytotoxic T cell activation (338). While the adaptive, both humoral and cellular, immune response will develop memory of antigens encountered, innate immunity mainly functions as a non-specific defence system. Sophisticated networks of intracellular sensors evolved by the cells (e.g. protein kinase receptors, toll-like receptors, single-stranded RNA inducible genes) detect early viral infections and activate the immune response pathways (369-373).

1.7.1.Adaptive Immune Response

One of the immune system's major functions is the production of immunoglobulins (Igs) or antibodies which bind to and help eliminate any foreign material that might enter the body (374). Each antibody binds to a particular epitope or determinant. Although an antigen may have many epitopes that react with many different antibodies, an individual antibody binds to only one specific epitope. Antibody production plays an important role in controlling foreign infections, especially by viruses (375).

1.7.1.1.B Cells and Antibody Production

Antibodies are produced by B lymphocytes (B cells) in the body (374, 376). These cells are produced and mature in the bone marrow. B cell maturation serves as the basis for immunological diversity. To protect individuals against

pathogens, antibodies directed against more than 10^7 different antigens must be produced (377). This is achieved by genetic rearrangement in B cells via four different mechanisms: joining and rearrangement of variable region gene segments, somatic hypermutation of variable regions, class switch recombination of constant heavy regions, and gene conversion of variable genes. Rearranged variable regions are produced during B cell maturation while somatic hypermutation and class switch recombination are triggered by antigen recognition (378). Through all the variance and mutations, the production of antibodies directed at self-antigens is unavoidable. However, B cells recognising self-antigens get terminated preventing autoimmune reactions (379).

During infection or immunisation, antigens enter the bloodstream and are counteracted by the immune system's defensive response of antibody production. At the initial stages of infection, the higher number of antigens in the blood promote antibody production. After seroconversion, the period during which a specific antibody develops and becomes detectable in blood, the amounts of antibody and antigen in the blood equalise. Furthermore, the immune system preserves an immunological memory of the infection to aid in rapid detection and immunological protection against reinfection (377).

1.7.1.2.Antibody Structure

Antibodies are made up of two distinct parts: variable fragment (Fv) which recognises an epitope and the constant region (Fc) that grants effector functions such as antibody-dependent cell-mediated cytotoxicity and activation of the classical complement pathway (380). Each antibody contains two sets of light and heavy chains linked by disulphide bonds. While the light chain contains one variable and one constant region, the heavy chain is made up of one variable and three to four constant regions. There are five primary classes of Igs: IgG, IgM, IgA, IgD, and IgE (381). There are two key differences between the antibody classes: the amino acid sequences of the heavy chain constant regions and the number of subunits (382, 383).

Antibody production and secretion in the body follows B cell activation. Once secreted antibodies can contribute to the immune response through several

modes of action: they can block pathogen-receptor interactions hindering infection, neutralise toxins and viruses, activate the complement cascade via the classical pathway, interact with effector cells to trigger antibody dependent cell-mediated cytotoxicity (ADCC), and mediate phagocytosis of pathogens.

1.7.1.3.Humoral Immune Response

During maturation, B cells develop independently of antigens. However, mature B cells, with specific B-cell receptors formed of a CD79 signal transduction domain and antigen-recognising single isotype immunoglobulin domain (i.e. IgD, IgM, IgA, IgG, or IgE), continually move through secondary lymphoid organs searching for antigens. Once one is encountered, B cells act as antigen presenting cells triggering a humoral response. B cell binds to the antigen which leads to its subsequent endocytosis by the lymphocyte (384). The antigen is later processed in the B cell and is presented on the cell surface bound to the groove of the major histocompatibility complex (MHC). The presentation of these antigens recruits helper T lymphocytes which bind to the antigen-expressing B cells. The cytokines secreted by the helper T cell drive B cell proliferation and maturation into antibody-producing plasma cells. This is essential for the development of B cell memory (385, 386). Released into the blood by mature B cells, antibodies lock onto matching antigens forming antibody-antigen complexes. These are later cleared by the complement cascade or by the liver and the spleen.

In the case of “original antigenic sin,” a concept first proposed by Thomas Francis in 1960s, the production of the aforementioned neutralising antibodies is not always as effective (375). The concept implies that when the epitope present on an antigen varies slightly in the case of a secondary infection, then the immune system relies on memory of the earlier infection rather than mounting another primary immunological response which would allow faster and stronger response. This usually results in an inadequate immunological response towards the new strain and in some cases, such as the dengue virus and human immunodeficiency virus (HIV) infection, result in antibody-dependent enhancement (ADE) (387, 388). In the case of ADE cross-reactive antibodies against the new strain are unable to neutralise the new virus fully.

Therefore, binding of such antibodies triggers internalisation of the virus by macrophages and dendritic cells involved in the complement cascade enhancing the virus entry and infection.

1.7.1.3.1.Antibody-mediated neutralisation of viruses

Antibodies (Abs) play numerous roles in clearance of viruses from organisms. The synergistic effects of both neutralising and non-neutralising antibodies contribute greatly to both adaptive and innate immune responses (389, 390). The significance of antibody-mediated immunity has been well-established in the literature through protection by passive immunisation studies utilising immunodeficient animals (391, 392).

The interactions between antibody paratope (i.e. antigen binding site) and antigen epitopes (i.e. immunogenic determinants on viruses, usually on envelope proteins which are recognised by antibodies) dictate antibody-virus binding and is required to achieve neutralisation. During a humoral antibody response, B cells that express Abs with the highest affinity directed towards the virus grow through clonal expansion (393-396). While these Abs usually demonstrate the most potent neutralising activity (397-399), other Abs with lower affinities or non-specific interactions can be involved in so-called “hit-and-run” neutralisation (400). These Abs dissociate after inducing conformational changes in the viral envelopes which may affect their infectivity (390).

Therefore, the coating of viruses by Abs is thought to be required for an efficient block of infection. Several mechanisms of neutralisation have been described in the prevention of different viruses from infecting cells. Most neutralising antibodies (nAbs) hinder interactions between the viral envelopes and their respective receptors (401). This block can be through either direct competition by nAb binding to receptor recognition epitope or in some cases through steric hindrance (e.g. mouse mammary virus) (402-404). Another mechanism that prevents viral attachment to cells is Ab-mediated aggregation or cross-linking of viral particles (405, 406). However, in such cases complete neutralisation or protection might not be observed as aggregated viral particles can still infect cells, albeit a lower number of cells. Alternatively, Abs can

interfere with post-attachment interactions between viruses and receptors or co-receptors blocking or reducing internalisation of the virions (e.g. some antibodies against influenza virus) (407-409). Lastly, there are several post-endocytosis mechanisms identified: interference with fusion in endosomal vesicles and with uncoating of the virus, and inhibition of initial metabolic steps (389, 394-396, 401, 404, 408, 410-414).

All in all, the task of viral infection blocking, dictated by antibody binding, comprises intricate mechanisms to achieve potent protection. While *in vitro* assays will select for nAbs with highest affinities and dominant neutralisation mechanisms directed towards viral attachment and early infection functions, a potent humoral response would likely to be multi-hit exploiting several mechanisms at the same time through concerted efforts of several nAbs (389, 390, 401).

1.7.1.4.T Cell-Mediated Immunity

T cell-mediated immunity comprises the second branch of the adaptive immune response (415). It involves recognition and clearance of pathogens or pathogen-infected cells (416). The two major types of T cells, CD4+ helper and CD8+ cytotoxic, originate from the bone marrow progenitors and mature in the thymus (417).

The immune response commences when naïve T cells encounter antigen presenting cells (e.g. dendritic cells, macrophages) expressing antigens and co-stimulatory molecules. This leads to differentiation of T cells into effector cells, production of cytokines and chemokines as well as further activation of macrophages and natural killer cells (415, 418). While CD8+ cytotoxic T cells are able to induce apoptosis of viruses, pathogens, and infected cells (419-421), CD4+ helper cells are involved in the secondary signalling pathways to induce a potent antibody-based response as well as producing cytokines (422-424). The concerted efforts of these effector T cells mediate infection clearance (425, 426). These specialised subsets of T cells target viral proteins and antigens that are more likely to be conserved amongst different subtypes and pathogens, in contrast to epitope-specific antibody-dependent immunity, therefore, conferring broader protection (422, 427).

1.7.2.Innate Immune Response

Innate immune responses against viruses depend on innate pattern-recognition receptors of organisms (428-430). These receptors are key sensors which recognise conserved microbial motifs called pathogen associated molecular patterns (PAMPs) (431-435). These motifs, including genomic materials such as genomic DNA, single-stranded or double-stranded RNA and surface proteins, are in most cases essential for the survival of the pathogen and hence cannot be modified for immune evasion.

Toll-like receptors (TLRs), an evolutionarily conserved family of type I membrane glycoproteins, are the major pattern-recognition receptors utilised by the innate immune cells including macrophages, dendritic cells, B cells, and T cells. They are expressed constitutively in these cells regardless of function, immunological memory, and life-cycle stage (373, 436). However, the levels of expression are not static and can be modulated effectively in response to a recognised pathogen, cytokine signalling or inflammatory stress (431, 437).

Amongst the TLR family members, TLR2 and TLR4, expressed on the extracellular cell surface, are involved in viral glycoprotein recognition (432, 438). On the other hand, TLR3, 7, 8, and 9, almost exclusively expressed in intracellular compartments of the immune cells, recognise viral genomic materials. Regardless of which PAMP is recognised, TLR activation leads to type I interferon production. This robust antiviral response activates other cells through autocrine or endocrine signalling pathways (439-441).

Especially secretion of type I interferon is key to modulation of both innate and subsequent adaptive immune responses (442, 443). It induces dendritic cell maturation which leads to antigen presentation to T cells via MHCs, further cytokine secretion and triggering of adaptive immune responses. Dendritic cells are also involved in the secretion of chemokines that mediate both CD8+ and CD4+ T cell activation as well as recruitment of other phagocytic cells (442).

In return, pathogens, especially viruses have evolved strategies to circumvent this response. Most common ones include inhibition of type I interferon

response, prevention of antigen presentation to immune cells, and blocking of cell death induction (444-450).

1.7.2.1.Complement-Mediated Immunity

The complement cascade is an essential part of the innate immunity and is a major effector mechanism of humoral immunity (451-453). The cascade is made up of more than thirty proteins produced mainly by hepatocytes, macrophages, and gastrointestinal epithelial cells. The proteins in the cascade interact with each other regulating activation enzymatically. The cascade can follow three different pathways, the classical, alternative, and the lectin route. All three pathways result in the formation of the membrane attack complex (MAC) which induces lysis of many types of cells (454).

The classical pathway is triggered by antibody binding to antigens. This results in a conformational change in the constant region of the antibody exposing the complement binding site. Complement component C1 recognises this site and upon binding goes through conformational changes and enzyme activations which in return magnify its signal (455).

The alternative pathway functions though antibody-independent mechanisms. This pathway can proceed on many microbial surfaces and leads to the generation of distinct C3 convertase. It is initiated by hydrolysis of C3 into C3b. A number of mechanisms ensure that when C3b binds to host cells, complement-regulatory proteins stop complement activation (456, 457).

Lastly, the lectin pathway uses a protein very similar to C1 to trigger the cascade. Mannose-binding lectin (MBL) recognises structural patterns and interacts with mannose residues and some other specific sugars on the pathogen surface. Through this binding MBL initiates the immune response (455, 458).

1.7.2.1.1.Complement-mediated inactivation of viruses and viral vectors

Oncolytic therapy utilising viruses like VSVind has yielded promising results in the treatment of a variety of cancers (459-465). However, neutralisation of these viruses by nonimmune sera can potentially block the viral infection and

diminish the efficacy of the systemic therapy. This also applies to viral vectors pseudotyped with envelopes from such viruses. Serum inactivation poses a major concern in the development of these vectors for *in vivo* gene therapy (466).

Wild-type VSVind and VSVind.G pseudotyped viral vectors have been shown to be sensitive to neutralisation by fresh human, mouse, and dog sera (266, 466-470). This anti-VSV activity is mediated by serum IgM and the complement components, mainly C1q (467). Furthermore, presence of the galactosyl(α1-3)galactosyl (αGal) epitope on these oncoviruses, when they are produced by cell lines expressing the sugar, was found to make them less stable in human serum as well as more vulnerable to complement killing via natural anti-αGal antibodies (470).

One way to circumvent these problems is to pseudotype vectors with serum-resistant envelopes. Glycoproteins of some members of the vesiculovirus family, COCV, MARAV, and PIRYV, unlike VSVind, have been reported to be resistant to complement-mediated neutralisation by human serum (200, 467, 471). Therefore, there have been attempts to adapt these viral envelopes in vector systems as well as to produce recombinant chimeric VSVind G proteins (202, 467). Another strategy that has been fruitful is the synthetic modification of the envelope. Specifically, poly-ethylene glycosylation (PEGylation) of a VSVind.G pseudotyped HIV-1-based virus vectors has shown to protect the vectors from complement-mediated inactivation by human and mouse sera while not affecting transduction efficiency *in vitro* (466). Developing oncolytic viruses or vectors with envelopes that can resist serum inactivation may provide the opportunity for systemic administration. Furthermore, it also could aid in lowering the dose necessary to achieve therapeutic levels of gene expression and, therefore, minimising the vector or virus-associated toxicity.

1.7.3.Immune Responses Against *in vivo* Oncolytic Virotherapy and Gene Therapies

Rhabdoviruses such as VSVind and MARAV have been developed into promising oncolytic and vaccine vectors, and their clinical evaluation is

underway (356, 472-476). Their efficacy in the treatment of a variety of human cancers has been validated preclinically (459-465). VSVind is a preferred candidate for oncolytic virus development due to its broad tropism, short replication cycle, and high sensitivity to interferon-mediated antiviral activity (341, 356, 477-482).

However, the primary immune response elicited following administration of VSVind leads to the production of neutralising antibodies which limit multiple rounds of administration (483). In contrast, some other viruses such as lymphocytic choriomeningitis virus and arenavirus, are not as immunogenic and do not generate a robustly-neutralising antibody response (484).

Previous reports claim that VSVind is neutralised by several mammalian sera (see section 1.7.2.1.1) (468-470). The complement system not only acts as the first line of defence towards these viruses but also aids the adaptive branch of the immune system (485). The neutralising activities of antibodies against viral epitopes are enhanced by the complement (486, 487).

Furthermore, in the case of gene therapies innate and adaptive immune responses against viral-vector derived antigens limit the efficacy of LVs as well as affect the longevity and therapeutic effectivity of the transgene expression (488). Therefore, so far while *ex vivo* gene therapies utilising LVs have been successful in the clinic, *in vivo* administration of LVs is still in its preclinical stage (489). Historically it has been shown that systemic LV administration induce inflammatory responses which include the rapid production of cytokines such as interleukin-1 (IL-1), IL-6, tumour necrosis factor α (TNFα), and type I interferons (IFNα and IFNβ) (490). Furthermore, efficient transduction of antigen-presenting cells by LVs prime the adaptive branch of the immune system and activate T cell responses (435). Induction of a potent CTL response following systemic administration of LVs pseudotyped with glycoproteins from Ebola virus, lymphocytic choriomeningitis virus, Mokolo virus, and VSVind has led to a robust anti-transgene response resulting in clearance of transduced cells from the organism (491, 492). Although this ability to generate CTL responses via LV administration has been exploited to generate antitumour immunity or achieve a robust immune response through

vaccine vectors (493-495), this is a major concern in achieving sustained transgene expression in gene therapies.

In addition, induction of cell-mediated immunity also primes B cells to produce high-affinity antibodies against vector components via helper T cell-dependent pathways (489, 496). Thus far, production of strongly neutralising antibodies directed towards matrix and capsid proteins of LVs (i.e. p17 and p24 respectively) has been observed (496-501). Although these antibodies did not affect sustained transgene expression, they limited the efficacy of a subsequent administration of the same vector (497). Generation of high-affinity antibodies directed towards the envelope glycoproteins of LVs is postulated to be as problematic, but, this remains to be fully explored in preclinical models (488).

Currently, extensive research is underway developing more tolerogenic vectors to either avoid or override the innate immune response pathways (488, 502). In addition, better understanding both the humoral and T cell-mediated immunity against the systemic administration of LVs will enable personalisation of therapies as well as dampening the anti-vector and anti-transgene effects ensuring longevity of the vectors and transduced cells in the organism for successful gene therapies.

1.8.Rationale

VSVind.G confers broad tropism and efficient cellular uptake. In combination with the low seroprevalence of neutralising anti-VSVind.G antibodies in humans, VSVind.G psudotyped recombinant viruses and viral vectors have substantial potential as *in vivo* gene delivery systems. Similarly, vesiculovirus research is expanding expeditiously following their adaptation to oncolytic virotherapy and gene therapy research. Despite this there exists a gap in knowledge regarding the antigenic and immunogenic characteristics of vesiculovirus glycoproteins. Identification of well-characterised antibodies as well as strongly neutralising epitopes on glycoprotein bring substantial utility to the development of G protein containing advanced therapy medicinal products.

Lentiviral vectors are a particularly promising group of ATMPs as they can transduce non-dividing cells efficiently and enable transgene integration leading to stable expression. Their use in cellular therapies and gene editing approaches are paving the way for novel curative treatments for a variety of hereditary and acquired diseases. However, this untapped potential cannot be fully exploited due to the induction of humoral and cell mediated immune responses *in vivo* limiting the scope and efficacy of therapies. Therefore, a detailed investigation of the characteristics of such responses as well as the generation of a proof-of-principle method to circumvent them will have significant implications for the potentials of cancer immunotherapy and gene therapy. In addition, it will allow for the development of improved therapies tailored for every individual to achieve sustained therapeutic effects.

1.9. Aims of Thesis

In this thesis, research exploring antigenic and immunogenic characteristic of six vesiculovirus G proteins was undertaken.

In the first part of the thesis (Chapter 3), I have attempted to identify a commercially available reagent which will be valuable for vesiculovirus and VesG-based gene therapy research. I characterised the interactions of two commercially available monoclonal anti-VSVind.G antibodies with other vesiculovirus G proteins. This work comprised the identification of their binding epitopes, examining the strength of cross-neutralisation of VesG-LV, and investigation of their neutralisation mechanisms.

In the final part of the thesis, the innate and adaptive immune responses elicited against VesG were examined. In Chapter 4, I aimed to deduce the sensitivity of VesG to complement-mediated inactivation by fresh mammalian sera. Further work was conducted with the intention of identifying the region(s) on the G proteins that conferred resistance or sensitivity. This work was expanded in Chapter 5, where the primary immune response elicited following systemic administration of LVs and methods to avoid it were studied. As a proof-of-principle for a repeated LV administration approach in clinical gene therapy and oncolytic virotherapy applications, I was able to demonstrate that

inhibitory effects of pre-existing anti-envelope immunity could be circumvented via the use of a heterogeneous panel of pseudotypes enabling systemic re-administration of LVs.

2 Materials and Methods

All buffer recipes and primer sequences are listed in an appendix at the end of this chapter.

2.1.Cell Culture

In all experiments, human embryonic kidney (HEK) 293T cells were used. HEK293T cells are a derivative of HEK293 cells that were originally isolated from an aborted human embryo in 1973 (503). In contrast to HEK293 cells, HEK293T cells express the large SV40 T antigen which allows them to be transfected with high efficiencies and grow in much higher rate than their parental cell line (504). These characteristics make HEK293T cells a good candidate for LV production (505).

The cell line was maintained in Dulbecco's Modified Eagle Medium (DMEM) (Sigma-Aldrich, St Louis, MO) supplemented with 10% heat-inactivated Foetal Calf Serum (Gibco, Carlsbad, CA), 2mM L-Glutamine (Gibco), 100 units/ml

Penicillin (Gibco), 100µg/ml Streptomycin (Gibco). All cells were kept in cell culture incubators at 37ºC and 5% CO_2.

2.2.Gene Transfer to Mammalian Cells

2.2.1.Transfection of Cells for G Protein Expression

Single plasmid transfection was used to express VesG on HEK293T cell surface. HEK293T cells were seeded on the day prior to transfection at $4x10^6$ cell per 10cm plate density. These cells were transfected by lipofection using FuGENE6 (Promega, Madison, WI). First, 5µg/plate of G protein-encoding plasmid was mixed with 10µl/plate of dH_2O. The mixture was then added to a solution of OptiMEM (Gibco) (85µl/plate) and FuGENE6 (1:5 µg of DNA: µl of FuGENE6), incubated at room temperature for 20 minutes and then added dropwise to each 10cm plate of HEK293T cells (the medium was changed with fresh DMEM just before the addition of DNA/OptiMEM/FuGENE6). The details of the plasmids used are in section 2.3.1.7. The cells were harvested 48h later to be used in various flow cytometry assays.

2.2.2.Transient Lentiviral Vector Production and Concentration

Three-plasmid co-transfection into HEK293T cells was used to make pseudotyped LV as described previously (155). Briefly, $2x10^7$ HEK293T cells were seeded in 15cm plates. 24 hours later, they were transfected using FuGene6 (Promega, Madison, WI) with following plasmids: 3.75µg of SIN pHV.GFP (green fluorescent protein (GFP) expressing vector plasmid (198, 506)) or pCCL.FLuc.2A.eGFP (firefly luciferease and enhanced GFP expressing vector plasmid (507)), 2.5 µg of p8.91 (Gag-Pol and Rev expression plasmid (508)), and 2.5 µg of envelope expression plasmids (see *Table 2-2)*. 4h after transfection the medium was changed to OptiMEM supplemented with 2mM L-Glutamine, 100 units/ml Penicillin, and 100µg/ml Streptomycin. Vector containing media (VCM) was collected 48h and 72h after transfection, passed through Whatman Puradisc 0.45µm cellulose acetate filters (SLS, UK) and concentrated ~100-fold by ultra-centrifugation at 22,000

rpm (87,119xg) for 2 hours at 4ºC in Beckmann Optima LK-90 ultracentrifuge using the SW-28 swinging bucket rotor (radius 16.1cm). The virus was resuspended in cold plain OptiMEM on ice, aliquoted, and stored at -80ºC.

2.3.Plasmid Cloning

2.3.1.Transformation, Amplification, and Purification

2.3.1.1.Transformation of Bacterial Cells with Plasmid DNA

2.3.1.1.1.Transformation of competent cells with plasmid DNA

5-alpha high-efficiency competent *Escherichia coli* (NEB, Ipswich, MA) were thawed on ice for 10min. 2µl of 100ng of plasmid or 50ng of ligation mix (see section 2.3.1.6) was added to 50µl of competent cells, incubated on ice for 30min and heat shocked at 42ºC for precisely 30sec. The heat-shocked cells were then placed on ice for a further 5min before addition of 950µl of SOC (super optimal broth with catabolite repression) medium (provided by the manufacturer). The cells were then incubated in a shaker at 250rpm at 37ºC for ~1 hour. In the transformation of bacteria with a ligation mix 250µl (of SOC and transformed bacteria) was spread onto an agar plate containing 100µg/ml ampicillin (Sigma-Aldrich). In the transformation of plasmid DNA for large-scale harvest (see section 2.3.1.3.2) 100µl (of SOC and transformed bacteria) was spread onto an agar plate containing 100µg/ml ampicillin (Sigma-Aldrich).

2.3.1.1.2.Transformation of XL10-Gold ultracompetent cells with mutant plasmid DNA

XL10-Gold ultracompetent cells (Agilent, Santa Clara, CA) were transformed with the mutated plasmid DNA produced via site-directed mutagenesis method (see section 2.4.2.). The cells were gently thawed on ice and aliquoted a volume of 45µl to prechilled 15ml BD Falcon polypropylene round-bottom tubes. Then, 2µl of β-mercaptoethanol (provided by the manufacturer) was added to the cells followed by 10min incubation on ice. After, 2µl of mutagenesis reaction mix was added to the cell-β-mercaptoethanol mixture, incubated on ice for 30min and heat shocked at 42ºC for precisely 30sec in a

water bath. The heat-shocked cells were then placed on ice for a further 2min before addition of 500µl of NZY$^+$ broth (see Appendix). The cells were then incubated in a shaker at 250rpm at 37ºC for ~1 hour. After the incubation 250µl (of NZY$^+$ and transformed bacteria) was spread onto an agar plate containing 100µg/ml ampicillin (Sigma-Aldrich).

2.3.1.2.PCR Colony Screening

Polymerase chain reaction (PCR) was used to screen antibiotic resistant colonies for the correct constructs. GoTaq HotStart Green Master Mix (Promega) was prepared in a final volume of 25µl per reaction. Colonies were picked with a pipette tip, streaked on an agar plate containing 100µg/ml ampicillin (Sigma-Aldrich), and then transferred to PCR mastermix. PCR cycling conditions were 98ºC, 5min; 30 cycles (98ºC, 30sec; X ºC, 30sec; 72ºC, 30sec/kb of insert); 72ºC, 7min. The annealing temperature, denoted as X ºC, was set as the lowest melting temperature of the primer pair used in the PCR. Melting temperatures were calculated using the NEB T_m Calculator: (http://tmcalculator.neb.com/#!/).

Table 2-1: PCR Master Mix for Colony Screens.

Reagent	Amount per reaction (µl)
GoTaq Hot Start Green Master Mix, (2X)	12.5
Primer Forward, 10µM	2.5
Primer Reverse, 10µM	2.5
DNA template, 100ng	1
Nuclease-free Water	To a final volume of 25µl

2.3.1.3.Preparation of Plasmid DNA

2.3.1.3.1.General method for small-scale plasmid amplification

For each small-scale plasmid amplification (mini-prep), a single bacterial colony was picked from an agar plate and transferred to 5ml LB Broth with

100µg/ml ampicillin (Sigma-Aldrich) and grown overnight at 37ºC, shaking at 250rpm.

All plasmids were purified from bacterial cultures using the QIAprep spin miniprep kit (Qiagen, Germany). Overnight LB cultures were pelleted by centrifugation at 4000rpm (3452xg) for 30min. The bacteria were then resuspended in Buffer P1 and exposed to a high pH detergent by the addition of Buffer P2 which leads to denaturing of plasmid and genomic DNA, as well as proteins. The alkaline conditions caused by the buffer completely disrupt the base pairing, but the closed circular structure of the plasmids ensures that the two strands of complementary DNA do not separate in the short duration of exposure. By adding Buffer N3 the lysate was neutralised, leaving the plasmid DNA in the supernatant, which later was purified via anion-exchange chromatography. After elution of the plasmid DNA from the exchange resin via Buffer EB, DNA concentrations were determined using a NanoDrop (Spectrophotometer, ND-1000).

2.3.1.3.2.Large-scale plasmid harvest

For large scale plasmid harvest, a single bacterial colony was picked from an agar plate and transferred to 100ml LB Broth with 100µg/ml ampicillin (Sigma-Aldrich) and grown overnight at 37ºC, shaking at 250rpm. After overnight incubation, the cells were pelleted by centrifugation at 4000rpm (3452xg) for 30min. All plasmids were purified from bacterial cultures using QIAprep midiprep kit (Qiagen, Germany) in a similar manner as described in the previous section. The detailed protocol can be found at:

https://www.qiagen.com/us/resources/download.aspx?id=c164c4ce-3d6a-4d18-91c4-f5763b6d4283&lang=en.

2.3.1.4.Restriction Endonuclease Enzyme Digests

Several restriction endonuclease enzymes were used, all obtained from New England Biolabs. In a typical reaction, up to 2µg of plasmid DNA was digested with 5 units of enzyme/µg DNA, 1X of the CutSmart Buffer provided by the manufacturer and nuclease-free water (Qiagen) made up to a final reaction

volume of 50µl. The reaction mix was incubated at 37ºC for 30-60min and digestion was stopped with the DNA loading dye provided by the manufacturer.

2.3.1.5.DNA Dephosphorylation Reactions

Shrimp alkaline phosphatase (NEB) was used according to manufacturer's instructions to dephosphorylate the 5' end of DNA backbone before ligation reactions. In a sample reaction, ~1µg of DNA was mixed with 2µl of 10X CutSmart Buffer (provided by the manufacturer), 1µl of 1,000 units/ml shrimp alkaline phosphatase, and nuclease-free water to a final volume of 20µl. The mixture was incubated at 37ºC for 30min and reaction was later stopped by incubation at 65ºC for 5min. DNA concentration was measured via a NanoDrop (Spectrophotometer, ND-1000) and the dephosphorylated backbone was used in ligation reactions without any further purifications.

2.3.1.6.DNA Ligation Reactions

Ligations of DNA were used to clone new plasmids. T4 DNA ligase (NEB) was used in all reactions. In a typical reaction, 50ng of backbone DNA was used, with a 1:3 molar ratio of backbone to insert DNA in a final concentration of 1X ligase buffer (provided by the manufacturer) made up to a final volume of 20µl with nuclease-free water (Qiagen). The reaction was incubated at room temperature for 4 hours and chilled on ice until bacterial transformation or stored at -20ºC.

2.3.1.7.Plasmid Details

All VesG envelopes were cloned into the high-expression plasmid backbone pMD2, driven by a CMV promoter (*Figure 2-1).* Amino acid sequences for VSVnj.G (UniProt Accession Number: P04882), PIRYV.G (UniProt Accession Number: Q85213), MARAV.G (UniProt Accession Number: F8SPF4), VSVala.G (UniProt Accession Number: B3FRL4) were retrieved from UniProt. Codon-optimised genes were ordered from Genewiz (South Plainfield, NJ) and subcloned into the backbone following previously described methods.

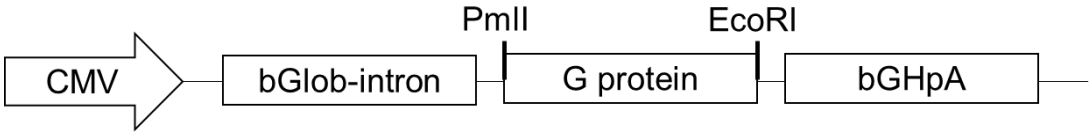

Figure 2-1: Configuration of G-protein Expressing Plasmids. The expression is driven by a human cytomegalovirus (CMV) promoter. The G-protein is flanked by an upstream bovine beta-globin intron and a downstream bovine growth hormone poly-A site. The restriction endonuclease enzyme sites used for subcloning are marked.

The list of all plasmids used is summarised in *Table 2-2.*

Table 2-2: Summary of Plasmids Used. Where the details of plasmids are published reference is given, otherwise the name of the person who provided the plasmid is given. "Self-made" plasmids are produced by me using the PCR, digestion, and ligation protocols described.

Plasmid	Source	Type of Vector
pMD.VSVind.G (pMD.G)	Plasmid Factory (Germany) (146)	G protein expression plasmids
pMD2.COCV.G	Kiem Group (202)	
pMD2.VSVnj.G	Self-made	
pMD2.PIRYV.G	Self-made	
pMD2.MARAV.G	Self-made	
pMD2.VSVala.G	Self-made	
pRDpro-LF	Khaled Sanber (Collins/Takeuchi Group) (198)	
pMD2.1A-4A &1B-4B.G[1]	Self-made; chimeric G proteins originally produced by Maha Tijani (Collins/Takeuchi group)	Chimeric G protein expression plasmids
pMD2.Cocal-mutants&	Self-made (see section 2.4.2)	Mutant G protein expression plasmids

pMD.VSVind-mutants (Total 22) [1]		
pMD2.Ind1-3&COCV1-3	Self-made (see section 2.4.2)	Chimeric G protein expression plasmids for complement sensitivity experiments
p8.91	Plasmid Factory (Germany) (146)	*Gag-pol* and *rev* expression plasmid
pCCL.FLuc.2A.eGFP	Waddington Group (507)	Lentiviral vector with SIN LTR
SIN pHV.GFP	Sean B. Knight (Collins/Takeuchi Group) (506)	Lentiviral vector with SIN LTR

[1]The plasmids are named after the individual chimeric G-proteins and mutants which can be found in section 3.3.3.

2.4.Polymerase Chain Reaction (PCR)

PCR was used for various purposes. For plasmid cloning, Phusion DNA polymerase (NEB) was used. For the generation of mutant G proteins, PfuUltra DNA polymerase (Agilent) and for diagnostic purposes, GoTaq polymerase (Promega) was used (see section 2.3.1.2).

2.4.1.PCR Method

Phusion High-Fidelity PCR Kit (NEB) was used to perform the PCR reactions. Phusion polymerase was provided in an inactive form, requiring incubation at 98ºC for 5min before the enzyme became active. Hence, at room temperature, the enzyme was not active and did not exert any endonuclease activity that would cause primer degradation enabling reaction set up at room temperature. All primers used were obtained from Sigma-Aldrich. A typical PCR reaction was set up with a final reaction volume of 50µl (*Table 2-3)*. The reactions were carried out in a PCR thermal cycler (Applied Biosystems, GenAmp PCR

system 2700) with settings shown in *Table 2-4.* XºC which denotes the annealing temperature was determined as previously explained.

Table 2-3: PCR Composition for Phusion.

Reagent	Amount per reaction (µl)
5X Phusion HF/GC Buffer	10
Primer Forward, 10µM	2.5
Primer Reverse, 10µM	2.5
DNA template, 100ng	1
dNTPs, 10mM	1
Phusion DNA polymerase (1 unit/50µl reaction)	0.5
Nuclease-free Water	To a final volume of 50µl

Table 2-4: Cycling Conditions for Phusion PCR.

Step	Temperature (ºC)	Time
1	98	5min
2	98	30sec
3	X	30sec
4	72	1min/kb
Repeat steps 2-4, 35 times		
5	72	7min

2.4.2.Site-Directed Mutagenesis (SDM) PCR for Mutant G Production

Site-directed mutagenesis (SDM) method was utilised to produce G protein mutants that were used in epitope mapping experiments. For this, Agilent QuikChange II XL Site-Directed Mutagenesis Kit was used.

Initially, primers that would have the desired nucleotide changes were designed using the QuikChange Primer Design Tool (http://www.genomics.agilent.com/primerDesignProgram.jsp). All primers used were obtained from Sigma-Aldrich.

In a typical SDM reaction, double-stranded DNA (dsDNA) template plasmid was mixed with the forward and reverse primers of the desired mutation, the reaction buffer, dNTP mix, QuikSolution (provided by the manufacturer) and dH_2O to a final volume of 50µl (*Table 2-5).* The reaction setup was completed by adding 1µl of PfuUltra High-Fidelity DNA Polymerase (2.5 units/µl) (provided by the manufacturer).

Table 2-5: Reaction Setup of SDM PCR.

Reagent	Amount per reaction (µl)
10X Reaction Buffer	5
Primer Forward, 125ng	X[1]
Primer Reverse, 125ng	X[1]
DNA template, 10ng	X[1]
dNTP mix	1
QuikSolution	3
Nuclease-free Water	To a final volume of 50µl

[1]X represents the volume of the reagent that equates to the indicated mass.

Each reaction was then carried out using a PCR thermal cycler (Applied Biosystems, GenAmp PCR system 2700) using the cycling parameters outlined in *Table 2-6.*

Table 2-6: Cycling Conditions for SDM PCR.

Step	Temperature (ºC)	Time
1	95	1min
2	95	50sec
3	60	50sec
4	68	1min/kb of plasmid length
Repeat steps 2-4, 18 times		
5	68	7min

Following the PCR step of the mutagenesis reaction, the tubes were placed on ice for 2 minutes to cool the reaction below 37ºC. The amplified mutant and original template dsDNA mix was then digested by directly adding 1µl of DpnI (10 Units/µl) (provided by the manufacturer) restriction endonuclease to each amplification reaction and incubation at 37ºC for 1 hour. This allowed the digestion of the parental, nonmutated supercoiled dsDNA to be digested by DpnI which cuts *dam* methylated DNA. Mutant DNA was then transformed into ultracompetent cells as described in section 2.3.1.1.2.

2.5. Agarose Gel Electrophoresis

Agarose gel electrophoresis was used to separate DNA of different sizes, to analyse PCR products, and to separate digested plasmid DNA fragments in cloning.

2.5.1. Agarose Gels

Agarose gels of 1% were made by dissolving agarose (Sigma-Aldrich) in buffer Tris/Borate/EDTA (TBE). For the 1% gel, 1g of agarose was added to 100ml of TBE, placed in a 950W microwave oven (Proline, UK) on high setting for 2 min, manually shaking approximately every 30sec. Once agarose was dissolved, it was cooled before adding 0.1µl/ml SyberSafe DNA gel stain (Invitrogen, Carlsbad, CA). Gels were set in various casting trays with various sizes of combs depending on need and were left to set at room temperature for 45-60min.

2.5.2. Electrophoresis

To separate DNA fragments, the agarose gel, set in the gel tray was placed in an electrophoresis tank, with the line of wells closest to (parallel to) the cathode. A 1kb GeneRuler DNA Ladder (Thermo-Fisher Scientific, UK) was added to 1 well and DNA samples (containing DNA loading dye (Thermo-Fisher Scientific)) were added to the other wells. The gels were run using constant voltage of 100V for 90min. The gel was then placed on a UV transilluminator (UVP, UK) to visualise the DNA bands, following which a photo was taken. If necessary bands were extracted using a scalpel (Swann-Morton, UK).

2.5.3. Extraction of DNA from Agarose Gel Fragments

DNA was extracted from gel fragments cut out after electrophoresis using QIAquick gel extraction kit (Qiagen), according to the manufacturer's guidelines. In summary, the gel fragments were dissolved in Buffer QG, centrifuged through an anion exchange resin to which DNA binds in acidic conditions. After washing with Buffer PE, DNA was eluted with Buffer EB (high pH).

2.6.Flow Cytometry

Flow cytometry analysis was used to determine the G protein expression on the plasma cell membrane and the existence of GFP or eGFP to titrate lentiviral vectors and check for infection in various assays.

2.6.1.Single Population Live Cell Gating and Single Cell Analysis

Flow cytometry analysis was done using fluorescence-activated cell sorting (FACS), a specialised type of flow cytometry in which cells are carried by a liquid flow in a way so that they pass through laser light beams one cell at a time for sensing. Then a detector measures the forward-scattered light (FSC) and side scattered light (SSC), as well as dye-specific fluorescence signals. FSC is proportional to the cell size while SSC is a measure of cell granularity. All flow cytometry experiments were carried out using FACSCanto II (BD Biosciences, San Jose, CA) machine and FACS Diva analysis software (BD Biosciences).

To analyse the data, FlowJo single cell analysis software (BD Biosciences) was utilised. First, the negative control cells, HEK293T cells, were gated for single cell population based on FSC and SSC data to eliminate any dead cells and debris. These gated cells represent the working population, “live cells,” for the assay analysis. To eliminate any unspecific antibody binding or background GFP expression levels (measured by fluorescein isothiocyanate (FITC) signal), these negative control cells were gated with regards to their single fluorescence signal strengths. The samples were analysed to determine percentages of GFP positive cells, single parameter fluorescence histograms, and median fluorescence intensity values.

2.6.2.Infection Assays and Determining GFP Expression Levels

2.6.2.1.Titration of Lentiviral Vectors

The functional titre of each vector preparation was determined via flow cytometry analysis for GFP expression following transduction of HEK293T cells. This was quantified as transduction units (TU) per ml which represented a functional measure of the number of cells that can be transduced with a given volume of the viral vector. For this HEK293T cells were seeded in 12-well plates at $2x10^5$ cell/well density in 2ml of medium containing 8µg/ml polybrene (Merck-Millipore). Approximately 3-4 hours later, 5-fold serial dilutions of the vector preparations using plain OptiMEM (Gibco) were made and 200µl of each dilution for unconcentrated preparations and 50µl of each dilution for concentrated preparations was added to each well. 48 hours post-transduction cells were trypsinised and analysed via flow cytometry for GFP expression. Titres were calculated from virus dilutions with 1-30% GFP expression according to the following equation:

$$\text{Titre}\left(\frac{\text{TU}}{\text{ml}}\right) = \frac{(\text{no. of cells seeded}) \times (\%\ \text{of GFP+ve cells}) \times (\text{dilution factor})}{(\text{the volume of virus preparation added (ml)})}$$

2.6.2.2.Antibody Neutralisation Assay

To determine whether commercially available anti-VSVind.G antibodies and murine serum samples obtained in *in vivo* experiments neutralise VesG pseudotyped LVs an infection assay was performed. Briefly, HEK293T cells were seeded in a 96-well plate at a density of $2x10^4$ cells/well with 200µl of medium containing 8µg/ml polybrene. Approximately 3 hours later, antibodies/sera were serially diluted in plain OptiMEM to 12 different concentrations/dilutions ranging from 0.5mg/ml (1:2 dilution) to $1.6x10^{-7}$ mg/ml (1:6,250,000 dilution). 10µl of an LV dilution at $4.0x10^5$ TU/mL titre was mixed 1:1 v/v with each antibody dilution or plain OptiMEM, incubated at 37ºC for 1h, and plated on the cells. 48 hours after challenging the cells with the antibody-

LV mixes, cells were trypsinised and analysed for GFP expression by flow cytometry.

Measured GFP percentages were normalised for each VesG and denoted as "infection%" following the equation below:

$$\text{Infection\%} = \frac{\text{Titre of Antibody/Serum}-\text{LV mix added sample}}{\text{Titre of OptiMEM}-\text{LV mix added sample}} \times 100$$

In the *in vivo* studies titres were normalised to the infection rates measured after mixing the LVs with dilutions of sera obtained from PBS control mice.

The data obtained from the above analysis was plotted against antibody concentration/antiserum dilution using the graphing and statistics software GraphPad Prism 5. Furthermore, non-linear regression analysis was carried out using the same software to fit neutralisation ([inhibitor] vs. response) curves and calculate IC50 values.

2.6.2.3.Serum Sensitivity Assay

Approximately 3 hours prior to infection, HEK293T cells were seeded in 12-well plates at $2x10^5$ cell/well density in 2ml of complete medium containing 8µg/ml polybrene (Merck-Millipore). Later 2.5µl of VesG-LV at $1.6x10^7$ TU/ml titre were mixed with plain OptiMEM (Gibco), fresh mammalian sera (human [cat#: S1764], guinea pig [cat#:S1639] , rabbit [cat#:S7764], Sigma-Aldrich), mouse (cat#: IMS-C57BL6-COMPL, Patricell, Nottingham, UK), and heat-inactivated mammalian sera (at 56°C for 1h) 1:20 v/v, incubated at 37ºC for 1h, and plated on the cells. 48 hours later cells were harvested and analysed via flow cytometry for GFP expression. Relative infection rates for all samples within individual VesG-LV were calculated using the equation below:

$$\text{Infection\%} = \frac{\text{Titre of serum mixed sample}}{\text{Titre of plain OptiMEM mixed sample}} \times 100$$

2.6.3.Investigation of Antibody Binding

2.6.3.1.Fluorescence Quantification

All antibody binding assays were carried out using flow cytometry as described in section 2.6.1. Antibody binding was analysed using single parameter fluorescence histograms comparing sample stains to negative control cell stains. In order to calculate affinities of antibodies to different VesG and determine their relative expression levels on the plasma membrane quantitative fluorescence cytometry method was utilised.

2.6.3.1.1.Use of molecules of equivalent soluble fluorochrome (MESF) system

Quantum Alexa Fluor 647 MESF kit (Bangs Laboratories, Fishers, IN) was utilised for all quantitative fluorescence cytometry experiments. This is a microsphere kit that enables the standardisation of fluorescence intensity units. Beads with a pre-determined number of fluorophores are run on the same day and at the same fluorescence settings as stained cell samples to establish a calibration curve that relates the instrument channel values (i.e. median fluorescence intensity (MFI)) to standardised fluorescence intensity (MESF) units.

For this Alexa Fluor 647 labelled and blank microspheres were run on the same day and settings on FACSCanto II, each fluorescence peak was gated using the full width at half maximum gating and MFI values were calculated. Using QuickCal software (provided by the manufacturer, http://www.bangslabs.com/quickcal) the standard curve of MESF vs. MFI was drawn and detection threshold of the machine was calculated (*Figure 2-2)*. MESF values of all antibody stained cell samples were determined using this calibration curve and the software.

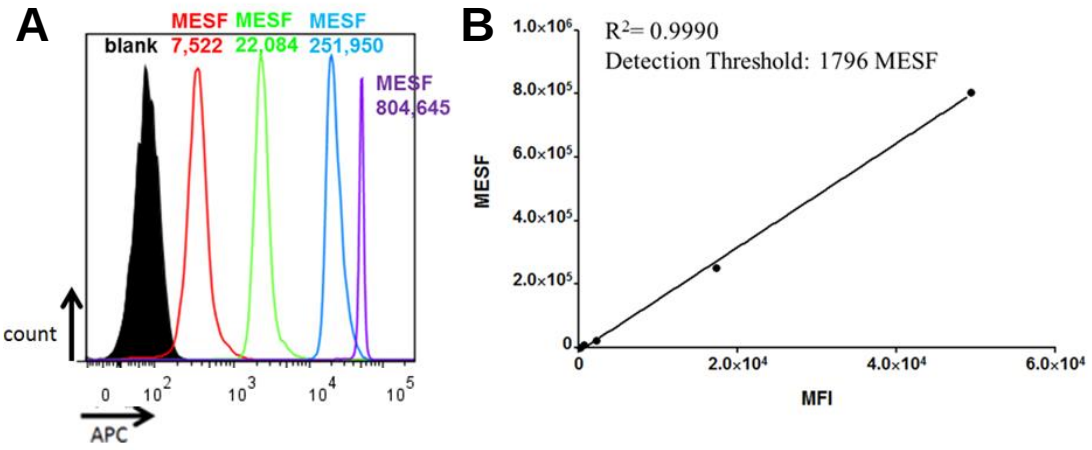

C

Bead Fluorophore Number	Median Fluorescence Intensity (MFI)
Blank (0)	193
7,522	653
22,084	2156
251,950	17300
804,654	49300

Figure 2-2: Standard Curve for Fluorescence Quantification. (A) Histograms showing the different fluorescence intensities of the control beads with specific numbers of fluorophores. Using these numbers summarised in the above table **(C),** QuikCal software (provided by the manufacturer) generated the standard curve used to relate MFI values to the number of fluorophores **(B).** This calculation also allowed the determination of the detection threshold of the FACSCanto II used in these experiments. This value was regarded as background or zero for the rest of the affinity assays.

2.6.3.2.Extracellular Antibody Binding Assay

HEK293T cells were transfected as described in section 2.2.1. 48 hours later cells were harvested, washed twice with phosphate-buffered saline (PBS) and plated in U-bottom 96-well plates at identical densities. Cells were then incubated with serial dilutions of extracellular antibodies ranging from 0.1mg/ml to $2x10^{-7}$ mg/ml in 1% bovine serum albumin (BSA) (Sigma-Aldrich) in PBS in a total reaction volume of 200µl for 30min at 4ºC (where a single dilution was used, it is indicated in the figure legends throughout the thesis). After washing twice with PBS (Sigma-Aldrich) to remove unbound antibodies, the cells were incubated for another 30min at 4ºC with their respective

fluorophore-conjugated secondary antibodies (detailed list of all antibodies used can be found in the appendix at the end of the chapter) in 1% BSA in PBS in total reaction volume of 200µl. Cells were then washed twice, fixed in 2% paraformaldehyde (PFA) in PBS, and analysed by flow cytometry.

2.6.3.3.Intracellular Antibody Binding Assay

HEK293T cells were transfected as described in section 2.2.1. 48 hours later cells were harvested, washed twice with PBS and plated in U-bottom 96-well plates at identical densities. Cells were then fixed for 20min at room temperature with 1% PFA (Sigma-Aldrich) in PBS and washed twice with PBS. Following this, cells were permeabilised by incubation at room temperature for 10min in 0.05% saponin (Sigma-Aldrich) in PBS, washed twice in PBS, and blocked with 1% BSA in PBS for 60min at room temperature. Blocked cells were then stained with 1:500 dilution of the anti-VSVind.G antibody P5D4 (Sigma-Aldrich) in 1% BSA in PBS for 60min at room temperature in a total reaction volume of 200µl. After washing with PBS twice to remove unbound antibodies, the cells were incubated with the respective secondary antibody in the same buffer composition for another hour at room temperature. Following two washes with PBS and resuspension in PBS, the stained cell samples were analysed via flow cytometry.

2.6.4.Infection Assay to Evaluate the Role of Low-density Lipoprotein Receptor (LDLR) in Lentiviral Entry

To determine whether the human LDLR plays a role in mediating infection of pseudotyped LVs, an infection assay was performed in the presence and absence of soluble recombinant LDLR (sLDLR). HEK293T cells were seeded at a density of $2x10^4$ cells/well in 96-well plates in 100µl of complete medium. 3 hours later these cells were incubated, for 30mins at 37ºC, with four different concentrations of sLDLR (0.05µg/ml, 0.5µg/ml, 1.5µg/ml, and 3µg/ml) (R&D Systems, Minneapolis, MN). The cells were then challenged with GFP encoding VesG or RDpro-pseudotyped LVs at two MOIs (0.1 or 0.5) in a total volume of 120µl. 48h later transduced cells were analysed for GFP expression by flow cytometry.

2.6.5.sLDLR Binding to G Protein Expressing Cells

Following transfection protocol detailed previously in section 2.2.1, cells were plated in U-bottom 96-well plates at equal densities. Cells were then either incubated with the extracellular polyclonal VSV-Poly (a kind gift from Dr Hiroo Hoshino, Gunma University, Japan (263, 509, 510)) or anti-RDpro antiserum (NCI, Rockville, MD) at 1:200 and 1:500 dilutions respectively following the protocol in section 2.6.3.2 or 3µg/ml of sLDLR in 1%BSA in PBS in a total reaction volume of 100µl. The cells that were incubated with 1%BSA/PBS were then stained. After washing twice with PBS, cells stained with anti-VSVind.G and anti-RDpro antibodies were incubated with their respective secondary antibodies. On the other hand, the cells incubated with sLDLR were stained with an anti-6His-tag antibody, ab18184 (Abcam, UK) against the C-terminal 6His-tag on sLDLR to probe for sLDLR binding following the protocol in section 2.6.3.2. Cells were then washed twice with PBS, fixed in 2% PFA in PBS, and analysed via flow cytometry.

2.7.Surface Plasmon Resonance

Analyses were performed using a BIAcore T100 instrument (GE Healthcare, Chicago, IL). Wild-type (wt) VSVind.G produced by thermolysin limited proteolysis of viral particles, Gth (a kind gift from Drs Yves Gaudin and Aurélie Albertini) (270, 297), (0.04 mg/mL) and monoclonal antibody (mAb) 8G5F11 (0.03 mg/mL) in sodium acetate buffers (10mM, pH 4.5 and 4.0 respectively) were immobilised on a CM5 sensor chip using the amine coupling system according to the manufacturer's instructions. To measure mAb affinity to VSVind.G, 8G5F11 (MW 155kDa) and IE9F9 (MW 155kDa) were suspended in HBS-EP (0.01M HEPES pH7.4, 0.15M NaCl, 3mM EDTA, 0.005v/v Tween20®) and passed over the immobilised Gth at the various concentrations. To measure VesG-LV avidity against 8G5F11, LV preparations were suspended in HBS-EP buffer and passed over the immobilised mAb at various titres. The dissociation constants were calculated using BIAevaluation software according to the manufacturer's instructions. For the competitive binding assay, multiple injections of mAbs at 10µg/mL

concentration was performed followed by the injection of soluble recombinant LDLR (R&D Systems, Minneapolis, MN) at an identical concentration.

2.8.SDS-PAGE and Immunoblotting

G protein expressing HEK293T cells in 10cm plates were washed with ice-cold PBS twice and then were lysed with 0.40ml per plate of lysis buffer [(25mM TrisHCl pH7.5, 150mM NaCl, 1% v/v Triton X-100) supplemented with Roche cOmplete™ protease inhibitor cocktail (Sigma-Aldrich)]. The lysates were centrifuged (17,000xg, 20 mins) and the supernatants containing the cellular proteins were collected. Protein concentrations were determined using a Pierce BCA Protein assay reagent kit (Thermo-Fisher Scientific) using BSA as the standard. After normalisation of protein concentrations, samples were boiled at 95ºC for 5 mins in 5X Laemmli buffer (0.5M Tris-HCl pH6.8, 10% glycerol, 2% sodium duodecylsulfate (SDS), 0.2 mg/ml Bromophenol blue, 5% β-Mercaptoethanol, and 0.1M dithiothreitol (DTT)) and were resolved by electrophoresis in a 4% (wt/vol) SDS-polyacrylamide staking gel, followed by 10% (wt/vol) resolving gel for 2h at 120 volts. Proteins were then transferred onto a nitrocellulose membrane (GE Healthcare), blocked with 5% (wt/vol) skimmed milk in PBS-T (washing buffer; PBS with 0.1% (v/v) Tween20), and incubated with the indicated antibodies in the blocking buffer. Secondary antibodies were visualised by ECL™ Prime Western Blotting Reagent (GE Healthcare). Gth was visualised via Ponceau S staining of the nitrocellulose membrane after protein transfer.

2.9.Animal Studies Investigating Lentiviral Vector Immunogenicity

2.9.1.Mice

All animal studies described were done according to protocols approved by Biological Services Division (BSD) at the National Institute for Biological Standards and Control (NIBSC) and within the remit of a Home Office Project License (PPL 70/8091). Animals were purchased from Charles River Laboratories (Kent, UK). 6 to 8-week-old female Balb/c mice with a minimum weight of 18g were used for both experiments.

Mice were immunised and boosted with wild-type VSVind.G protein produced by thermolysin limited proteolysis of viral particles (Gth) (270, 297) subcutaneously using the Sigma Adjuvant System (Sigma-Aldrich) at 0.08mg/mL antigen concentration. LVs were administered intravenously into the tail vein.

Blood sampling was performed by tail vein bleeding. Serum was obtained by centrifuging clotted blood samples at 10,000xg for 15 minutes at 4ºC. Serum was stored at -20ºC until further use.

At the termination of the studies, the animals were killed by exsanguination under terminal anaesthesia and several organs including lungs, liver, spleen, kidneys, and lymph nodes were autopsied and kept in sterile PBS on ice until further processing. Organ samples were processed on the day of harvest for luminescence or snap-frozen and stored at -80ºC until further analysis.

2.9.2.*In Vivo* Bioluminescence Imaging

Transduction efficacy, transgene expression, and biodistribution of the viral vectors were monitored using IVIS Spectrum *In Vivo* Imaging System (Perkin Elmer, Waltham, MA). Mice were injected intraperitoneally with D-Luciferin (Perkin Elmer, Waltham, MA) in PBS at 150mg per kilogram body weight dose prior to subjection to general anaesthesia via isoflurane inhalation in the induction chamber. Mice were then transferred to the imaging chamber while anaesthesia was maintained, and images were captured between 10 to 15 minutes post D-Luciferin injection. Mice were monitored during recovery after imaging. Images were analysed, and radiance determined via region of interest (ROI) analysis using Living Image® software (Perkin Elmer).

2.9.3.Enzyme-linked Immunosorbent Assay (ELISA) for Detection of anti-G Protein Antibodies

An enzyme-linked immunosorbent assay (ELISA) was used to detect anti-VSVind.G antibodies in murine sera. For this VSVind.G-LVs were produced as previously described, purified on a 20% sucrose (Sigma-Aldrich) cushion, and resuspended in sterile PBS. Total protein concentration of the LV

preparations was determined using a Pierce BCA Protein Assay Kit according to manufacturer's instructions using BSA as the standard.

A coating mix of 25µg/mL total protein in PBS was prepared and each well of Nunc Maxisorp ELISA plate (Thermo-Fisher Scientific, UK) was coated at a volume of 100µl/well overnight at 4ºC. The plate was washed three times with 200µl of PBS before the samples were incubated with 200µl/well of blocking buffer, 2% fish gelatine (Sigma-Aldrich) in PBS, for 1h at 37ºC. The plate was washed three times with 300µl/well of washing buffer, PBS-0.05% (v/v) Tween20®, before 100µl/well of serum samples and mAb controls diluted in diluent buffer, 10%FCS (heat-inactivated) in PBS, were added to the wells and incubated at 37ºC for 2h. After another three washes, the samples were incubated with the secondary antibody, horseradish peroxidase (HRP)-conjugated anti-mouse IgG (GE Healthcare) diluted 1:5000 in diluent buffer for 1h at 37ºC. Following three washes, 100µl/well of Ultra TMB-ELISA Substrate (Thermo-Fisher Scientific) was added to each well incubated at room temperature for 10 minutes and the reaction was stopped by adding isovolume of 4N sulfuric acid. The absorbance was determined at 450nm using a SpectraMax M5 Microplate Reader (Molecular Devices, San Jose, CA).

2.9.4.Luminescence Assay to Determine Luciferase Expression in Organ Samples

Upon receipt, samples from autopsied organs were cut and weighed individually using a high-sensitivity balance (Sartorius, Germany). Using gentleMACS™ C Tubes and gentleMACS™ Dissociator (Miltenyi Biotec, Germany) single-cell suspensions were obtained in 500µl PBS via tissue dissociation. These cells were washed once with PBS and plated on white 96-well plates (Thermo-Fisher Scientific) in triplicates at a volume of 100µl/well following resuspension in PBS. Bright-Glo luciferase assay system (Promega) was utilised to quantify relative protein expression levels. For this, isovolume of the Bright-Glo substrate was added onto the single cell suspensions, incubated at room temperature for 5min and luminescence was measured using MicroBeta2 2450 Microplate Counter (PerkinElmer). Measured relative light units (RLU) were normalised to g of tissue weight.

2.9.5.Extraction of Genomic DNA (gDNA) from Murine Organ Samples

Genomic DNA was obtained from murine tissue samples for quantitative PCR analysis. For this organic DNA extraction was performed using TRIzol (Thermo-Fisher Scientific) according to manufacturer's instructions. gDNA pellets were resuspended in 200-500µl of AE buffer (10mM Tris-Cl, 0.5mM EDTA, pH 9.0).

DNA concentration of gDNA was then quantified by a NanoDrop spectrophotometer through measurement of absorbance at 260nm (OD260). Multiplication of OD260 by 50 resulted in the concentration of DNA in ng/µl. Purity of the gDNA samples was established by the ratio of absorbance at 260nm to 280nm as well as 230nm to 260nm. All samples had a ratio close to $A_{230:260:280}$ 1:1.8:1 which is indicative that the DNA is largely free from contaminants such as proteins, organic compounds, and RNA.

2.9.6.Quantification of Reverse-transcribed LV Copies by Quantitative PCR (qPCR)

qPCR was used to quantify reverse-transcribed LV copies in tissues of interest. In all qPCR reactions QuantiTect SYBR Green PCR Kit (Qiagen, Germany) was utilised. The SYBR Green dye is an asymmetrical cyanine dye used as a nucleic acid stain in molecular biology. The dye preferentially binds to double stranded DNA, resulting in a DNA-dye complex that absorbs blue light and emits green light. As the specific DNA sequence is amplified by the polymerase (e.g. Taq DNA polymerase) the amount of double stranded DNA thus bound SYBR Green amount and the fluorescence of the sample increase. The number of PCR cycles taken to reach a threshold fluorescence (Ct) gives a measure of how much specific DNA sequence was present in the sample at the beginning of the qPCR program. Meanwhile, the presence of ROX, a passive reference dye, compensates for non-PCR-related variations in fluorescence detection. As fluorescence from ROX dye does not change during the qPCR, PCR-related fluorescent signals can be normalised using the ROX signal. Furthermore, to control for non-specific DNA amplification, which

is a potential drawback of SYBR Green-based detection, a melting curve is run, whereby the thermocycler detects the melting point of the PCR product. Detection of a single melting point is indicative of a single PCR product.

To convert the Ct value into a useful measure of DNA amount, absolute quantification was used throughout this thesis. Therefore, standards containing known quantities of the DNA sequence of interest were included in the qPCR, and Ct values from these were used to calculate a standard curve. *Table 2-7* contains an example of the calculations used to make up standards. Linear regression was later utilised to calculate the number of copies of the DNA sequence of interest in the reactions containing gDNA according to the standard curve.

Table 2-7: Sample Calculations for Standards Prepared for qPCR. Calculations for standards made for qPCR using HIV leader primers to detect reverse-transcribed LV provirus copies. The size of the plasmid was used to calculate the molecular weight of the molecule which was then used to calculate the weight of 10^{10} plasmid copies in nanograms (ng). 10^{10} plasmid copies/2µl aliquot of the plasmid was prepared in nuclease-free water which was then serially diluted to obtain 10^8, 10^7, 10^6, 10^5, 10^4, 10^3, 10^2, 10^1 plasmids/2µl.

Standard	Concentration (ng/ul)	Plasmid Size (bp)	Molecular Weight (Da)	Mass (g)	Weight of 10^{10} copies (ng)
pJet-Infect[1]	815	3397	2242020	$3.7x10^{-18}$	37.23

[1]Plasmid generated by Christopher Perry, Takeuchi Group.

As the concentration of DNA can vary amongst samples and nanodrop is not a highly accurate method to quantify DNA concentration, a control is needed to ensure that the integrity of the qPCR result is not compromised. Usually this is the quantification of an endogenous gene that has a known copy number per cell (for qPCR on gDNA). For all qPCR experiments presented in this thesis murine glyceraldehyde-3-phosphate dehydrogenase (*Gapdh)* was used as the endogenous control (*Table 2-8)*.

Table 2-8: Primers and Standards Used in qPCR.

Component	Standard	Primer	Primer Sequence
LV provirus	pJet-Infect[1]	3'LTR_FW	CCCAACGAAGACAAGATCTGC
		5'LTR_RS	TCCCATCGCGATCTAATTCTCC
Murine *Gapdh*	*Gapdh*[2]	mGAPDH_FW	ACGGCAAATTCAACGGCAC
		mGAPDH_RS	TAGTGGGGTCTCGCTCCTGG

[1]Plasmid generated by Christopher Perry, Takeuchi Group.

[2]Standard was amplified and quantified from the endogenous gene, a kind gift from Prof Simon Waddington's Group.

The same method was carried out for the setup of all qPCRs. A master mix was assembled according to *Table 2-9*. 23µl of the master mix was dispensed into each well (including 12 well for standards and 2 wells for template-negative controls) of a 96-well qPCR plate (Agilent, Santa Clara, CA). Next, 2µl of the standard, sample or water per reaction was added to corresponding wells to make a final volume of 25µl in each well.

qPCR plates containing the PCR master mix, standards, and samples were sealed with an optically clear adhesive tape (Thermo-Fischer Scientific) and centrifuged briefly to collect the samples. A Stragene Mx3005P qPCR System (Agilent) was used to run qPCR reactions with settings shown in *Table 2-10* and the data were analysed using the MxPro Software (Agilent).

Table 2-9: Composition of Reactions for SYBR Green-Based Quantification.

Component	Concentration	Volume per reaction (µl)
Primer FW	10 µM	1
Primer RS	10 µM	1
Quantitect SYBR Green Master Mix	-	12.5
Nuclease-Free Water	-	8.5
Template gDNA	-	2
Total Reaction Volume	-	25

Table 2-10: Cycling Conditions for SYBR Green-Based Quantification.

Step	Temperature (ºC)	Time
1	95	15min
2	95	15sec
3	55	30sec
4	72	30sec
Repeat steps 2-4, 40 times		
5	Melting curve	

2.10.Statistical Analyses

All statistical analyses were performed using the GraphPad Prism 5 software (Graphpad software, La Jolla, CA). Details of all tests, including the calculated p-values, are indicated in respective figure legends.

2.11. Appendix

2.11.1. Primers

All primer sequences in the subsequent sections are written 5' – 3'.

2.11.1.1. Primers Used in Cloning of Vectors

Table 2-11: Primers Used in Cloning of A and B Chimaeras

Vector	Primer Name	Primer Sequence
pMD2.1A.G[1] pMD2.2A.G	COCV-FW-PmlI	GCAAATCACGTGGCCACCATGAATTTTCTTCTCTTGACC
pMD2.3A.G pMD2.4A.G	VSVind–RS-EcoRI	GAGATGAACCGACTTGGAAAGTAAGAATTCATTTGC
pMD2.1B.G pMD2.2B.G	VSVind-FW-PmlI	GAAATTCACGTGGCCACCATGAAGTGCCTTTTG
pMD2.3B.G pMD2.4B.G	COCV-RS-EcoRI	AGCCGCTTCAGGAAGTGAGAATTCTTTTCC

[1] A and B chimaeras originally produced by Maha Tijani, Collins/Takeuchi group.

Table 2-12: Primers Used in Cloning Chimeric and Mutant G proteins.

Mutant	Primer Name	Primer Sequence
C1.1	C1.1-FW	CACAGTTCTCGTTCAGTCGTGGT TCCAGAGATCATACCCACCATCT TAGAGAT
	C1.1-RS	ATCTCTAAGATGGTGGGTATGAT CTCTGGAACCACGACTGAACGAG AACTGTG
C1.2	C1.2-FW	GAGATCATACCCACCATCCTAGA GAGGATAGGATTGTCGATGTC
	C1.2-RS	GACATCGACAATCCTATCCTCTC TAGGATGGTGGGTATGATCTC
C1.3	C1.3-FW	CATCTTAGAGATGATAGGAGCGG CGATGTCGACGCGGATATAGCG AGTCTCG
	C1.3-RS	CGAGACTCGCTATATCCGCGTCG ACATCGCCGCTCCTATCATCTCT AAGATG
C1.4	C1.4-FW	ATCCTAGAGAGGATAGGAGCGG CGATGTCGACGCGGATATAGCG AGTCTC
	C1.4-RS	GAGACTCGCTATATCCGCGTCGA CATCGCCGCTCCTATCCTCTCTA GGAT
C8.1	C8.1-FW	GTTTGAGTTCGTGGACAAGGACG TCTACGCAGC
	C8.1-RS	GCTGCGTAGACGTCCTTGTCCAC GAACTCAAAC
C8.2	C8.2-FW	GCTGCGTAGACGTCCTTGTCCGC CATCTCAAACCACACGCCG
	C8.2-RS	CGGCGTGTGGTTTGAGATGGCG GACAAGGACGTCTACGCAGC
C8.3	C8.3-FW	TTGGCGGCTGCGAAGAGGTCCT TGTCCGCCATCTCAAACCACACG CCGG

	C8.3-RS	CCGGCGTGTGGTTTGAGATGGC GGACAAGGACCTCTTCGCAGCC GCCAA
V1.1	V1.1-FW	CCACAGTTCCCTTTCTGTCTGAG ATCCACTGATCTTTCCGACCATT CTTGAGAGG
	V1.1-RS	CCTCTCAAGAATGGTCGGAAAGA TCAGTGGATCTCAGACAGAAAGG GAACTGTGG
V1.2	V1.2-FW	ACTGATCTTTCCGACCATTTTTGA GATGATTGGAGCAGCAATATCG
	V1.2-RS	CGATATTGCTGCTCCAATCATCT CAAAAATGGTCGGAAAGATCAGT
V1.3	V1.3-FW	ATTCTTGAGAGGATTGGATTATC AATATCGATTCTGATGTATCTGGT CTCAAAGTATTTTAGGGTAC
	V1.3-RS	GTACCCTAAAATACTTTGAGACC AGATACATCAGAATCGATATTGAT AATCCAATCCTCTCAAGAAT
V1.4	V1.4-FW	CCATTTTTGAGATGATTGGATTAT CAATATCGATTCTGATGTATCTG GTCTCAAAGTATTTTAGGGTACC A
	V1.4-RS	TGGTACCCTAAAATACTTTGAGA CCAGATACATCAGAATCGATATT GATAATCCAATCATCTCAAAAATG G
LSR	LSR-FW	GAGATCTTACCCACCATCCTAGA GAGGATAGGATTGTCGATGTC
	LSR-RS	GACATCGACAATCCTATCCTCTC TAGGATGGTGGGTAAGATCTC
AA	AA-FW	ACCATCTTAGAGATGATAGGAGC GGCGATGTCGATGCGGATATAG C
	AA-RS	GCTATATCCGCATCGACATCGCC GCTCCTATCATCTCTAAGATGGT

V	V-FW	GGATTGTCGATGTCGACGCGGATATAGCGAGTC
	V-RS	GACTCGCTATATCCGCGTCGACATCGACAATCC
K	K-FW	TGGTAGTTCCACTGATCTTTCCGACCATTCTTGAG
	K-RS	CTCAAGAATGGTCGGAAAGATCAGTGGAACTACCA
I	I-FW	GAGCAGCAATATCGATTCTGATGTATCTGGTCTCAAAG
	I-RS	CTTTGAGACCAGATACATCAGAATCGATATTGCTGCTC
G	G-FW	CAGCAAAGAGATCCTTACCAGCCATCTCGAACCAG
	G-RS	CTGGTTCGAGATGGCTGGTAAGGATCTCTTTGCTG
A	A-FW	GGCTGCAGCAAAGAGAGCCTTATCAGCCATCTC
	A-RS	GAGATGGCTGATAAGGCTCTCTTTGCTGCAGCC
N	N-FW	GGCTGCAGCAAAGAGATTCTTATCAGCCATCTCGA
	N-RS	TCGAGATGGCTGATAAGAATCTCTTTGCTGCAGCC
SQ	SQ-FW	ATCCCACAGTTCCCTTTCTGTCTGAGATCCACTGATCATTCCGACCATTC
	SQ-RS	GAATGGTCGGAATGATCAGTGGATCTCAGACAGAAAGGGAACTGTGGGAT
DN	DN-FW	GACCATTCTTGAGAGGATTGGATTATCAATATCGACTCTGATGTATCTGGT

	DN-RS	ACCAGATACATCAGAGTCGATATTGATAATCCAATCCTCTCAAGAATGGTC
ISK	ISK-FW	ACTGATCATTCCGACCATTTTTGAGATGATTGGAGCAGCAATATCG
	ISK-RS	CGATATTGCTGCTCCAATCATCTCAAAAATGGTCGGAATGATCAGT
VSVind.G COMPLEMENT CHIMAERAS (IND 1-3)	VSV-RS-OUT	ATCAAGAATTCTTACTTTCCAAGTCGGTTCATC
	VSV-FW-OUT	ATCAACACGTGGCCACCATGAAGTGCCTTTTG
	VSV-RS	GAGGTCTGAGATGGAGCGGAAATTGTAGCTCCCACTGGACAC
	VSV-FW	GCCACCATGAAGTGCCTTTTGTACTTAGCC
	V1.1-RS	AAAAACGTTATCTCTGTGTCAATGAGGTTAGAATCACATAGCCC
	V1.1-FW	TATGTGATTCTAACCTCATTGACACAGAGATAACGTTTTTTTCCG
	V1.2-RS	GATGGGAGTCTGACTCCCCAGTGTTTGCAATAATTCATTTTGCAG
	V1.2-FW	AAATGAATTATTGCAAACACTGGGGAGTCAGACTCCCATC
	V2.1-RS	GAGGGCAGCCTTACCCCGGCATGCTTGCAGTATTGCATTTTGC
	V2.1-FW	AAATGCAATACTGCAAGCATGCCGGGGTAAGGCTGCC
	V2.2-RS	GAGGTCTGAGATGGAGCAGAAATTGTAGCTCCCACTGGACACTC
	V2.2-FW	GTCCAGTGGGAGCTACAATTTCTGCTCCATCTCAGACCTCAG
COCV.G COMPLEMENT	COCV-RS-OUT	ATCAAGAATTCTCACTTCCTGAAGCGGCTC

CHIMAERAS (COCV 1-3)	COCV-FW-OUT	ATCAACACGTGGCCACCATGAATTTTCTTCTCTTG
	COCV-RS	TCACTTCCTGAAGCGGCTCATCTC
	COCV-FW	GCCACCATGAATTTTCTTCTCTTGAC
	C1.1-RS	AAGAAGGTGATGTCCATGGACACCAGTGTGGCGTCGCAAAG
	C1.1-FW	GGCTTTGCGACGCCACACTGGTGTCCATGGACATCACCTTCTTCTCAG
	C1.2-RS	GGAGGGCAGCCTTACCCCGGCATGCTTGCAGTATTGCATTTTGCAG
	C1.2-FW	AAAATGCAATACTGCAAGCATGCCGGGGTAAGGCTGCCC
	C2.1-RS	CTGATGGGAGTCTGACTCCCCAGTGTTTGCAATAATTCATTTTGCAG
	C2.1-FW	TGCAAAATGAATTATTGCAAACACTGGGGAGTCAGACTCCCATCAG
	C2.2-RS	TGAGGTTTGTGTCGGTGCGGAGATACTTGACCCTTCTGGGCATTC
	C2.2-FW	GCCCAGAAGGGTCAAGTATCTCCGCACCGACACAAACCTC
Chimeric VesG	VSV-flanking RS	GAATTCTTACTTTCCAAGTCGGTTCATCTC
	PIRY-flanking FW	ATCAACACGTGTCTAGAGCCACCATGGATC
	NJ-flanking FW	ATCAACACGTGTCTAGAGCCACCATGCTG
	COCV-flanking FW	ATCAACACGTGGCCACCATGAAT
	PIRY-inner FW	CCAGGGATGGTTCAGTAGTTGGAAAAGC

PIRY-inner RS	GCTTTTCCAACTACTGAACCATC CCTGGATC
NJ-inner FW	GAGGGCTGGTTCAGTAGTTGGAA AAGC
NJ-inner RS	GCTTTTCCAACTACTGAACCAGC CCTCCAC
COCV-inner FW	GAAGGTTGGTTTAGTAGTTGGAA AAGCTCT
COCV-inner RS	CCAACTACTAAACCAACCTTCGA TAAGCTC

2.11.2.Buffers

Table 2-13: Buffers.

Protocol	Buffer/Reagent Name	Composition
Bacterial Amplification	Luria-Bertani (LB) Agar	1% bacto tryptone 0.5% bacto yeast 0.5% NaCl (pH 7.0) 15g/L bactoagar
	Luria-Bertani (LB) Broth	1% bacto tryptone 0.5% bacto yeast 0.5% NaCl (pH 7.0)
	NZY^+ Broth	Per litre: 10g of NZ amine (casein hydrolysate) 5g of yeast extract 5g of NaCl, pH 7.5 12.5ml of 1M $MgCl_2$ 12.5 ml of 1M $MgSO_4$ 20ml of 20% (w/v) glucose
Elution Buffers	EB	10mM Tris-Cl, pH 8.5
	AE	10mM Tris-CL, pH 9.0 0.5mM EDTA
Electrophoresis	TBE	89 mM Tris (pH 7.6) 89 mM boric acid 2 mM EDTA
SDS-PAGE and Immunoblotting	Lysis Buffer	5mM TrisHCl pH7.5 150mM NaCl 1% v/v Triton X-100) supplemented with Roche cOmplete™ protease inhibitor cocktail
	Laemmli Buffer	50 mM Tris, pH6.8 10% Glycerol 2% SDS 5% 2-Mercapthoethanol 0.2 mg/ml Bromophenol blue 0.1 M DTT
	Running Buffer	25 mM Tris, pH8.5 200 mM Glycine 0.1% sodium dodecyl sulphate (SDS)
	Transfer Buffer	100 mM Tris, pH6.8 200 mM Glycine 20% Methanol
	4% Stacking Gel	125 mM Tris-HCl, pH6.8 4% Acrylamide/bis

		10% SDS 0.1% Tetramethylethylenediamine (TEMED) 1% Ammonium persulphate (APS)
	10% Resolving Gel	125 mM Tris-HCl, pH8.8 10% Acrylamide/bis 10% SDS 0.1% TEMED 1% APS
	Ponceau S Staining Solution	1g Ponceau S 50ml acetic acid Make up to 1L with ddH2O
Surface Plasmon Resonance	HBS-EP	10mM HEPES 150mM NaCl 3mM EDTA 0.005% Polysorbate 20

2.11.3.Antibodies

Table 2-14: Primary Antibodies Used.

Against	Antibody	Host	Isotype	Manufacturer/ Source, Catalogue Number	Dilution
VSVind.G	8G5F11	Mouse	IgG2a kappa	Kerafast (Boston, MA), originally Lyles (511) EB0010	Varied
	IE9F9	Mouse	IgG2a kappa	Kerafast (Boston, MA), originally Lyles (511) EB0012	Varied
	VSV-Poly	Goat	N/A[1]	Dr Hoshino (Gunma, Japan) (263, 509, 510)	Varied
	P5D4	Mouse	IgG1	Sigma-Aldrich, St Louis, MO SAB4200695	1:500
Human GAPDH	GAPDH	Mouse	IgM	Sigma-Aldrich, G8795	1:5,000
RDpro	Anti-RD114 antiserum	Goat	N/A	NCI	1:500
6XHis-tag	Monoclonal anti-6His-tag	Mouse	IgG2b	Abcam, UK, ab18184	1:500

[1]Not applicable, polyclonal

Table 2-15: Secondary Antibodies Used.

Antibody	Host	Manufacturer/Source, Catalogue Number	Dilution
Alexa Fluor® 647 AffiniPure Goat Anti-Mouse IgG (subclasses 1+2a+2b+3), Fcγ Fragment Specific	Goat	Jackson Immunoresearch, UK 115-605-164	1:500
Alexa Fluor® 647 AffiniPure Rabbit Anti-Goat IgG, Fc Fragment Specific	Rabbit	Jackson Immunoresearch, UK 305-605-046	1:500
Anti-6X His tag® antibody (FITC)	Rabbit	Abcam, UK, ab1206	1:500
Amersham ECL Mouse IgG, HRP-linked whole Antibody	Sheep	GE Healthcare NA931	1:5,000

2.11.4.G Proteins

Table 2-16: Accession Numbers of Vesiculovirus and Rabies Virus G Proteins.

Virus	UniProtKB/Swiss-Prot Accession Number	Genbank Accession Number
Vesicular stomatitis Indiana virus (VSVind) – San Juan strain	P03522	M35219
Maraba virus (MARAV)	F8SPF4	HQ660076
Cocal virus (COCV)	O56677	AF045556
Vesicular stomatitis Alagoas virus (VSVala)	B3FRL4	ACB47442
Vesicular stomatitis New Jersey virus (VSVnj) – Ogden strain	P04882	V01214
Piry virus (PIRYV)	Q85213	D26175
Chandipura virus (CHAV) - I653514 strain	P13180	AY614717.1
Carajas virus (CJSV)	A0A0D3R1Y6	AY335185.1
Isfahan virus (ISFV)	Q5K2K4	AJ810084.2
Rabies virus (RABV) – CVS-11 strain	O92284	EU126641.1

3 The Interactions of Monoclonal Anti-VSVind.G Antibodies with the G Proteins of Other Major Vesiculoviruses

3.1.Overview

The rhabdovirus, vesicular stomatitis virus Indiana strain (VSVind), has been used to study glycoprotein processing, viral assembly, and humoral and cellular antiviral immune responses. Because the virus lyses infected cells, it is now being developed for clinical oncolytic virotherapy (512-514). Furthermore, its envelope G protein (VSVind.G) is the most commonly used envelope to pseudotype lentiviral vectors and has been used in many experimental and clinical studies (146, 264, 265). VSVind.G's crystal structure, fusogenic residues, serum sensitivity, and cell fusion and entry mechanisms have been identified (269, 270, 297, 321, 515, 516).

Pseudotyping is producing virus particles or viral vectors using the surface glycoprotein of a different virus, resulting in a pseudotyped virus particle (260, 261, 517). Pseudotyping can be used to modify the tropism of LVs and

increase their stability since the choice of envelope glycoprotein determines many biophysical and infectious characteristics of a particular LV pseudotype (518). VSVind.G pseudotyped particles can produce high titres and their stability allows for LV concentration by ultracentrifugation. They can also transduce a wide range of cells including important gene therapy targets such as haematopoietic stem cells and T cells. However, viral vectors that bear the VSVind envelope are particularly sensitive to human serum which limits their potential for *in vivo* applications (266). In addition, it has been reported that VSVind.G is cytotoxic and cannot be constitutively expressed (267, 519). This led some investigators to use inducible promoters to drive envelope expression in packaging cell lines and look for alternative envelopes (197, 520, 521). Recently G proteins derived from the other vesiculovirus subfamily members Cocal, Piry, and Chandipura viruses, have been proposed as alternative envelopes for lentiviral vector production due to some possible advantages over VSVind.G (200, 202, 471).

Although some antigenic and biochemical characteristics of VSVind.G have been reported, there is little known about the other vesiculovirus G proteins (VesG), and there is a general lack of reagents available to identify and characterise them. In the past, monoclonal antibodies (mAbs) have been used to study the antigenic determinants found on viral glycoproteins, for example the hemaegglutinin (HA) of influenza virus, the gp70 protein of murine leukaemia virus (MLV), gp120 of human immunodeficiency virus (HIV-1), and rabies virus G protein (522-526). These previous studies have identified epitopes essential in virus neutralisation (526-528). Also, mAbs have proven useful in viral pathogenesis studies as mutants selected for escape from neutralising antibodies, often have altered pathogenicity compared to their wild-type counterparts (529-531).

There are several commercial mAbs which recognise the C-terminal cytoplasmic tail of VSVind.G since the eleven amino acid determinant YTDIEMNRLGK is used as a peptide-tag to purify, visualise, and study other proteins of interest (531). Moreover, in the early 1980s, a group of researchers has produced many mAbs against VSVind.G and VSVnj.G with the purpose of dissecting antigenic determinants to characterise the G proteins (511, 532).

Later, their work was developed by other groups leading to a broad characterisation of VSVind.G epitopes (312, 512, 533). Currently, two of these antibodies are available commercially (*Table 3-1).* Compared to this antibody research on VSVind.G and VSVnj.G, there are currently no available monoclonal antibodies that were raised against G proteins of other vesiculoviruses.

Table 3-1: List of Commercially Available Monoclonal Anti-VSVind.G Antibodies.

Name	Manufacturer	Epitope
F-6*	Santa Cruz Biotechnology	C-terminal
P5D4*	Sigma-Aldrich	C-terminal
EPR12997*	Abcam	C-terminal
8G5F11 (I1)	Kerafast (511)	Extracellular
IE9F9 (I14)	Kerafast (511)	Extracellular

*There are other commercially available mAbs which recognise the same epitope as the listed antibodies.

The current knowledge on the major antibody binding sites on VSVind.G dates to the research done by the Lefrancois and Wagner groups in the 1980s (312, 512, 533). The mAbs that were used to carry out these characterisation studies were produced using the hybridoma method (511). Spleen cells from mice that were either hyper-immunised or given a single injection of wt VSVind or VSVnj were utilised as the antibody-producing part of the hybridoma cell lines. Out of the 58 isolated hybridomas that produced antibodies, 38 produced antibodies towards the G proteins of either VSVind or VSVnj. The reactivity of the mAbs was classified by ELISA, competitive binding assays, and their ability to neutralise viral infection. The neutralising antibodies, eleven for VSVnj.G (*Table 3-2*) and sixteen for VSVind.G (*Table 3-3*), were then used to determine antibody binding epitopes on the glycoproteins.

Table 3-2: Review of Anti-VSVnj.G mAbs Produced by Lefrancois *et al*[a].

Designation	Neutralising Activity	Cross-reactivity with VSVind.G	Neutralising Epitope Recognised[b]	Competition with mAbs
N1	+	NR[c]	I	All compete only with mAbs within the same designated group/epitope
N2	+	NR	I	
N3	+	NR	I	
N4	+	NR	I	
N5	+	NR	I	
N6	+	NR	II	
N7	+	NR	II	
N8	+	NR	II	
N9	+	NR	III	
N10	+	NR	III	
N11	+	NR	IV	-
N12	-	-	N/A[d]	Enhances binding of other non-neutralising mAbs
N13	-	-	N/A	
N14	-	-	N/A	
IN2	-	+	N/A	Varying levels of competition with I17 and non-neutralising anti-VSVind.G mAbs
IN5	-	+	N/A	
IN6	-	+	N/A	

[a]Information collated from (312, 511, 532, 533).

[b]Epitopes were designated arbitrarily based on the mAb groups identified via binding competition assays.

[c]Not reported

[d]Not applicable

Table 3-3: Review of Anti-VSVind.G mAbs Produced by Lefrancois *et al*[a].

Designation	Neutralising Activity	Cross-reactivity with VSVnj.G	Neutralising Epitope Recognised	Competition with mAbs (Epitope Designation)
I1 (8G5F11)	+	NR[b]	A_1	A, C
I2	+	-	A_2	A, C
I3	+	-	A_2	A, C
I4	+	NR	A_3	A, C
I5	+	-	A_3	A, C
I6	+	NR	A_3	A, C
I7	+	NR	A_3	A, C
I8	+	-	A_1	A, C
I9	+	NR	A_3	A, C
I10	+	NR	B	B, C
I11	+	NR	B	B, C
I12	+	NR	B	B, C
I13	+	NR	B	B, C
I14 (IE9F9)	+	-	B	B, C
I15	+	NR	C	A, B, C
I16	+	NR	C	A, B, C
I17	+	+ (non-neutralising)	D	competes with non-neutralising mAbs
IN1	-	-	N/A[c]	Varying levels of competition with I17 and non-neutralising anti-VSVnj.G mAbs
IN3	-	+	N/A	
IN4	-	+	N/A	
IN7	-	+	N/A	

[a]Information collated from (312, 511, 532, 533)

[b]Not reported

[c]Not applicable

Determination of these sites was carried out using competitive binding assays. Briefly, ELISA plates were coated with virus particles, then dilutions of unlabelled competitor antibodies were added, followed by an ^{125}I-labelled mAb. Plates were incubated at 37ºC, unbound antibody was washed away, and a gamma counter was used to determine bound radioactivity in counts per minute (CPM). The percentage competition was then calculated (*Equation 3-1).* This work was further built upon by both groups who investigated the binding of the same antibodies as well as some others to chimeric, truncated, and mutated version of VSVind.G, further mapping the epitopes.

$$\%Competition: \frac{cpm_{Absence\ of\ Competitior} - cpm_{Presence\ of\ Comp.}}{cpm_{Absence\ of\ Competitior}} x100 \quad \text{[Equation 3-1]}$$

Overall, four distinct neutralising, non-overlapping epitopes were identified on VSVnj.G, while the topological relationship of the VSVind.G epitopes was more complicated (511, 533). VSVnj.G epitopes that are involved in neutralisation are located at the centre of the 517 amino acid long glycoprotein. The broad locations of the antigenic sites are residues 214-289, which contains three epitopes, and 43-267 (512) (*Table 3-2)*.

Some conserved determinants between VSVind.G and VSVnj.G have been discovered. These epitopes are non-neutralising presumably because neutralising antibodies exert stronger selective pressure for the evolution of the antigenic variant (532, 533). Antibodies that bound to these epitopes (NJ15-17 and I17-20) were mostly cross-reactive and demonstrated varying levels of competition (*Tables 3-2 and 3-3)*.

VSVind.G antigenic sites were more extensively analysed. While one epitope is mapped to cysteine-rich residues at an N-terminal domain of the glycoprotein, two others are located towards the cysteine-poor C-terminal domain (512). The epitopes, named A, B, and C, though found in highly conserved regions of both glycoproteins are unique to VSVind.G. These three antibody binding sites, have varying degrees of interaction and overlap (*Figure 3-1)* (532). In addition, a fourth epitope, D, utilised only by a single

neutralising antibody, I17 (*Table 3-3),* was described, however, its location on the G protein hasn't been elucidated.

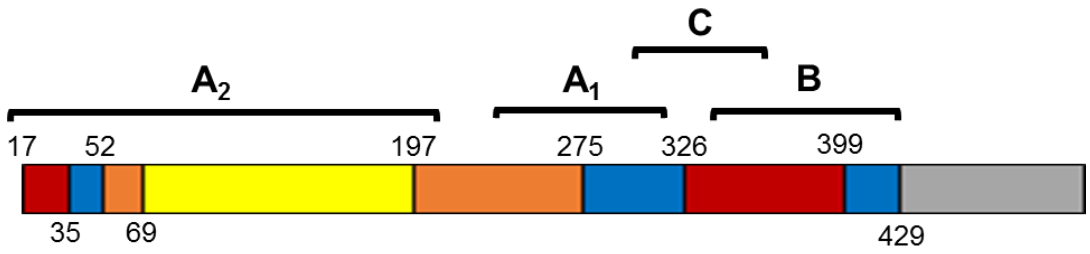

Figure 3-1: Identified Antigenic Epitopes of VSVind.G Mapped on a Linear Diagram of the G Protein. The three major epitopes, A (A_1 and A_2), B, and C and their approximate locations are identified on the diagram. As the location of epitope C has not been precisely identified, its position is mapped tentatively. The domain architecture of VSVind.G is represented in a linear diagram, colour-coded by domain (red: DI, lateral domain; blue: DII, trimerisation domain; orange: DIII, PH domain, yellow: DIV, fusion domain; grey: transmembrane and C-terminal domains). Domain boundaries are numbered according to the G protein precursor (i.e. including the signal peptide). Diagram adapted from (270).

a. *Epitope A*

The dominant neutralising epitope for VSVind.G, A, is divided into two major regions A_1 and A_2 that are separated in the primary structure of the protein. Although a third subdomain for epitope A, A_3, has been described, its location hasn't been reported. Both continuous and discontinuous determinants have been identified in these two antigenic sites located at 263-317 and 17-200 respectively (312, 512). In the mutants selected by A_1 mAbs an extremely high rate of amino acid substitution has been observed (312). Combined with the extensive lack of structural constraints in the region, the results indicate that A_1 may be a continuous epitope analogous to highly variable continuous antigenic loops elucidated in the influenza virus (524).

Furthermore, A_2 epitope shows varying interactions with the A_1 epitope through reciprocal binding and competition (511, 533). The most likely reason behind this comes from the 3D crystal structure of the glycoprotein (see section 1.6.2.3.2). Both epitopes lie divided between domains II and III of VSVind.G, therefore, although spread apart in primary structure, in the tertiary conformation of the protein epitopes may be in very close proximity to each other (297).

It is reported that 8G5F11's epitope lies in the antigenic variant A_1 (297, 312, 511). As 8G5F11 has neutralising activity, it might bind to the fusion loops of trimeric domain II. On the other hand, 8G5F11's neutralising effects might come from reciprocal interactions with epitope A_2.

b. *Epitope B*

Reported to have a partial overlap with epitope A possibly through tertiary folding, epitope B is towards the C-terminal end of the extracellular domain of the glycoprotein. It is reported to be located at residues 339-428 (312, 512). IE9F9's epitope is also thought to be within this antigenic determinant which corresponds to the domain I of VSVind.G (297).

c. *Epitope C*

Although the exact location of this epitope is not yet identified, it is known to be in close proximity of epitope A (533). The antibodies that bind to epitopes A and C demonstrate reciprocal competition which is thought to be occurring due to steric hindrance (511). In addition, due to high reciprocal competition between the antibodies binding to both epitopes, it is postulated that epitope B and epitope C have an overlapping region (312, 533).

In summary, the major antigenic sites of rhabdoviruses are in the lateral and PH domains of the viruses (270, 522). Similar to this, the neutralising epitopes of VSVind.G are located in domains I, II, and III (297, 312). Since segments containing the antigenic determinants are the most exposed parts of VSVind.G, it is most probable that other vesiculoviruses have similar antigenic regions in their corresponding domains (246, 312, 522). However, the lack of cross-reaction and cross-neutralisation reported between VSVind.G and VSVnj.G mAbs highlights that sequence of these antigenic sites may differ.

Both receptor recognition and membrane fusion by wild-type VSVind and other vesiculoviruses, as well as the pseudotyped particles, are mediated by the viral glycoprotein. This is a type I membrane protein with a single transmembrane domain, which homotrimerises and protrudes from the viral surface (270, 534, 535). The G protein mediates viral attachment by interacting with a cellular receptor. In the case of VSVind.G, the low-density lipoprotein receptor (LDLR) and its family members have been demonstrated to be the cellular receptor responsible for viral entry (321, 322). It has been shown that LDLR is the primary entryway for VSVind.G pseudotyped particles in various cell lines that includes a human epithelial cell line. Furthermore, viral infection was inhibited in a dose-dependent manner by soluble LDLR molecules and was entirely blocked following the addition of receptor-associated protein (RAP) which binds to other LDLR family members [74]. Similar dose-dependent partial inhibition of COCV infection has also been demonstrated (200).

Recently Nikolic and colleagues have demonstrated that VSVind.G is able to bind two cysteine-rich (CR) domains, CR2 and CR3, of LDLR with similar affinities (323). The crystal structure of both domains with VSVind.G show that both CR2 and CR3 interact with the same site on the glycoprotein in its pre-fusion form. This epitope is split apart when the G protein in its post-fusion form, hence, rendering the proteins unable to interact.

CR domain binding to VSVind.G is dictated by basic residues H24 and K63 on VSVind.G which dock onto acidic residues in CR2 and CR3 (D69/73/79, E80 and D108/112/118, E119 respectively) that coordinate calcium ions and R370 which interacts with carbonyl groups of W66 and F105 on CR2 and CR3 respectively (323). This type of binding is similar to the ones employed by LDLR family members to bind to their endogenous ligands (324, 328, 329, 536). However, these key residues are not conserved amongst vesiculoviruses. Therefore, the use of this epitope and the use of LDLR per se cannot be generalised to other vesiculoviruses. Indeed, CHAV.G which does not possess the basic residues in the positions corresponding to 63 and 370 on VSVind.G does not bind to the CR domains (323).

Therefore, a study to characterise antigenic sites amongst the VesG would provide valuable insights into virus neutralisation and receptor recognition. Identification of antibodies that recognise VesG will not only be valuable for vesiculovirus research but also aid in the development of G protein-containing advanced therapy medicinal products and vaccine vectors.

3.2. Aims

In this chapter, I aimed to identify anti-VSVind.G antibodies that can cross-react with other vesiculovirus G proteins. In addressing this aim, I utilised antibodies with extracellular binding epitopes: two commercially available monoclonal antibodies, 8G5F11 and IE9F9, as well as a goat polyclonal antibody VSV-Poly. Furthermore, critical amino acid residues that dictate antibody binding were identified and the neutralisation mechanisms of mAbs were investigated.

3.3.Results

3.3.1.Cross-reactivity of Anti-VSVind.G Antibodies with Other VesG

To investigate antibody binding to different vesiculovirus G proteins, I constructed vectors expressing the six different VesG: VSVind.G, COCV.G, VSVnj.G, PIRYV.G, VSVala.G, and MARAV.G. Codon-optimised G protein genes were subcloned in the pMD2 plasmid backbone, which is widely used to express VSVind.G in lentivector productions (202). Feline endogenous retrovirus RD114 derived RDpro envelope (515, 517) was used as a negative control. Using these constructs commercially available monoclonal anti-VSVind.G antibodies, 8G5F11, IE9F9, and P5D4, and goat polyclonal VSV-Poly were investigated for binding.

Briefly, HEK293T cells were transiently transfected to express the G proteins on the cell surface. These cells were then incubated with the antibodies and analysed via flow cytometry 48 hours post-transfection. Stained HEK293T cells were first gated for single cell population, i.e. “live cells” (*Figure 3-2A*). Following which the live cell populations were analysed for median fluorescence intensity (MFI). Mock-transfected cells and cells incubated with fluorophore-conjugated secondary antibody only were included as further negative controls (*Figure 3-2B*).

Amongst the extracellular antibodies tested IE9F9 only bound to VSVind.G (*Figure 3-2C*). However, anti-VSVind.G monoclonal antibody 8G5F11 and polyclonal VSV-Poly both could recognise various VesG with different binding strengths depicted by the shifts in MFIs of the histograms. PIRYV.G, the most distant vesiculovirus G investigated, with approximately 40% identity to VSVind.G on amino acid level, could be recognised by VSV-Poly while 8G5F11 did not bind to it. Lastly, a weak cross-reaction was also observed between the anti-VSVind.G mAb P5D4 which binds to the cytoplasmic tail of the G protein and COCV.G.

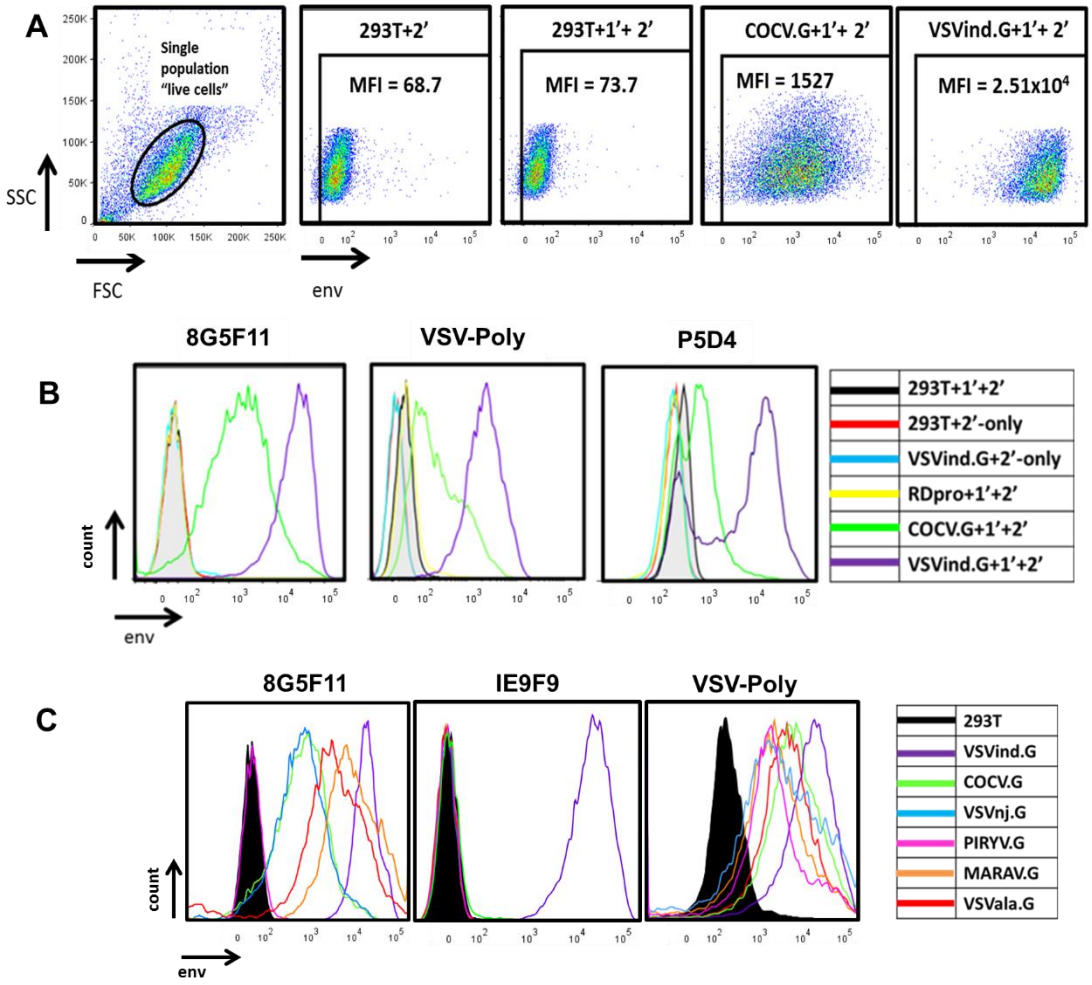

Figure 3-2: Overview of Gating and Flow Cytometry Analyses Depicting Antibody Cross-reactivity. (A) Single population cells were gated on mock-transfected HEK293T cells as "live cells." This gating was used for all further analyses. Live cells were also gated at zero (0) for median fluorescence intensity (MFI) measurements. This panel represents the scatter plots of 8G5F11 staining shown in **(B)**. **(B)** Gated live cell populations of all controls and samples were plotted as histograms to distinguish unspecific background binding from true antibody cross-reaction. 8G5F11, mAb with ectodomain epitope; VSV-Poly polyclonal Ab; P5D4, mAb with endoplasmic epitope. Unrelated feline endogenous virus RD114 derived RDpro envelope (515, 517) was used as negative control. P5D4 staining was carried out after permeabilisation of transfected cells. **(C)** Histograms represent the binding of the antibodies to the VesG expressed on the surface of transfected HEK293T cells. The strength of cross-reaction is depicted via the different MFIs of the histograms. Data shown is one of the three repeats performed.

3.3.2.Characterisation of IE9F9 and 8G5F11 Interactions with G Proteins

Chimeric G proteins were then synthesised to confirm that the difference in MFI values of 8G5F11 binding to VesG was indicative of the mAb affinity towards VesG and not a difference in relative expression levels of the G proteins. The endogenous transmembrane and C-terminal domains of VesG were switched with that of VSVind.G (*Figure 3-3A*). Following expression of these chimeric G proteins in HEK293T cells, 8G5F11 and IE9F9 binding saturation was investigated using quantitative flow cytometry (see section 2.6.3.1) while the relative expression levels of the G proteins were monitored using P5D4 (*Figure 3-3B and C*). 8G5F11 demonstrated a wide range of affinities towards VesG: while its affinity for MARAV.G was comparable to that of VSVind.G, its interactions with COCV.G and VSVnj.G were much weaker.

mAb-G protein interactions were further investigated via surface plasmon resonance to perform a more quantitative analysis. First, in order to quantify mAb binding to G protein monomers under conformationally correct folding, wild-type (wt) VSVind.G produced by thermolysin limited proteolysis of viral particles (Gth) (270, 297) was immobilised on a CM5 chip and was tested for the dose-dependent binding of two extracellular mAbs (*Figure 3-3D*). The dissociation constants (Kd) which indicate the binding affinity of antibodies to Gth were measured as 2.76nM and 14.7nM for 8G5F11 and IE9F9 respectively. These values matched and corroborated the results acquired via quantitative flow cytometry. To further explore 8G5F11-VesG cross-reactivity, the mAb was immobilised, and VesG-LV binding to the antibody was quantified. Since pseudotyped lentiviral particles contain many trimeric G protein spikes (321), this analysis of the interaction between the viral particles and the mAb reflects avidity. A specific, vector dose-dependent (i.e. increasing binding response with increasing titres) binding of VSVind.G was detected which saturated faster than the mAb-Gth interaction (*Figure 3-3E*). Furthermore, when equal doses of VesG-LV at $1x10^8$ TU/ml were injected on immobilised 8G5F11, similar patterns and strengths of binding were observed to that of quantitative flow cytometry, in the order of strength of VSVind,

MARAV, VSVala, Cocal, and VSVnj (Figure 3-3F). Unrelated RDpro envelope pseudotyped LVs were utilised as negative control to deduce unspecific interaction of enveloped particles with immobilised mAb. PIRYV.G-LV demonstrated a similar response to that of RDpro-LV indicative of the lack of binding between the G protein and 8G5F11.

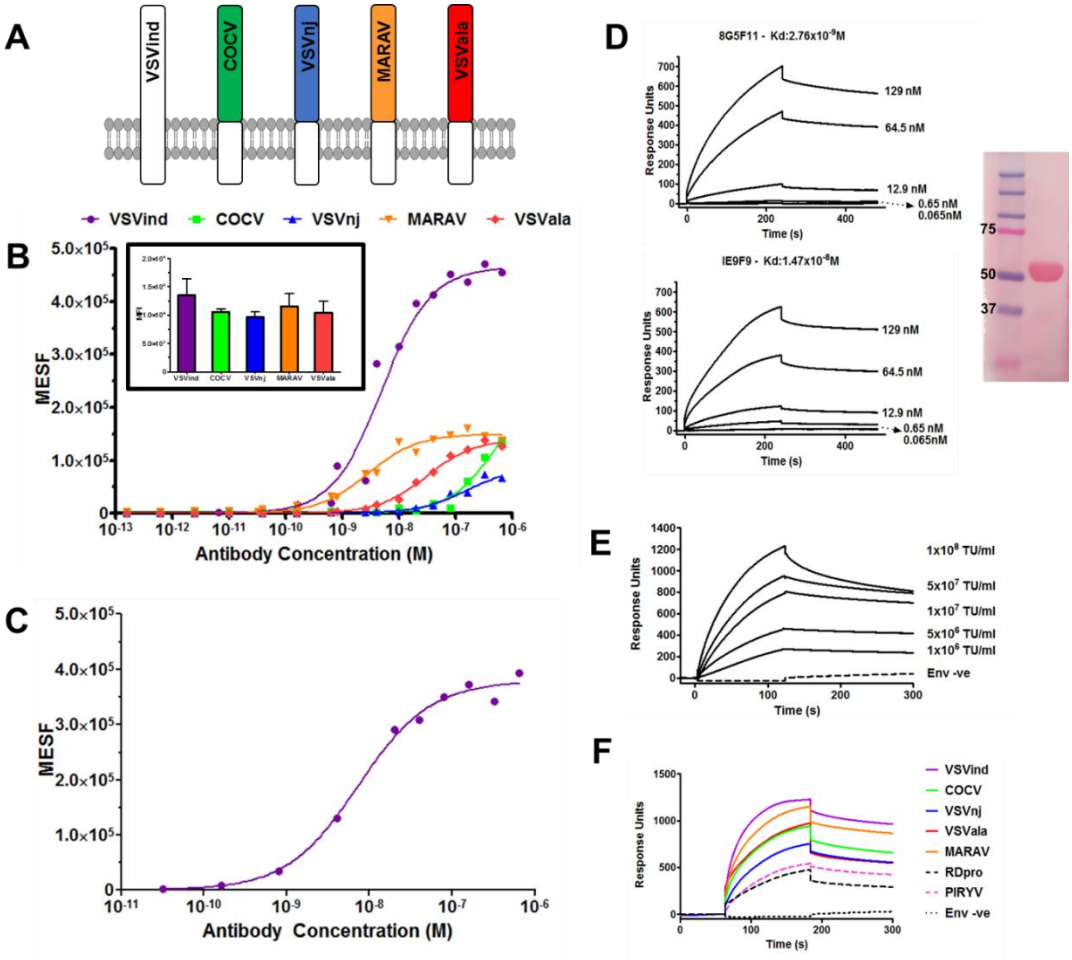

Figure 3-3: Investigation of 8G5F11 and IE9F9 Affinities Towards VSVind.G and Characterisation of 8G5F11 Cross-reactivity. (A) Schematic representation of the chimeric vesiculovirus G proteins with VSVind.G transmembrane and C-terminal domains. **(B)** HEK293T cells expressing these chimeric VesG were incubated with serial dilutions of 8G5F11 and analysed via flow cytometry. MFIs of the fluorescent signals were converted into the number of fluorophores using the MESF standard curve (see *Figure 2-2),* the background signal from mock-transfected HEK293T cells was subtracted, and binding saturation curves were plotted. The distinct affinities of the mAb towards different VesG are demonstrated by the shift in the slope of the binding curves. The curves were fitted and dissociation constants

(Kd) calculated using the software GraphPad Prism 5 modelling the interaction as 1:1 specific binding: VSVind.G: $2.64x10^{-9}$M, COCV.G: $5.88x10^{-7}$M, VSVnj.G: $1.57x10^{-7}$M, MARAV.G: $4.13x10^{-9}$M, VSVala.G: $3.09x10^{-9}$M. Data shown represent the mean of three repeats performed in duplicates. **(inset)** The expression levels of the chimeric G proteins were determined via intracellular P5D4 staining. Data shown represent the mean +/- standard deviation (SD) of three repeats performed in duplicates. **(C)** Binding saturation analysis of IE9F9 and VSVind.G. The dissociation constant of this interaction was calculated as $4.8x10^{-9}$M. **(D)** Surface plasmon resonance (SPR) analysis of **(top)** 8G5F11 and **(bottom)** IE9F9 binding to immobilised Gth in HBS-EP buffer. **(right)** SDS/PAGE of Gth (15µg) visualised via Ponceau S stain. The molecular mass markers (kDa) are shown on the left lane. **(E)** Surface plasmon resonance analysis of VSVind.G-LV binding to immobilised 8G5F11 in HBS-EP buffer. **(F)** Surface plasmon resonance analysis of Ves.G-LV ($1x10^8$ TU/ml) binding to immobilised 8G5F11 in HBS-EP buffer. The binding curves are normalised with regards to the relative response of unenveloped LV particles (Env -ve) which was regarded as the background. SPR data shown is one of the three repeats performed.

3.3.3.Determination of Neutralisation Activity of Anti-VSVind.G Antibodies

Three antibodies, 8G5F11, IE9F9, and VSV-Poly, were further evaluated for their ability to neutralise VSVind.G and VesG pseudotyped LVs (*Figure 3-4*). For this, a flow cytometry-based infection assay in the presence of the antibodies was developed. Briefly, GFP encoding LVs (LV.GFP) pseudotyped with VesG were incubated with serial dilutions of the antibodies in 1:1 v/v ratio at 37ºC for 1 hour. After the incubation, this LV-antibody mix was plated on HEK293T cells seeded 4h prior in 96 well plates with a total volume of 200µl. GFP expression of the cells were measured 48h after infection and results were normalised to control infection by LVs incubated with plain OptiMEM in parallel.

8G5F11 demonstrated varying strengths of neutralisation against VesG pseudotyped LVs, IC50 values ranging from 11.5ng/ml to 86.9µg/ml (*Figure 3-4A*). There was, however, a limited correlation between G proteins' binding strength and sensitivity of LV to neutralisation. While COCV.G and VSVala.G bound to 8G5F11 stronger compared to VSVnj.G, LVs pseudotyped with either G proteins were less sensitive to neutralisation than VSVnj.G-LV. (*Figure 3-2 and 3-3*). IE9F9 neutralised only VSVind.G-LV at an IC50 of 137ng/ml, about twelve-folds weaker than 8G5F11 (*Figure 3-4B*). In the case of VSV-Poly, I only observed cross neutralisation at high serum concentrations (*Figure 3-4C*). Furthermore, although VSV-Poly bound to PIRYV.G, it did not neutralise PIRYV.G-LVs.

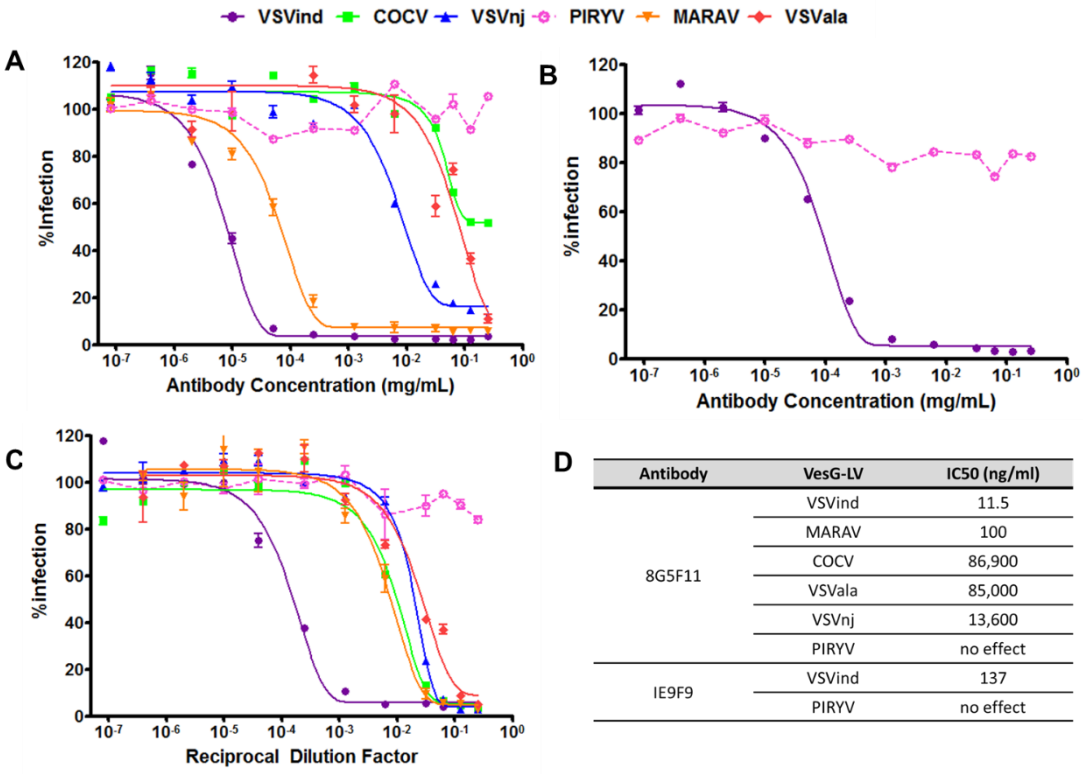

D

Antibody	VesG-LV	IC50 (ng/ml)
8G5F11	VSVind	11.5
	MARAV	100
	COCV	86,900
	VSVala	85,000
	VSVnj	13,600
	PIRYV	no effect
IE9F9	VSVind	137
	PIRYV	no effect

Figure 3-4: Neutralisation Activity Observed by mAbs and VSV-Poly. Neutralisation of VesG-LV by **(A)** 8G5F11, **(B)** IE9F9, and **(C)** VSV-Poly. Solid lines signify the neutralisation effect observed while the dotted lines indicate the lack of neutralisation. **(D)** Calculated IC50 values for 8G5F11 and IE9F9, depicting the potency of neutralisation. The curves were fitted using the software GraphPad Prism 5 modelled as an [inhibitor] vs response curve with variable Hill Slopes and IC50 values calculated. Data shown represent the mean +/- SD of three repeats performed in duplicates.

3.3.4.Investigation of Key Amino Acid Residues that Dictate Binding and Neutralisation via Epitope Mapping

I have identified that the two commercially available anti-VSVind.G antibodies are both strongly neutralising against VSVind.G-LV. However, they differ considerably in their ability to recognise other VesG. The epitopes these mAbs bind to might be the underlying reason behind this difference in characteristics. To address this, an epitope mapping analysis was undertaken. First, a series of chimeric G proteins between VSVind.G and COCV.G, A-chimaeras and B-chimaeras (produced by Maha Tijani, Collins/Takeuchi group, see *Table 2-2)*, were constructed (*Figure 3-5A*) and LVs pseudotyped with these chimeric proteins were investigated for their sensitivity to neutralisation by both mAbs (*Figure 3-5B and C*). The results enabled narrowing down of the epitopes of these mAbs to lie between amino acid (aa) residues 137-369 on VSVind.G. Combining this work with previously published data on 8G5F11 and IE9F9's epitopes obtained through mutant virus escape assays (*Figure 3-6A)* (312, 511, 512, 532, 533) I concentrated on two distinct regions on VSVind.G and synthesised twenty-two different mutant G proteins via site-directed mutagenesis to study the epitopes (*Figure 3-6*). The mutants were then evaluated for display and pseudotyping functionality (*Figure 3-7A*). All were confirmed to be functional and could successfully pseudotype LVs yielding comparable titres to their wild-type (wt) counterparts. Furthermore, they could be detected by extracellular VSV-Poly and intracellular P5D4 staining implying a lack of significant protein display and structure conformation issues (*Figure 3-7B*).

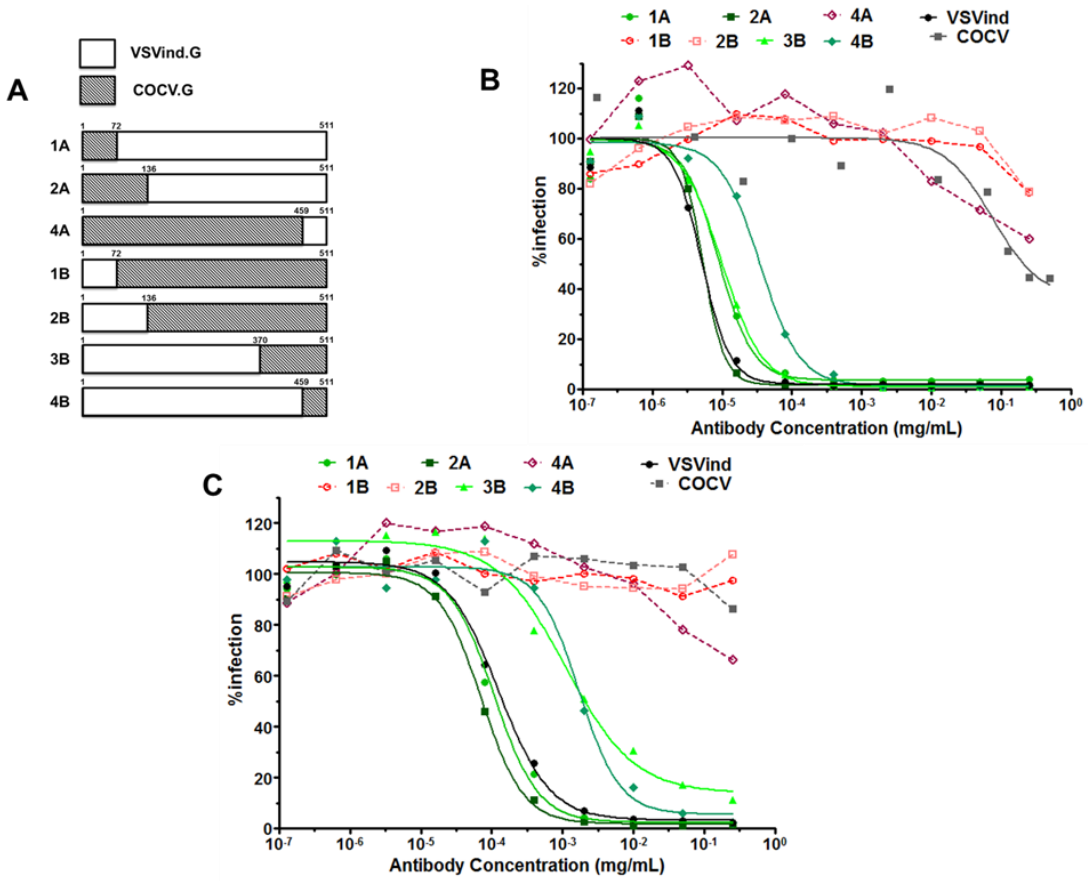

Figure 3-5: Sensitivity of Chimeric VSVind.G/COCV.G Proteins to Neutralisation by mAbs. **(A)** The design and the cross-over points of the chimeric G proteins are represented in linear diagrams, in which white bars stand for wild-type (wt) VSVind.G sequences and wt COCV.G sequences are represented by black hatched bars. The cross-over point between the two wt sequences is indicated by the amino acid number above the bar. Chimaera 3A, mirror image of 3B in terms of G protein construction, was non-functional and, therefore, was omitted from analyses. The neutralisation curves for chimeric G proteins plotted for **(B)** 8G5F11 and **(C)** IE9F9. Solid lines signify the neutralisation observed. The results indicated that the epitopes of both mAbs lie between aa residues 137-369 on VSVind.G. The curves were fitted using the software GraphPad Prism 5 modelled as an [inhibitor] vs response curve with variable Hill Slopes. Data shown represent the mean from three experiments performed in triplicates.

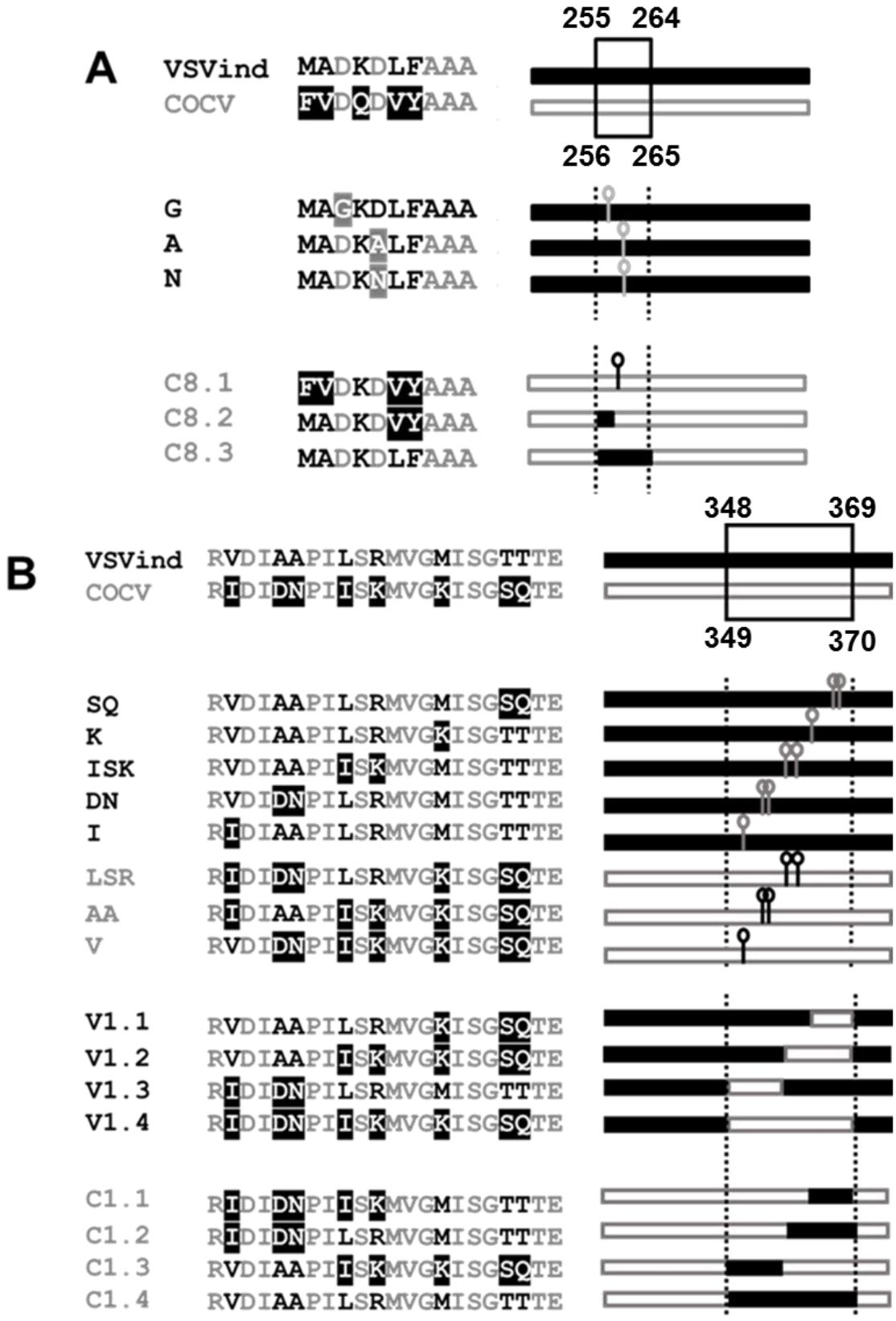
A
VSVind MADKDLFAAA
COCV FVDQDVYAAA
255 264
256 265
G MAGKDLFAAA
A MADKALFAAA
N MADKNLFAAA
C8.1 FVDKDVYAAA
C8.2 MADKDVYAAA
C8.3 MADKDLFAAA
B
VSVind RVDIAAPILSRMVGMISGTTTE
COCV RIDIDNPISKMVGKISGSQTE
348 369
349 370
SQ RVDIAAPILSRMVGMISGSQTE
K RVDIAAPILSRMVGKISGTTTE
ISK RVDIAAPISKMVGMISGTTTE
DN RVDIDNPILSRMVGMISGTTTE
I RIDIAAPILSRMVGMISGTTTE
LSR RIDIDNPILSRMVGKISGSQTE
AA RIDIAAPISKMVGKISGSQTE
V RVDIDNPISKMVGKISGSQTE
V1.1 RVDIAAPILSRMVGKISGSQTE
V1.2 RVDIAAPISKMVGKISGSQTE
V1.3 RIDIDNPILSRMVGMISGTTTE
V1.4 RIDIDNPISKMVGKISGSQTE
C1.1 RIDIDNPISKMVGMISGTTTE
C1.2 RIDIDNPILSRMVGMISGTTTE
C1.3 RVDIAAPISKMVGKISGSQTE
C1.4 RVDIAAPILSRMVGMISGTTTE

Figure 3-6: Mutants and Chimeric G Proteins Produced for Epitope Mapping. Mutants and chimaeras produced for epitope mapping of monoclonal antibodies **(A)** 8G5F11 and **(B)** IE9F9. Names and linear representations of the mutants and chimaeras are listed on either side of the amino acid alignments of the regions where mutations were made. The boundaries are labelled with respective amino acid numbers. Amino acid alignment legend: black, residues from wt VSVind.G; white with a black background, residues from wt COCV.G; grey, shared residues; white with a grey background, previously identified mutants (312). Linear G protein representations: dotted lines represent the regions that the mutations were carried out. Black bars represent wt VSVind.G sequences while grey-bordered bars are for wt COCV.G residues. A bar and a circle denote point mutations.

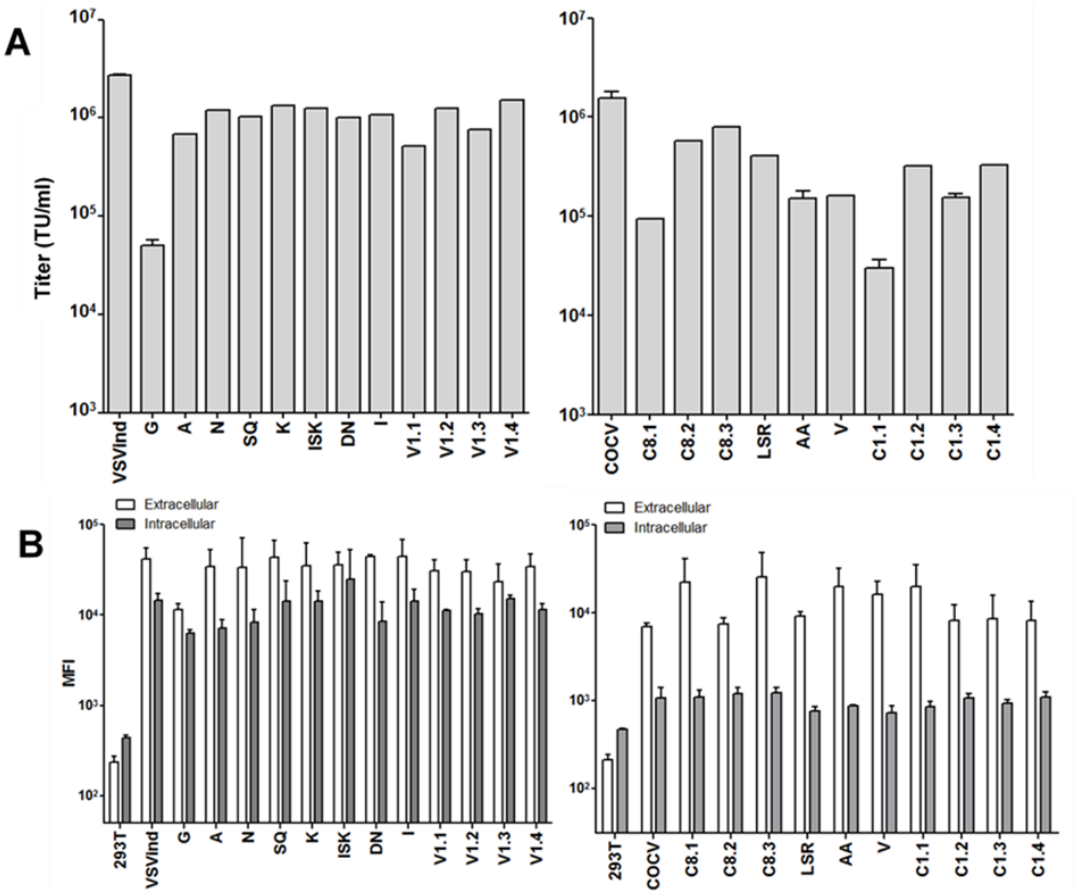

Figure 3-7: Investigation of Mutant G Protein Functionality and Display. **(A)** LVs pseudotyped with wt and mutant G proteins were titrated on HEK293T cells in parallel. The cell supernatant vector titres achieved are plotted for **(left)** VSVind.G and **(right)** COCV.G mutants. The data represent the average +/- SEM of two separate vector productions. **(B)** HEK293T cells were transfected to express the mutant G proteins on their surface. They were then incubated with intracellular P5D4 and extracellular VSV-Poly antibodies to examine the relative expression levels of **(left)** VSVind and **(right)** COCV mutant G compared to their wt counterparts. The data represent average +/- SD of three repeats performed in duplicates.

First, mAb binding to these mutants were examined via flow cytometry. Extracellular VSV-Poly and intracellular P5D4 stains determined relative expression levels of the mutants. For both sets, the relative difference between expression levels of mutant and wt proteins was in most cases less than two-fold (*Figure 3-8A and B*). In the case of 8G5F11, binding to VSVind.G mutants was reduced by approximately 100-folds while the amino acid switches on COCV.G enabled these mutants to bind to 8G5F11 at similar levels to that of wt VSVind.G (*Figure 3-8C*). This change in binding could also be observed on a western blot. While none of the VSVind.G mutants could be visualised, 8G5F11 could bind to COCV.G chimaera C8.3 (*Figure 3-8E*). It can be inferred from these results that aa 257-259 (DKD) are the predominant residues that dictate 8G5F11 binding to G proteins.

On the other hand, for IE9F9 no statistically significant changes in antibody binding were observed for VSVind.G mutants except for chimaeras V1.2 and V1.4 (*Figure 3-8D*). However, there was a substantial gain of binding effect for COCV.G mutants. While IE9F9 does not bind to wt COCV.G, mutations of amino acid residues LSR and AA (*Figure 3-6*) alone led to significant increases in the fluorescence signal, thus, antibody binding. C1.4 with both LSR and AA had a comparable MFI level to that of wt VSVind.G.

Neutralisation profile of both VSVind.G and COCV.G mutants was also examined (*Figure 3-8F-I*). While 8G5F11 did not neutralise VSVind.G mutants (*Figure 3-8F*), COCV.G mutants demonstrated varying degrees of sensitivity with the strongest binder being the most sensitive (*Figure 3-8H*). On the other hand, this was not the case for IE9F9 mutants. The mAb blocked VSVind.G mutant V1.2 pseudotyped LV infection in a dose-dependent manner, while V1.4-LVs were resistant to IE9F9 neutralisation (*Figure 3-8G*). Furthermore, no effect was observed on COCV.G mutant LV infection even though all bound to the mAb, some at similar levels to wt VSVind.G (*Figure 3-8I*). The data show that while 8G5F11 employs a neutralisation mechanism that is universally effective amongst the VesG it binds to, IE9F9's is VSVind.G specific, and mAb binding does not necessarily result in neutralisation.

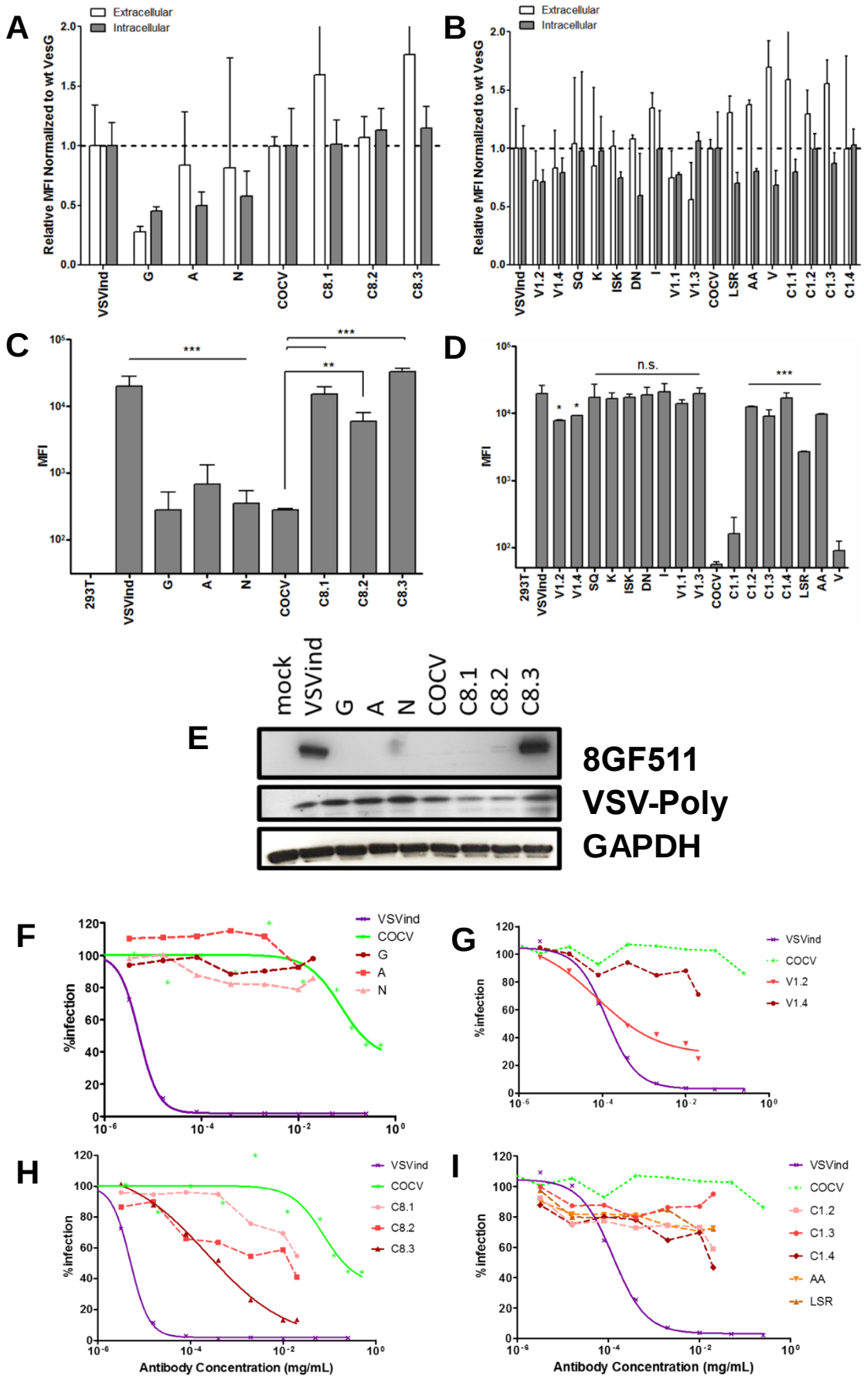
A
Extracellular
Intracellular
Relative MFI Normalized to wt VesG
VSVind
G
A
N
COCV
C8.1
C8.2
C8.3
B
Extracellular
Intracellular
Relative MFI Normalized to wt VesG
VSVind
V1.2
V1.4
SQ
K
ISK
DN
I
V1.1
V1.3
COCV
LSR
AA
V
C1.1
C1.2
C1.3
C1.4
C
MFI
293T
VSVind
G
A
N
COCV
C8.1
C8.2
C8.3
D
MFI
n.s.
293T
VSVind
V1.2
V1.4
SQ
K
ISK
DN
I
V1.1
V1.3
COCV
C1.1
C1.2
C1.3
C1.4
LSR
AA
V
E
mock
VSVind
G
A
N
COCV
C8.1
C8.2
C8.3
8GF511
VSV-Poly
GAPDH
F
%infection
VSVind
COCV
G
A
N
G
%infection
VSVind
COCV
V1.2
V1.4
H
%infection
VSVind
COCV
C8.1
C8.2
C8.3
Antibody Concentration (mg/mL)
I
%infection
VSVind
COCV
C1.2
C1.3
C1.4
AA
LSR
Antibody Concentration (mg/mL)

Figure 3-8: Investigation of Antibody Binding to Mutant G proteins and Neutralisation of Mutant-LVs. HEK293T cells were transfected to express the mutant G proteins on their surface. **(A-B)** The cells expressing chimeric mutants were stained with extracellular VSV-Poly (white bars) and intracellular P5D4 (grey bars) as expression control for the G proteins. The measured MFI values were normalised to the wt VesG signals for each set of mutants. The same population of cells were also incubated with **(C)** 8G5F11 and **(D)** IE9F9 at saturating concentrations. One-way ANOVA analysis with Dunnett's post-test was performed to compare the MFI values of mutant G proteins to that of their wild-type counterpart. Legged lines denote the significance of a single comparison, while straight lines signify all the individual comparisons within the group share the denoted significance unless otherwise stated (*, $p<0.05$; **, $p<0.01$; ***, $p<0.001$). This assay was performed three times in duplicates; mean +/- SD is plotted above. **(E)** Western blot analysis of 8G5F11 binding to wt and mutant G proteins. Data shown is one of the three repeats performed. The neutralisation curves for select mutant G-LV are plotted for **(F and H)** 8G5F11 and **(G and I)** IE9F9. Solid lines signify the neutralisation effect observed. **(F and G)** Previously reported reductions in binding for VSVind.G mutants translated into either complete or partial resistance to neutralisation by both antibodies. For COCV.G mutants **(H and I),** the mutations conferred the G proteins sensitivity to neutralisation by 8G5F11 but not by IE9F9. The curves were fitted using the software GraphPad Prism 5 modelled as an [inhibitor] vs response curve with variable Hill Slopes. Data shown represent the mean from three experiments performed in independent triplicates.

3.3.5.Investigation of Neutralisation Mechanisms Utilised by the mAbs: Binding Competition with Low-density Lipoprotein Receptor (LDLR)

Antibodies neutralise viruses and viral vectors by several mechanisms. Many neutralising antibodies (nAbs) prevent virions from interacting with cellular receptors (389). VSVind.G's primary receptor has been identified as the low-density lipoprotein receptor (LDLR) (321, 323). All six VesG investigated throughout this work have high degrees of sequence homology on amino acid level (i.e. five >50% and three >70%) and are phylogenetically and serologically closely related. Therefore, I hypothesised that the primary cellular entryway might be conserved amongst VesG.

To evaluate this, first, the interaction between soluble recombinant LDLR (sLDLR) and G proteins expressed on the surface of HEK293T cells was investigated. As with previous assays, RDpro envelope was utilised as a negative control since its primary receptor has been identified as ASCT-2, a neutral amino acid transporter (60, 537, 538). Briefly, RDpro and VesG expressing cells were incubated with respective antibodies and sLDLR in parallel. VSV-Poly was used to determine envelope expression for VesG and goat anti-RD114 antiserum for RDpro expression. A separate aliquot of the same cell population was also incubated with sLDLR and was probed for the C-term 6XHis-tag on the recombinant protein to determine binding to G proteins. All cells were then analysed via flow cytometry. While all proteins were successfully expressed on the cell surface, all VesG but PIRYV.G bound to sLDLR (*Figure 3-9A*). PIRYV.G, like the unrelated RDpro envelope, did not interact with the recombinant receptor protein.

This discrepancy in binding was further explored through an infection inhibition assay. HEK293T cells were challenged with VesG and RDpro pseudotyped LVs at two multiplicities of infection (MOI) in the presence and absence of sLDLR. In line with the binding profiles, PIRYV.G-LV and RDpro-LV infections were unaffected by the presence of sLDLR in the media (*Figure 3-9B*). On the other hand, VesG-LV infection was blocked in a dose-dependent manner with on average 90% infection inhibition achieved with 3µg/mL sLDLR for all

pseudotypes at both MOIs. The infection hindrance observed or lack thereof in the case of PIRYV.G, combined with the binding data, strongly suggested that the remaining five VesG shared LDLR as their main receptor for viral entry into cells.

Therefore, I investigated the competition in binding VSVind.G between mAbs and LDLR via SPR as a potential neutralisation mechanism for the mAbs (*Figure 3-9C*). VSVind.G (Gth, see section 3.3.2), immobilised on the chip surface, was saturated with repeated injections of 8G5F11 and IE9F9. This was followed by an injection of recombinant soluble human LDLR (sLDLR), and its binding to Gth was examined. While sLDLR was able to bind to Gth following 8G5F11 saturation as well as without antibody exposure (buffer control), this interaction was almost completely abrogated by IE9F9. These data suggest that IE9F9, but not 8G5F11, neutralises VSVind.G-LV by blocking the G protein-receptor interaction either through steric hindrance or direct competition.

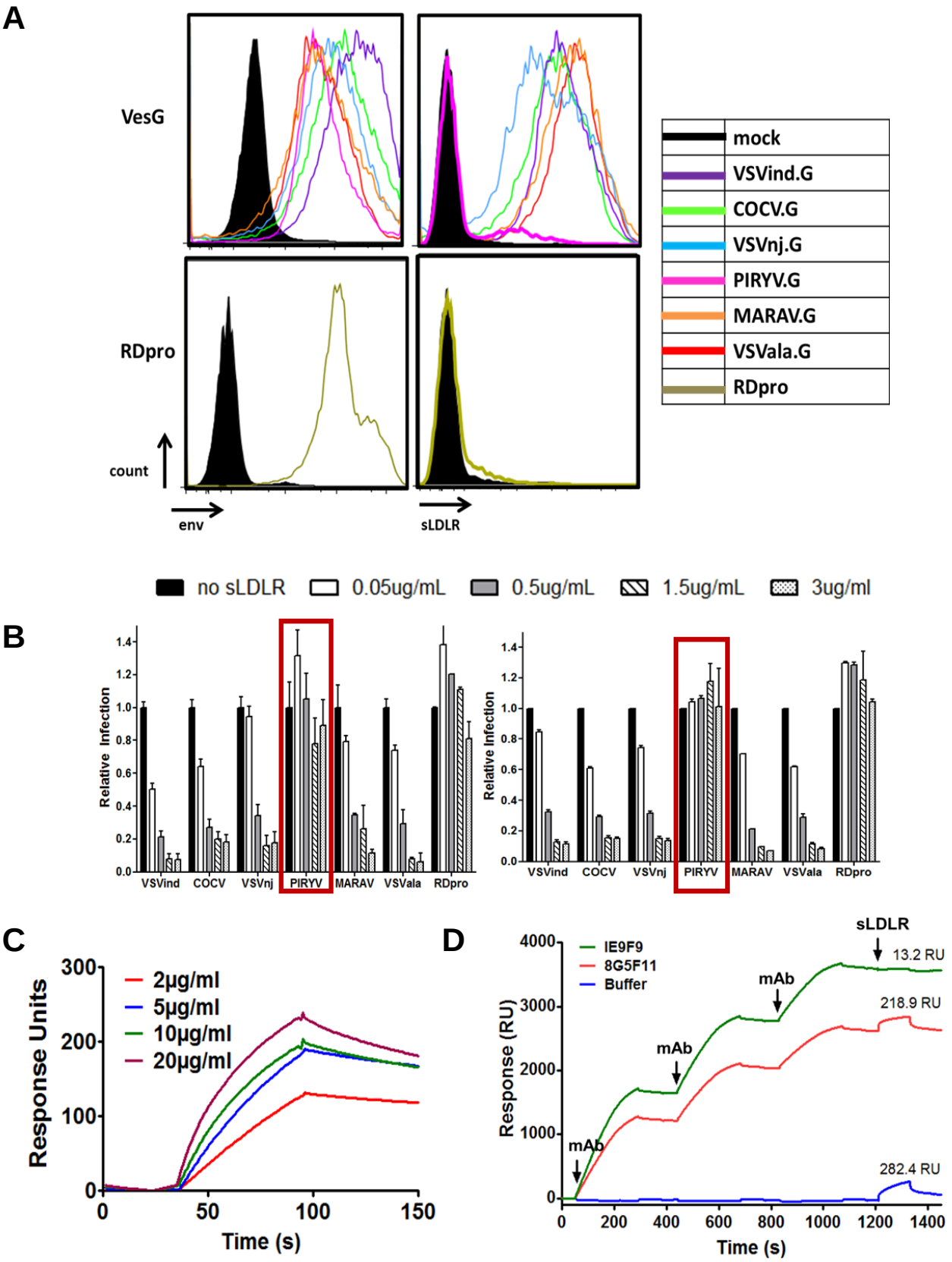
A
VesG
RDpro
count
env
sLDLR
mock
VSVind.G
COCV.G
VSVnj.G
PIRYV.G
MARAV.G
VSVala.G
RDpro
B
no sLDLR
0.05ug/mL
0.5ug/mL
1.5ug/mL
3ug/ml
Relative Infection
VSVind
COCV
VSVnj
PIRYV
MARAV
VSVala
RDpro
C
Response Units
2μg/ml
5μg/ml
10μg/ml
20μg/ml
Time (s)
D
IE9F9
8G5F11
Buffer
Response (RU)
mAb
sLDLR
13.2 RU
218.9 RU
282.4 RU
Time (s)

Figure 3-9: Exploring sLDLR VesG Interactions and How mAb Binding Affects Receptor Recognition. **(A)** VesG and RDpro expressing HEK293T cells were incubated with **(left)** VSV-Poly and anti-RD114 antiserum to determine envelope expression and **(right)** sLDLR in parallel. The cells were then probed with the respective secondary antibodies to determine envelope expression and anti-6XHis-tag antibody for sLDLR binding. PIRYV.G did not bind to sLDLR while other VesG showed similar levels of interaction with the soluble receptor protein (The maximum difference between the calculated MFI values was <3-fold)**.** Data shown is one of the three repeats performed. **(B)** HEK293T cells were challenged with GFP expressing VesG and RDpro pseudotyped LV at MOIs **(left)** 0.1 and **(right)** 0.5 in the absence and presence of sLDLR. The infection rates were analysed 48h later via flow cytometry and were normalised to that of sLDLR-free samples. Percentage GFP of sLDLR-free samples ranged 2-10% and 13-30% for MOI 0.1 and 0.5 respectively. Data shown represent relative infection +/- SD from three experiments performed in duplicates. **(C)** Concentration scouting of recombinant LDLR binding to immobilised Gth. LDLR was injected over Gth to determine its binding levels to the G protein at various concentrations. From the relative binding responses 10µg/ml was determined to be the optimal concentration to be used in the competitive binding study. The data presented represent one of the three repeats performed. **(D)** 8G5F11 and IE9F9 were injected over immobilised Gth at 10µg/ml concentration three times to achieve binding saturation. Following this, sLDLR was injected over the chip at the same concentration, and its binding to Gth was measured. As negative control, an identical sLDLR injection was performed following multiple injections of HBS-EP running buffer. Measured sLDLR binding levels are indicated above the binding response curves and times of injections are marked with arrows. The data presented represent one of the three repeats performed.

3.4.Discussion

As discussed in section 3.1, lentiviral vectors pseudotyped with VSVind.G have several beneficial characteristics including high-titres, physical stability, and broad cell tropism. However, there are a couple of major problems associated with the use of this envelope: VSVind.G is reported to be cytotoxic to cells, therefore, it is thought to be difficult to express it constitutively in stable packaging cell lines, and VSVind.G-LVs are sensitive to complement-mediated inactivation (193, 266, 267, 466-469). Therefore, several G proteins of the other members of the vesiculovirus subfamily are proposed as alternative envelopes to pseudotype LVs (200, 202, 471). However, currently, there are no commercially available reagents to identify or characterise these new G proteins.

Historically antibody-based research has been utilised effectively to elucidate antigenic determinants in various viral envelopes. The structure-function studies of neutralising antibodies have led to invaluable findings with regards to viral evolution, pathogenesis, and essential targets of innate and adaptive immune responses (526-531).

VSVind.G crystal structure has been extensively studied with regards to viral fusion, receptor attachment, and infection (269, 270, 290, 297, 307, 323). However, its antigenic sites and neutralising epitopes remain to be fully characterised. Current knowledge on VesG binding antibodies dates back to late twentieth century, during which several scientists have investigated cross-reacting and cross-neutralising mAbs between VSVind.G and VSVnj.G (511) and have loosely mapped four major antigenic sites (312, 512, 533).

In the past several decades VSVind has developed into a potent and efficient oncolytic virotherapy platform while numerous successful gene therapies have been conducted using VSVind.G pseudotyped LVs in the laboratory and the clinic (2, 539). However, the anti-VesG antibody research has not developed as rapidly and extensively. Currently, the majority of the anti-VSVind.G monoclonal antibodies commercially available are directed towards the C terminal tail of the G protein. The eleven amino acid long epitope located there (i.e. YTDIEMNRLGK) is widely utilised as a peptide-tag to purify and analyse

various other proteins of interest. 8G5F11 and IE9F9, produced for antigenic site studies (511), are the only two commercially available mAbs against ectodomain epitopes.

In this chapter, I undertook a detailed investigation of the two commercially available monoclonal anti-VSVind.G antibodies with ectodomain epitopes: 8G5F11 and IE9F9. Unlike 8G5F11 which could recognise a variety of vesiculovirus G proteins and neutralise VesG pseudotyped LVs, IE9F9 only bound to VSVind.G. Moreover, VSV-Poly, a polyclonal anti-VSVind.G antibody, demonstrated binding and neutralising activities similar to 8G5F11.

Intriguingly, 8G5F11 bound to even distant relatives of VSVind.G, e.g. VSVnj.G, with high affinity implying its epitope might be well-conserved amongst the vesiculoviruses. However, there was a lack of correlation between the affinities derived from binding saturation analyses and phylogenetic relatedness. mAb's interaction with COCV.G, one of the closest relatives of VSVind.G with 72% homology on amino acid level, was approximately 250-fold weaker compared to VSVind.G (*Figure 3-3B*).

Fine mapping of 8G5F11's epitope provided possible explanations for this discrepancy. I identified that the predominant residues for 8G5F11 binding are located at positions 257-259 (DKD) on VSVind.G. In this key determinant two negatively charged aspartic acid residues flank the positively charged lysine. Antibody binding was significantly reduced when either of the aspartic acid residues was mutated into a neutral amino acid (*Figure 3-8C*). These mutations possibly prevent the formation of salt-bridges and destabilise the structure of the α-helix in which 8G5F11's epitope is located (269, 270, 297).

Comparison of the corresponding three residues on other VesG revealed insights demonstrating that 8G5F11 binding is considerably more dependent on the overall charges of the amino acid side chains rather than the types of residues (*Figure 3-10*). Since MARAV.G has identical residues at these positions 8G5F11 binds to this protein as strongly as it does to VSVind.G. However, the mAb's affinity for VSVala.G is almost identical to that of both VSVind.G and MARAV.G although the residues are not fully conserved. In VSVala.G the second aspartic acid residue is replaced with glutamic acid.

However, it is possible that the conservation of the second negative charge and the structural similarities between these two residues enable a robust G protein-antibody interaction. In contrast, in both COCV.G and VSVnj.G, although both aspartic acid residues are retained the positively charged amino acid in between is missing: the lysine is replaced with a hydrophilic, polar glutamine and a non-polar proline residue in these two G proteins respectively.

In VSVind.G's 3D structure several pH sensing residues, D268, D274, E276, and D395 (330), are located in the vicinity of the epitope. In addition, it is known that salt-bridges between E286-K290 (331, 332) act as stabilisers in the pre-fusion structure of the protein. The charge distribution of 8G5F11's binding site enables the epitope to fold into an α-helical conformation which most probably contributes to the aforementioned interactions (269, 270, 297). The absence of such charge distribution in COCV.G and VSVnj.G implies that although these G proteins are phylogenetically closely related, they might be structurally distinct. Lastly, the corresponding aa residues in PIRYV.G, VEQ, have electrostatically and structurally different characteristics to that of lysine and aspartic acid leading to the lack of interaction between the mAb and G protein.

A

VSVind.G	252	WFEMADKDLFAA----A	264
COCV.G	253	WFEFVDQDVYAA----A	265
VSVnj.G	252	WFQIMDPDLDKTVRDLP	268
VSVala.G	253	WFEMVDKELLES----V	265
MARAV.G	252	WFELVDKDLFQA----A	264
PIRYV.G	252	WMGLNVEQSIREKKISA	268

B

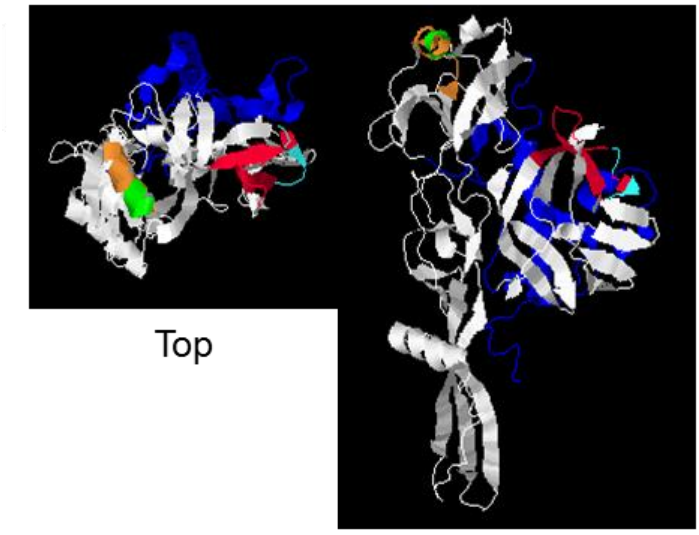

Pre-fusion

C

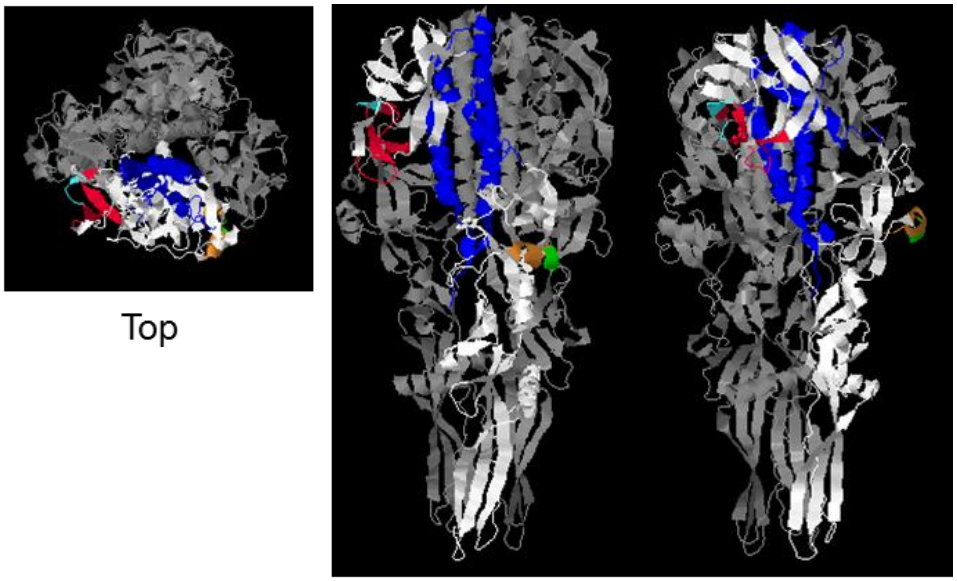

Post-fusion

Figure 3-10: 8G5F11 and IE9F9 Epitopes Mapped onto the 3D Crystal Structure of VSVind.G. **(A)** Comparison of 8G5F11's epitope in other VesG through amino acid alignment. Amino acid residues for the vesiculovirus G proteins were retrieved from UniProt. The sequences were aligned using ClustalOmega online multiple sequence alignment tool (EMBL-EPI) (see *Table 2-16)*, and the alignments were visualised using JalView software (294). The boundaries are labelled with respective amino acid numbers. Dashed lines represent gaps introduced to maximise matching of amino acid residues. Blue shading indicates percent identity; dark blue: 80-100%, medium blue: 60-80% light blue: 40-60%, and no colour indicating <40% identity. Amino acid residues that dictate 8G5F11 binding are highlighted in a red box. Epitopes recognised by 8G5F11 and IE9F9 mapped onto VSVind.G **(B)** pre-fusion and **(C)** post-fusion (PBD IDs: 5I2S and 5I2M respectively 3D crystal structures. Blue, trimerisation domain; orange, 8G5F11 epitope; red, IE9F9 epitope. The key amino acids discussed in the chapter are also identified 352-353 (AA), and 356-358 (LSR) are turquoise, 257-259 (DKD) are green. Epitope mapping and colouring of the 3D crystal structures were performed using JalView.

Furthermore, I demonstrated that IE9F9 binds a β-sheet rich domain of the VSVind G protein (270, 297). In contrast to the significant abrogation of binding observed between 8G5F11 and VSVind.G mutants, a similar loss of function effect was not observed between IE9F9 and the mutants. This signifies that the antibody might be relying on other structural cues and environmental charges around it for binding or can utilise a secondary epitope. However, by switching the corresponding residues on COCV.G with VSVind.G's, I was able to identify two determinants, AA and LSR, located at positions 352-353 and 356-358 respectively on VSVind.G, which are key to this mAb's binding.

Overall, all three antibodies examined demonstrated neutralising activities. 8G5F11 had the greatest ability to cross-neutralise; inhibiting infections of LVs pseudotyped with five of the six vesiculovirus G proteins tested. However, for the mAb higher affinity towards a G protein did not translate into stronger neutralisation (*Figures 3-3 and 3-4*). This suggests that innate differences between VesG, such as protein structure, might be playing a role in LV neutralisation. Since the structures of VesG other than VSVind.G and CHAV.G are not yet delineated, it is hard to point out the key factors and mechanisms involved accurately.

However, 8G5F11's epitope lies close to the cross-over point between pleckstrin homology and trimerisation domains of VSVind.G (270, 297, 323, 331, 332). In the proximity of the epitope, several hinge segments have been identified which undergo large rearrangements in their relative orientations while the G protein refolds from pre- to post-fusion conformation in the low-pH conditions of the endosomes following endocytosis (269, 323, 331). Therefore, I propose that 8G5F11 might be hindering this process ultimately preventing viral fusion and infection. As pH-induced conformational changes during viral fusion is a shared characteristic amongst VesG (540), hence, this might be the feature 8G5F11 exploits to cross-neutralise VesG-LV.

Moreover, I have identified that IE9F9 blocks VSVind.G from binding to its primary receptor: LDLR (*Figure 3-9C*). The crystal structure of VSVind.G in complex with LDLR have been recently delineated. Co-crystallisation of the

bound receptor-G protein complex revealed that VSVind.G can interact with two distinct cysteine-rich domains (CR2 and CR3) of LDLR (323). Several determinants on VSVind.G mediate the interactions between the G protein and the CR domains; one of which lies between residues 366-370. This is only seven amino acids away from the critical determinants AA and LSR. Hence, it can be concluded that IE9F9 blocks receptor binding via physical hindrance. Sequence alignment of VesG revealed that neither AA nor LSR is conserved within the genus. Therefore, although I have demonstrated several other vesiculovirus G proteins interact with LDLR, the use of this epitope cannot be generalised to the other members of the genus, making IE9F9's epitope and neutralisation mechanism specific to VSVind.G. mAb's lack of cross-reactivity and cross-neutralisation (*Figures 3-3 and 3-4*) as well as its failure to neutralise COCV.G mutants when its epitope is inserted into the wt G protein *(Figure 3-8*) strengthens the theory that the LDLR binding epitope is not conserved amongst VesG. Nikolic and colleagues have demonstrated that VSVind.G has specifically evolved to interact with the CR domains of LDLR and other LDLR family members (323). The other members of the receptor family have already been identified as secondary ports of entry for the virus (321). Complete neutralisation achieved with IE9F9 (*Figure 3-4B*) indicates that the other LDLR family members might be interacting with the same epitope on VSVind.G as well.

Following VSVind.G-LVs success in clinical gene therapies, more research has been focused on generating stable packaging cell lines (PCLs) for long-term, low-cost, high-yield LV production (196, 541, 542). Thus far, several PCLs have been generated using inducible promoters to drive VSVind.G expression (197, 520, 521). In addition, a few other vesiculovirus G proteins have been proposed as promising candidates owing to their several advantages over VSVind.G (200, 202, 471). Collins/Takeuchi group's (UCL/NIBSC, UK) efforts have led to the establishment of WinPac cells to which both RD114 derived RDpro envelope (198) and COCV.G envelope been adapted (manuscript accepted) (543). Availability of a mAb which binds to various VesG provides the opportunity for these G proteins to be utilised in PCL generation in order to exploit possible differences in tropism and serum

resistance, as it provides the opportunity for researchers to detect and track envelope expression cells as well as use the mAb in various LV characterisation and infection assays.

Further work on the two strongly neutralising epitopes 8G5F11 and IE9F9 recognise regarding their immunodominance will be instrumental. A detailed immunogenic characterisation of these epitopes may provide valuable insights on host-pathogen interactions and adaptive immune response targets towards LVs and viruses in gene therapy or oncolytic virotherapy applications. Furthermore, biomathematical analyses on degrees of epitope conservation could help researchers understand more about the co-evolution of the genus vesiculovirus. Thus, further structure-function studies on VSVind.G and other VesG should be performed exploring both 8G5F11 and IE9F9 binding and neutralisation. The information acquired from these studies may provide the opportunity for modifying VSVind.G or adapting other VesG to improve G protein-containing advanced therapy medicinal products and VSVind-based vaccine vectors.

A couple of the experiments performed in this chapter had minor limitations; first of which was the binding affinity analysis shown in *Figure 3-3B.* To control expression levels, intracellular antibody staining was utilised against the VSVInd.G tail added onto VesG. Despite intracellular P5D4 signal was comparable for all VesG, VSVind.G demonstrated approximately four-times higher maximum binding levels to 8G5F11 compared to other VesG. This might be because although the chimeric VesG are expressed at similar levels to wt VSVind.G (determined by P5D4 staining) a smaller number of G protein spikes might be present on the cell surface either due to inherent properties of VesG or to protein trafficking issue. Another explanation for the binding levels might be that 8G5F11's epitope might not be accessible to the mAb when VesG other than VSVind.G assume their homodimeric or homotrimeric conformations, therefore, reducing the number of bound 8G5F11 molecules on the cell surface. The second one was the competitive binding experiment performed using SPR (see *Figure 3-9D).* Although mAb saturation was aimed to be achieved using a slow injecting method with high mAb concentration, the Biacore T100 utilised in the experiments did not allow for more than three

injections thus leaving both IE9F9 and 8G5F11 binding levels below saturation. But despite this limitation the desired hindrance effect was observed. All in all, taken together the work presented in this chapter identifies a commercially available reagent that can be widely utilised in VesG research.

4 Sensitivity of Lentiviral Vectors Pseudotyped with Vesiculovirus G Proteins to Inactivation by Mammalian Sera

4.1.Overview

Innate immune responses are the first line of defence against viral infections and lentiviral vectors (489). This response is generated by the complement system, phagocytes, and antigen presenting cells (APCs) (502).

The complement cascade is one of the central pathways of defence of the immune system (451-453). The cascade, made up of more than thirty proteins, can follow three different pathways; classical, alternative, and the lectin route all leading to cell lysis (454). The complement response by nonimmune sera against versatile vectors utilised in oncolytic virotherapy such as VSVind and MARAV is a severe drawback of systemic therapy for cancer. Also, a similar barrier needs to be addressed with regards to *in vivo* viral vector gene therapy

as serum inactivation of the viral pseudotypes diminishes the effectiveness of otherwise highly efficient vectors (466).

Involved in all three pathways, C3 serves as the pivotal component of the complement-mediated immunity. C3 is activated following its cleavage into two functional subunits: C3a and C3b. C3a is involved in modulation of inflammation while C3b is an opsonin which can covalently bind to any adjacent surfaces and mark it for phagocyte recruitment (544).

The classical pathway has a recognition molecule, C1q (545, 546). C1q deposition is dictated mostly via charged patterns. It can recognise numerous molecules including immune complexes containing natural IgG and IgM which are involved in lentiviral vector inactivation (547). C1q can also bind to molecular patterns displayed on surfaces of the pathogens (e.g. bacterial lipopolysaccharides, viral capsid peptidoglycans, and endotoxins) (545, 548). As C1q can interact with more than a hundred molecules, classical pathway activation can occur both in an immune complex-dependent or -independent manner. Thus, complement activation relies on the versatility of the target pattern recognition molecules that can discriminate between pathogen-associated molecules and host cells.

The alternative pathway is activated by spontaneous hydrolysis of C3 into C3b. In addition to contributing to membrane attack complex formation, the pathway also functions as a positive feedback mechanism amplifying the activation of C3 initiated via the classical or the lectin pathway (549). Variety of complement regulatory proteins mediate the functions of this pathway (550). Incorporation of membrane associated regulators found on human cell lines, for example CD55 and CD59, is a known mechanism of evasion utilised by viruses such as HIV-1, human T-lymphotropic virus-1, and human cytomegalovirus (551, 552). During the production of lentiviral vectors, the envelope protein expressed on the producer cells may interact differently with these membrane-associated proteins restricting their incorporation onto the vector membrane or blocking their functions conferring sensitivity to complement-mediated inactivation (266, 551, 553, 554).

The lectin pathway functions through MBL, a lectin that can recognise and bind to a variety of carbohydrates on pathogen surfaces (555). Once bound it can either act as an opsonin or further activate the complement cascade. Although specific function of the lectin pathway in innate immunity against viral vectors is yet to be elucidated, these carbohydrate-protein interactions have been shown to neutralise viral infections (549). Notably, MBL can bind to HIV-1 infected cells and HIV-1 envelope protein gp120 (556, 557) leading to opsonisation of HIV-1 particles (558). Recently, several studies have demonstrated that with Ebola virus, dengue virus, West Nile virus and retroviral vectors pseudotyped with glycoproteins from these viruses are susceptible to MBL-mediated neutralisation (559, 560).

Serum sensitivity of wt VSVind and VSVind.G-LV is well-established in the literature (266, 466-470). IgM antibodies and complement components of nonimmune human, mouse, and dog sera have been reported to neutralise these vectors (467). Furthermore, α-galactosylation of these vectors was found to make them more vulnerable to complement-mediated killing (470). Recent studies have demonstrated the dose-dependent nature of complement-mediated LV inactivation. The high titre vector preparations utilised *in vivo* rapidly saturate this neutralising response hence explaining the achievement of successful gene transfer in some animal models such as dogs despite previously established LV neutralising activities (174, 561, 562).

The complement system can also exert unfavourable pressure on LV efficacy by mediating phagocytosis through complement receptors and further activation of innate responses rather than blocking efficient gene transfer to target cells (502). Therefore, it may still be beneficial to avoid complement activation. There is evidence that alternative LV pseudotypes (e.g. RDpro, COCV.G, PIRYV.G) (200, 471, 515, 517), or co-display of complement regulatory proteins on vector particles (563), or synthetic modification (e.g. PEGylation) of envelope proteins (466), or mutant envelopes produced by directed evolution (564) can confer resistance to complement-mediated inactivation. Furthermore, the amount of complement sensitive envelope spikes on the LV surface and the presence of complement-blocking antibodies

in the vector preparation also play a role in preserving LV infectivity in human serum samples (562).

When complement cascade components and LV-binding antibodies opsonise LV particles resulting in phagocytosis by macrophages and APCs, these cells act as detectors for pathogen-associated molecular pathways and can promote inflammation and activate adaptive immune responses through antigen presentation (428, 435, 565). LV RNA and proviral DNA can engage toll-like receptor (TLR) 3 and TLR7 inducing a robust type I interferon (IFN) response (489, 490, 566, 567). In addition, a transient increase in proinflammatory cytokines has been observed within hours of LV administration (174). These cytokines can limit the gene delivery efficiency of the vectors and promote adaptive immune responses through APCs (490, 567) and antigen-specific T cell responses (435). Therefore, developing viral vectors with envelopes that can resist complement-mediated inactivation or avoid complement cascade activation may allow optimal gene transfer to target cells after systemic *in vivo* delivery while minimising vector-related toxicity and negating the need for high repetitive dosing.

4.2. Aims

The work presented in this chapter was aimed at characterising VesG envelopes for their sensitivity to complement-mediated inactivation by fresh human serum. The scope of the work was later expanded to include some other mammalian sera. Lastly, some mix-and-match chimeric constructs were investigated to map the region(s) on the G proteins that are responsive to serum inactivation.

4.3.Results

4.3.1.Inactivation of VesG Pseudotyped LVs by Mammalian Sera

One limitation of VSVind.G-LV is that, in humans, serum neutralisation of LVs reduces their effectiveness *in vivo.* Therefore, I wanted to investigate the sensitivity of other VesG-LV to inactivation by human serum complement (*Figure 4-1)*. For this, GFP encoding LVs (LV.GFP) pseudotyped with VesG and RDpro envelopes were incubated in serum-free media, heat-inactivated (HI) or fresh human serum for 1h at 37ºC and plated onto HEK293T cells. Infectious titres of the LVs were measured 48h later via flow cytometry.

When the titres were normalised to that of serum-free samples, the loss of titres for all envelopes incubated in HI serum was less than 30%, indicating the inactivation of LVs by fresh human serum was due to the heat-labile component which includes the complement cascade proteins. The level of serum inactivation varied significantly ($p<0.001$) between VSVind.G and three other VesG, COCV.G, PIRYV.G, and MARAV.G. While VSVind.G-LVs lost more than 70% of their original titre, COCV.G, MARAV.G, and PIRYV.G-LVs showed similar levels of inactivation resistance to that of RDpro-LVs which is known to withstand complement inactivation. On the other hand, VSVnj.G and VSVala.G-LVs were, like VSVind.G, highly sensitive to fresh human serum.

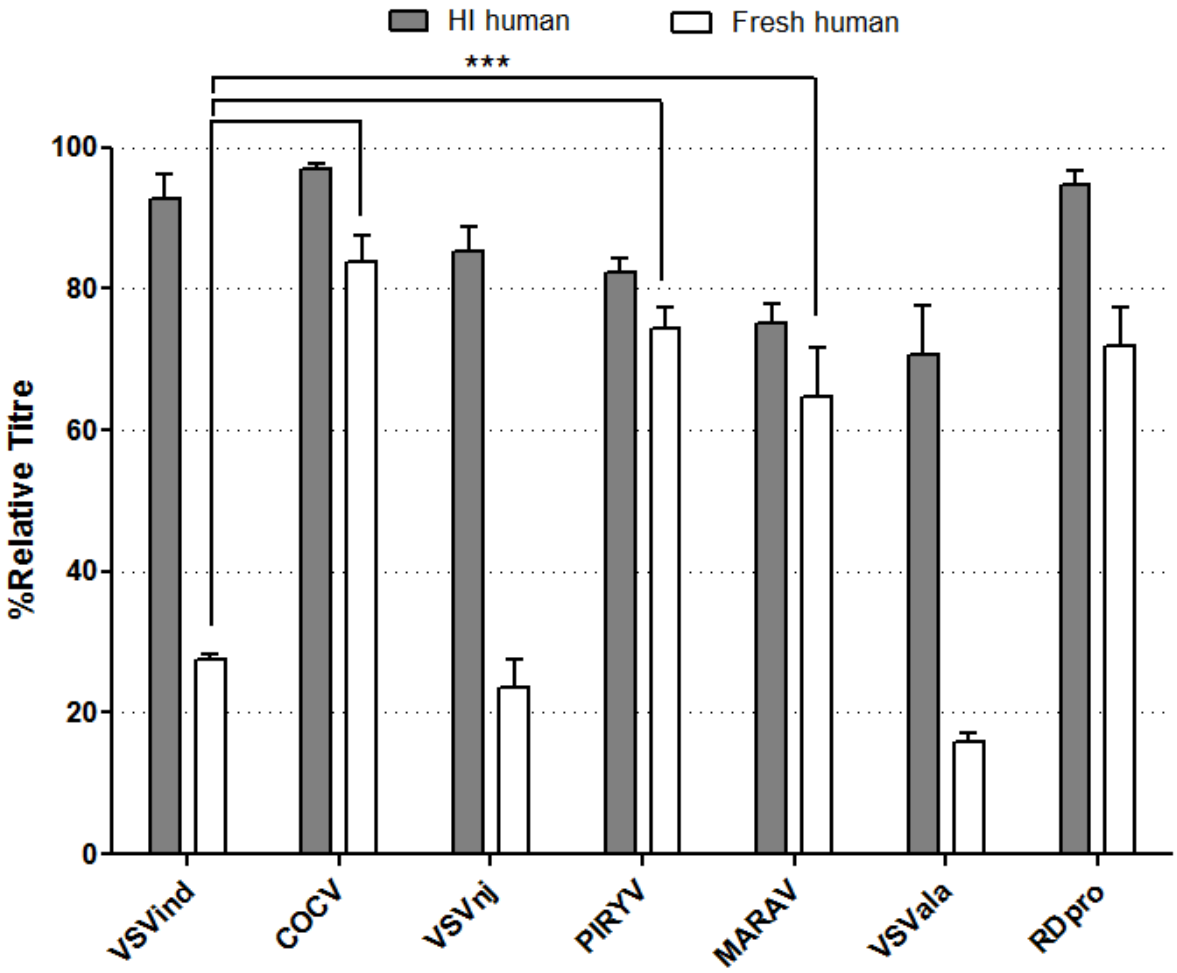

Figure 4-1: Neutralisation of Lentiviral Pseudotypes by Fresh Human Serum. VesG and RDpro pseudotyped LV.GFP were incubated with serum-free media, fresh or heat-inactivated (HI) human serum at 37ºC for 1h and plated on 293T cells. The infectious titres of the LVs were measured 48h later via flow cytometry and were normalised to that of serum-free samples. While the loss of titres for HI samples **(grey)** was less than 30% for all LV, the level of inactivation by fresh serum **(white)** varied significantly amongst VesG-LV. Percentage GFP of serum-free samples ranged 10-30%. Data shown represent relative titres +/- SD for four experiments performed in duplicates. One-way ANOVA analysis with Dunnett's post-test was performed to compare relative titres. (*** $p<0.001$)

The study was then expanded to include sera from other mammalian species, specifically mouse, rabbit, and guinea pig: animal models commonly used in gene therapy studies (568). The relative sensitivity of LVs to neutralisation by these sera was compared as above (*Figure 4-2).* Overall, COCV.G, PIRYV.G, and MARAV.G envelopes proved to be intrinsically more resistant to complement-mediated inactivation by mammalian sera compared to VSVind.G and VSVnj.G. On average, the reduction of overall titres of COCV.G, PIRYV.G, and MARAV.G-LV for all three sera were 20-30%, while VSVind.G-LV titres decreased by 50-90%. Lastly, VSVala.G was more resistant to inactivation by these mammalian sera than by human serum, performing better than VSVind.G and VSVnj.

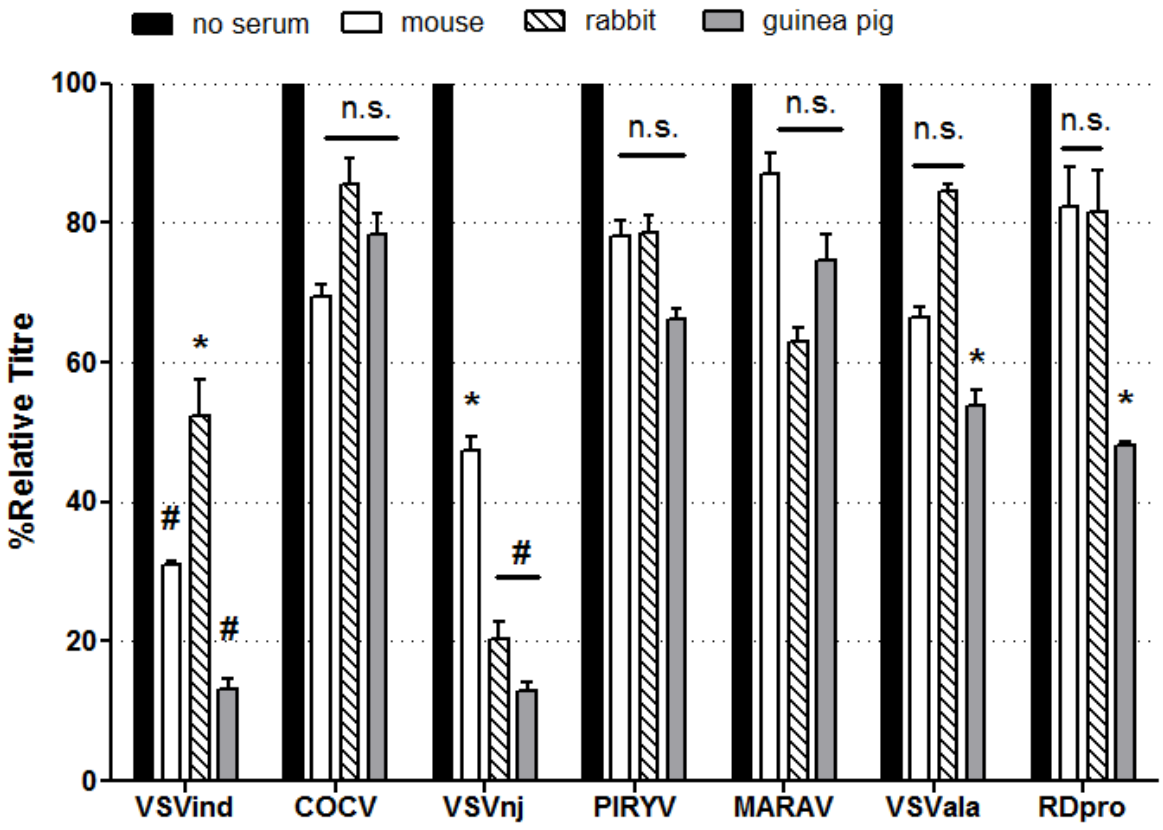

Figure 4-2: Serum Neutralisation of VesG-LV by Mammalian Sera. Serum sensitivity of VesG and RDpro pseudotyped LV.GFP were measured as previously described. Measured titres were then normalised to that of serum-free samples. Reduction of titre by heat-inactivated sera was <30% for all LV (data not shown). Percentage GFP of serum-free samples ranged 10-30%. Data shown represent relative titres +/- SD for three experiments performed in duplicates. One-way ANOVA analysis with Tukey's post-test was performed to compare relative titres to that of HI samples. (# $p<0.001$, * $p<0.05$, n.s. not significant).

4.3.2.Mapping the VSVind.G Region Responsible for Serum Sensitivity

Having identified envelope G proteins with different levels of resistance to serum neutralisation, I wanted to investigate the determinants that conferred serum resistance. For this, I aimed to determine the region(s) on VSVind.G which sensitised the G protein to complement-mediated neutralisation.

Briefly, some mix-and-match chimeric G-proteins between VSVind.G and COCV.G (produced by Maha Tijani, Collins/Takeuchi group, see *Table 2-2*) were investigated for their relative resistance to human and mammalian sera (*Figure 4-3)*. Chimeric G pseudotyped LVs were incubated with serum-free media, fresh or HI sera and plated onto cells. Titres were measured 48h later via flow cytometry and were normalised to that of serum-free samples.

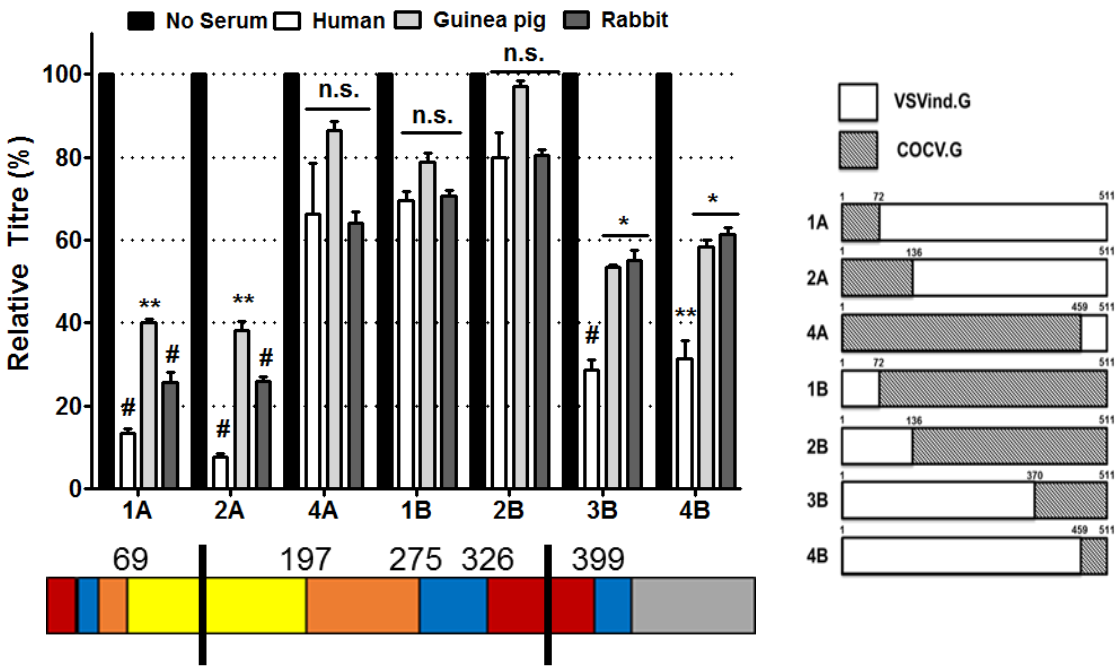

Figure 4-3: Serum Neutralisation of LVs Pseudotyped with Chimeric G Proteins. (A) Serum sensitivity of the chimeric G was measured as previously described. Reduction of titre by heat-inactivated sera was <30% for all LV (data not shown). Percentage GFP of serum-free samples ranged 10-30%. Data shown represent relative titres +/- SD for four experiments performed in duplicates. One-way ANOVA analysis with Tukey's post-test was performed to compare relative titres to that of HI samples. (# $p<0.001$, ** $p<0.01$ * $p<0.05$, n.s. not significant). **(B)** Two sets of mix-and-match constructs were investigated; A-chimaeras and B-chimaeras. The design and the cross-over points of the chimeric G-proteins are represented in linear diagrams, in which white bars stand for wt VSVind.G sequences, and hatched bars represent wt COCV.G sequences. Numbers indicate the cross-over point between the two wt sequences. **(C)** A linear diagram depicting VSVind.G's domain architecture, colour-coded by domain (Lateral domain, red; trimerisation domain, blue; PH domain, orange; fusion domain, yellow; transmembrane domain and C-terminal tail, grey). Several domain boundaries are labelled (16 amino acid long signal peptide of VSVind.G is omitted from the diagram). The deduced responsive region to complement-mediated inactivation is marked with bold black lines. Diagram adapted from (270).

Relative levels of inactivation revealed a general trend amongst the chimeric envelopes. LVs pseudotyped with chimaeras 1A, 2A, 3B, and 4B which consisted mostly of VSVind.G got inactivated by all sera considerably more than the other three pseudotypes. The levels of reduction of titres were on average similar to that of wt VSVind.G. On the other hand, LVs pseudotyped with chimaeras mostly consisting of COCV.G, 4A, 1B, and 2B, resisted serum inactivation similar to wt COCV.G-LVs. It can be deduced from the data that the region that is responsive to complement activity by fresh mammalian sera lies between the amino acid residues 138-369 on wt VSVind.G. This region comprises most of the pleckstrin homology domain and parts of the fusion, trimerisation, and lateral domains (297).

The identified region on VSVind.G was further analysed through pairwise amino acid sequence distance analysis (*Figure 4-4).* Aligned amino acid sequences for all six VesG were investigated for the evolutionary divergence between them. Pairwise distances of COCV.G, MARAV.G, VSVala.G, VSVnj.G, and PIRYV.G vs VSVind.G, individually and as a group, were calculated via the Kimura model using the analysis platform SSE (569-571). This analysis is based on the dissimilarity amongst the investigated group or between the pair of VesG. The pairwise evolutionary distance between two protein sequences is estimated as a single value as a function of dissimilarity. Dissimilarity is defined as “the fraction of positions in which both sequences differ” (572). Since these sequence differences, in most cases, are results of multiple evolutionary events, calculated pairwise variance underestimates the actual evolutionary distances. Kimura model for amino acid evolution is a rough yet quick and simple model that approximates PAM distances. A PAM distance or 1-PAM unit describes an amount of evolution which will change, on average, 1% of the amino acid sequence of a protein. Because Kimura model approximates PAM values, it shares the limitations of the PAM matrices. Hence, it does not take into account the similarity of the amino acid differences but rather only relies on the diversity of the residues (i.e. a switch between two non-polar residues vs. a switch from a non-polar residue to a charged residue). Despite this, Kimura model is still a suitable and viable analysis tool to visualise

the phylogenetic diversity between VesG which the source of complement resistance might be.

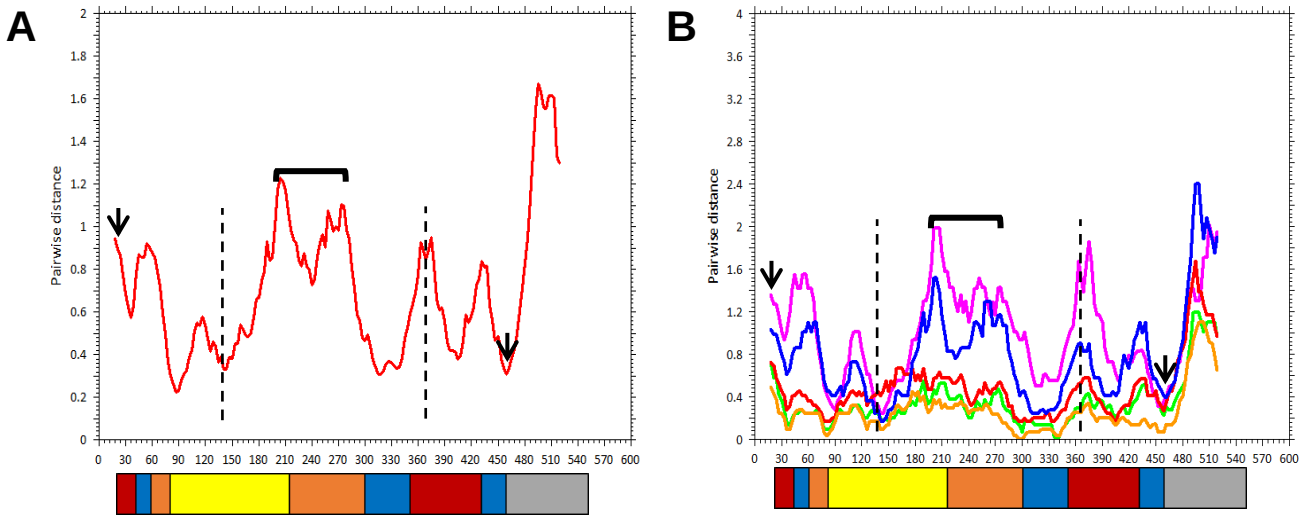

Figure 4-4: Multiple Alignment Amino Acid Sequence Homology Plots. Pairwise amino acid sequence analysis was carried out on six VesG amino acid alignment via Kimura model using the analysis platform SSE (569). **(A)** The global evolutionary divergence of five VesG (COCV, MARAV, VSVala, VSVnj, and PIRYV) vs VSVind.G. **(B)** Pairwise distance plots of each VesG vs VSVind.G (pink, PIRYV.G; blue, VSVnj.G; red, VSVala.G; green, COCV.G; orange, MARAV.G). The inset graph focuses on the VesG divergence between residues 137 and 369. In both graphs, the x-axis denotes the residue location, and y-axis stands for the average pairwise divergence at a specific residue. The linear domain architecture of VSVind.G is plotted below the graphs to match corresponding locations of the residues; the colour code of the G protein domains is identical to *Figure 4-3.* Black dotted lines mark the deduced sensitive region, and the square bracket indicates where the PH domain is located within the region. The black arrows mark the end of the signal peptide and the beginning of the transmembrane domain for VSVind.G.

It can be inferred from the global average divergence plot that the PH domain, located within the responsive region, is the most diverse domain in the ectoplasmic part of the G proteins. The individual pairwise homology graphs confirm this overall observation for each G protein since the PH domain remains to be the most variable region in the ectodomain of all five VesG compared to VSVind.G.

Two sets of chimeric G proteins between VSVind.G and COCV.G were synthesised to further investigate PH domain's involvement in complement-mediated serum inactivation (*Figure 4-5).* The two identified hypervariable regions were switched between the two glycoproteins. All chimaeras except COCV2 were functional and could pseudotype LVs reaching crude titres comparable to wt VSVind.G and COCV.G. The five functional chimeric G proteins were then tested for their sensitivity to complement-mediated inactivation by human, rabbit, and guinea pig serum.

No statistically significant changes in sensitivity were observed for the VSVind.G chimaeras Ind1, Ind2, and Ind3. LVs pseudotyped with these three G proteins got inactivated by all three sera losing on average >80% of their original titres. However, switching VSVind.G's PH domain into COCV.G had significant effects on the G protein's serum resistance ($p<0.001$). Both the partial switch (i.e. COCV2) and full switch (i.e. COCV3) conferred serum sensitivity to COCV.G for all sera tested substantially reducing the transduction ability of the LVs. It can be inferred from these results that COCV.G's serum resistance is the result of the amino acid changes in its PH domain mediated most probably by evolutionary divergence through immune pressure.

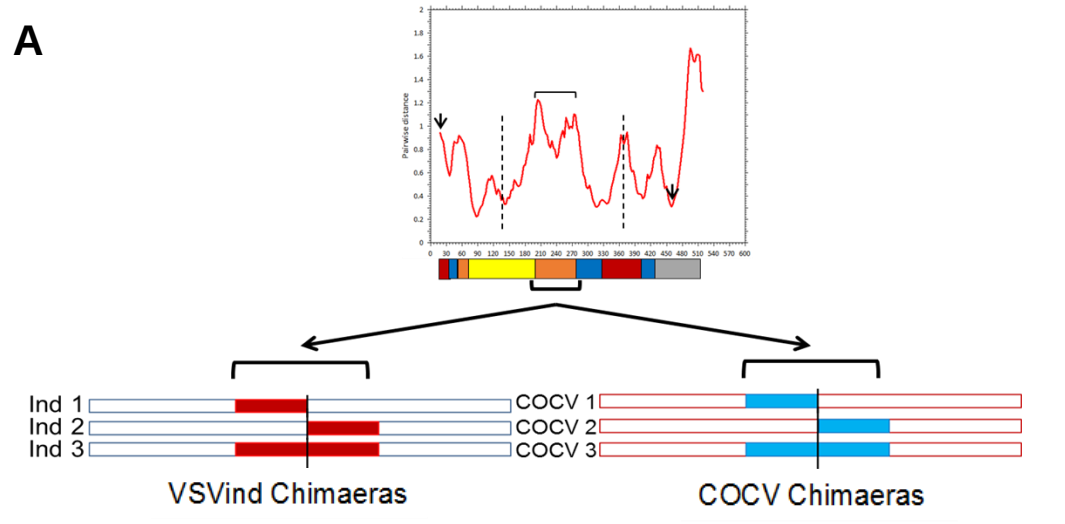
A
Ind 1
Ind 2
Ind 3
COCV 1
COCV 2
COCV 3
VSVind Chimaeras
COCV Chimaeras

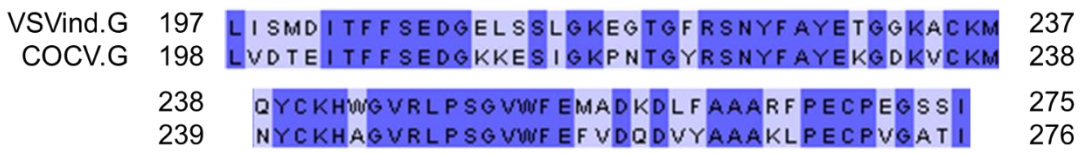
B
VSVind.G 197 LISMDITFFSEDGELSSLGKEGTGFRSNYFAYETGGKACKM 237
COCV.G 198 LVDTEITFFSEDGKKESIGKPNTGYRSNYFAYEKGDKVCKM 238
238 QYCKHWGVRLPSGVWFEMADKDLFAAARFPECPEGSSI 275
239 NYCKHAGVRLPSGVWFEFVDQDVYAAAKLPECPVGATI 276

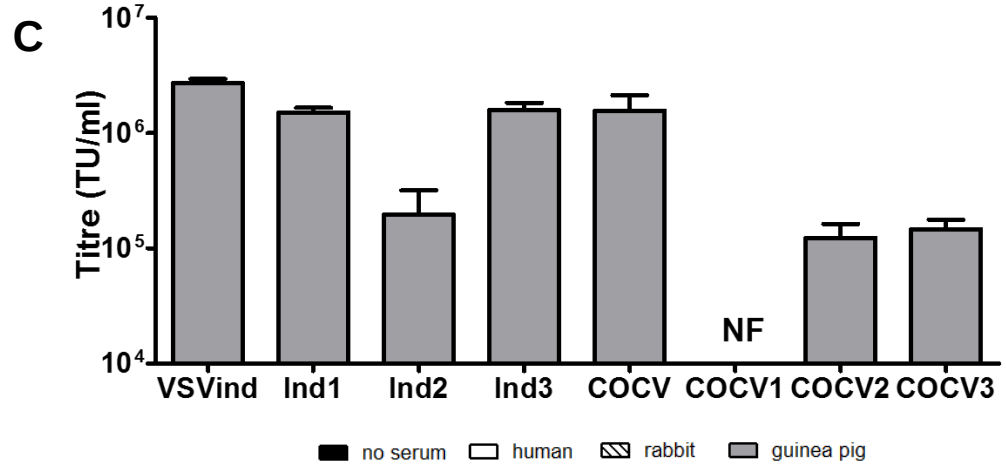
C
Titre (TU/ml)
10^7
10^6
10^5
10^4
NF
VSVind
Ind1
Ind2
Ind3
COCV
COCV1
COCV2
COCV3
no serum
human
rabbit
guinea pig

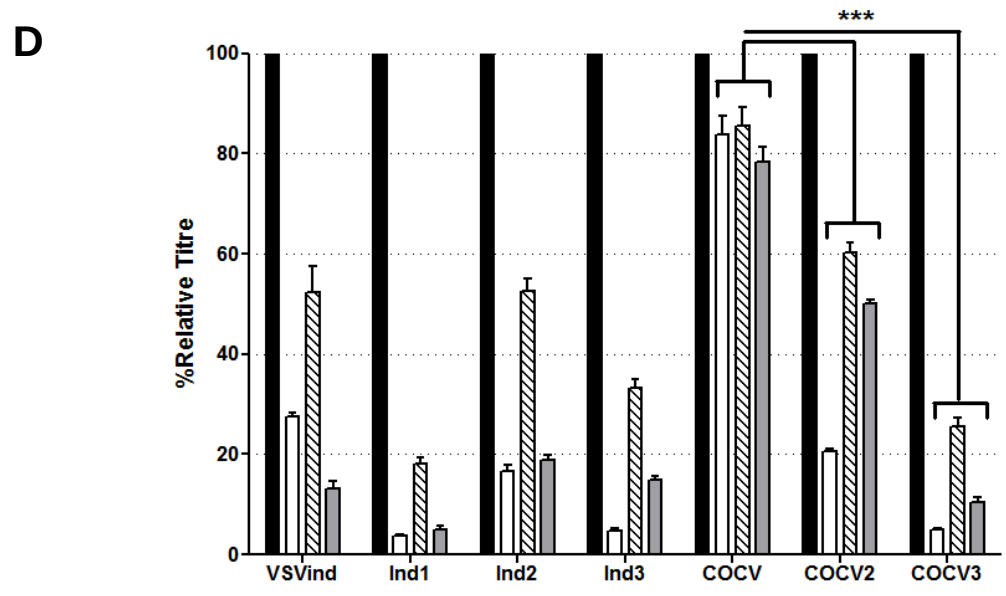
D
***
%Relative Titre
100
80
60
40
20
0
VSVind
Ind1
Ind2
Ind3
COCV
COCV2
COCV3

Figure 4-5: VSVind.G PH Domain Confers Serum Sensitivity. **(A)** Two sets of VSVind.G and COCV.G chimaeras were produced by switching parts of or the entire hypervariable PH domains. wt VSVind sequences are denoted by the colour blue wt COCV.G sequences are with red. The switches performed are indicated with solid coloured bars. **(B)** Comparison of PH domains of VSVind.G and COCV.G through amino acid alignment, domain boundaries are labelled. Amino acid sequences for the G proteins were retrieved from UniProt (See *Table 2-16)*. The sequences were aligned using ClustalOmega online multiple sequence alignment tool (EMBL-EPI), and the alignments were visualised using JalView software (294). Blue shading indicates percent identity: dark blue, 80-100%; light blue, 60-80%. **(C)** All chimeric G proteins but COCV1 were functional and could pseudotype LVs reaching crude titres comparable to their wt counterparts. NF: non-functional. Data presented represent mean titres +/- SD of three independent vector preparations. **(D)** Serum sensitivity of the chimeric G was measured as previously described. While no statistically significant changes were observed in serum sensitivity for VSVind.G chimaeras, COCV.G became substantially more sensitive to human, guinea pig, and rabbit complement-mediated inactivation. Data shown represent relative titres +/- SD for three experiments performed in duplicates. Reduction of titre by heat-inactivated sera was <30% for all LV (data not shown). Percentage GFP of serum-free samples ranged 10-30%. One-way ANOVA analysis with Dunnett's multiple comparison post-test was performed to compare the reduction of titres of LVs pseudotyped with chimeric G proteins to that of wt Gs (*** $p<0.001$).

4.4.Discussion

The sensitivity of the VSVind.G pseudotyped lentiviral vector to human complement-mediated inactivation is a drawback. Combined effects of natural serum IgM and complement are responsible for the observed neutralising activity (467). This neutralisation occurs slowly and is not completely abrogated by heat-inactivation, i.e. destruction of the complement. The mechanism of the limited independent neutralisation of IgM is thought to be either through viral aggregation or hindrance of G protein-receptor interactions (467, 573).

The complement cascade does not only function as a lytic system targeting pathogens. It is also a highly effective surveillance tool which can modulate other branches of the immune system (545, 546). It acts as the first line of defence against pathogens, altered and malfunctioning host cells (485). A pathogen infection triggers the activation of the complement cascade which comprises the central component of the innate immunity. While complement activation ultimately results in triggering of the adaptive immune response which stimulates the host to produce antibodies, complement suppresses the infection through inflammation, opsonisation, phagocytosis, and destruction of the pathogen (546).

Several approaches have been explored to evade the innate immune system or limit its activation to achieve better transduction efficiencies in gene therapy and oncolytic virotherapy: use of infected cells as carriers to protect and transport the virus to sites of tumour growth, synthetic modification of envelope G proteins of viral vectors and viruses to prevent antibody neutralisation, to generate neutralisation-resistant variants of VSVind.G through directed evolution and incorporation of factors such as CD46, CD55, and CD59 into the vector to modulate serum responses (466, 468, 550, 564, 574-577) . However, each method has limitations.

Therefore, serum resistant envelopes such as feline endogenous retrovirus RD114 derived envelopes (e.g. RDpro) and COCV.G have been utilised as alternatives (200, 517). However, RDpro pseudotypes lentiviral vectors less efficiently compared to VSVind.G (i.e. approximately 100-folds lower titres)

and thus its *in vivo* use has been limited so far (578, 579), whereas no current studies have reported *in vivo* use of COCV.G.

Furthermore, VSVind virus has been extensively studied and characterised as a promising oncolytic platform as it can selectively kill cancerous cells both *in vitro* and *in vivo* (346, 356, 477-481, 514). Several preclinical studies have confirmed its effectiveness against human cancers (353, 357, 459, 465, 580-587). Therefore, effective systemic delivery of the virus in oncolytic therapy or pseudotyped lentiviral vector in gene therapy is critical for achieving therapeutic effects (467).

I have demonstrated that three vesiculovirus G proteins, COCV.G, PIRYV.G, and MARAV.G, are relatively resistant to this neutralisation mediated by the serum complement. To achieve long-term therapeutic efficacy and sustained gene expression in clinical gene therapy, repeated administration of viral vectors may be necessary. Therefore, serum-resistance of these G proteins grants them an advantage over VSVind.G pseudotyped vectors for their future use in *in vivo* applications.

Furthermore, I have identified, on VSVind.G, the region which is responsive to serum inactivation. It lies in between the amino acid residues 137-369. This region comprises most of the PH domain of the G protein which is reported to be the most diverse and antigenically active ectoplasmic domain amongst vesiculovirus G proteins. As MARAV.G and COCV.G have 80% and 72% sequence homology to VSVind.G on amino acid level, it is most probable that the structure, the overall charges, and the presence or absence of specific epitopes on this domain is responsible for the relative resistance between these envelopes.

Two hypervariable regions were identified which lie within sensitive determinant comprising the PH domain. Their role in conferring serum sensitivity or resistance to VSVind.G and COCV.G were investigated using chimeric proteins. When the PH domain of VSVind.G was switched into COCV.G (determined through amino acid alignment) partially or entirely, it conferred sensitivity to wt COCV.G against human, rabbit, and guinea pig sera. This indicated that VSVind.G's PH domain contains epitopes that enable IgM

binding and C1q deposition. However, the reverse did not confer resistance to wt VSVind.G. This implies that although VSVind.G's PH domain contains complement sensitive triggers, not all are localised in that domain. In line with these findings, through directed evolution studies, several mutations in VSVind.G have previously been identified that confer the G protein serum resistance. Out of the three key mutations, S162T, T230N, and T368A (564), although all three are within the sensitive region initially determined (i.e. aa 137-369), only T230 lies within the PH domain. To sum up, VSVind.G has several other serum sensitive triggers located throughout the G protein and not only at the hypervariable PH domain, therefore, replacing this domain with one from COCV.G does not confer resistance.

It is still unknown whether the slow neutralising effect of the complement system would be sufficient enough to shut down vector efficacy following systemic administration. However, it is a part of a network of the innate immune response that harnesses phagocytes and antigen presenting cells (489). IgM and activated complement system components can opsonise LVs, but also can trigger the sensors associated with pathogen-associated molecular patterns (PAMPs) eventually promoting inflammation and activating adaptive branches of the immune system (428, 435, 565). It has been shown that proviral DNA robustly activates innate immunity sensors and induces a powerful type I interferon response by activating TLR3 and TLR7 (489, 490, 566, 567). In addition, LVs' ability, especially VSVind.G-LVs', to efficiently transduce myeloid dendritic cells directly contributes to this TLR-dependent induction of IFN and cytotoxic T cell response (588-590). The PAMPs present in the vector backbone stimulate dendritic cells (and other APCs) to process the transgene and present it to CD4+ and CD8+ T cells through major histocompatibility complexes (591) irrespective of mode of uptake (592-595).

Several studies have demonstrated a rapid but transient increase in proinflammatory cytokine secretion in dogs and mice following systemic delivery of LVs (174, 489). These cytokines might not only interfere with LV transduction but also can recruit inflammatory cells and activate APCs triggering the adaptive immune response (435, 490, 567).

One of the current approaches to prevent the activation of the innate immune system is to use cocktails of monoclonal antibodies and small molecules to inactivate cytokines and costimulatory molecules or specifically target and block subsets of immune cells (596-602). In addition to these immunomodulatory molecules, drug-based strategies have also been explored. Anti-inflammatory glucocorticoids such as dexamethasone have been tested as preconditioning regimens prior to LV administration to increase vector delivery efficacy and limit the activation of the innate immune response (566, 603).

The specifics of the innate immune response to lentiviral vectors and how it is modulated according to vector titre, envelope, and administration method remains to be fully explored. Regardless, the mechanisms through which the innate immune system tackles LVs should be judiciously analysed to develop less immunogenic gene therapies. It may prove useful to perform site-directed mutagenesis studies on VSVind.G and serum-resistant VesG to deduce any possible C1q deposition sites as well as to map IgM and serum IgG interaction epitopes to understand further the innate characteristics of these envelopes which confer them serum-resistance. Moreover, the effects of utilising pre-treatment regimens of complement inhibitors and incorporating complement-antagonising molecules on the vector surface on gene delivery efficacy and vector stability can be investigated in established preclinical animal models.

Such approached will also allow for the circumvention of the limitations of *in vitro* serum sensitivity assays. The most crucial of which, that also affected the work presented in this chapter, is despite isolated or reconstituted sera are utilised in physiological concentrations *in vitro* incubation of heat labile complement cascade proteins with LVs or wild-type viruses substantially magnify the inhibitory effects exhibited by the sera. Therefore, results obtained and conclusions derived may not reflect *in vivo* circumstances or the native characteristics of LV pseudotypes and viruses (see Chapter 5 discussion).

5 Circumventing the Humoral Immune Response Against Envelope G protein of Lentiviral Vectors for *In Vivo* Gene and Oncolytic Virotherapy

5.1.Overview

Lentiviral vectors are potent gene delivery platforms in the treatment of both hereditary and acquired diseases (488). Currently, LVs are utilised in 7% of all gene therapy clinical trials worldwide with one-fifth targeting monogenic diseases (502, 604). Despite this, *in vivo* LV gene therapy is still at preclinical development stage (50, 174, 605, 606) while *ex vivo* therapies using haematopoietic stem and progenitor cells and T lymphocytes are in clinical use (28, 607-610). A significant obstacle in *in vivo* LV gene therapy advancement is the immune responses directed towards LVs which may limit the efficacy and safety of the therapy (488, 611).

Administration of vectors may induce a primary immune response against the LV envelope or core proteins [14]. In this case, although the efficacy and safety of the initial vector administration should not be affected, the effect of

subsequent doses of therapy may be limited. Indeed, production of antibodies through CD4+ T cell-mediated mechanisms directed towards vector proteins has been observed following systemic administration of vectors (497). Although the development of these antibodies did not limit transduction efficiency, strongly neutralising antibodies toward the matrix (p17) and capsid proteins (p24) limited the efficacy of a subsequent administration of the same vector. On the other hand, the effects of neutralising anti-envelope antibodies to LV efficacy remains to be fully explored in animal models (489).

LVs acquire plasma membrane proteins of the producer cells as well as their envelope proteins during the complex assembly and budding processes. Since, in most cases, vectors are produced in the immortalised human cell line HEK293T, they acquire an array of proteins from the producer cells. Upon recognition by the immune system or opsonisation of LVs by APCs, these proteins may trigger robust immune responses both in animal models and in patients (562). Some studies have demonstrated allogeneic major histocompatibility complex class I (MHC-I) mediated T cell activation in human cells *in vitro* and a robust anti-MHC-I immune response *in vivo* following LV administration to mice (502, 562, 612). Furthermore, it has been elucidated that the generation of antibodies against MHC epitopes plays a substantial role in the inactivation of LVs (562). Therefore, the presence of such allo-antibodies might reduce LV transduction efficacy dramatically and lead to phagocytosis and cytotoxic T cell (CTL)-mediated killing of LV-transduced autologous cell in *in vivo* and *ex vivo* gene therapies. To prevent this response raised against MHC-I on the vector surface, MHC-I negative LV production has been explored through genetic inactivation of beta-2 macroglobulin gene in the producer cell. This has substantially reduced LV's ability to induce human T cells immunity (562).

Another major hurdle for successful *in vivo* LV gene therapies is achieving long-term transgene maintenance and expression. Thus, considerable effort has been dedicated to the development of vector platforms that can promote transgene expression at therapeutic levels through transgene specific immunological tolerance (498, 613-616). The immune response elicited towards the transgene product following LV administration ranges between

active immunity, ignorance, and active immune tolerance (502). This can vary depending on several factors: the nature of the transgene product, the LV titre, transduced tissues, and type of genetic disorder targeted. The transgene is more likely to be tolerated if it shares homology with other self-antigens or is partially known to the immune system (617). The ubiquitously used VSVind.G envelope confers broad cell tropism to LVs, including macrophages and dendritic cells. Therefore, transduced APCs presenting the transgene product can efficiently prime CD8+ CTLs, which when activated, can clear transgene expressing cells from the organism (492, 618). This property of vectors has been extensively exploited to induce anti-tumour and anti-pathogen immune responses following administration of LV encoding tumour associated antigens (493, 494).

Local delivery of LVs facilitates better access to the target tissues and reduces the risk of spread of vector and transgene products, therefore, limiting the specific anti-vector immune responses. This method has been utilised effectively especially targeting immune privileged tissues such as eyes or parts of the central nervous system (50, 497, 605, 619, 620). However, when an extensive systemic expression of the transgene product is required, the inherent capacity of the LVs to transduce antigen presenting cells (APCs) plays a crucial role in inducing adaptive immune responses (498). An approach developed to circumvent this was to incorporate several repeats of target sequences of micro RNAs (miRNA) into the 3' end of the transcript to block bone-marrow derived professional APCs (621). The therapeutic efficacy of this technique has been documented in haemophilia B mice, where sustained correction of coagulation was achieved using miRNAs (622, 623).

Additionally, recognition of the transgene by antibodies also poses a concern toward the success of gene therapies (624). Generation of neutralising antibodies towards the transgene enhances the clearance of the encoded proteins especially in cases where systemic expression is utilised (489). For example, the function of enzymes and factors delivered via LVs in murine haemophilia A models have been curtailed substantially through antibody-mediated immune responses thus limiting the efficacy of the treatments (499, 500). Furthermore, such immune responses will persist in patients through the

development of memory B cells and limit re-administration of the treatment (624).

The activation of cell-mediated and humoral adaptive immunity leads to the generation of immune responses directed towards both vector and transgene-derived antigens (502). LV derived antigens, i.e. envelope and capsid proteins, are expected to induce immune responses both in humans and animal models following intravenous administration (497). The capacity of the immune system's memory will likely render subsequent doses of the same vector less effective. However, a detailed characterisation of this immune response remains to be investigated in animal models (502). As LVs, like many other viruses and viral vectors, may also activate innate immune responses in parallel to adaptive immune pathways, their administration may exacerbate any anti-vector or anti-transgene immune responses due to induction of inflammatory pathways (623). Therefore, combined therapies may need to be tailored for successful and sustained therapeutic gene delivery *in vivo.*

In this chapter the focus will be mainly on the anti-envelope response elicited following systemic administration of LVs and how to overcome it in a murine animal model. Furthermore, the transgene expression and the localisation of transduced cells will also be investigated to provide some preliminary data on the *in vivo e*ffects of the immune system against LVs.

5.2. Aims

The anti-vector immune response elicited following systemic administration of LVs *in vivo* remains to be investigated extensively. It is expected that a possible anti-envelope response induced by the LV injection will be problematic for repeated administration of viral vectors or viruses with the same envelope. Therefore, I aimed to explore the effects of adaptive immune response against intravenous LV administration focusing on the following three points of investigation:

1. Does the administration of VesG-LV induce a neutralising anti-G immune response? Is this response broadly neutralising?
2. How will the elicited immune response against a VesG affect the secondary vector dose efficacy?
3. Can a potent neutralising anti-G response be circumvented via the usage of a heterogeneous panel of envelopes sequentially?

5.3.Results

5.3.1.Induction of a Neutralising Anti-envelope Response Following Intravenous LV Administration

A potential humoral immune response against the envelope G proteins of LVs is a major concern regarding transgene delivery efficacy of the vectors and remains to be fully explored. Although VSVind.G is sensitive to inactivation by fresh mammalian sera from humans, mice, guinea pigs, and rabbits *in vitro* (see Chapter 4), the potency of this inactivation has not been investigated *in vivo,* nor has the induction of anti-envelope antibodies following LV administration. Therefore, I aimed to determine whether intravenous (IV) administration of VSVind.G-LV would lead to the production of envelope-specific neutralising antibodies.

Three female Balb/c mice were injected with $5x10^7$ TU/mouse of VSVind.G-LV (titres determined by titration on HEK293T cells) through their tail vein, and blood samples were collected after twenty-one days, allowing for maturation of the immune response. Sera were isolated, pooled (to investigate the overall response), and neutralising activity was determined through the *in vitro* neutralisation assay described in section 3.3.3. Although VSVind.G-LV infection was blocked in a dose-dependent manner, a similar effect was observed for LVs pseudotyped with the unrelated RDpro envelope (*Figure 5-1A dotted lines*). This unspecific neutralising activity implied that the hindrance of LV infection was due to antibodies directed against the human proteins on the vector surface which were acquired during the production as the vectors bud out of HEK293T cells. This anti-human response was thought to be against proteins encoded by the human leukocyte antigen (HLA) complex, as a similar non-specifically neutralising response was previously observed during early attempts of HIV-1 vaccine production (625). In addition, a similar MHC-I directed immune response has been reported in haemophilia B mouse models (562).

To distinguish the anti-human response from anti-VSVind.G response, 150µl of pooled sera was first incubated with $1x10^7$ HEK293T cells on ice for 1h and

the neutralisation assay was carried out. This incubation successfully removed anti-human antibodies as, after adsorption, the neutralising activity against RDpro-LV was lost. This then revealed a strongly neutralising anti-VSVind.G response (*Figure 5-1A solid lines*). This response was specific to VSVind.G as LVs pseudotyped with the other five VesG remained infectious (*Figure 5-1B*).

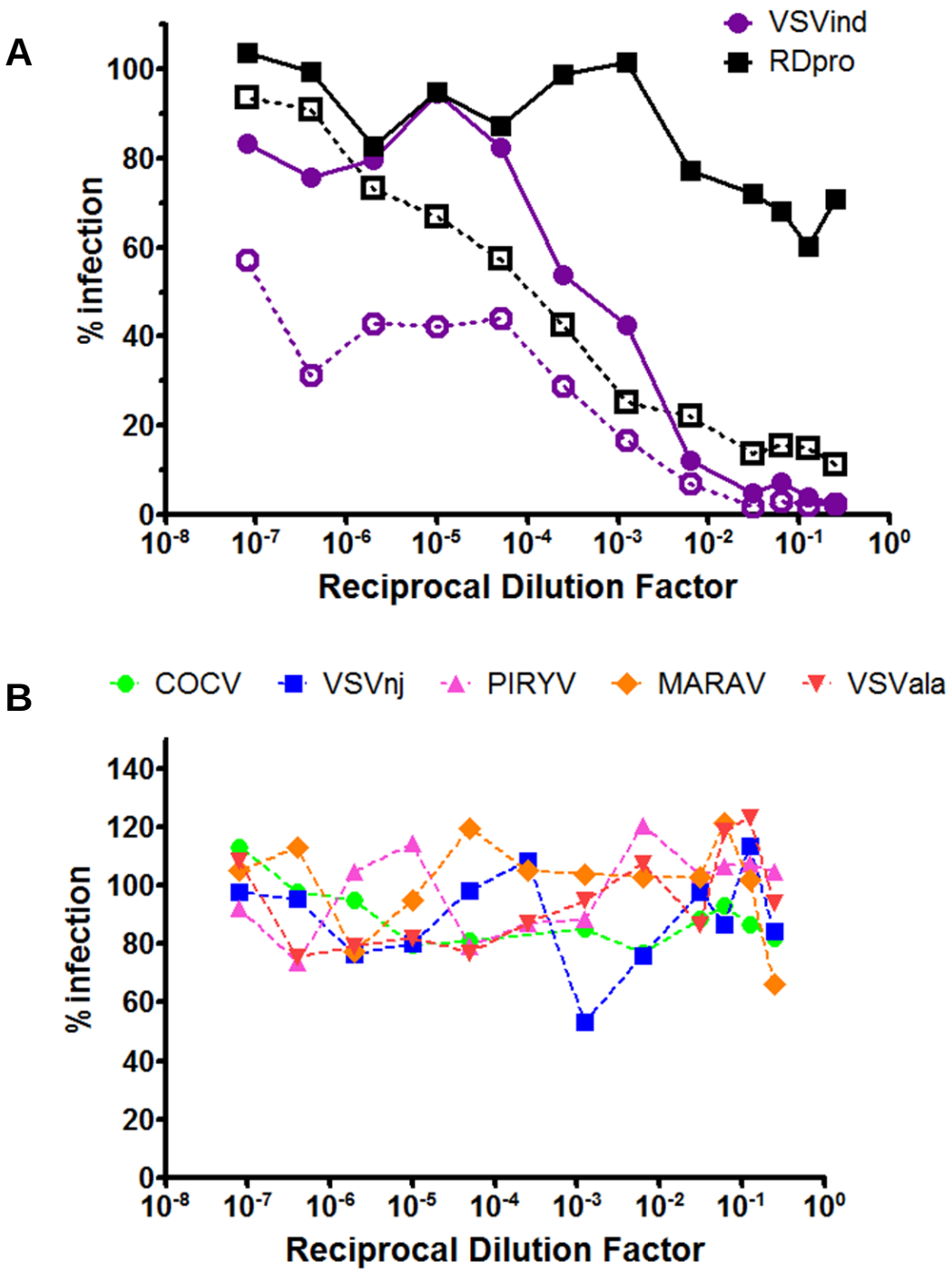

Figure 5-1: Intravenous LV Administration Elicits a Specific Neutralising Anti-envelope Response. **(A)** Neutralisation activity of pooled sera on VSVind.G and RDpro pseudotyped LVs pre- **(dotted lines with clear symbols)** and post-adsorption **(solid lines with filled symbols)** with HEK293T cells. **(B)** The neutralising activity observed was exclusively against VSVind.G as no reduction in infectivity was observed for the other five VesG pseudotyped LVs. Data shown represent the mean of three repeats performed in duplicates. Data presented in this section were obtained as a part of a larger *in vivo* study described in section 5.3.2.

5.3.2.Investigation of the Effects of Pre-existing Anti-envelope Immunity to a Subsequent LV Administration

The neutralising humoral response induced by LV administration identified in the previous section may become a substantial problem limiting the efficacy of subsequent administration of LVs pseudotyped with the same envelope where repeated injections of the vectors are necessary to achieve therapeutic levels of transgene expression. To investigate this, I designed a subsequent challenge study. However, the anti-HEK293T response following IV LV injection made a different immunisation protocol necessary. Therefore, an immunisation-boost regimen using wild type VSVind.G protein (Gth, see Chapter 3) (270, 297) was chosen to prompt the anti-G response.

Mice were immunised and boosted subcutaneously (SC) with 4µg of Gth protein mixed with Sigma Adjuvant System® Oil on either side (for a total of 8µg of protein/mouse) two weeks apart (*Figure 5-2A*). Three weeks later, the immune response group (i.e. immunisation+challenge; IC) were challenged with intravenous injection of $5x10^7$ TU/mouse VSVind.G-LV encoding both firefly luciferase (FLuc) and enhanced green fluorescent protein (eGFP). Immunisation-only (IO) and challenge-only (CO) groups were either only immunised and received PBS injections or received a vector dose following immunisation/boost with the adjuvant only (*Figure 5-2B*). The study was terminated at two time points; five days (D5) and twenty-one days (D21) post-challenge at which time terminal bleeds were collected and lungs, kidneys, lymph nodes, livers, and spleens were harvested. During the study, none of

the mice showed signs of distress (observation) and no substantial changes in body weights were observed (*Figure 5-2C*). Throughout the study, serum antibody levels were assessed via the blood samples collected through tail vein bleeds. The LV transduction efficacy as well as initial and sustained transgene expressions were assessed by *in vivo* bioluminescence imaging and several post-termination assays including analysis FLuc activity in harvested organs and quantitative PCR were performed.

A

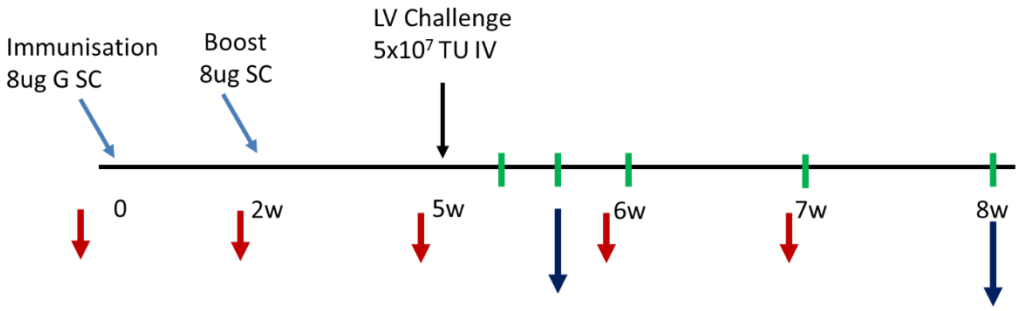

B

GROUP	MOUSE #	IMMUNISATION	BOOST	CHALLENGE
PBS	1	× (PBS)	× (PBS)	× (PBS)
Immunisation-only **(IO)**	3	✓	✓	× (PBS)
Challenge-only **(CO)**	6	× (Adjuvant-only)	× (Adjuvant-only)	✓
Immunisation + Challenge **(IC)**	6	✓	✓	✓

C

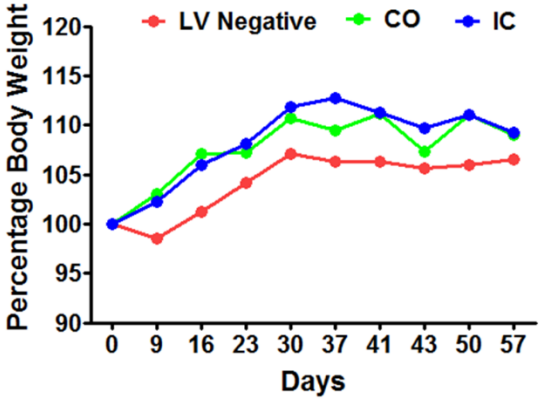

D

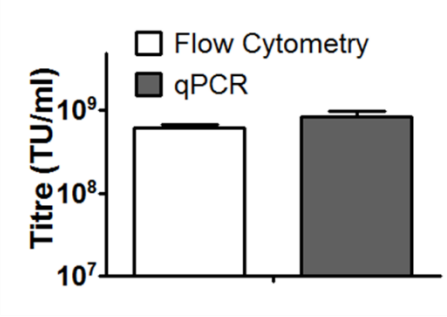

E

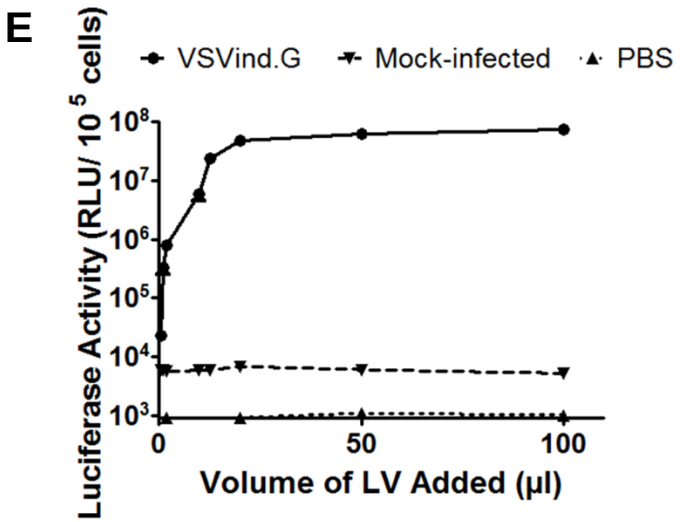

Figure 5-2: Design of LV Challenge Study Exploring the Effects of Pre-existing Anti-envelope Immunity on Subsequent LV Administrations. **(A)** Timeline of the study. Immunisation and boost points are identified by light blue arrows while the black arrow indicates the time of LV challenge. Red arrows designate the times blood samples were collected through tail vein bleeds. Green lines show the days mice were imaged. Dark blue arrows indicated the early and late termination dates. On the early termination day; three mice, selected at random on the day, were culled from the CO and IC groups while rest of the mice were culled at the end of the study. w: weeks. **(B)** Study groups including the PBS (non-treatment control) group are summarised in a table indicating the injections at immunisation, boost, and challenge. **(C)** Bodyweights (bw) of mice throughout eight weeks normalised to that of at the beginning of the study. Each data point represents the mean bw of all mice in the indicated group. Standard deviation of each data point for all the groups was <5%. LV negative includes both PBS and IO groups. **(D)** Infectious titres and **(E)** luciferase activity of the VSVind.G-LV batch used in this study. Infection assays on HEK293T cells were carried out as outlined in section 2.6.2. Quantitative PCR and luciferase activity assays were performed as outlined in sections 2.9.4 and 2.9.6. Data shown represent mean +/- SEM of two experiments performed in duplicates.

Prior to the LV challenge the serum antibody levels in immunised mice were assessed, and the induced immune response was characterised to ensure a VSVind.G specific neutralising response was elicited. Serum antibody levels were determined via enzyme-linked immunosorbent assay (ELISA) against VSVind.G-LV. Monoclonal anti-VSVind.G antibody 8G5F11 was utilised as a positive control and blood samples obtained pre-study were used to determine background levels caused by unspecific binding of antibodies and/or matrix effect in high serum concentrations (*Figure 5-3A-C*). In both the IO and IC groups signals were detected indicating the presence of anti-VSVind.G antibodies. The signal could be titrated by serial dilutions showing dose-dependence. On the other hand, no substantial absorbance difference was observed between pre-study and pre-challenge serum antibody levels for any of the mice in the CO group (*Figure 5-3B)* and the PBS one (*Figure 5-3A square*). Further characterisation revealed that the induced humoral response was neutralising and VSVind.G specific (*Figure 5-3D-E*). Analyses of serum samples revealed that the humoral immune response induced via Gth immunisation exhibited similar properties to the one elicited against an IV LV

administration. The study continued with VSVind.G-LV challenge. Mice in IC and CO groups received $5x10^7$ TU/mouse of LVs expressing Fluc and eGFP (LV.FLuc-eGFP) via tail vein injections (see *Figure 5-5* for vector construct map). Luciferase expression was monitored via bioluminescence imaging for twenty-one days (*Figure 5-4).* Starting from day 2 post-challenge a strong luciferase signal could be detected in CO mice mainly localised at the liver, spleen, and inguinal and auxiliary lymph nodes (*Figure 5-4A)*. This signal was sustained for two weeks. On day fourteen total clearance of the luciferase signal from the liver and spleen was observed, however, luciferase expression in the lymph nodes and the tracheal region was remained constant until the termination of the study.

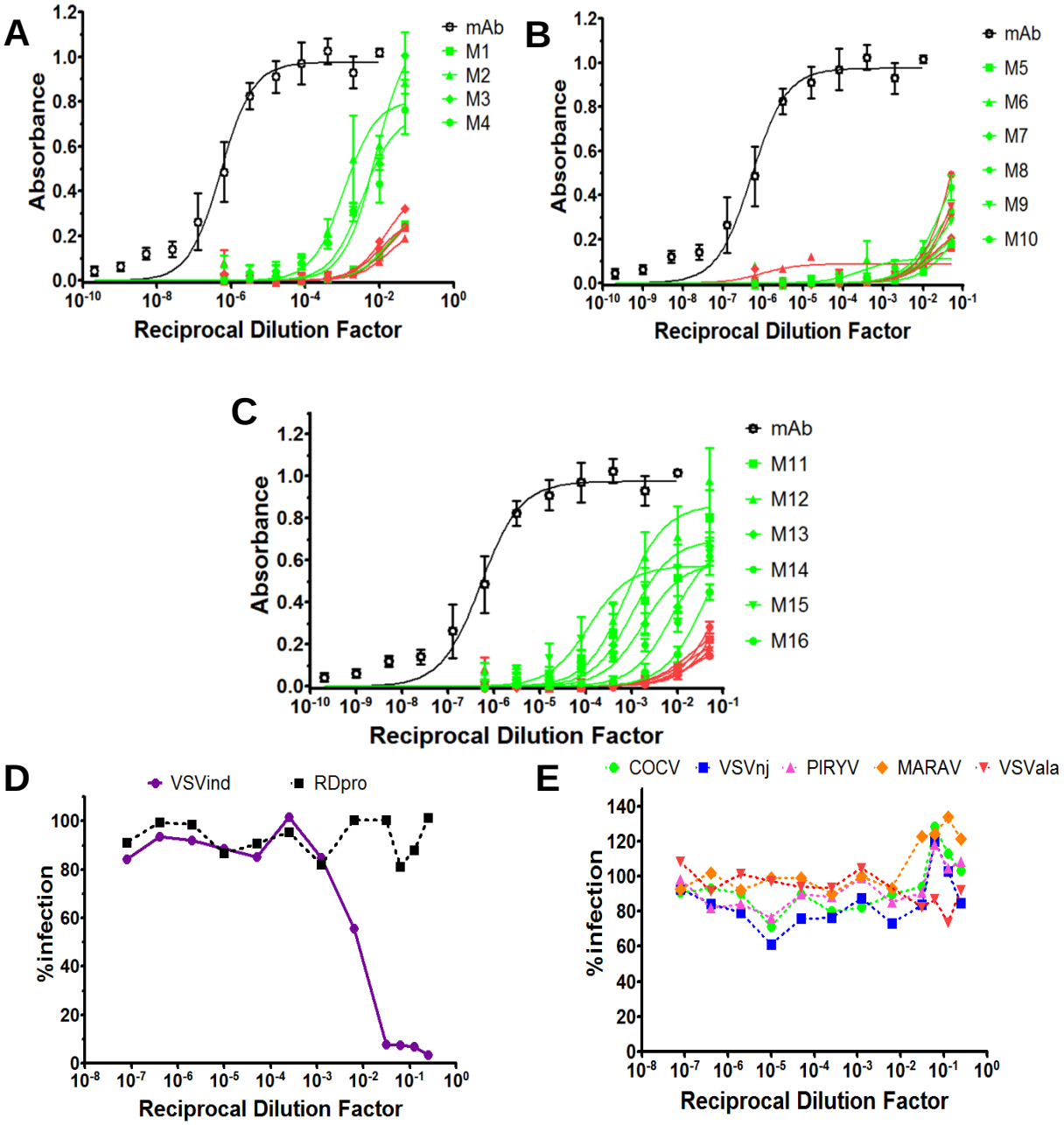

Figure 5-3: Pre-challenge Antibody Levels and Neutralising Activity Induced via Gth Immunisation. Wells were coated with 25 µg/ml of VSVind-LV and were incubated with serial dilutions of serum samples to determine anti-VSVind.G serum antibody levels for mice in **(A)** PBS (M1, i.e. mouse 1) and IO (M2, M3, M4), **(B)** CO, and **(C)** IC groups. The antibody levels were determined by measuring absorbance at 450nm. Anti-VSVind.G mAb 8G5F11 was used as positive control and was utilised to compare the values obtained from different plates. mAb concentrations ranged from 10 µg/ml to 0.2 pg/ml. Green lines represent pre-challenge serum samples, and red lines denote pre-study serum samples for each mouse. Each mouse is denoted with a different symbol. Immunised IO and IC groups displayed varying levels of

antibodies while no substantial absorbance difference was observed between the pre-study and pre-challenge serum samples for PBS (M1) and CO groups. The curves were fitted in GraphPad Prism 5 modelling the interaction as 1:1 specific binding. Data shown represent the mean +/- SD of three repeats performed in duplicates. Neutralisation activity of pooled IO sera on **(D)** VSVind.G and RDpro pseudotyped LVs and **(E)** other VesG-LV. Data shown represent the mean of three repeats performed in duplicates.

In the CO group, overall measured radiance levels throughout the study were significantly lower compared to that of the IC group ($p<0.0001$) (*Figure 5-4B).* In addition, a multiple comparison of each imaging time point revealed significant differences in luciferase expression in the CO group compared to IC group and naïve mice (*Figure 5-4B).* In the IC group, luciferase expression could not be detected, and the radiance of mice in the IC group remained comparable to that of LV negative mice for the whole study (overall average radiances $2.01x10^5$ and $1.24x10^5$ p/sec/cm^2/sr respectively). Thus, the induced anti-envelope immunity significantly reduced the efficacy of a subsequent viral vector injection utilising the envelope homologous to the immunogen. On the other hand, in the CO group sustained tissue transduction was achieved in the lymph nodes and tracheal region, but, transgene expression clearance was observed in the liver and spleen two weeks after injection. A similar vector clearance has been previously reported in the liver (490).

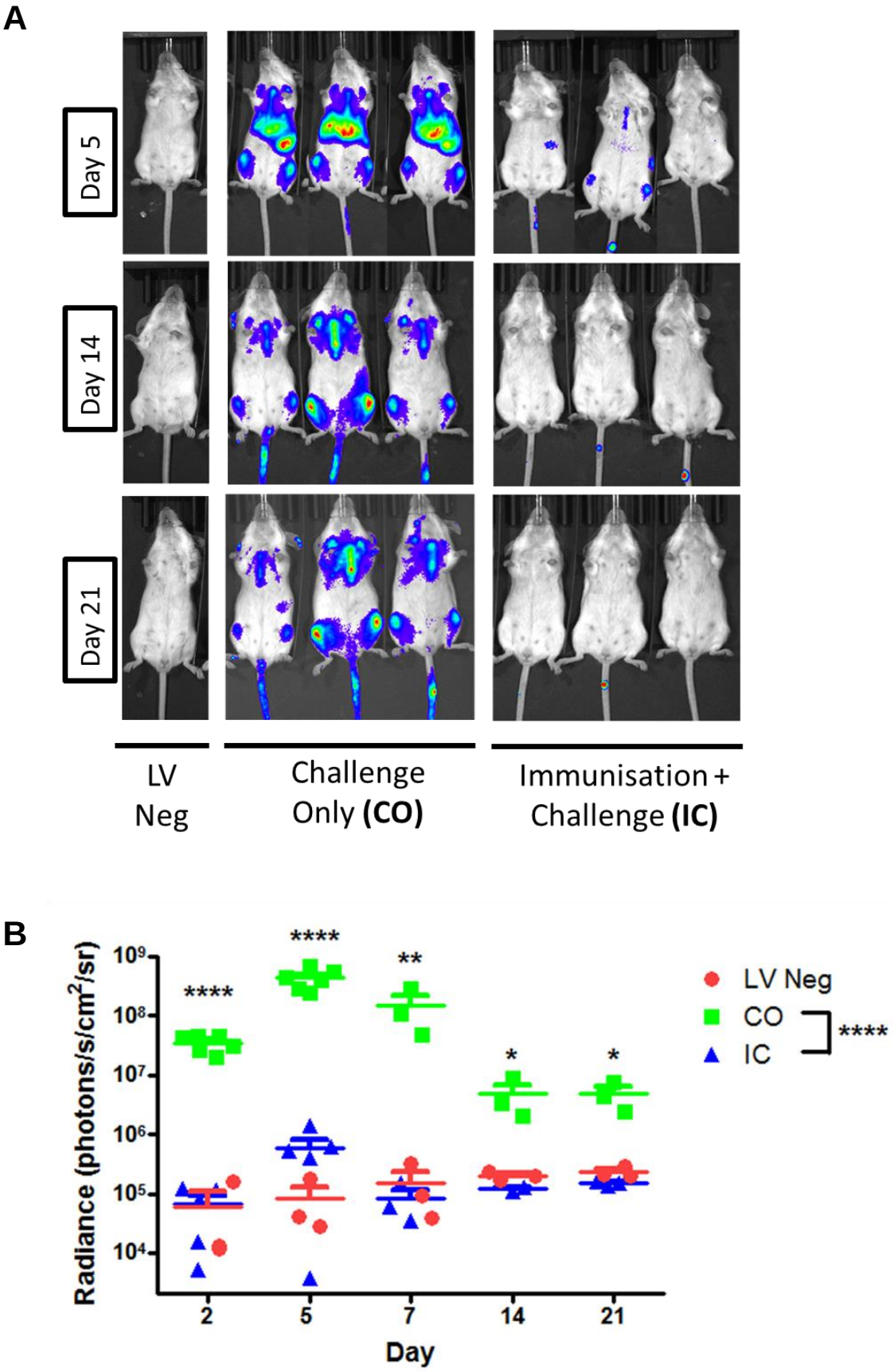
A
Day 5
Day 14
Day 21
LV Neg
Challenge Only (CO)
Immunisation + Challenge (IC)
B
Radiance (photons/s/cm²/sr)
10⁹
10⁸
10⁷
10⁶
10⁵
10⁴
****
****
**
*
*
2
5
7
14
21
Day
LV Neg
CO
IC
****

Figure 5-4: Pre-existing Anti-VSVind.G Immunity Abrogates the Efficacy of a Subsequent VSVind.G-LV Administration. **(A)** Representative bioluminescence images of transduced and naïve mice at three time points of day 5, 14, and 21 post-challenge. Localisation and the intensity of the luciferase signal are depicted in a heat map. **(B)** Photon emission from each mouse was quantified as radiance (p/s/cm^2/sr) post-imaging using region of interest analysis in Living Image® software. Each dot represents a mouse, and the horizontal bar shows the median. Two-way ANOVA followed by Bonferroni's multiple comparison test was performed to analyse the significance of luciferase expression differences in LV negative, CO group, and IC mice at each imaging time point (indicated on the graph) as well as overall throughout the study (indicated on the legend). In all comparisons the difference between LV neg and IC samples were not significant (not shown). (**** $p<0.0001$, ** $p<0.01$, * $p<0.05$). Neg: negative.

To investigate the biodistribution of VSVind.G-LVs and examine the effects of the pre-existing immunity and observed vector clearance on the transgene expression in transduced tissues, kidneys, lungs, livers, spleens, and lymph nodes (inguinal and auxiliary) were harvested from each mouse on both termination dates (day 5-D5 and day 21-D21 post-challenge). First, luciferase activity was quantified in the tissues using the Bright-Glo™ luciferase assay system and was normalised to the weight of the tissue (*Figure 5-5A-D).* Corroborating the bioluminescence imaging results, in CO-D5 samples, the most robust luciferase activity was measured in the liver, spleen, and lymph nodes. Although some signal was detected in the lungs in both D5 and D21 samples, it was not statistically significant, and no difference in luciferase activity was observed in the kidneys compared to that of the negative control.

Furthermore, the inhibition of viral vector transduction was also evident in organs harvested from IC mice compared to CO mice. Significant differences in luciferase activity were observed in the liver ($p<0.001$) and spleen ($p<0.01$) while in all tissues investigated there were no statistically significant differences between the luciferase activity of IC samples and LV negative samples implying LV transduction was blocked by the pre-existing anti-envelope immunity.

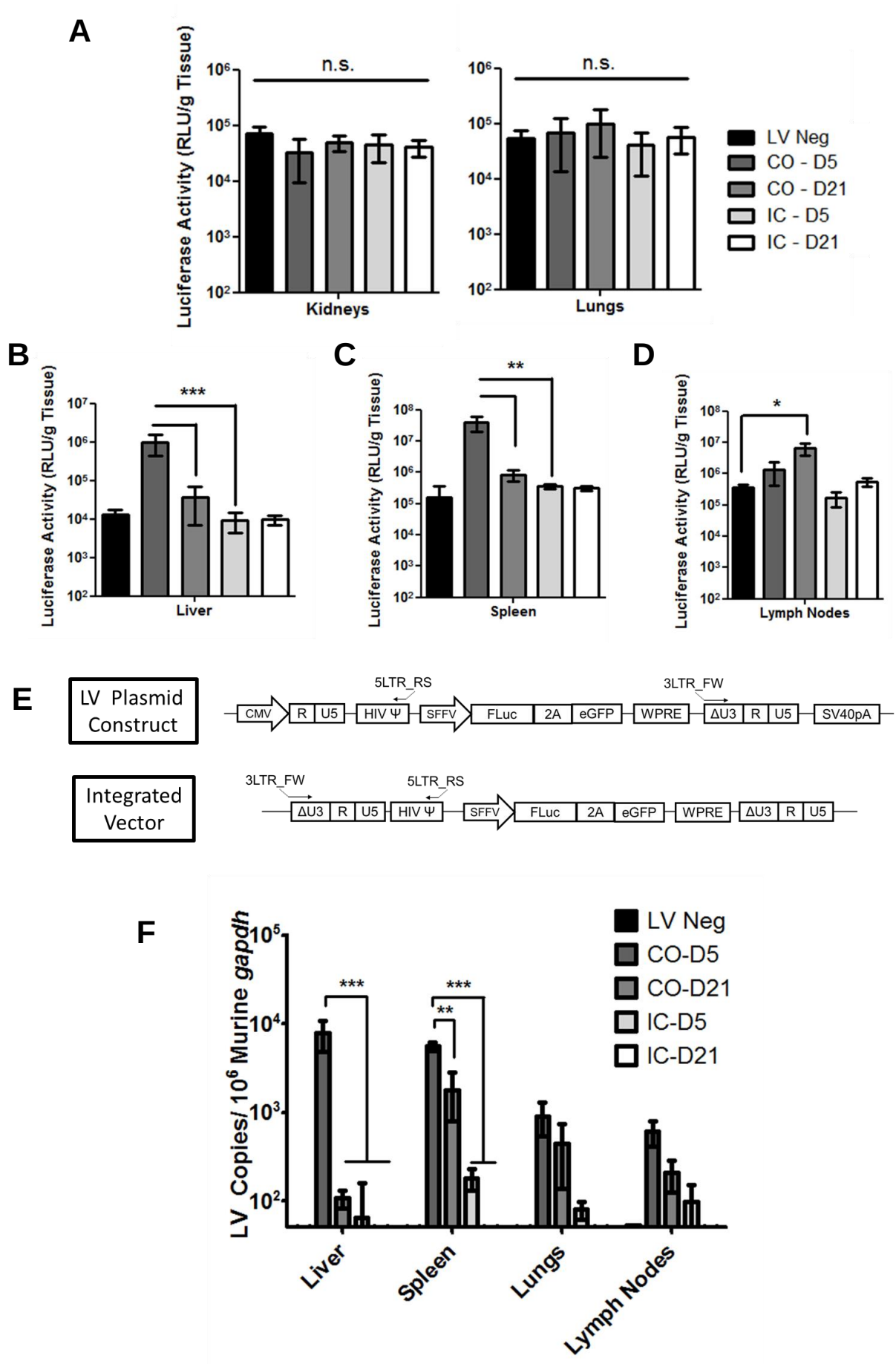
A
Luciferase Activity (RLU/g Tissue)
n.s.
n.s.
Kidneys
Lungs
LV Neg
CO - D5
CO - D21
IC - D5
IC - D21
B
***
Liver
C
**
Spleen
D
*
Lymph Nodes
E
LV Plasmid Construct
5LTR_RS
3LTR_FW
CMV
R
U5
HIV Ψ
SFFV
FLuc
2A
eGFP
WPRE
ΔU3
SV40pA
Integrated Vector
F
LV Copies/ 10^6 Murine gapdh
Liver
Spleen
Lungs
Lymph Nodes

Figure 5-5: Investigation of LV Transduction Efficacy via Analyses of Organ Samples. Tissue samples from harvested organs were collected, weighed, and homogenised. Luciferase activity in all samples was measured using the Bright-Glo™ luciferase assay system and was normalised to the weight of the organ. D5: early sacrifice group, D21: late sacrifice group. **(A)** Luciferase activity measured in the kidneys and lungs. A complete shutdown of transduction in IC samples and viral clearance in D21 samples were confirmed via lack of luciferase activity in both **(B)** liver and **(C)** spleen. **(D)** On the other hand, in CO mice, sustained gene expression was achieved in the lymph nodes. Data shown represent mean +/- SD of luciferase activity measured. Legged lines denote the significance of a single comparison, while straight lines signify all the individual comparisons within the group share the denoted significance unless otherwise stated. For **(B), (C),** and **(D)** One-way ANOVA analysis was performed with Tukey's multiple comparison post-test (*** $p<0.001$, ** $p<.0.01$, * $p<0.05$). **(E)** Schematic representation of the qPCR primers mapped on the LV vector sequence pre- and post-reverse transcription. Reverse transcription reorganises the vector genome bringing the primers together forming the qPCR amplicon. **(F)** LV provirus was quantified by amplification of reverse transcribed LV genome via qPCR. The calculated copy numbers were normalised to that of murine *gapdh* in each tissue. Data presented represent mean +/- SEM of the qPCR assay performed in triplicates. Legged lines denote the significance of a single comparison, while straight lines signify all the individual comparisons within the group share the denoted significance unless otherwise stated. One-way ANOVA analysis was performed with Tukey's multiple comparison post-test (*** $p<0.001$, ** $p<.0.01$, * $p<0.05$). Neg: negative.

I then quantitated LV provirus in tissues to gain insights on mechanisms of vector clearance observed in bioluminescence imaging. For this, genomic DNA was extracted from tissue samples and was analysed via qPCR (*Figure 5-5E-F).* To avoid amplifying any plasmid DNA which might have been delivered into the mice via the tail vein injections distinct set of primers were designed which would allow quantification of reverse-transcribed copies of the vector genome (*Figure 5-5E).* Murine *gapdh* was also quantified in parallel to assess the quality of the extracted genomic DNA samples and was further utilised to normalise calculated LV copy numbers in each tissue. In the liver, the reverse transcribed provirus DNA copies were significantly higher ($p<0.001$) in the CO-D5 samples compared to the other groups. On the other hand, in the spleen, while some reduction in LV genome copies was observed between CO-D5 and CO-D21 this was less prominent ($p<0.01$). Furthermore, the hindering effects of pre-existing immunity could be observed in both IC-D5 and IC-D21 groups which had substantially lower levels of LV copies ($p<0.001$). Reverse transcribed LV copies were also detected in lung and lymph node samples, albeit in lower levels, confirming the biodistribution of the LVs established above (*Figure 5-5A-D)*.

All in all, the data acquired demonstrate that pre-existing immunity directed against the envelope G protein of LVs significantly hinders gene delivery in subsequent vector administrations. This may pose a substantial problem in gene therapy and oncolytic virotherapy where repeated vector and virus administration may be necessary.

5.3.3.LV Administration Boosts Pre-existing Anti-Envelope Immunity

In section 5.3.1, I have demonstrated that IV injection of viral vectors into naïve mice elicits a specific, robust neutralising anti-envelope response. Therefore, LV challenge of pre-immunised mice may boost the immune system prompting an even stronger response which blocks vector transduction. To investigate this, I explored the neutralising activity of the sera isolated from the end of test terminal bleeds of IC-D21 mice. As previously described, sera were pooled, adsorbed to HEK293T cells, and incubated with VSVind.G and VesG

pseudotyped LVs (*Figure 5-6).* As expected, IV LV injection to mice pre-immunised with Gth strengthened the neutralising anti-envelope response shifting the IC50 (i.e. serum dilution where 50% neutralisation is achieved) value approximately fifty-folds (from 0.007 to 0.0001) (*Figure 5-6A).* This response elicited by the combination of SC immunisation and IV vector injection was ten times more potent than the one induced by LV challenge only (IC50 0.0001 and 0.001 respectively).

Interestingly, although LV administration and Gth immunisation alone did not produce any detectable cross-neutralising antibodies against VesG (*Figures 5-1B and 5-3E),* sera of IC-D21 mice demonstrated weak neutralising activity against MARAV.G and COCV.G pseudotyped LVs. The potency of neutralisation by the mouse sera displayed similar characteristics to that of VSV-Poly (*Figure 3-3C)* although lacked the broad cross-neutralising activity observed with the polyclonal antibody. MARAV.G and COCV.G are the closest phylogenetic relatives of VSVind.G (see *Figure 1-5*) and may share several immunodominant epitopes resulting in antibody cross-reactivity and neutralisation. Furthermore, although *in vitro* neutralisation strength of the pooled serum is weak (IC50 0.2 for COCV.G and 0.06 for MARAV.G), this might still lead to *in vivo* protection against or partial hindrance of MARAV.G- and COCV.G-LVs.

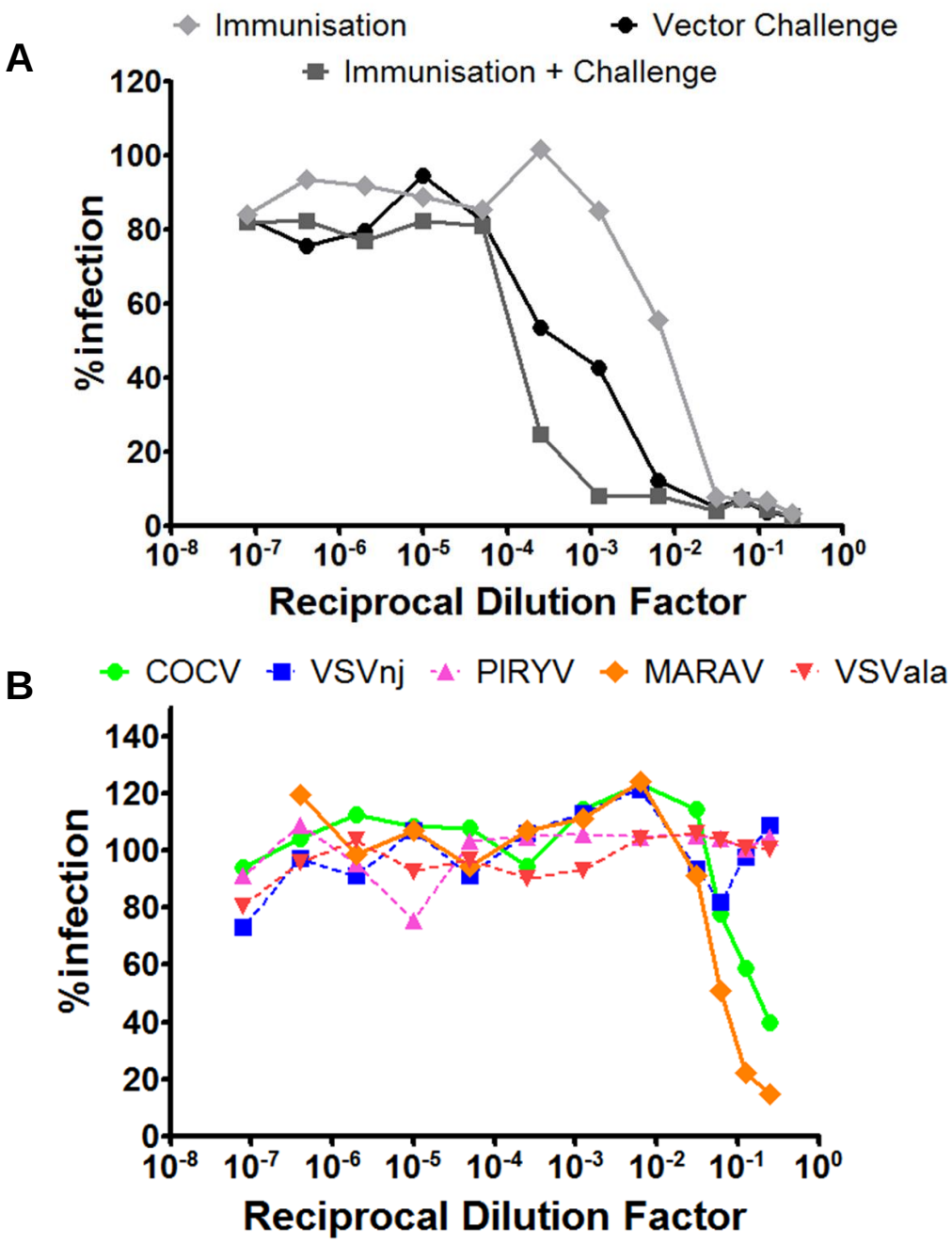

Figure 5-6: LV Challenge of Pre-immunised Mice Strengthens the Immune Response.
(A) The strength of VSVind.G-LV neutralisation activity elicited by Gth immunisation, LV challenge, and the combination of both. Calculated IC50 values: immunisation (IO-D21 sera pooled), 6.96×10^{-3}; vector challenge (CO-D21 sera pooled), 1.20×10^{-3}; immunisation+challenge (IC-D21 sera pooled), 1.51×10^{-4}. **(B)** Cross-neutralising activity of sera isolated from IC-D21 terminal bleeds. Solid lines signify the neutralisation effect observed while the dotted lines indicate the lack of neutralisation. Data shown represent the mean of three repeats performed in duplicates. To calculate IC50 values, curves were fitted using the software GraphPad Prism 5 modelled as an [inhibitor] vs response curve with variable Hill Slopes.

5.3.4.Utilising a Heterogeneous Panel of Envelopes Circumvents Humoral Anti-envelope Response

The viral vector immunogenicity study (section 5.3.2) demonstrated that SC immunisation with Gth elicited a strong enough immune response to protect the mice against a subsequent LV challenge. In *in vitro* studies the IC50 of this neutralising activity was approximately ten-folds higher (i.e. weaker neutralisation) compared to that of the response induced by IV VSVind.G-LV injection (*Figure 5-6A)*. This implies that if sequential LV administration is utilised, the first dose administered would confer resistance against the subsequent ones. But, a heterogeneous panel of envelopes could be utilised to side-step the anti-vector immunity allowing for sequential injections to achieve desired levels of therapeutic transgene expression and anti-tumour effect.

To test this theory, four VesG, VSVind.G, COCV.G, MARAV.G, and PIRYV.G, were selected. A study with the same Gth immunisation-boost regimen was designed (*Figure 5-7A-B).* However, after priming the immune system for anti-VSVind.G immunity mice were challenged with either VSVind.G-LV or other VesG-LVs. LV gene delivery efficacy was assessed utilising bioluminescence imaging and the study was terminated seven days post challenge.

The study design allowed examination of the following points:

1) Evasion of pre-existing anti-envelope immunity by using vectors pseudotyped with envelopes phylogenetically related to VSVind.G.
2) Effects of complement resistance to *in vivo* gene delivery (*in vitro* effect in *Figure 4-2).*
3) Evolution of the immune response following administration of LV with different pseudotypes.

Like the previous study, no adverse health effects were observed throughout the study (*Figure 5-7C).* Pre-challenge serum antibody levels were assessed via LV-based ELISA to ensure the presence of a VSVind.G specific humoral response (*Figure 5-7D).* In IO and all IC groups anti-VSVind.G antibodies were detected, with measured absorbance levels comparable to that of the

A

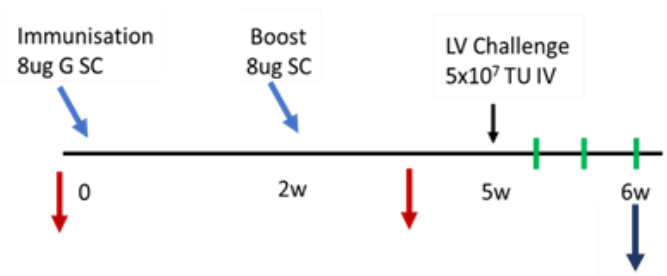

B

GROUP	ENVELOPE	MOUSE #	IMMUNISATION	BOOST	CHALLENGE
PBS	N/A	1	× (PBS)	× (PBS)	× (PBS)
Immunisation-only **(IO)**	N/A	3	✓	✓	× (PBS)
Challenge-only **(CO)**	VSVind	3	× (Adjuvant-only)	× (Adjuvant-only)	✓
	COCV	6	× (Adjuvant-only)	× (Adjuvant-only)	✓
	MARAV	6	× (Adjuvant-only)	× (Adjuvant-only)	✓
	PIRYV	6	× (Adjuvant-only)	× (Adjuvant-only)	✓
Immunisation + Challenge **(IC)**	VSVind	3	✓	✓	✓
	COCV	6	✓	✓	✓
	MARAV	6	✓	✓	✓
	PIRYV	6	✓	✓	✓

C

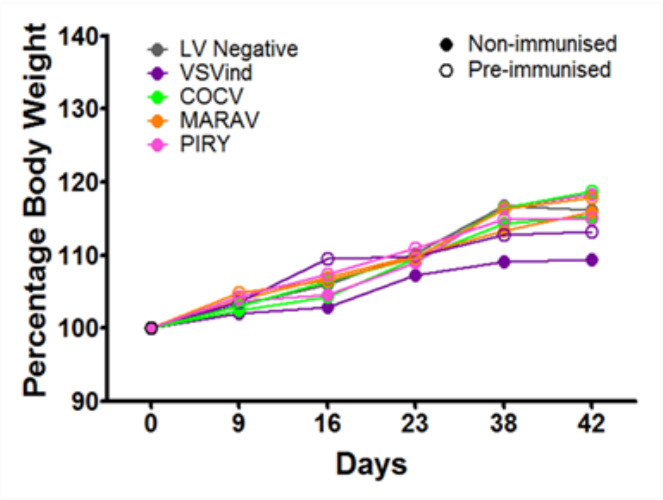

D

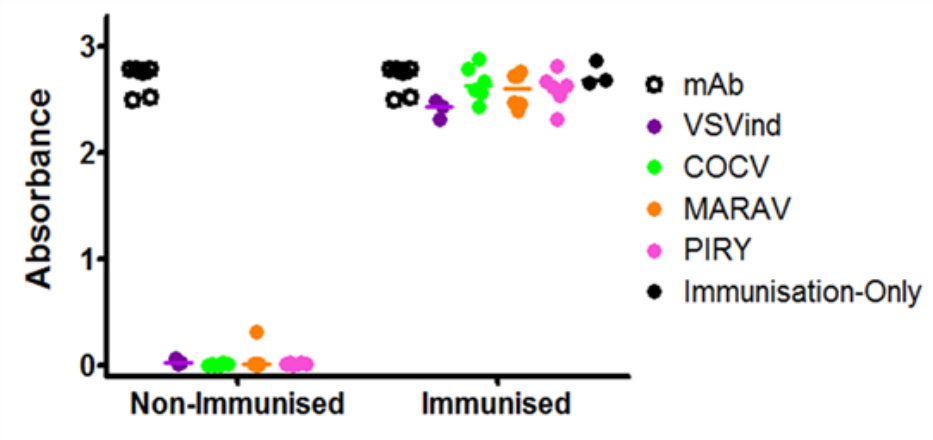

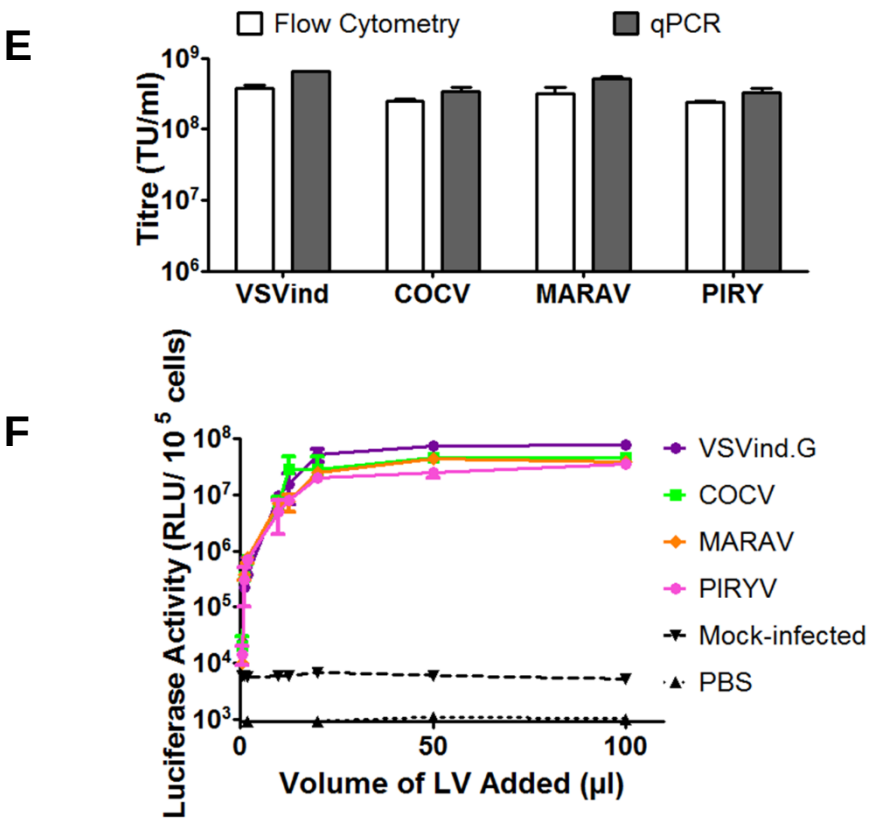

Figure 5-7: Design of VesG-LV Challenge Study Exploring G Protein Immunogenicity and Immune Evasion. (A) Timeline of the study. Immunisation and boost points are identified by light blue arrows while the black arrow indicates the time of LV challenge. Red arrows designate the times blood samples were acquired through tail vein bleeds. Green lines show the days mice were imaged. Dark blue arrow indicates termination of the study where terminal bleeds and post-mortem organ harvest were performed. w: weeks. **(B)** Study groups including the PBS (non-treatment control) group are summarised in a table indicating the injections at immunisation, boost, and challenge time points. Power analysis was performed on the radiance data acquired from the previous study (see section 5.3.2). Comparison of the radiances from LV negative and LV positive samples yielded a signal:noise ratio of 2.8. Hence for 80% power assuming a 5% significance level a sample size of three mice or higher was needed per experimental group. N/A: not applicable. **(C)** Bodyweights (bw) of mice throughout eight weeks normalised to that of at the beginning of the study. Each data point represents the mean bw of all mice in the indicated group. Standard deviation of each data point for all the groups was <5%. LV negative includes both PBS and IO groups. **(D)** Pre-challenge anti-VSVind.G serum antibody levels of immunised and non-immunised mice were determined via LV-based ELISA. mAb 8G5F11 was used as positive control to compare values obtained from different plates (10µg/ml). Single dilution of 1:100 pre-study and pre-challenge serum samples were added to wells coated with identical concentrations (25µg/ml) of VSVind.G-LVs in triplicates. Absorbance of pre-study samples was regarded as

background (overall <0.1 for all samples) and subtracted from that of pre-challenge samples. Each dot represents a mouse, and the horizontal bar shows the median. Data shown are the mean absorbance difference obtained from two repeats performed in triplicates. **(E)** Infectious titres and **(F)** luciferase activity of the VSVind.G-LV batch used in this study. Infection assays on HEK293T cells were carried out as outlined in section 2.6.2. Quantitative PCR and luciferase activity assays were performed as outlined in sections 2.9.4 and 2.9.6. Data shown represent mean +/- SEM of two experiments performed in duplicates.

control mAb 8G5F11. Following, the mice in CO and IC groups were challenged with $5x10^7$ TU/mouse of VesG-LV.Fluc-eGFP via tail vein injections. Gene delivery and expression were monitored for seven days by bioluminescence imaging at three time points (*Figure 5-8).* A similar biodistribution pattern was observed for all four pseudotypes: luciferase expression mainly detected in the four organs previously investigated.

In non-immunised mice, initial levels of gene delivery of all pseudotypes were comparable (median radiances VSVind.G: $1.23x10^8$ p/s/cm^2/sr, COCV.G: $3.67x10^7$ p/s/cm^2/sr, MARAV.G: $3.73x10^7$ p/s/cm^2/sr, PIRYV.G: $5.01x10^7$ p/s/cm^2/sr). Overall, these levels remained constant for all pseudotypes throughout seven days indicating that sustained gene expression can be achieved with all envelopes.

On the other hand, LV challenges of VSVind.G immunised mice revealed intriguing differences regarding the Gs' capacity to evade the humoral immune response. Like the previous study, VSVind.G-LV gene delivery was blocked entirely as indicated by the radiance at similar levels to the naïve mice. Both COCV.G and MARAV.G pseudotyped LV could circumvent the pre-existing immunity. Although radiance of IC mice challenged with these two pseudotypes was reduced compared to the CO mice, it was substantially higher than that of VSVind.G-LV (>100-fold on day 2-5). In *Figure 5-5B,* I have shown that following VSVind.G-LV challenge of pre-immunised mice cross-neutralising antibodies against COCV.G and MARAV.G are produced implying that there may be some conserved immunodominant epitopes on these closely related G proteins. In line with the neutralising activity observed previously,

A

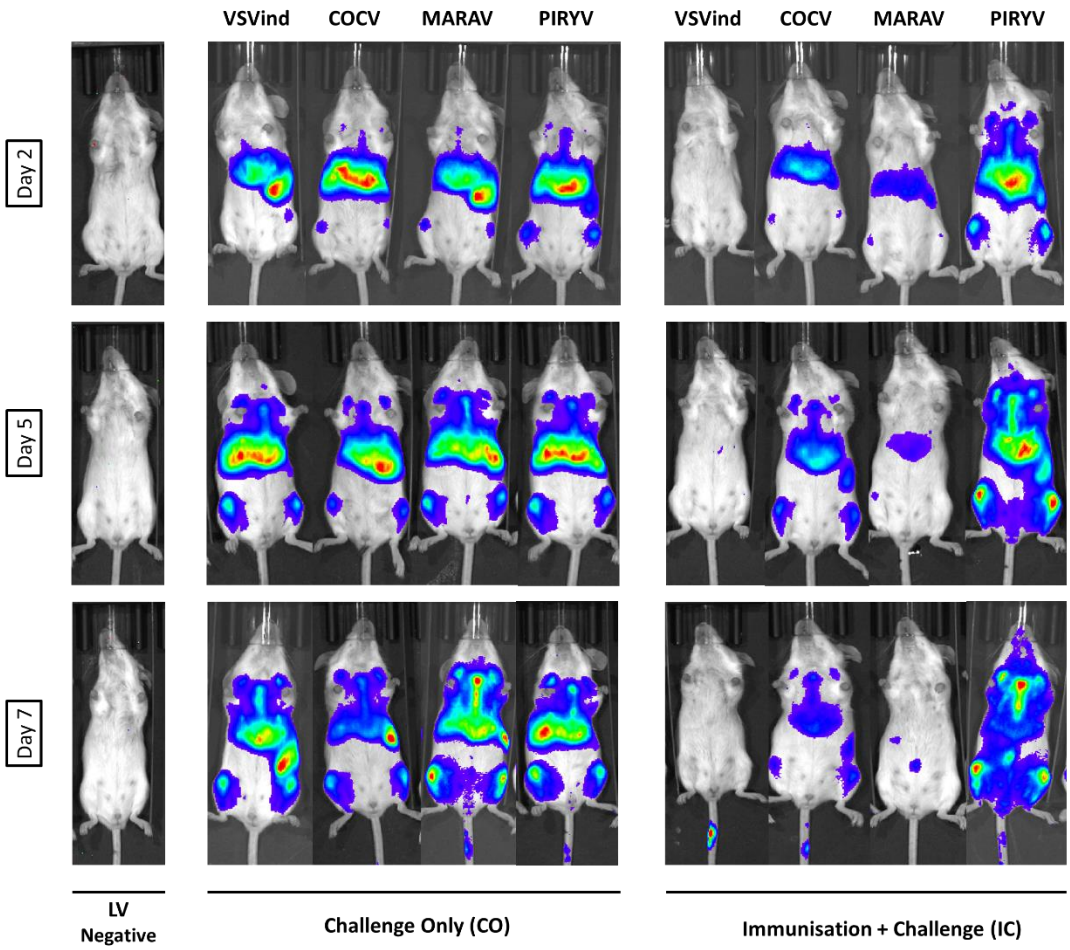

B

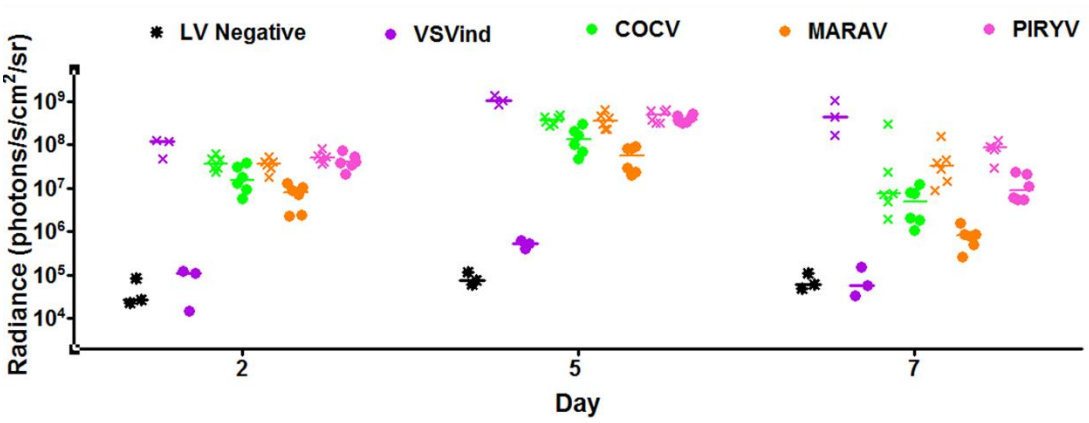

C

		Day 2	Day 5	Day 7
Challenge Only	LV Neg vs VSVind	p<0.0001	p<0.0001	p<0.0001
	VSVind vs COCV	n.s.	n.s.	p<0.001
	VSVind vs MARAV	n.s.	n.s.	p<0.001
	VSVind vs PIRYV	n.s.	n.s.	p<0.01

		Day 2	Day 5	Day 7
Immunisation + Challenge	LV Neg vs. VSVind	n.s.	n.s.	n.s.
	LV Neg vs. COCV	n.s.	p<0.05	n.s.
	LV Neg vs. MARAV	n.s.	n.s.	n.s.
	LV Neg vs. PIRYV	p<0.0001	p<0.0001	p<0.01

Figure 5-8: Evading Pre-existing Anti-VSVind.G Immunity by Using a Heterogeneous VesG Panel. **(A)** Representative bioluminescence images of transduced and naïve mice at three time points of day 2, 5, and 7 post-challenge. Localisation and the intensity of the luciferase signal are depicted in a heat map. The envelopes of the challenge vector are indicated at the top of the images, and the experimental groups are located at the bottom. The time points when the images were acquired are indicated on the left. **(B)** Photon emission from each mouse was quantified as radiance (p/s/cm^2/sr) post-imaging using region of interest analysis in Living Image® software. Each data point represents a mouse, and the horizontal bar shows the median. Different colours indicate the pseudotype of the challenge vector, solid dots stand for the IC group and crosses the CO group. **(C)** Two-way ANOVA followed by Bonferroni's multiple comparison test was performed to compare relative radiance levels in CO and IC groups. Comparisons summarised in a table. Neg: negative; n.s.: not significant.

MARAV.G-LV's gene delivery efficacy was transient as bioluminescence levels dropped considerably by day 7. On the other hand, sustained FLuc expression with COCV.G-LV in the IC group was achieved at comparable levels to the CO group and approximately 100-folds higher than VSVind.G. Strikingly PIRYV.G-LV efficacy was unaffected throughout and significantly higher levels of transgene expression was achieved ($p<0.0001$ on day 2 and 5, $p<0.01$ on day7).

Following termination of the study seven days post-challenge, gene transduction efficacy was investigated (*Figure 5-9)*. As previously described, the luciferase activity was measured following organ homogenisation using the Bright-Glo™ luciferase assay system. The overall biodistribution was similar for all four pseudotypes implying general broad tropism of all envelopes. Furthermore, all pseudotypes were efficient in transducing spleen cells reaching on average 100-fold higher luciferase activity compared to that of naïve samples. One of the undelying reasons behing this might be that the internal promoter used in the vector construct, driven from spleen focus-forming virus (SFFV) (*Figure 5-5E),* might be more active or efficient in the spleen cells.

Furthermore, IC samples support the overall results obtained via bioluminescence imaging. While the luciferase activity in organs transduced with MARAV.G-LV is at comparable levels to the VSVind.G-LV transduced and naïve samples, COCV.G-LV challenged mice exhibited substantially higher levels of activity (~ten-folds higher in the spleen and lymph nodes). In addition, PIRYV.G-LV challenged mice expressed FLuc at significantly higher levels in all four organs ($p<0.01$ in liver and spleen; $p<0.05$ in lungs and lymph nodes) which is comparable to that of CO mice injected with PIRYV.G-LVs.

These data demonstrated that PIRYV.G-LV outperformed the other pseudotypes completely evading the humoral immune response. While COCV.G-LV transduction is partially blocked, viable levels of transgene expression were detected, and immune evasion could be bolstered with a higher dose.

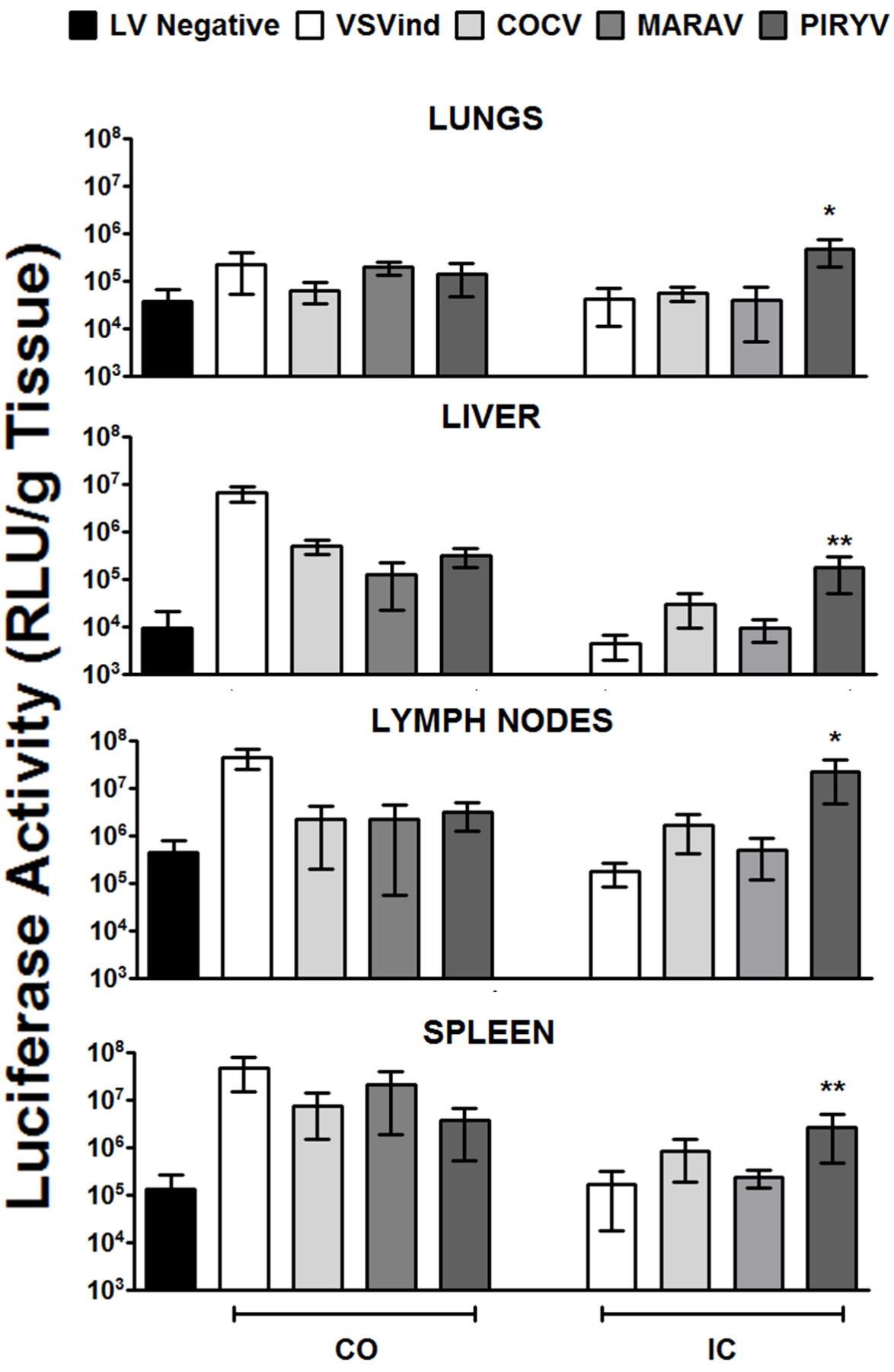
LV Negative
VSVind
COCV
MARAV
PIRYV
LUNGS
LIVER
LYMPH NODES
SPLEEN
Luciferase Activity (RLU/g Tissue)
10^8
10^7
10^6
10^5
10^4
10^3
*
**
*
**
CO
IC

Figure 5-9: Investigation of LV Transduction Levels Through Luciferase Activity in Organ Samples. Tissue samples from harvested organs were collected, weighed, and homogenised. Luciferase activity in all samples was measured utilising the Bright-Glo™ luciferase assay system and was normalised to the weight of the organ. CO: Challenge-only, IC: Immunisation+Challenge. Data shown represent mean +/- SD of luciferase activity measured. One-way ANOVA analysis was performed with Dunnett's multiple comparison post-test comparing luciferase activity of IC samples to that of LV negative mice (** $p<0.01$, * $p<0.05$).

5.3.5.Investigation of VesG Immunogenicity in the Presence and Absence of Anti-VSVind.G Immunity

In section 5.3.3, I have demonstrated that IV injection of viral vectors boosted the immune system prompting an even stronger response and leading to the production of cross-neutralising antibodies. Therefore, investigation of immune response evolution in response to VesG-LV challenge could provide essential insights on VesG immunogenicity. For this *in vitro* neutralisation assays were carried out. As previously described sera were isolated from terminal bleeds of CO and IC group mice, pooled, adsorbed to HEK293T cells and incubated with VesG-, VSVind.G-, and RDpro-LVs encoding GFP. GFP expression was measured 48h later via flow cytometry and neutralising activity was determined by normalising CO/IC-group responses to that of PBS group (*Figure 5-10)*.

First, VesGs' ability to induce anti-G neutralising response following LV injection to naïve mice was explored (*Figure 5-10A-C)*. Pooled sera from CO mice challenged with COCV.G-LV (CO-COCV.G), and MARAV.G-LV (CO-MARAV.G) demonstrated neutralising activities against their respective pseudotypes. The IC50 values for both neutralisation profiles were comparable implying similar levels of immunogenicity (*Figure 5-10E).* Interestingly, while the response against COCV.G-LV was specific, MARAV.G-LV administration yielded cross-neutralising antibodies against VSVind.G; once again indicating homology between immunodominant neutralising

epitopes between these two closely related G proteins. On the other, surprisingly, CO-PIRYV.G did not hinder PIRYV.G-LV infectivity.

Furthermore, the presence of an anti-VSVind.G immunity at the time of the LV challenge boosted the production of neutralising anti-VesG antibodies (*Figure 5-10D).* When the *in vitro* neutralisation assay was carried out using IC sera, stronger neutralising responses were observed for all pseudotypes. While IC50 values of COCV.G and MARAV.G infections decreased by approximately two- and four-folds respectively, PIRYV.G-LV infection was partially hindered (<50%).

A similar trend was evident for the neutralising anti-VSVind.G response. All VesG-LV challenges but PIRYV.G-LV boosted the pre-existing immunity resulting in stronger VSVind.G-LV neutralisation (*Figure 5-10E).* While VSVind.G challenge had the most potent effect enhancing the neutralising response by approximately 100-folds, both COCV.G and MARAV.G-LV administrations resulted in the production of cross-neutralising antibodies and a modest improvement on pre-existing G immunity. All in all, the evolution of the immune response post-LV administration highlighted that PIRYV.G-LVs is less immunogenic compared to the other three VesG-LVs.

A

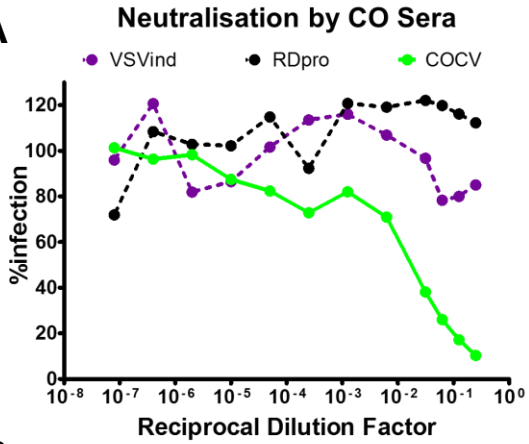

B

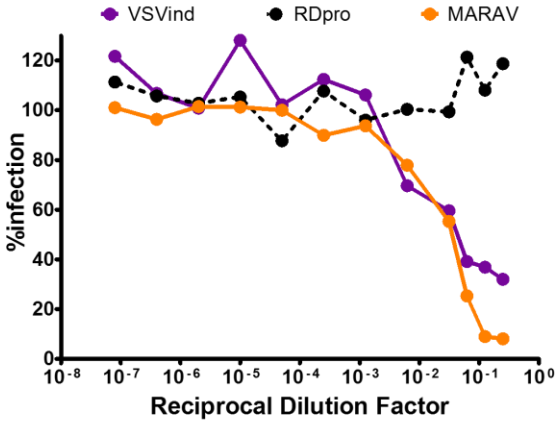

C

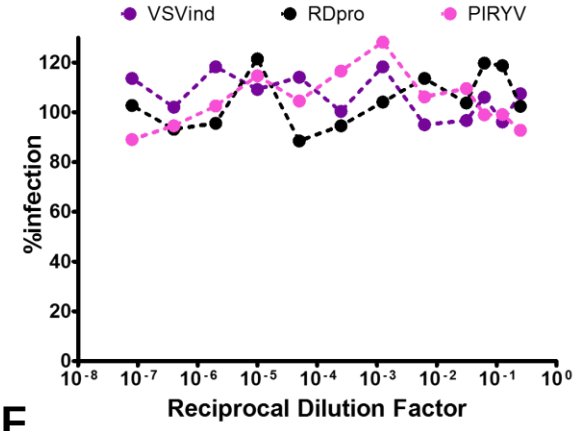

D

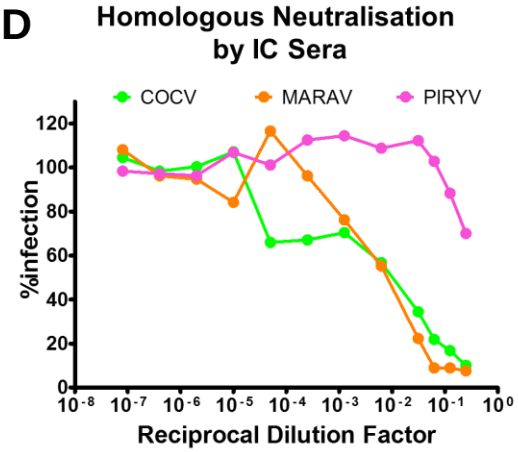

E

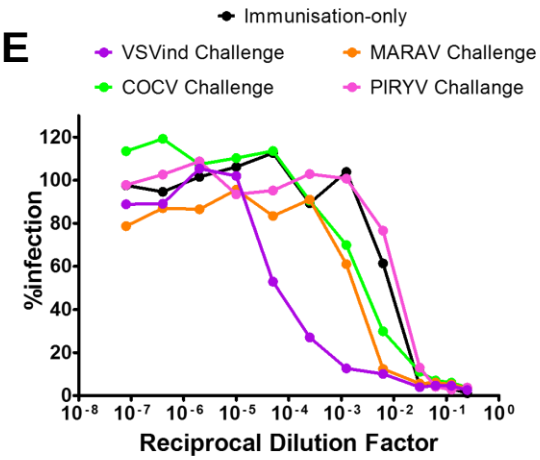

F

Pooled Sera	VesG-LV	IC50 (Reciprocal Dilution Factor)
CO-COCV.G	COCV	1.68×10^{-2}
	VSVind	no effect
CO-MARAV.G	MARAV	3.09×10^{-2}
	VSVind	5.15×10^{-2}
CO-PIRYV.G	PIRYV	no effect
	VSVind	no effect
IC-COCV.G	COCV	1.07×10^{-2}
IC-MARAV.G	MARAV	8.03×10^{-3}
IC-PIRYV.G	PIRYV	>4

Figure 5-10: Neutralising Antibody Response After VesG-LV Administration. After isolation from terminal bleeds sera from each study group were pooled (e.g. CO mice challenged with COCV.G: CO-COCV.G; IC mice challenged with PIRYV.G: IC-PIRYV.G etc.) and adsorbed onto HEK293T cells. Following, *in vitro* neutralisation assays were carried as previously described. RDpro-LVs were utilised as negative control to detect any remaining anti-human neutralising response post-adsorption. Neutralising activities of **(A)** CO-COCV.G, **(B)** CO-MARAV.G, and **(C)** CO-PIRYV.G. **(D)** Neutralising activity of IC-COCV.G, -MARAV.G, and -PIRYV.G against their respective pseudotypes. **(E)** Neutralising activity of IC-VesG sera against VSVind.G-LV compared to the neutralising activity observed after SC Gth immunisation. Solid lines signify the neutralisation effect observed while the dotted lines indicate the lack of neutralisation. Calculated IC50 values: Immunisation-only, $7.15x10^{-3}$; COCV, $5.21x10^{-3}$; MARAV, $2.49x10^{-3}$; PIRYV, $1.90x10^{-2}$; VSVind, $1.52x10^{-4}$. Data shown represent the mean of three repeats performed in duplicates. **(F)** Table summarising measured IC50 values of the observed neutralising activity of CO- and IC-VesG sera. To calculate IC50 values, curves were fitted using the software GraphPad Prism 5 modelled as an [inhibitor] vs response curve with variable Hill Slopes.

5.4.Discussion

Lentiviral vector systems are promising gene therapy vehicles owing to their ability to integrate into the host cell genome (626). This is thought to allow more prolonged and more stable transgene expression. Also, they are less immunogenic than other vector systems such as high capacity adenoviruses (627-629). Previous studies have shown sustained transgene expression and successful therapies in experimental animal models in the absence of immune responses (626, 630-634).

In several preclinical gene therapy and oncolytic virotherapy studies requirement of repeated vector and virus administration has been a cause of concern with regards to the safety and efficacy of subsequent vector administration due to the induced immune responses (497). Extensive research is being done to evade, manipulate, and suppress undesirable immune responses. Some of the promising strategies involve altered delivery techniques such as administration to immune-privileged sites, exploited organ-specific immune responses, and immunomodulatory regimens prior to vector administration (488).

In this chapter, I have explored the anti-vector primary immune response elicited following the systemic administration of LVs and its effect on subsequent administrations. As hypothesised in literature, I have demonstrated that IV injection of VSVind.G-LVs into naïve mice induces a potent and specific neutralising anti-envelope response (*Figure 5-1).* Interestingly, the challenge of naïve mice also revealed a potent anti-vector response which blocked infection of LVs pseudotyped with unrelated RDpro envelope *in vitro.* This is thought to be mediated by antibodies that recognise antigens acquired by the vectors during production from HEK293T cells (e.g. MHC-I and -II) and, therefore, may be an anti-host response. This underlined a major obstacle in studying repeated administration of viral vectors to non-immune privileged sites in animal models. In addition, the generation of such allo-antibodies may lead to cytotoxicity and allogeneic immune responses in both *in vivo* and *ex vivo* gene therapies in patients.

Due to this effect, in the following studies, the immune system was primed via subcutaneous injection of wild-type VSVind.G protein, Gth (270, 297). The protein is produced and purified through limited proteolysis cleavage of wt viral particles and hence retains its immunogenicity. Furthermore, through x-ray crystallography studies it has been demonstrated that Gth, in solution, can assume monomeric and trimeric forms as well as go through pH-dependent conformational changes (290, 331). Owing to these characteristics, Gth injections coupled with an adjuvant system elicited a VSVind.G specific neutralising immune response similar to one following intravenous VSVind.G-LV administration (*Figure 5-3D-E).*

It has been long discussed in the literature that the induction of a primary immune response, although wouldn't affect the initial vector injection, could be problematic for subsequent administrations (488, 489, 502). In this chapter, the potency of a pre-existing anti-envelope immunity has been demonstrated. VSVind.G-LV gene delivery efficacy was significantly reduced to the point of complete abrogation *(Figures 5-4 and 5-5).* However, utilising a phylogenetically distant relative of VSVind.G, PIRYV.G, I was able to demonstrate repeated administration is achievable (*Figure 5-8).* The efficacy of MARAV.G-LVs was substantially reduced while PIRYV.G-LVs completely avoided the pre-existing immunity. On the other hand, COCV.G got partially neutralised but achieved sustained gene delivery which may be boosted to higher levels with increased dosage. The degree of immune evasion achieved by the three different pseudotypes could be explained with regards to phylogenetic relatedness (see *Figure 1-5).* MARAV.G and COCV.G are two of the closest relatives of VSVind.G with 78% and 72% homology on amino acid level respectively. *In vitro* neutralisation assays performed using the sera isolated from terminal bleeds of pre-immunised mice challenged with VSVind.G-LVs displayed weak but neutralising cross-reactivity against these two pseudotypes (*Figure 5-6B).* This implies that these three closely-related G proteins share immunodominant epitopes where neutralising antibodies recognise. Furthermore, they may also share several other immunogenic determinants where non-neutralising antibodies bind to. These antibodies most probably contribute to concerted efforts of the immune system through

several mechanism: coating the viral vectors and leading to vector aggregation, aiding the deposition of complement cascade proteins leading to vector opsonisation, and contributing to antigen presentation stimulating the activation of macrophages and cytotoxic T cells (389, 390, 401, 415, 422, 467). This would explain the more robust viral transduction hindrance observed *in vivo* compared to modest vector neutralisation *in vitro.* On the other hand, PIRYV.G, with only 40% amino acid homology, may lack these determinants rendering the antibodies unable to bind to the glycoprotein.

On the other hand, administration of these four different pseudotypes led to distinct humoral immune responses. Following IV injection of VesG-LV into naïve mice, envelope specific neutralising antibodies were detected for VSVind.G, COCV.G, and MARAV.G but not for PIRYV.G *(Figure 5-10A-D)*. PIRYV.G-LV infection was blocked partially (<50%) only with IC-PIRYV.G sera, while complete neutralisation was observed for both CO- and IC-VesG sera for other pseudotypes. In addition, similarly, further administration of VSVind.G-, COCV.G-, and MARAV.G-LVs boosted the pre-existing anti-VSVind.G immunity in the IC groups while PIRYV.G-LV injection had no effect *(Figure 5-10E).* It can be deduced from the data that PIRYV.G in comparison to the other three G proteins is much less immunogenic and might need three or four boosts/sequential administrations to elicit a robust neutralising response. This difference, once more, follows phylogenetic relatedness. Furthermore, a recent study in which the low pH conformation of another vesiculovirus, Chandipura virus (CHAV), was investigated has revealed several evolutionary variances amongst VesG (246). Comparison of CHAV.G 3D structure and previously elucidated VSVind.G structures (270, 297) highlighted selective pressure of primary immune responses with regards to the main antigenic sites of the G proteins. Although the general structure-function of both G protein trimers remained universally constant, close examination of local structures especially the ones that undergo substantial conformational changes between pre- and post-fusion forms revealed that VesG could be classified into two subgroups. While VSVind.G, COCV.G, MARAV.G, VSVnj.G, and VSVala.G were clustered together, CHAV.G and PIRYV.G were in the second group with several other G proteins (246). The

overall structural differences between PIRYV.G and the other tested VesG could lead to substantially different antigen presentation in their PH domains. Therefore, the way antigenic domains are structured may dictate the immunogenicity difference as well as the lack of cross-neutralisation observed with pooled mice sera and goat polyclonal antibody VSV-Poly (see Chapter 3). Another reason behind the lack of neutralising PIRYV.G-LV antibodies, may be the number of glycoprotein spikes acquired by LVs during assembly and budding from the producer cells. PIRYV.G-LVs may have a considerably smaller number of glycoproteins compared to the other VesG-LV, therefore, providing the immune system with fewer immunogenic targets leading to a weaker response. Therefore, it will be important to quantify whether the amount of G protein on the surface of the LVs are similar.

Furthermore, the promotion of sustained transgene expression at therapeutic levels has proven to be complicated. CTL-mediated rapid clearance of transduced cells has been considered the major hurdle to overcome in establishing immune tolerance (492, 618). Furthermore, ubiquitously utilised VSVind.G envelope has been demonstrated to exacerbate this as VSVind.G pseudotypes are very efficient in transducing APCs hence enhancing and accelerating CD8+ CTL priming. In line with the literature, total vector clearance from the liver and spleen was observed fourteen days post vector administration to naïve mice *(Figure 5-4).* Further genomic analyses of LV provirus in liver and spleen samples revealed that while almost all transduced cells were getting cleared from the liver, in the spleen a combination of cell clearance and gDNA modifications (e.g. promoter methylation) may be involved in the anti-transgene immune response as a substantial number of LV provirus copies were detected in CO-D21 samples (*Figure 5-5F).* However, this may also be due to a transduced cell population persisting and proliferating in the spleen (588).

Transgene delivery levels in the CO group mice, in both studies, provided insights on *in vivo* effectiveness of complement-mediated viral vector inactivation. Serum sensitivity of wt VSVind and VSVind.G-LV is well established in the literature (266, 466-470). Recent studies have demonstrated the dose-dependent nature of complement-mediated LV

inactivation (174, 561, 562). The data shown in section 4.3.1 established that COCV.G, MARAV.G, and PIRYV.G are substantially more resistant to complement-mediated inactivation by both human and mouse sera (See *Figure 4-2).* It has been postulated that the titres utilised *in vivo* are high enough to saturate this neutralising response. *In vivo* bioluminescence imaging and luciferase activity detected in organs harvested post-mortem have confirmed this (*Figure 5-8).* While high levels of transgene expression were achieved with serum resistant pseudotypes, VSVind.G-LV transduction efficiency was comparable to or better than these pseudotypes. This highlights that, although >70% reduction of titres is observed *in vitro* compared to <30% for serum-resistant pseudotypes*, in vivo* transduction efficiency remains unaffected in this experimental setting.

In the past two decades, both VSVind and attenuated strains of Maraba virus have developed into potent and flexible vaccine vectors in oncolytic virotherapy (476, 514). There has been extensive research on both vesiculoviruses to improve viral survival, oncoselectivity, oncotoxicity, safety, and tumour immunity. Several approaches targeting these issues have been to use M (356, 483, 635-639) and G mutants (640-642), incorporation of immunomodulatory (480, 643, 644) and cancer suppressor (645) molecules into the virus, and utilising/co-expressing foreign glycoproteins to retarget the virus (353, 582, 646-651).

Premature clearance of the oncolytic viruses as well as virus sequestration has been one of the major hurdles in oncolytic virotherapy. Several approaches in delivery methods to mask the virus from neutralising antibodies (i.e. immunoshielding) (577, 652-654), incorporation of genes or molecules favouring virus survival (644, 655), and combination therapies (656-659) have been explored with variable success. If adopted, the heterogenous envelope panel approach will allow evasion of oncolytic vectors from circulating neutralising antibodies, non-specific host proteins, complement system, and other innate and pre-existing immune responses. This will also prevent the creation of overcomplicated recombinant viruses to elude host antiviral responses which may compromise the biosafety of the treatments.

Sustained gene expression, especially in the liver and spleen (*Figures 5-4 and 5-5),* remains an issue in systemic LV administration. Further work characterising the primary and innate immune responses (e.g. cytokines released) induced following LV administration may be performed, and APC transduction efficiency of different pseudotypes can be explored. This will allow tailoring or expansion of the envelope panel to included less immunogenic G proteins permitting double/triple LV administrations without eliciting a potent humoral response.

In addition, the anti-host response identified will be problematic if repeated systemic administration of LVs aimed to be studied further. There are several approaches including the use of humanised animal models, modification of LV production methods to incorporate different cell lines, and masking/blocking these antigens prior to LV administration. However, each has several drawbacks (e.g. cost, lower vector titres, decreased vector stability) and requires extensive investigation and optimisation.

Lastly, a couple of limitations were identified pertaining to the second LV challenge study designed. First, as mentioned in *Figure 5-7* power analysis of the data obtained in the first study allowed for the use of at least three mice per experimental group in this study. Therefore, IO, CO, and IC groups were designed accordingly. Despite this PBS group (non-immunised, non-challenged) only had one mouse which is underrepresented. However, as described in section 2.6.2.2 only the serum obtained from this mouse was used in neutralisation assays (see *Figures 5-1, 5-3, 5-6, 5-10)* and it was not included in other analyses. Therefore, the underrepresentation of the PBS does not invalidate the study which is otherwise adequately powered. More importantly, prior to LV challenge total LV particle number was not characterised for the pseudotypes. Although all pseudotypes had similar functional titres, determined by both flow cytometry and qPCR, and displayed comparable levels of luciferase activity following HEK293T infection, number of non-functional particles could have affected the immune response elicited. But the lack of cross-neutralising antibodies produced following Gth immunisation (see *Figure 5-3E)* meant that the presence of any non-functional G protein bearing particles would not alter the inhibitory effects of pre-existing

anti-envelope immunity substantially. Regardless establishment of total LV particle number for all pseudotypes and normalisation of challenge doses to total particle number as well as functional particle number would have strengthened the study.

In the past, translation from animal models to human therapeutics gene therapy has not always been straightforward. However, taken together, the work presented in this chapter serves as the proof-of-principle for a vector administration method in gene therapy and oncolytic virotherapy. This method will allow tailoring a panel of pseudotypes for every individual as well as cell target permitting repeated systemic administration of vectors and viruses to achieve sustained therapeutic levels of transgene expression and anti-tumour effects.

6 General Discussion

Lentiviral vectors (LVs) are promising tools for gene therapy. Recent clinical trials have demonstrated the translation of their effectiveness in preclinical laboratory studies to curative therapies (28, 30, 48, 607). Vesicular stomatitis virus Indiana strain G protein (VSVind.G) is the most commonly used envelope glycoprotein to pseudotype lentiviral vectors for experimental and clinical applications. Furthermore, the wild-type virus has been developed into a potent and versatile oncolytic viral and vaccine vector (514). Recently, G proteins derived from other vesiculoviruses (VesG), for example, Cocal virus and Piry virus, have been proposed as alternative LV envelopes with possible advantages compared to VSVind.G (manuscript accepted) (200, 202, 471, 543). Therefore, research focusing on the characterisation of VesG will be useful for vesiculovirus research, development of G protein containing advanced therapy medicinal products, and VesG's adaptation into preclinical and clinical gene therapies.

In this work, I have addressed a gap in vesiculovirus research by exploring antigenic and immunogenic characteristics of VesG. I investigated two anti-VSVind.G monoclonal antibodies for their ability to cross-react with other VesG, namely COCV.G, VSVnj.G, VSVala.G, MARAV.G and PIRYV.G. Understanding how cross-neutralising antibodies interact with other G proteins may be of interest in the context of host-pathogen interactions and may give some insights on the targets of adaptive and innate immune responses triggered in *in vivo* applications of VesG containing vectors. However, currently, there are no commercially available reagents to identify and characterise the majority of VesG. The prototype G protein, VSVind.G, has been extensively studied with regards to its crystal structure, receptor attachment, and pH-mediated cell fusion (269, 270, 290, 297, 323). But, as discussed in section 3.1, the current information about its antigenic sites, antibody binding epitopes, and immune response targets date back to 1980s.

Furthermore, although vesiculoviruses research has been growing anti-VesG antibody research has not developed as rapidly and extensively.

In Chapter 3, I undertook a detailed characterisation of two anti-VSVind.G mAbs, 8G5F11 and IE9F9. Initial investigations revealed that while IE9F9 was a VSVind.G specific antibody, 8G5F11 could bind to various VesG and neutralise LVs pseudotyped with these G proteins. Following site-directed mutagenesis work, the epitopes that these mAbs recognise and the key amino acids dictating these interactions were identified. The binding and neutralisation profiles of the mAbs to wild-type and mutant G proteins revealed intriguing characteristics. Binding to an epitope located on an α-helix in VSVind.G's PH domain (270, 297), 8G5F11 has a broad ability to cross-neutralise; blocking infections of LVs pseudotyped with five out of the six VesGs tested. Yet, the strength of neutralisation activity observed did not correlate with the affinity of the mAb towards the VesG, suggesting that innate structural differences (relating to the antigen-Ab quaternary structure) amongst VesG may be involved in LV neutralisation. On the other hand, I identified that IE9F9 inhibits the binding between VSVind.G and its primary receptor LDLR (321, 323), suggesting that the IE9F9 epitope has a critical role in the receptor recognition. I have also demonstrated that other vesiculoviruses, namely COCV, MARAV, VSVala, and VSVnj, utilise LDLR for cell infection. However, the residues that dictate IE9F9 binding are not conserved amongst the genus. Furthermore, I have demonstrated that IE9F9 cannot neutralise mutant COCV.G-LV even when its epitope is inserted into the G protein. Taken together, these strengthen the theory that although the use of the receptor might be shared, the receptor recognition epitope is not conserved amongst VesG.

Another aspect of VesG important for their *in vivo* application and investigated in this project is their sensitivity to fresh mammalian serum and the related inactivation of VesG-LVs (266, 467, 469, 470, 516). This neutralising activity is dependent on the concerted efforts of serum IgM and the complement system (467). Several approaches have been explored to evade this innate immune response allowing for higher transduction efficiencies in gene therapy and oncolytic virotherapy. The use of virus-infected cells as carriers,

biochemical modification of LV envelopes to incorporate serum response modulators, and pseudotyping of vectors with serum resistant envelopes are some of the most ubiquitously explored ones (466, 468, 550, 564, 574, 576, 577). However, each has limitations and the sensitivity to complement-mediated neutralisation remains to be one of the major concerns in the systemic delivery of vectors and viruses (467).

The work presented in Chapter 4 has focused on investigating VesG with regards to their relative serum resistance in comparison to VSVind.G. Serum neutralisation assays have revealed while VSVnj.G and VSVala.G, like VSVind.G, are sensitive, COCV.G, PIRYV.G, and MARAV.G are substantially more resistant to inactivation by fresh human, mouse, guinea pig, and rabbit sera. Further investigation of some mix-and-match chimeric constructs between VSVind.G and COCV.G targeting two identified hypervariable regions revealed that VSVind.G's PH domain confers sensitivity to inactivation by human, rabbit, and guinea pig sera. However, switching this domain on VSVind.G with that of a serum-resistant G protein (i.e. COCV.G) does not rescue titres and protect against complement-mediated neutralisation. Three key mutations on VSVind.G, S162T, T230N, and T368A (564), have been previously identified through directed evolution studies which confer serum resistance to the G protein. Out of the three only one, T230 lie within the hypervariable PH domain, but all are located within the broader responsive domain identified. Therefore, the data implies that S162 and T368 can still confer sensitivity in the absence of T230 for VSVind.G.

Furthermore, despite the establishment of serum sensitivity *in vitro,* it remains to be fully explored whether the slow neutralising activity of the complement cascade would be sufficient to block transduction *in vivo*. In Chapter 5, I demonstrated that high levels of transgene expression could be achieved with VSVind.G pseudotypes, comparable to that of serum resistant pseudotypes (i.e. COCV.G, MARAV.G, PIRYV.G), following systemic administration of LV into naïve mice. This highlights that despite in Chapter 4 VSVind.G-LV titres were reduced by fresh mouse serum by >70%, *in vivo* transduction efficiency remained unaffected in these experimental settings. Therefore, it can be inferred that LV titres utilised *in vivo* may be high enough to saturate the

complement response, rendering the data on *in vitro* sensitivity irrelevant for preclinical and clinical systemic administrations of LVs. This conclusion is supported by the fact that previously high transgene expression was achieved in dogs utilising VSVind.G-LVs even though VSVind.G was also sensitive to fresh dog serum *in vitro* (174).

However, the specifics of how vector titres and choice of envelope modulate the innate immune response against LVs remain to be fully explored. It may be of value to undertake site-directed mutagenesis studies to identify key epitopes and determinants involved in C1q deposition, serum IgM binding, and possibly alternative and MBL pathway activation and modulation on VSVind.G and other VesG. This may lead to insights on G protein characteristics which confer serum resistance and why serum resistance does not correspond to phylogenetic relatedness (i.e. two closest relatives of VSVind.G, COCV.G and MARAV.G are serum resistant, while more distant ones, VSVnj.G and VSVala.G are sensitive). Lastly, more extensive and decisive studies are necessary to conclusively deduce whether *in vitro* serum-sensitivity translates into *in vivo* reduction of LV transduction or virus infection.

Instead anti-vector and anti-transgene immune responses remain to be limiting factors in the systemic administration of LVs. Although extensive research is being done on how to evade, modulate, and manipulate these undesirable immune responses, they still pose a safety and efficacy concern for repeated administration of vectors.

In Chapter 5, I have explored the humoral immune response elicited following systemic delivery of LVs and its inhibitory effect on a subsequent administration. Tail vein injection of naïve mice with VSVind.G-LV induced a specific and neutralising anti-VSVind.G response. Furthermore, infection inhibition studies revealed another neutralising response which blocked infection of LVs pseudotyped with RDpro envelope. This is thought to be due to neutralising antibodies directed towards human antigens vectors acquire during budding from HEK293T-based producer cells, as the antibodies could be removed from serum samples via adsorption to cells. Although this anti-HEK293T response may not be as robust in clinical gene therapy, MHC

molecules incorporated into the vectors during production may act as alloantigens following APC transduction and trigger an alloreactive T cell-mediated adaptive immune response (562).

Furthermore, as postulated in the literature, the pre-existing anti-envelope antibodies significantly reduced the efficacy of a subsequent intravenous administration of the same vector pseudotype. However, by utilising a heterogenous panel of pseudotypes, comprising the three serum-resistant VesG proteins, I demonstrated that repeated LV administration is achievable. While PIRYV.G-LV efficacy was unaffected, COCV.G- and MARAV.G-LV transductions were partially blocked. This implied that the three closely related G proteins COCV.G, MARAV.G and VSVind.G shared immunodominant determinants that were targeted by the concerted efforts of both adaptive and innate branches of the immune system. A recent study exploring the crystal structure of another VesG, CHAV.G, revealed that the evolutionary divergence observed in the hypervariable PH domain amongst the genus is a results of the selective immune pressures (246). Therefore, there may be structure-derived immunogenic and antigenic differences that dictate the extent of immune evasion by different VesG. Furthermore, Lefrancois and colleagues have demonstrated that the antibodies generated in response to wild-type VSVind and VSVnj infections in mice both target neutralising and non-neutralising epitopes (511, 532, 533). While neutralising antibodies were serotype-specific, non-neutralising ones demonstrated cross-reactivity between VSVind.G and VSVnj.G. However, both types of antibodies may aid in the antiviral response as neutralising IgGs can exploit shared determinants to cross-neutralise while non-neutralising but cross-reactive IgGs and IgMs may aid in pathogen trapping by complement receptors on dendritic cells and T-cell mediated clearance of the vectors (338, 660).

Several obstacles remain ahead of *in vivo* LV gene therapy's efficient translation into the clinic. Namely, induced immune responses against LV antigens have been limiting the repeated administration of vectors (497, 502) and anti-producer cell response identified will be problematic if repeated systemic administration of LVs is aimed to be studied further and this may lead to mild autoimmune responses in patients as well (562, 612). Furthermore,

premature clearance of oncolytic vectors and transduced cells have been one of the major hurdles in achieving long-term therapeutic effects (618). Therefore, extensive research has been undertaken to develop approaches in producing alloantigen free LVs (562), exploiting immunoshielding methods to mask viral antigens (502, 577, 652-654), and utilising LVs and oncolytic viruses in combination therapies to suppress the antiviral immune response (656-659).

Taken together, the work presented in Chapter 5 demonstrates a proof-of-concept for a vector administration method in gene therapy and oncolytic virotherapy. By utilising a personally tailored panel of envelopes, this method will permit repeated IV administration of LVs or oncolytic viruses with minimal hindrance in transduction efficiencies.

6.1.Future Directions

The work presented in this thesis has provided insights related to antigenic and immunogenic co-evolution of vesiculoviruses. Studies focusing on IE9F9 and 8G5F11 neutralisation of VesG-LV uncovered mechanistic similarities towards anti-influenza haemagglutinin head-binding (specifically neutralising via receptor blocking) and stem-binding (broadly neutralising via inhibiting membrane fusion) antibodies (661, 662). I intend to further investigate the neutralisation mechanism employed by 8G5F11 and narrow down the step(s) in viral attachment and cell entry it acts on. Further studies on the antigen-Ab quaternary structure would be interesting with regards to exploring vesiculovirus infection and G-protein mediated fusion.

In addition, my experiments revealed that PIRYV.G, unlike the other VesG tested, does not utilise LDLR as its primary receptor. Nikolic and colleagues have recently reported that a phylogenetically close relative of PIRYV.G, CHAV.G, also does not bind to LDLR (323). As described in section 5.4, another study from the same group has also grouped vesiculoviruses into two subgroups with regards to their inherent differences in their pH sensitive switches and local structures (246). While the G proteins in the first group (e.g. VSVind.G, COCV.G, VSVnj.G, VSVala.G, MARAV.G) share LDLR as their

receptor, the primary receptor(s) for the G proteins in the second group is unknown. Therefore, identification of PIRYV.G's main receptor and investigation of whether its use is conserved within the second vesiculovirus subgroup (e.g. CHAV.G, ISFV) will provide vital information on vesiculovirus infection evolution and tissue tropism.

Furthermore, through several chimeric constructs I have identified that the PH domain of VSVind.G confers serum sensitivity. However, the data also demonstrated that there are determinant(s) outside the PH domain which contribute to this innate sensitivity. Further fine mapping of C1q deposition and serum IgM binding sites on VSVind.G may be of interest in generating serum-resistant variants to be incorporated into ATMP and gene therapy applications. In addition, the presence of determinants involved in activation and modulation of alternative and MBL routes of the complement cascade could allow for further optimisation of these glycoproteins for *in vivo* use.

Lastly, I was able to demonstrate that a pre-existing neutralising anti-envelope can be evaded by using a heterogenous panel of envelopes. This work provides a proof-of-principle that systemic re-administration of LVs is achievable. However, further optimisation of the methods is necessary for its successful translation into preclinical and clinical gene therapy and oncolytic virotherapy applications. First and foremost, the anti-HEK293T response described in section 5.3.1 should be further investigated in humanised mouse models and/or non-human primate models to deduce whether a similar allogeneic response would limit vector re-administration. Following which studies exploring tailoring the vectors for tissue targeting and investigation solutions to premature clearance of the transgene may be undertaken.

Bibliography

1. Kay MA. State-of-the-art gene-based therapies: the road ahead. Nat Rev Genet. 2011;12(5):316-28.
2. Dunbar CE, High KA, Joung JK, Kohn DB, Ozawa K, Sadelain M. Gene therapy comes of age. Science. 2018;359(6372).
3. Sambrook J, Westphal H, Srinivasan PR, Dulbecco R. The integrated state of viral DNA in SV40-transformed cells. Proc Natl Acad Sci U S A. 1968;60(4):1288-95.
4. Mann R, Mulligan RC, Baltimore D. Construction of a retrovirus packaging mutant and its use to produce helper-free defective retrovirus. Cell. 1983;33(1):153-9.
5. Rosenberg SA, Aebersold P, Cornetta K, Kasid A, Morgan RA, Moen R, et al. Gene transfer into humans--immunotherapy of patients with advanced melanoma, using tumor-infiltrating lymphocytes modified by retroviral gene transduction. N Engl J Med. 1990;323(9):570-8.
6. Scholler J, Brady TL, Binder-Scholl G, Hwang WT, Plesa G, Hege KM, et al. Decade-Long Safety and Function of Retroviral-Modified Chimeric Antigen Receptor T Cells. Science Translational Medicine. 2012;4(132).
7. Parkhurst MR, Yang JC, Langan RC, Dudley ME, Nathan DAN, Feldman SA, et al. T Cells Targeting Carcinoembryonic Antigen Can Mediate Regression of Metastatic Colorectal Cancer but Induce Severe Transient Colitis. Molecular Therapy. 2011;19(3):620-6.
8. Di Stasi A, Tey SK, Dotti G, Fujita Y, Kennedy-Nasser A, Martinez C, et al. Inducible apoptosis as a safety switch for adoptive cell therapy. N Engl J Med. 2011;365(18):1673-83.
9. Linette GP, Stadtmauer EA, Maus MV, Rapoport AP, Levine BL, Emery L, et al. Cardiovascular toxicity and titin cross-reactivity of affinity-enhanced T cells in myeloma and melanoma. Blood. 2013;122(6):863-71.
10. Morgan RA, Yang JC, Kitano M, Dudley ME, Laurencot CM, Rosenberg SA. Case Report of a Serious Adverse Event Following the Administration of T Cells Transduced With a Chimeric Antigen Receptor Recognizing ERBB2. Molecular Therapy. 2010;18(4):843-51.
11. Park TS, Rosenberg SA, Morgan RA. Treating cancer with genetically engineered T cells. Trends Biotechnol. 2011;29(11):550-7.
12. Collins M, Thrasher A. Gene therapy: progress and predictions. Proc Biol Sci. 2015;282(1821):20143003.
13. Aiuti A, Cattaneo F, Galimberti S, Benninghoff U, Cassani B, Callegaro L, et al. Gene therapy for immunodeficiency due to adenosine deaminase deficiency. N Engl J Med. 2009;360(5):447-58.
14. Gaspar HB, Cooray S, Gilmour KC, Parsley KL, Zhang F, Adams S, et al. Hematopoietic stem cell gene therapy for adenosine deaminase-deficient severe combined immunodeficiency leads to long-term immunological recovery and metabolic correction. Sci Transl Med. 2011;3(97):97ra80.
15. Candotti F, Shaw KL, Muul L, Carbonaro D, Sokolic R, Choi C, et al. Gene therapy for adenosine deaminase-deficient severe combined

immune deficiency: clinical comparison of retroviral vectors and treatment plans. Blood. 2012;120(18):3635-46.
16. Hacein-Bey-Abina S, Hauer J, Lim A, Picard C, Wang GP, Berry CC, et al. Efficacy of Gene Therapy for X-Linked Severe Combined Immunodeficiency. New Engl J Med. 2010;363(4):355-64.
17. Gaspar HB, Cooray S, Gilmour KC, Parsley KL, Adams S, Howe SJ, et al. Long-term persistence of a polyclonal T cell repertoire after gene therapy for X-linked severe combined immunodeficiency. Sci Transl Med. 2011;3(97):97ra79.
18. Chinen J, Davis J, De Ravin SS, Hay BN, Hsu AP, Linton GF, et al. Gene therapy improves immune function in preadolescents with X-linked severe combined immunodeficiency. Blood. 2007;110(1):67-73.
19. Stein S, Ott MG, Schultze-Strasser S, Jauch A, Burwinkel B, Kinner A, et al. Genomic instability and myelodysplasia with monosomy 7 consequent to EVI1 activation after gene therapy for chronic granulomatous disease. Nat Med. 2010;16(2):198-204.
20. Ott MG, Schmidt M, Schwarzwaelder K, Stein S, Siler U, Koehl U, et al. Correction of X-linked chronic granulomatous disease by gene therapy, augmented by insertional activation of MDS1-EVI1, PRDM16 or SETBP1. Nat Med. 2006;12(4):401-9.
21. Bianchi M, Hakkim A, Brinkmann V, Siler U, Seger R, Zychlinsky A, et al. Restoration of NET formation by gene therapy in CGD controls aspergillosis. Human Gene Therapy. 2009;20(11):1467-.
22. Kang EM, Choi U, Theobald N, Linton G, Long Priel DA, Kuhns D, et al. Retrovirus gene therapy for X-linked chronic granulomatous disease can achieve stable long-term correction of oxidase activity in peripheral blood neutrophils. Blood. 2010;115(4):783-91.
23. Kang HJ, Bartholomae CC, Paruzynski A, Arens A, Kim S, Yu SS, et al. Retroviral gene therapy for X-linked chronic granulomatous disease: results from phase I/II trial. Mol Ther. 2011;19(11):2092-101.
24. Boztug K, Schmidt M, Schwarzer A, Banerjee PP, Diez IA, Dewey RA, et al. Stem-cell gene therapy for the Wiskott-Aldrich syndrome. N Engl J Med. 2010;363(20):1918-27.
25. Aiuti A, Biasco L, Scaramuzza S, Ferrua F, Cicalese MP, Baricordi C, et al. Lentiviral Hematopoietic Stem Cell Gene Therapy in Patients with Wiskott-Aldrich Syndrome. Science. 2013;341(6148):865-U71.
26. Hacein-Bey Abina S, Gaspar HB, Blondeau J, Caccavelli L, Charrier S, Buckland K, et al. Outcomes following gene therapy in patients with severe Wiskott-Aldrich syndrome. JAMA. 2015;313(15):1550-63.
27. Cavazzana-Calvo M, Payen E, Negre O, Wang G, Hehir K, Fusil F, et al. Transfusion independence and HMGA2 activation after gene therapy of human beta-thalassaemia. Nature. 2010;467(7313):318-22.
28. Cartier N, Hacein-Bey-Abina S, Bartholomae CC, Veres G, Schmidt M, Kutschera I, et al. Hematopoietic Stem Cell Gene Therapy with a Lentiviral Vector in X-Linked Adrenoleukodystrophy. Science. 2009;326(5954):818-23.
29. Biffi A, Sessa M, Montini E, Naldini L. HSC gene therapy trial for Metachromatic Leukodystrophy. Human Gene Therapy. 2011;22(10):A7-A8.

30. DiGiusto DL, Krishnan A, Li L, Li H, Li S, Rao A, et al. RNA-based gene therapy for HIV with lentiviral vector-modified CD34(+) cells in patients undergoing transplantation for AIDS-related lymphoma. Sci Transl Med. 2010;2(36):36ra43.
31. Louis CU, Savoldo B, Dotti G, Pule M, Yvon E, Myers GD, et al. Antitumor activity and long-term fate of chimeric antigen receptor-positive T cells in patients with neuroblastoma. Blood. 2011;118(23):6050-6.
32. Pule MA, Savoldo B, Myers GD, Rossig C, Russell HV, Dotti G, et al. Virus-specific T cells engineered to coexpress tumor-specific receptors: persistence and antitumor activity in individuals with neuroblastoma. Nat Med. 2008;14(11):1264-70.
33. Kochenderfer JN, Yu Z, Frasheri D, Restifo NP, Rosenberg SA. Adoptive transfer of syngeneic T cells transduced with a chimeric antigen receptor that recognizes murine CD19 can eradicate lymphoma and normal B cells. Blood. 2010;116(19):3875-86.
34. Kochenderfer JN, Dudley ME, Feldman SA, Wilson WH, Spaner DE, Maric I, et al. B-cell depletion and remissions of malignancy along with cytokine-associated toxicity in a clinical trial of anti-CD19 chimeric-antigen-receptor-transduced T cells. Blood. 2012;119(12):2709-20.
35. Kochenderfer JN, Dudley ME, Kassim SH, Somerville RP, Carpenter RO, Stetler-Stevenson M, et al. Chemotherapy-refractory diffuse large B-cell lymphoma and indolent B-cell malignancies can be effectively treated with autologous T cells expressing an anti-CD19 chimeric antigen receptor. J Clin Oncol. 2015;33(6):540-9.
36. Brentjens RJ, Riviere I, Park JH, Davila ML, Wang X, Stefanski J, et al. Safety and persistence of adoptively transferred autologous CD19-targeted T cells in patients with relapsed or chemotherapy refractory B-cell leukemias. Blood. 2011;118(18):4817-28.
37. Brentjens RJ, Davila ML, Riviere I, Park J, Wang X, Cowell LG, et al. CD19-targeted T cells rapidly induce molecular remissions in adults with chemotherapy-refractory acute lymphoblastic leukemia. Sci Transl Med. 2013;5(177):177ra38.
38. Davila ML, Riviere I, Wang X, Bartido S, Park J, Curran K, et al. Efficacy and toxicity management of 19-28z CAR T cell therapy in B cell acute lymphoblastic leukemia. Sci Transl Med. 2014;6(224):224ra25.
39. Lee DW, Kochenderfer JN, Stetler-Stevenson M, Cui YK, Delbrook C, Feldman SA, et al. T cells expressing CD19 chimeric antigen receptors for acute lymphoblastic leukaemia in children and young adults: a phase 1 dose-escalation trial. Lancet. 2015;385(9967):517-28.
40. Kalos M, Levine BL, Porter DL, Katz S, Grupp SA, Bagg A, et al. T Cells with Chimeric Antigen Receptors Have Potent Antitumor Effects and Can Establish Memory in Patients with Advanced Leukemia. Science Translational Medicine. 2011;3(95).
41. Porter DL, Levine BL, Kalos M, Bagg A, June CH. Chimeric Antigen Receptor-Modified T Cells in Chronic Lymphoid Leukemia. New Engl J Med. 2011;365(8):725-33.

42. Maude SL, Frey N, Shaw PA, Aplenc R, Barrett DM, Bunin NJ, et al. Chimeric Antigen Receptor T Cells for Sustained Remissions in Leukemia. New Engl J Med. 2014;371(16):1507-17.
43. Maude SL, Shpall EJ, Grupp SA. Chimeric antigen receptor T-cell therapy for ALL. Hematology Am Soc Hematol Educ Program. 2014;2014(1):559-64.
44. Grupp SA, Kalos M, Barrett D, Aplenc R, Porter DL, Rheingold SR, et al. Chimeric Antigen Receptor-Modified T Cells for Acute Lymphoid Leukemia. New Engl J Med. 2013;368(16):1509-18.
45. Morgan RA, Dudley ME, Wunderlich JR, Hughes MS, Yang JC, Sherry RM, et al. Cancer regression in patients after transfer of genetically engineered lymphocytes. Science. 2006;314(5796):126-9.
46. Johnson LA, Morgan RA, Dudley ME, Cassard L, Yang JC, Hughes MS, et al. Gene therapy with human and mouse T-cell receptors mediates cancer regression and targets normal tissues expressing cognate antigen. Blood. 2009;114(3):535-46.
47. Robbins PF, Morgan RA, Feldman SA, Yang JC, Sherry RM, Dudley ME, et al. Tumor regression in patients with metastatic synovial cell sarcoma and melanoma using genetically engineered lymphocytes reactive with NY-ESO-1. J Clin Oncol. 2011;29(7):917-24.
48. Levine BL, Humeau LM, Boyer J, MacGregor RR, Rebello T, Lu XB, et al. Gene transfer in humans using a conditionally replicating lentiviral vector. P Natl Acad Sci USA. 2006;103(46):17372-7.
49. MacGregor RR. Clinical protocol. A phase 1 open-label clinical trial of the safety and tolerability of single escalating doses of autologous CD4 T cells transduced with VRX496 in HIV-positive subjects. Hum Gene Ther. 2001;12(16):2028-9.
50. Palfi S, Gurruchaga JM, Ralph GS, Lepetit H, Lavisse S, Buttery PC, et al. Long-term safety and tolerability of ProSavin, a lentiviral vector-based gene therapy for Parkinson's disease: a dose escalation, open-label, phase 1/2 trial. Lancet. 2014;383(9923):1138-46.
51. Chowdhury S, Ikeda Y. Retroviruses. In: Harrington K, Vile R, Pandha H, editors. Viral Therapy of Cancer: John Wiley & Sons, Ltd; 2008.
52. Telesnitsky A, Goff SP. Reverse Transcriptase and the Generation of Retroviral DNA. In: Coffin JM, Hughes SH, Varmus HE, editors. Retroviruses. Cold Spring Harbor (NY): Cold Spring Harbor Laboratory Press; 1997. p. 121-60.
53. Balvay L, Lastra ML, Sargueil B, Darlix JL, Ohlmann T. Translational control of retroviruses. Nat Rev Microbiol. 2007;5(2):128-40.
54. Baltimore D. RNA-dependent DNA polymerase in virions of RNA tumour viruses. Nature. 1970;226(5252):1209-11.
55. Temin HM, Mizutani S. RNA-dependent DNA polymerase in virions of Rous sarcoma virus. Nature. 1970;226(5252):1211-3.
56. Coffin JM, Hughes SH, Varmus HE. The Interactions of Retroviruses and their Hosts. In: Coffin JM, Hughes SH, Varmus HE, editors. Retroviruses. Cold Spring Harbor (NY)1997.
57. Hunter E. Viral Entry and Receptors. In: Coffin JM, Hughes SH, Varmus HE, editors. Retroviruses. New York, USA: Cold Spring Harbor Laboratory Press; 1997. p. 71-120.

58. Vogt VM. Retroviral virions and genomes. In: Coffin JM, Varmus HE, editors. Retroviruses. Cold Spring Harbor, NY: Cold Spring Harbor Laboratory Press; 1997. p. 27-71.
59. Collins JF, Bai L, Ghishan FK. The SLC20 family of proteins: dual functions as sodium-phosphate cotransporters and viral receptors. Pflugers Arch. 2004;447(5):647-52.
60. Overbaugh J, Miller AD, Eiden MV. Receptors and entry cofactors for retroviruses include single and multiple transmembrane-spanning proteins as well as newly described glycophosphatidylinositol-anchored and secreted proteins. Microbiol Mol Biol Rev. 2001;65(3):371-89, table of contents.
61. Dalgleish AG, Beverley PCL, Clapham PR, Crawford DH, Greaves MF, Weiss RA. The Cd4 (T4) Antigen Is an Essential Component of the Receptor for the Aids Retrovirus. Nature. 1984;312(5996):763-7.
62. Klatzmann D, Champagne E, Chamaret S, Gruest J, Guetard D, Hercend T, et al. Lymphocyte-T T4 Molecule Behaves as the Receptor for Human Retrovirus Lav. Nature. 1984;312(5996):767-8.
63. Maddon PJ, Mcdougal JS, Clapham PR, Dalgleish AG, Jamal S, Weiss RA, et al. Hiv Infection Does Not Require Endocytosis of Its Receptor, Cd4. Cell. 1988;54(6):865-74.
64. Albritton LM, Bowcock AM, Eddy RL, Morton CC, Tseng L, Farrer LA, et al. The Human Cationic Amino-Acid Transporter (Atrc1) - Physical and Genetic-Mapping to 13q12-Q14. Genomics. 1992;12(3):430-4.
65. Miller DG, Edwards RH, Miller AD. Cloning of the Cellular Receptor for Amphotropic Murine Retroviruses Reveals Homology to That for Gibbon Ape Leukemia-Virus. P Natl Acad Sci USA. 1994;91(1):78-82.
66. Miller DG, Miller AD. A Family of Retroviruses That Utilize Related Phosphate Transporters for Cell Entry. J Virol. 1994;68(12):8270-6.
67. van Zeijl M, Johann SV, Closs E, Cunningham J, Eddy R, Shows TB, et al. A human amphotropic retrovirus receptor is a second member of the gibbon ape leukemia virus receptor family. Proc Natl Acad Sci U S A. 1994;91(3):1168-72.
68. Takeuchi Y, Vile RG, Simpson G, O'Hara B, Collins MK, Weiss RA. Feline leukemia virus subgroup B uses the same cell surface receptor as gibbon ape leukemia virus. J Virol. 1992;66(2):1219-22.
69. Decroly E, Vandenbranden M, Ruysschaert JM, Cogniaux J, Jacob GS, Howard SC, et al. The convertases furin and PC1 can both cleave the human immunodeficiency virus (HIV)-1 envelope glycoprotein gp160 into gp120 (HIV-1 SU) and gp41 (HIV-I TM). J Biol Chem. 1994;269(16):12240-7.
70. Nisole S, Saib A. Early steps of retrovirus replicative cycle. Retrovirology. 2004;1:9.
71. Uchil PD, Mothes W. HIV Entry Revisited. Cell. 2009;137(3):402-4.
72. McClure MO, Sommerfelt MA, Marsh M, Weiss RA. The pH independence of mammalian retrovirus infection. J Gen Virol. 1990;71 (Pt 4):767-73.
73. Roe T, Reynolds TC, Yu G, Brown PO. Integration of murine leukemia virus DNA depends on mitosis. Embo J. 1993;12(5):2099-108.

74. Miller DG, Adam MA, Miller AD. Gene transfer by retrovirus vectors occurs only in cells that are actively replicating at the time of infection. Mol Cell Biol. 1990;10(8):4239-42.
75. Weinberg JB, Matthews TJ, Cullen BR, Malim MH. Productive human immunodeficiency virus type 1 (HIV-1) infection of nonproliferating human monocytes. J Exp Med. 1991;174(6):1477-82.
76. Zennou V, Petit C, Guetard D, Nerhbass U, Montagnier L, Charneau P. HIV-1 genome nuclear import is mediated by a central DNA flap. Cell. 2000;101(2):173-85.
77. Logue EC, Taylor KT, Goff PH, Landau NR. The Cargo-Binding Domain of Transportin 3 Is Required for Lentivirus Nuclear Import. J Virol. 2011;85(24):12950-61.
78. Lee MS, Craigie R. Protection of retroviral DNA from autointegration: involvement of a cellular factor. Proc Natl Acad Sci U S A. 1994;91(21):9823-7.
79. Yoshinaka Y, Katoh I, Copeland TD, Oroszlan S. Murine Leukemia-Virus Protease Is Encoded by the Gag-Pol Gene and Is Synthesized through Suppression of an Amber Termination Codon. P Natl Acad Sci USA. 1985;82(6):1618-22.
80. Berkowitz R, Fisher J, Goff SP. RNA packaging. Morphogenesis and Maturation of Retroviruses. 1996;214:177-218.
81. Freed EO. HIV-1 replication. Somat Cell Mol Genet. 2001;26(1-6):13-33.
82. AIDS*info* Glossary of HIV/AIDS-Related Terms. 9th Edition ed: National Institute of Health; 2018. HIV Life Cycle; p. 101.
83. Deng H, Liu R, Ellmeier W, Choe S, Unutmaz D, Burkhart M, et al. Identification of a major co-receptor for primary isolates of HIV-1. Nature. 1996;381(6584):661-6.
84. Garg H, Blumenthal R. Role of HIV Gp41 mediated fusion/hemifusion in bystander apoptosis. Cell Mol Life Sci. 2008;65(20):3134-44.
85. Shah AJ, Smogorzewska EM, Hannum C, Crooks GM. Flt3 ligand induces proliferation of quiescent human bone marrow CD34+CD38- cells and maintains progenitor cells in vitro. Blood. 1996;87(9):3563-70.
86. Schuitemaker H, van 't Wout AB, Lusso P. Clinical significance of HIV-1 coreceptor usage. J Transl Med. 2011;9.
87. Goodenow MM, Collman RG. HIV-1 coreceptor preference is distinct from target cell tropism: a dual-parameter nomenclature to define viral phenotypes. J Leukocyte Biol. 2006;80(5):965-72.
88. Ashkenazi A, Shai Y. Insights into the mechanism of HIV-1 envelope induced membrane fusion as revealed by its inhibitory peptides. Eur Biophys J Biophy. 2011;40(4):349-57.
89. Marsh M, Helenius A. Virus entry: open sesame. Cell. 2006;124(4):729-40.
90. Stein BS, Gowda SD, Lifson JD, Penhallow RC, Bensch KG, Engleman EG. Ph-Independent Hiv Entry into Cd4-Positive T-Cells Via Virus Envelope Fusion to the Plasma-Membrane. Cell. 1987;49(5):659-68.

91. Miyauchi K, Kim Y, Latinovic O, Morozov V, Melikyan GB. HIV Enters Cells via Endocytosis and Dynamin-Dependent Fusion with Endosomes. Cell. 2009;137(3):433-44.
92. Kleiman L, Jones CP, Musier-Forsyth K. Formation of the tRNALys packaging complex in HIV-1. Febs Lett. 2010;584(2):359-65.
93. Marquet R, Isel C, Ehresmann C, Ehresmann B. Transfer-Rnas as Primer of Reverse Transcriptases. Biochimie. 1995;77(1-2):113-24.
94. Ratner L, Haseltine W, Patarca R, Livak KJ, Starcich B, Josephs SF, et al. Complete Nucleotide-Sequence of the Aids Virus, Htlv-Iii. Nature. 1985;313(6000):277-84.
95. Molling K, Bolognesi DP, Bauer H, Busen W, Plassmann HW, Hausen P. Association of viral reverse transcriptase with an enzyme degrading the RNA moiety of RNA-DNA hybrids. Nat New Biol. 1971;234(51):240-3.
96. Champoux JJ, Schultz SJ. Ribonuclease H: properties, substrate specificity and roles in retroviral reverse transcription. FEBS J. 2009;276(6):1506-16.
97. Schultz SJ, Champoux JJ. RNase H activity: structure, specificity, and function in reverse transcription. Virus Res. 2008;134(1-2):86-103.
98. Fuentes GM, Rodriguez-Rodriguez L, Palaniappan C, Fay PJ, Bambara RA. Strand displacement synthesis of the long terminal repeats by HIV reverse transcriptase. J Biol Chem. 1996;271(4):1966-71.
99. Clavel F. HIV drug resistance : viral strategies for treatment escape. Acta Pharmacol Sin. 2006;27:29-.
100. Praparattanapan J, Kotarathititthum W, Chaiwarith R, Nuntachit N, Sirisanthana T, Supparatpinyo K. Resistance-Associated Mutations after Initial Antiretroviral Treatment Failure in a Large Cohort of Patients Infected with HIV-1 Subtype CRF01_AE. Curr Hiv Res. 2012;10(8):647-52.
101. Preston BD, Poiesz BJ, Loeb LA. Fidelity of Hiv-1 Reverse-Transcriptase. Science. 1988;242(4882):1168-71.
102. Takeuchi Y, Nagumo T, Hoshino H. Low Fidelity of Cell-Free DNA-Synthesis by Reverse-Transcriptase of Human Immunodeficiency Virus. J Virol. 1988;62(10):3900-2.
103. Milone MC, O'Doherty U. Clinical use of lentiviral vectors. Leukemia. 2018;32:1529-41.
104. Campbell EM, Hope TJ. HIV-1 capsid: the multifaceted key player in HIV-1 infection. Nat Rev Microbiol. 2015;13(8):471-83.
105. Arhel NJ, Souquere-Besse S, Munier S, Souque P, Guadagnini S, Rutherford S, et al. HIV-1 DNA Flap formation promotes uncoating of the pre-integration complex at the nuclear pore. Embo J. 2007;26(12):3025-37.
106. Bukrinsky MI, Sharova N, McDonald TL, Pushkarskaya T, Tarpley WG, Stevenson M. Association of integrase, matrix, and reverse transcriptase antigens of human immunodeficiency virus type 1 with viral nucleic acids following acute infection. Proc Natl Acad Sci U S A. 1993;90(13):6125-9.
107. Craigie R, Bushman FD. HIV DNA integration. Cold Spring Harb Perspect Med. 2012;2(7):a006890.

108. Matreyek KA, Engelman A. Viral and Cellular Requirements for the Nuclear Entry of Retroviral Preintegration Nucleoprotein Complexes. Viruses-Basel. 2013;5(10):2483-511.
109. Fassati A, Gorlich D, Harrison I, Zaytseva L, Mingot JM. Nuclear import of HIV-1 intracellular reverse transcription complexes is mediated by importin 7. Embo J. 2003;22(14):3675-85.
110. Heinzinger NK, Bukrinsky MI, Haggerty SA, Ragland AM, Kewalramani V, Lee MA, et al. The Vpr Protein of Human-Immunodeficiency-Virus Type-1 Influences Nuclear-Localization of Viral Nucleic-Acids in Nondividing Host-Cells. P Natl Acad Sci USA. 1994;91(15):7311-5.
111. Gallay P, Hope T, Chin D, Trono D. HIV-1 infection of nondividing cells through the recognition of integrase by the importin/karyopherin pathway. P Natl Acad Sci USA. 1997;94(18):9825-30.
112. Hilditch L, Towers GJ. A model for cofactor use during HIV-1 reverse transcription and nuclear entry. Curr Opin Virol. 2014;4:32-6.
113. Bushman F, Lewinski M, Ciuffi A, Barr S, Leipzig J, Hannenhalli S, et al. Genome-wide analysis of retroviral DNA integration. Nat Rev Microbiol. 2005;3(11):848-58.
114. Mitchell RS, Beitzel BF, Schroder AR, Shinn P, Chen H, Berry CC, et al. Retroviral DNA integration: ASLV, HIV, and MLV show distinct target site preferences. PLoS Biol. 2004;2(8):E234.
115. Marshall HM, Ronen K, Berry C, Llano M, Sutherland H, Saenz D, et al. Role of PSIP1/LEDGF/p75 in Lentiviral Infectivity and Integration Targeting. Plos One. 2007;2(12).
116. Felice B, Cattoglio C, Cittaro D, Testa A, Miccio A, Ferrari G, et al. Transcription factor binding sites are genetic determinants of retroviral integration in the human genome. Plos One. 2009;4(2):e4571.
117. Cavalluzzo C, Christ F, Voet A, Sharma A, Singh BK, Zhang KYJ, et al. Identification of small peptides inhibiting the integrase-LEDGF/p75 interaction through targeting the cellular co-factor. J Pept Sci. 2013;19(10):651-8.
118. Christ F, Debyser Z. The LEDGF/p75 integrase interaction, a novel target for anti-HIV therapy (vol 435, pg 102, 2013). Virology. 2013;438(1):50-.
119. Aiyer S, Swapna GVT, Malani N, Aramini JM, Schneider WM, Plumb MR, et al. Altering murine leukemia virus integration through disruption of the integrase and BET protein family interaction. Nucleic Acids Res. 2014;42(9):5917-28.
120. De Rijck J, de Kogel C, Demeulemeester J, Vets S, El Ashkar S, Malani N, et al. The BET family of proteins targets moloney murine leukemia virus integration near transcription start sites. Cell Rep. 2013;5(4):886-94.
121. Debyser Z, Christ F, De Rijck J, Gijsbers R. Host factors for retroviral integration site selection. Trends Biochem Sci. 2015;40(2):108-16.
122. Llano M, Saenz DT, Meehan A, Wongthida P, Peretz M, Walker WH, et al. An essential role for LEDGF/p75 in HIV integration. Science. 2006;314(5798):461-4.
123. Llano M, Vanegas M, Fregoso O, Saenz D, Chung S, Peretz M, et al. LEDGF/p75 determines cellular trafficking of diverse lentiviral but not

murine oncoretroviral integrase proteins and is a component of functional lentiviral preintegration complexes. J Virol. 2004;78(17):9524-37.
124. Craigie R. Integration of HIV DNA into the host cell genome. Faseb J. 1997;11(9):A867-A.
125. Nabel G, Baltimore D. An Inducible Transcription Factor Activates Expression of Human-Immunodeficiency-Virus in T-Cells. Nature. 1987;326(6114):711-3.
126. Iglesias N, Stutz F. Regulation of mRNP dynamics along the export pathway. Febs Lett. 2008;582(14):1987-96.
127. Hakata Y, Yamada M, Mabuchi N, Shida H. The carboxy-terminal region of the human immunodeficiency virus type 1 protein Rev has multiple roles in mediating CRM1-related Rev functions. J Virol. 2002;76(16):8079-89.
128. Jin L, Guzik BW, Bor YC, Rekosh D, Hammarskjold ML. Tap and NXT promote translation of unspliced mRNA. Genes Dev. 2003;17(24):3075-86.
129. Neville M, Stutz F, Lee L, Davis LI, Rosbash M. The importin-beta family member Crm1p bridges the interaction between Rev and the nuclear pore complex during nuclear export. Curr Biol. 1997;7(10):767-75.
130. Wyatt R, Kwong PD, Desjardins E, Sweet RW, Robinson J, Hendrickson WA, et al. The antigenic structure of the HIV gp120 envelope glycoprotein. Nature. 1998;393(6686):705-11.
131. Kutluay SB, Zang T, Blanco-Melo D, Powell C, Jannain D, Errando M, et al. Global Changes in the RNA Binding Specificity of HIV-1 Gag Regulate Virion Genesis. Cell. 2014;159(5):1096-109.
132. Freed EO. HIV-1 assembly, release and maturation. Nat Rev Microbiol. 2015;13(8):484-96.
133. Martin-Serrano J, Neil SJ. Host factors involved in retroviral budding and release. Nat Rev Microbiol. 2011;9(7):519-31.
134. Khan MA, Aberham C, Kao S, Akari H, Gorelick R, Bour S, et al. Human immunodeficiency virus type 1 Vif protein is packaged into the nucleoprotein complex through an interaction with viral genomic RNA. J Virol. 2001;75(16):7252-65.
135. Kaplan AH, Zack JA, Knigge M, Paul DA, Kempf DJ, Norbeck DW, et al. Partial Inhibition of the Human-Immunodeficiency-Virus Type-1 Protease Results in Aberrant Virus Assembly and the Formation of Noninfectious Particles. J Virol. 1993;67(7):4050-5.
136. Pettit SC, Everitt LE, Choudhury S, Dunn BM, Kaplan AH. Initial cleavage of the human immunodeficiency virus type 1 GagPol precursor by its activated protease occurs by an intramolecular mechanism. J Virol. 2004;78(16):8477-85.
137. Miller AD, Jolly DJ, Friedmann T, Verma IM. A transmissible retrovirus expressing human hypoxanthine phosphoribosyltransferase (HPRT): gene transfer into cells obtained from humans deficient in HPRT. Proc Natl Acad Sci U S A. 1983;80(15):4709-13.
138. Pao W, Klimstra DS, Fisher GH, Varmus HE. Use of avian retroviral vectors to introduce transcriptional regulators into mammalian cells for

analyses of tumor maintenance. P Natl Acad Sci USA. 2003;100(15):8764-9.
139. Rayner JO, Dryga SA, Kamrud KI. Alphavirus vectors and vaccination. Rev Med Virol. 2002;12(5):279-96.
140. Lundstrom K. Alphavirus vectors for gene therapy applications. Curr Gene Ther. 2001;1(1):19-29.
141. Derse D, Martarano L. Construction of a recombinant bovine leukemia virus vector for analysis of virus infectivity. J Virol. 1990;64(1):401-5.
142. Milan D, Nicolas JF. Activator-dependent and activator-independent defective recombinant retroviruses from bovine leukemia virus. J Virol. 1991;65(4):1938-45.
143. Poznansky M, Lever A, Bergeron L, Haseltine W, Sodroski J. Gene transfer into human lymphocytes by a defective human immunodeficiency virus type 1 vector. J Virol. 1991;65(1):532-6.
144. Sakuma T, Barry MA, Ikeda Y. Lentiviral vectors: basic to translational. Biochem J. 2012;443(3):603-18.
145. Shimotohno K, Temin HM. Formation of infectious progeny virus after insertion of herpes simplex thymidine kinase gene into DNA of an avian retrovirus. Cell. 1981;26(1 Pt 1):67-77.
146. Naldini L, Blomer U, Gallay P, Ory D, Mulligan R, Gage FH, et al. In vivo gene delivery and stable transduction of nondividing cells by a lentiviral vector. Science. 1996;272(5259):263-7.
147. Delenda C. Lentiviral vectors: optimization of packaging, transduction and gene expression. Journal of Gene Medicine. 2004;6:S125-S38.
148. Miller AD. Development and Applications of Retroviral Vectors. In: Coffin JM, Hughes SH, Varmus HE, editors. Retroviruses. USA: Cold Spring Harbor Laboratory Pree; 1997. p. 437-74.
149. Hughes S, Kosik E. Mutagenesis of the region between env and src of the SR-A strain of Rous sarcoma virus for the purpose of constructing helper-independent vectors. Virology. 1984;136(1):89-99.
150. Lobel LI, Patel M, King W, Nguyen-Huu MC, Goff SP. Construction and recovery of viable retroviral genomes carrying a bacterial suppressor transfer RNA gene. Science. 1985;228(4697):329-32.
151. Reik W, Weiher H, Jaenisch R. Replication-competent Moloney murine leukemia virus carrying a bacterial suppressor tRNA gene: selective cloning of proviral and flanking host sequences. Proc Natl Acad Sci U S A. 1985;82(4):1141-5.
152. Terwilliger EF, Godin B, Sodroski JG, Haseltine WA. Construction and Use of a Replication-Competent Human Immunodeficiency Virus (Hiv-1) That Expresses the Chloramphenicol Acetyltransferase Enzyme. P Natl Acad Sci USA. 1989;86(10):3857-61.
153. Schmidt M, Rethwilm A. Replicating Foamy Virus-Based Vectors Directing High-Level Expression of Foreign Genes. Virology. 1995;210(1):167-78.
154. Miyoshi H, Blomer U, Takahashi M, Gage FH, Verma IM. Development of a self-inactivating lentivirus vector. J Virol. 1998;72(10):8150-7.
155. Soneoka Y, Cannon PM, Ramsdale EE, Griffiths JC, Romano G, Kingsman SM, et al. A transient three-plasmid expression system for

the production of high titer retroviral vectors. Nucleic Acids Res. 1995;23(4):628-33.
156. Sheridan PL, Bodner M, Lynn A, Phuong TK, DePolo NJ, de la Vega DJ, et al. Generation of retroviral packaging and producer cell lines for large-scale vector production and clinical application: Improved safety and high titer. Molecular Therapy. 2000;2(3):262-75.
157. Miller AD. Retrovirus packaging cells. Hum Gene Ther. 1990;1(1):5-14.
158. Papadakis ED, Nicklin SA, Baker AH, White SJ. Promoters and control elements: designing expression cassettes for gene therapy. Curr Gene Ther. 2004;4(1):89-113.
159. Dull T, Zufferey R, Kelly M, Mandel RJ, Nguyen M, Trono D, et al. A third-generation lentivirus vector with a conditional packaging system. J Virol. 1998;72(11):8463-71.
160. Donello JE, Loeb JE, Hope TJ. Woodchuck hepatitis virus contains a tripartite posttranscriptional regulatory element. J Virol. 1998;72(6):5085-92.
161. Schambach A, Galla M, Maetzig T, Loew R, Baum C. Improving transcriptional termination of self-inactivating gamma-retroviral and lentiviral vectors. Mol Ther. 2007;15(6):1167-73.
162. Schambach A, Bohne J, Baum C, Hermann FG, Egerer L, von Laer D, et al. Woodchuck hepatitis virus post-transcriptional regulatory element deleted from X protein and promoter sequences enhances retroviral vector titer and expression. Gene Ther. 2006;13(7):641-5.
163. Zufferey R, Donello JE, Trono D, Hope TJ. Woodchuck hepatitis virus posttranscriptional regulatory element enhances expression of transgenes delivered by retroviral vectors. J Virol. 1999;73(4):2886-92.
164. Ramezani A, Hawley TS, Hawley RG. Lentiviral vectors for enhanced gene expression in human hematopoietic cells. Mol Ther. 2000;2(5):458-69.
165. Zaiss AK, Son S, Chang LJ. RNA 3' readthrough of oncoretrovirus and lentivirus: implications for vector safety and efficacy. J Virol. 2002;76(14):7209-19.
166. Logan AC, Nightingale SJ, Haas DL, Cho GJ, Pepper KA, Kohn DB. Factors influencing the titer and infectivity of lentiviral vectors. Human Gene Therapy. 2004;15(10):976-88.
167. Riviere L, Darlix JL, Cimarelli A. Analysis of the Viral Elements Required in the Nuclear Import of HIV-1 DNA. J Virol. 2010;84(2):729-39.
168. Hacein-Bey-Abina S, Garrigue A, Wang GP, Soulier J, Lim A, Morillon E, et al. Insertional oncogenesis in 4 patients after retrovirus-mediated gene therapy of SCID-X1. J Clin Invest. 2008;118(9):3132-42.
169. Persons DA. Lentiviral vector gene therapy: effective and safe? Mol Ther. 2010;18(5):861-2.
170. Persons DA, Baum C. Solving the problem of gamma-retroviral vectors containing long terminal repeats. Mol Ther. 2011;19(2):229-31.
171. Stein S, Ott MG, Schultze-Strasser S, Jauch A, Burwinkel B, Kinner A, et al. Genomic instability and myelodysplasia with monosomy 7 consequent to EVI1 activation after gene therapy for chronic granulomatous disease. Nature Medicine. 2010;16(2):198-U05.

172. Case SS, Price MA, Jordan CT, Yu XJ, Wang L, Bauer G, et al. Stable transduction of quiescent CD34(+)CD38(-) human hematopoietic cells by HIV-1-based lentiviral vectors. Proc Natl Acad Sci U S A. 1999;96(6):2988-93.
173. Uchida N, Sutton RE, Friera AM, He D, Reitsma MJ, Chang WC, et al. HIV, but not murine leukemia virus, vectors mediate high efficiency gene transfer into freshly isolated G0/G1 human hematopoietic stem cells. Proc Natl Acad Sci U S A. 1998;95(20):11939-44.
174. Cantore A, Ranzani M, Bartholomae CC, Volpin M, Valle PD, Sanvito F, et al. Liver-directed lentiviral gene therapy in a dog model of hemophilia B. Sci Transl Med. 2015;7(277):277ra28.
175. Kong J, Kim SR, Binley K, Pata I, Doi K, Mannik J, et al. Correction of the disease phenotype in the mouse model of Stargardt disease by lentiviral gene therapy. Gene Ther. 2008;15(19):1311-20.
176. Ailles L, Schmidt M, Santoni de Sio FR, Glimm H, Cavalieri S, Bruno S, et al. Molecular evidence of lentiviral vector-mediated gene transfer into human self-renewing, multi-potent, long-term NOD/SCID repopulating hematopoietic cells. Mol Ther. 2002;6(5):615-26.
177. Cavalieri S, Cazzaniga S, Geuna M, Magnani Z, Bordignon C, Naldini L, et al. Human T lymphocytes transduced by lentiviral vectors in the absence of TCR activation maintain an intact immune competence. Blood. 2003;102(2):497-505.
178. Sutton RE, Reitsma MJ, Uchida N, Brown PO. Transduction of human progenitor hematopoietic stem cells by human immunodeficiency virus type 1-based vectors is cell cycle dependent. J Virol. 1999;73(5):3649-60.
179. Cattoglio C, Facchini G, Sartori D, Antonelli A, Miccio A, Cassani B, et al. Hot spots of retroviral integration in human CD34(+) hematopoietic cells. Blood. 2007;110(6):1770-8.
180. Wu XL, Li Y, Crise B, Burgess SM. Transcription start regions in the human genome are favored targets for MLV integration. Science. 2003;300(5626):1749-51.
181. Schroder ARW, Shinn P, Chen HM, Berry C, Ecker JR, Bushman F. HIV-1 integration in the human genome favors active genes and local hotspots. Cell. 2002;110(4):521-9.
182. Modlich U, Navarro S, Zychlinski D, Maetzig T, Knoess S, Brugman MH, et al. Insertional Transformation of Hematopoietic Cells by Self-inactivating Lentiviral and Gammaretroviral Vectors. Molecular Therapy. 2009;17(11):1919-28.
183. Montini E, Cesana D, Schmidt M, Sanvito F, Bartholomae CC, Ranzani M, et al. The genotoxic potential of retroviral vectors is strongly modulated by vector design and integration site selection in a mouse model of HSC gene therapy. Journal of Clinical Investigation. 2009;119(4):964-75.
184. Zufferey R, Dull T, Mandel RJ, Bukovsky A, Quiroz D, Naldini L, et al. Self-inactivating lentivirus vector for safe and efficient in vivo gene delivery. J Virol. 1998;72(12):9873-80.
185. Naldini L. In vivo gene delivery by lentiviral vectors. Thromb Haemost. 1999;82(2):552-4.

186. Logan AC, Lutzko C, Kohn DB. Advances in lentiviral vector design for gene- modification of hematopoietic stem cells. Curr Opin Biotech. 2002;13(5):429-36.
187. Kotsopoulou E, Kim VN, Kingsman AJ, Kingsman SM, Mitrophanous KA. A Rev-independent human immunodeficiency virus type 1 (HIV-1)-based vector that exploits a codon-optimized HIV-1 gag-pol gene. J Virol. 2000;74(10):4839-52.
188. Schneider R, Campbell M, Nasioulas G, Felber BK, Pavlakis GN. Inactivation of the human immunodeficiency virus type 1 inhibitory elements allows Rev-independent expression of gag and gag/protease and particle formation. J Virol. 1997;71(7):4892-903.
189. Maetzig T, Galla M, Baum C, Schambach A. Gammaretroviral vectors: biology, technology and application. Viruses. 2011;3(6):677-713.
190. Schambach A, Swaney WP, van der Loo JC. Design and production of retro- and lentiviral vectors for gene expression in hematopoietic cells. Methods Mol Biol. 2009;506:191-205.
191. Klages N, Zufferey R, Trono D. A stable system for the high-titer production of multiply attenuated lentiviral vectors. Mol Ther. 2000;2(2):170-6.
192. Segura MM, Mangion M, Gaillet B, Garnier A. New developments in lentiviral vector design, production and purification. Expert Opin Biol Ther. 2013;13(7):987-1011.
193. Burns JC, Friedmann T, Driever W, Burrascano M, Yee JK. Vesicular stomatitis virus G glycoprotein pseudotyped retroviral vectors: concentration to very high titer and efficient gene transfer into mammalian and nonmammalian cells. Proc Natl Acad Sci U S A. 1993;90(17):8033-7.
194. Farson D, Witt R, McGuinness R, Dull T, Kelly M, Song J, et al. A new-generation stable inducible packaging cell line for lentiviral vectors. Hum Gene Ther. 2001;12(8):981-97.
195. Broussau S, Jabbour N, Lachapelle G, Durocher Y, Tom R, Transfiguracion J, et al. Inducible packaging cells for large-scale production of lentiviral vectors in serum-free suspension culture. Mol Ther. 2008;16(3):500-7.
196. Ikeda Y, Takeuchi Y, Martin F, Cosset FL, Mitrophanous K, Collins M. Continuous high-titer HIV-1 vector production. Nature Biotechnology. 2003;21(5):569-72.
197. Throm RE, Ouma AA, Zhou S, Chandrasekaran A, Lockey T, Greene M, et al. Efficient construction of producer cell lines for a SIN lentiviral vector for SCID-X1 gene therapy by concatemeric array transfection. Blood. 2009;113(21):5104-10.
198. Sanber KS, Knight SB, Stephen SL, Bailey R, Escors D, Minshull J, et al. Construction of stable packaging cell lines for clinical lentiviral vector production. Sci Rep-Uk. 2015;5.
199. Marin V, Stornaiuolo A, Piovan C, Corna S, Bossi S, Pema M, et al. RD-MolPack technology for the constitutive production of self-inactivating lentiviral vectors pseudotyped with the nontoxic RD114-TR envelope. Mol Ther Methods Clin Dev. 2016;3:16033.
200. Trobridge GD, Wu RA, Hansen M, Ironside C, Watts KL, Olsen P, et al. Cocal-pseudotyped lentiviral vectors resist inactivation by human

serum and efficiently transduce primate hematopoietic repopulating cells. Mol Ther. 2010;18(4):725-33.
201. Wielgosz MM, Kim YS, Carney GG, Zhan J, Reddivari M, Coop T, et al. Generation of a lentiviral vector producer cell clone for human Wiskott-Aldrich syndrome gene therapy. Mol Ther Methods Clin Dev. 2015;2:14063.
202. Humbert O, Gisch DW, Wohlfahrt ME, Adams AB, Greenberg PD, Schmitt TM, et al. Development of Third-generation Cocal Envelope Producer Cell Lines for Robust Lentiviral Gene Transfer into Hematopoietic Stem Cells and T-cells. Mol Ther. 2016;24(7):1237-46.
203. White JM, Delos SE, Brecher M, Schornberg K. Structures and mechanisms of viral membrane fusion proteins: multiple variations on a common theme. Crit Rev Biochem Mol Biol. 2008;43(3):189-219.
204. . !!! INVALID CITATION !!! {}.
205. Garg H, Joshi A, Freed EO, Blumenthal R. Site-specific mutations in HIV-1 gp41 reveal a correlation between HIV-1-mediated bystander apoptosis and fusion/hemifusion. J Biol Chem. 2007;282(23):16899-906.
206. Chu VC, McElroy LJ, Chu V, Bauman BE, Whittaker GR. The avian coronavirus infectious bronchitis virus undergoes direct low-pH-dependent fusion activation during entry into host cells. J Virol. 2006;80(7):3180-8.
207. Freed EO, Mouland AJ. The cell biology of HIV-1 and other retroviruses. Retrovirology. 2006;3:77.
208. Seth S, Vincent A, Compans RW. Activation of fusion by the SER virus F protein: a low-pH-dependent paramyxovirus entry process. J Virol. 2003;77(11):6520-7.
209. Lamb RA, Jardetzky TS. Structural basis of viral invasion: lessons from paramyxovirus F. Curr Opin Struct Biol. 2007;17(4):427-36.
210. Harrison SC. Mechanism of membrane fusion by viral envelope proteins. Adv Virus Res. 2005;64:231-61.
211. Fouillot-Coriou N, Roux L. Structure-function analysis of the Sendai virus F and HN cytoplasmic domain: different role for the two proteins in the production of virus particle. Virology. 2000;270(2):464-75.
212. Modis Y, Ogata S, Clements D, Harrison SC. Structure of the dengue virus envelope protein after membrane fusion. Nature. 2004;427(6972):313-9.
213. Kielian M. Class II virus membrane fusion proteins. Virology. 2006;344(1):38-47.
214. Podbilewicz B. Virus and cell fusion mechanisms. Annu Rev Cell Dev Biol. 2014;30:111-39.
215. Modis Y. Class II Fusion Proteins. In: Pöhlmann S, Simmons G, editors. Viral Entry into Host Cells Advances in Experiental Medicine and Biology. 790. New York, NY: Springer; 2013.
216. Backovic M, Jardetzky TS. Class III viral membrane fusion proteins. Adv Exp Med Biol. 2011;714:91-101.
217. Heldwein EE, Lou H, Bender FC, Cohen GH, Eisenberg RJ, Harrison SC. Crystal structure of glycoprotein B from herpes simplex virus 1. Science. 2006;313(5784):217-20.

218. Kadlec J, Loureiro S, Abrescia NG, Stuart DI, Jones IM. The postfusion structure of baculovirus gp64 supports a unified view of viral fusion machines. Nat Struct Mol Biol. 2008;15(10):1024-30.
219. Baquero E, Albertini AA, Raux H, Buonocore L, Rose JK, Bressanelli S, et al. Structure of the low pH conformation of Chandipura virus G reveals important features in the evolution of the vesiculovirus glycoprotein. PLoS Pathog. 2015;11(3):e1004756.
220. Kim IS, Jenni S, Stanifer ML, Roth E, Whelan SP, van Oijen AM, et al. Mechanism of membrane fusion induced by vesicular stomatitis virus G protein. Proc Natl Acad Sci U S A. 2017;114(1):E28-E36.
221. Dietzgen RG, Kondo H, Goodin MM, Kurath G, Vasilakis N. The family Rhabdoviridae: mono- and bipartite negative-sense RNA viruses with diverse genome organization and common evolutionary origins. Virus Res. 2017;227:158-70.
222. Dietzgen R, Calisher CH, Kurath G, Kuzmin IV, Rodriguez LL, Stone DM, et al. Family *Rhabdoviridae.* In: King AMQ, Adams MJ, Carstens EB, Lefkowitz EJ, editors. Virus Taxonomy Ninth Report of the International Committee on Taxonomy of Viruses. Oxford: Elsevier Academic Press; 2011. p. 686-714.
223. Ge P, Tsao J, Schein S, Green TJ, Luo M, Zhou ZH. Cryo-EM model of the bullet-shaped vesicular stomatitis virus. Science. 2010;327(5966):689-93.
224. Mire CE, White JM, Whitt MA. A spatio-temporal analysis of matrix protein and nucleocapsid trafficking during vesicular stomatitis virus uncoating. PLoS Pathog. 2010;6(7):e1000994.
225. Dietzgen RG, Calisher CH, Kurath G, Kuzmin IV, Rodriguez LL, Stone DM, et al. Rhabdoviridae. Hungary: ICTV; 2016.
226. Walker PJ, Firth C, Widen SG, Blasdell KR, Guzman H, Wood TG, et al. Evolution of genome size and complexity in the rhabdoviridae. PLoS Pathog. 2015;11(2):e1004664.
227. Spiropoulou CF, Nichol ST. A Small Highly Basic-Protein Is Encoded in Overlapping Frame within the P-Gene of Vesicular Stomatitis-Virus. J Virol. 1993;67(6):3103-10.
228. Peluso RW, Richardson JC, Talon J, Lock M. Identification of a set of proteins (C' and C) encoded by the bicistronic P gene of the Indiana serotype of vesicular stomatitis virus and analysis of their effect on transcription by the viral RNA polymerase. Virology. 1996;218(2):335-42.
229. Schnell MJ, Mebatsion T, Conzelmann KK. Infectious Rabies Viruses from Cloned Cdna. Embo J. 1994;13(18):4195-203.
230. Whelan SPJ, Ball LA, Barr JN, Wertz GTW. Efficient Recovery of Infectious Vesicular Stomatitis-Virus Entirely from Cdna Clones. P Natl Acad Sci USA. 1995;92(18):8388-92.
231. Fernando BG, Yersin CT, Jose CB, Paola ZS. Predicted 3D Model of the Rabies Virus Glycoprotein Trimer. Biomed Research International. 2016.
232. Astray RM, Jorge SAC, Pereira CA. Rabies vaccine development by expression of recombinant viral glycoprotein. Arch Virol. 2017;162(2):323-32.

233. Gaudin Y, Ruigrok RWH, Tuffereau C, Knossow M, Flamand A. Rabies Virus Glycoprotein Is a Trimer. Virology. 1992;187(2):627-32.
234. Albertini AAV, Baquero E, Ferlin A, Gaudin Y. Molecular and Cellular Aspects of Rhabdovirus Entry. Viruses-Basel. 2012;4(1):117-39.
235. Lafon M. Rabies virus receptors. J Neurovirol. 2005;11(1):82-7.
236. Tuffereau C, Benejean J, Alfonso AMR, Flamand A, Fishman MC. Neuronal cell surface molecules mediate specific binding to rabies virus glycoprotein expressed by a recombinant baculovirus on the surfaces of lepidopteran cells. J Virol. 1998;72(2):1085-91.
237. Tuffereau C, Benejean J, Blondel D, Kieffer B, Flamand A. Low-affinity nerve-growth factor receptor (P75NTR) can serve as a receptor for rabies virus. Embo J. 1998;17(24):7250-9.
238. Tuffereau C, Schmidt K, Langevin C, Lafay F, Dechant G, Koltzenburg M. The rabies virus glycoprotein receptor p75(NTR) is not essential for rabies virus infection. J Virol. 2007;81(24):13622-30.
239. Lewis P, Fu YG, Lentz TL. Rabies virus entry at the neuromuscular junction in nerve-muscle cocultures. Muscle & Nerve. 2000;23(5):720-30.
240. Thoulouze MI, Lafage M, Schachner M, Hartmann U, Cremer H, Lafon M. The neural cell adhesion molecule is a receptor for rabies virus. J Virol. 1998;72(9):7181-90.
241. Gaudin Y, Ruigrok RWH, Knossow M, Flamand A. Low-Ph Conformational-Changes of Rabies Virus Glycoprotein and Their Role in Membrane-Fusion. J Virol. 1993;67(3):1365-72.
242. Whitt MA, Buonocore L, Prehaud C, Rose JK. Membrane-Fusion Activity, Oligomerization, and Assembly of the Rabies Virus Glycoprotein. Virology. 1991;185(2):681-8.
243. Beier KT, Saunders A, Oldenburg IA, Miyamichi K, Akhtar N, Luo LQ, et al. Anterograde or retrograde transsynaptic labeling of CNS neurons with vesicular stomatitis virus vectors. P Natl Acad Sci USA. 2011;108(37):15414-9.
244. Rodriguez LL, Pauszek SJ. Genus Vesiculovirus. In: Dietzgen RG, Kuzmin IV, editors. Rhabdoviruses: Molecular Taxonomy, Evolution, Genomics, Ecology, Host-vector Interactions, Cytopathology, and Control. United Kingdom: Caister Academic Press; 2012. p. 23-36.
245. de Souza WM, Acrani GO, Romeiro MF, Reis O, Tolardo AL, de Andrade AAS, et al. Complete genome sequence of Piry vesiculovirus. Arch Virol. 2016;161(8):2325-8.
246. Baquero E, Albertini AA, Raux H, Buonocore L, Rose JK, Bressanelli S, et al. Structure of the Low pH Confirmation of Chandipura Virus G Reveals Important Features in the Evolution of the Vesiculovirus Glycoprotein. PLoS Pathogens. 2015;3(11).
247. Pauszek SJ, Allende R, Rodriguez LL. Characterization of the full-length genomic sequences of vesicular stomatitis Cocal and Alagoas viruses. Arch Virol. 2008;153(7):1353-7.
248. Gallione CJ, Rose JK. Nucleotide-Sequence of a Cdna Clone Encoding the Entire Glycoprotein from the New-Jersey Serotype of Vesicular Stomatitis-Virus. J Virol. 1983;46(1):162-9.

249. Jonkers AH, Shope RE, Aitken THG, Spence L. Cocal virus, a new agent in Trinidad related to vesicular stomatitus virus, type Indiana Am J Vet. 1984;Res. 25:236–42.
250. Hanson RP. The natural history of vesicular stomatitis. Bacteriol Rev. 1952;16(3):179-204.
251. Martinez I, Wertz GW. Biological differences between vesicular stomatitis virus Indiana and New Jersey serotype glycoproteins: Identification of amino acid residues modulating pH-dependent infectivity. J Virol. 2005;79(6):3578-85.
252. Cargnelutti JF, Olinda RG, Maia LA, de Aguiar GM, Neto EG, Simoes SV, et al. Outbreaks of Vesicular stomatitis Alagoas virus in horses and cattle in northeastern Brazil. J Vet Diagn Invest. 2014;26(6):788-94.
253. Alonso A, Martins MA, Gomes Mda P, Allende R, Sondahl MS. Development and evaluation of an enzyme-linked immunosorbent assay for detection, typing, and subtyping of vesicular stomatitis virus. J Vet Diagn Invest. 1991;3(4):287-92.
254. Federer KE, Burrows R, Brooksby JB. Vesicular stomatitis virus--the relationship between some strains of the Indiana serotype. Res Vet Sci. 1967;8(1):103-17.
255. Letchworth GJ, Rodriguez LL, Del cbarrera J. Vesicular stomatitis. Vet J. 1999;157(3):239-60.
256. Cotton WE. Vesicular Stomatitis. Vet Med. 1927;22:169-75.
257. Hassler D, Braun R, Schwarz TF. [Deadly encephalitis epidemic in India caused by the Chandipura virus]. Dtsch Med Wochenschr. 2003;128(36):1817.
258. John TJ. Chandipura virus, encephalitis, and epidemic brain attack in India. Lancet. 2004;364(9452):2175; author reply -6.
259. Tandale BV, Tikute SS, Arankalle VA, Sathe PS, Joshi MV, Ranadive SN, et al. Chandipura virus: a major cause of acute encephalitis in children in North Telangana, Andhra Pradesh, India. J Med Virol. 2008;80(1):118-24.
260. Weiss RA, Boettiger D, Murphy HM. Pseudotypes of avian sarcoma viruses with the envelope properties of vesicular stomatitis virus. Virology. 1977;76(2):808-25.
261. Zavada J. The pseudotypic paradox. J Gen Virol. 1982;63 (Pt 1):15-24.
262. Lukashevich IS, Zavada J. Phenotypic mixing of vesicular stomatitis virus (VSV) with vaccinia virus. Acta Virol. 1982;26(6):524.
263. Hoshino H, Clapham PR, Weiss RA, Miyoshi I, Yoshida M, Miwa M. Human T-cell leukemia virus type I: pseudotype neutralization of Japanese and American isolates with human and rabbit sera. Int J Cancer. 1985;36(6):671-5.
264. Bhella RS, Nichol ST, Wanas E, Ghosh HP. Structure, expression and phylogenetic analysis of the glycoprotein gene of Cocal virus. Virus Res. 1998;54(2):197-205.
265. Reiser J, Harmison G, KluepfelStahl S, Brady RO, Karlson S, Schubert M. Transduction of nondividing cells using pseudotyped defective high-titer HIV type 1 particles. P Natl Acad Sci USA. 1996;93(26):15266-71.

266. DePolo NJ, Reed JD, Sheridan PL, Townsend K, Sauter SL, Jolly DJ, et al. VSV-G pseudotyped lentiviral vector particles produced in human cells are inactivated by human serum. Mol Ther. 2000;2(3):218-22.
267. Hoffmann M, Wu YJ, Gerber M, Berger-Rentsch M, Heimrich B, Schwemmle M, et al. Fusion-active glycoprotein G mediates the cytotoxicity of vesicular stomatitis virus M mutants lacking host shut-off activity. J Gen Virol. 2010;91(Pt 11):2782-93.
268. Kuzmin IV, Novella IS, Dietzgen RG, Padhi A, Rupprecht CE. The rhabdoviruses: biodiversity, phylogenetics, and evolution. Infect Genet Evol. 2009;9(4):541-53.
269. Roche S, Albertini AAV, Lepault J, Bressanelli S, Gaudin Y. Structures of vesicular stomatitis virus glycoprotein: membrane fusion revisited. Cell Mol Life Sci. 2008;65(11):1716-28.
270. Roche S, Rey FA, Gaudin Y, Brassanelli S. Structure of the pre-fusion form of the vesicular stomatitis virus glycoprotein g. Science. 2007;315:843-8.
271. Cartwright B, Talbot P, Brown F. The proteins of biologically active sub-units of vesicular stomatitis virus. J Gen Virol. 1970;7(3):267-72.
272. Kang CY, Prevec L. Proteins of vesicular stomatitis virus. II. Immunological comparisons of viral antigens. J Virol. 1970;6(1):20-7.
273. Baltimore D, Huang AS, Stampfer M. Ribonucleic acid synthesis of vesicular stomatitis virus, II. An RNA polymerase in the virion. Proc Natl Acad Sci U S A. 1970;66(2):572-6.
274. Davis NL, Wertz GW. Synthesis of vesicular stomatitis virus negative-strand RNA in vitro: dependence on viral protein synthesis. J Virol. 1982;41(3):821-32.
275. Rose JK, Welch WJ, Sefton BM, Esch FS, Ling NC. Vesicular stomatitis virus glycoprotein is anchored in the viral membrane by a hydrophobic domain near the COOH terminus. Proc Natl Acad Sci U S A. 1980;77(7):3884-8.
276. Travassos da Rosa AP, Tesh RB, Travassos da Rosa JF, Herve JP, Main AJ, Jr. Carajas and Maraba viruses, two new vesiculoviruses isolated from phlebotomine sand flies in Brazil. Am J Trop Med Hyg. 1984;33(5):999-1006.
277. Libersou S, Albertini AA, Ouldali M, Maury V, Maheu C, Raux H, et al. Distinct structural rearrangements of the VSV glycoprotein drive membrane fusion. J Cell Biol. 2010;191(1):199-210.
278. Sieczkarski SB, Whittaker GR. Differential requirements of Rab5 and Rab7 for endocytosis of influenza and other enveloped viruses. Traffic. 2003;4(5):333-43.
279. Le Blanc I, Luyet PP, Pons V, Ferguson C, Emans N, Petiot A, et al. Endosome-to-cytosol transport of viral nucleocapsids. Nat Cell Biol. 2005;7(7):653-U25.
280. Carneiro FA, Ferradosa AS, Da Poian AT. Low pH-induced conformational changes in vesicular stomatitis virus glycoprotein involve dramatic structure reorganization. J Biol Chem. 2001;276(1):62-7.
281. Clague MJ, Schoch C, Zech L, Blumenthal R. Gating Kinetics of Ph-Activated Membrane-Fusion of Vesicular Stomatitis-Virus with Cells -

Stopped-Flow Measurements by Dequenching of Octadecylrhodamine Fluorescence. Biochemistry-Us. 1990;29(5):1303-8.
282. Gaudin Y, de Kinkelin P, Benmansour A. Mutations in the glycoprotein of viral haemorrhagic septicaemia virus that affect virulence for fish and the pH threshold for membrane fusion. J Gen Virol. 1999;80:1221-9.
283. Roche S, Gaudin Y. Evidence that rabies virus forms different kinds of fusion machines with different pH thresholds for fusion. J Virol. 2004;78(16):8746-52.
284. Rose JK, Gallione CJ. Nucleotide sequences of the mRNA's encoding the vesicular stomatitis virus G and M proteins determined from cDNA clones containing the complete coding regions. J Virol. 1981;39(2):519-28.
285. Masters PS, Bhella RS, Butcher M, Patel B, Ghosh HP, Banerjee AK. Structure and Expression of the Glycoprotein Gene of Chandipura Virus. Virology. 1989;171(1):285-90.
286. Brun G, Bao XK, Prevec L. The relationship of Piry virus to other vesiculoviruses: A re-evaluation based on the glycoprotein gene sequence. Intervirology. 1995;38(5):274-82.
287. Kumar S, Stecher G, Tamura K. MEGA7: Molecular Evolutionary Genetics Analysis Version 7.0 for Bigger Datasets. Mol Biol Evol. 2016;33(7):1870-4.
288. Jones DT, Taylor WR, Thornton JM. The rapid generation of mutation data matrices from protein sequences. Comput Appl Biosci. 1992;8(3):275-82.
289. Kotwal GJ, Capone J, Irving RA, Rhee SH, Bilan P, Toneguzzo F, et al. Viral membrane glycoproteins: comparison of the amino terminal amino acid sequences of the precursor and mature glycoproteins of three serotypes of vesicular stomatitis virus. Virology. 1983;129(1):1-11.
290. Albertini AA, Merigoux C, Libersou S, Madiona K, Bressanelli S, Roche S, et al. Characterization of Monomeric Intermediates during VSV Glycoprotein Structural Transition. Plos Pathogens. 2012;8(2).
291. Sun X, Roth SL, Bialecki MA, Whittaker GR. Internalization and fusion mechanism of vesicular stomatitis virus and related rhabdoviruses. Future Virol. 2010;5(1):85-96.
292. Garnier J, Gaye P, Mercier JC, Robson B. Structural properties of signal peptides and their membrane insertion. Biochimie. 1980;62(4):231-9.
293. Kreil G. Transfer of Proteins across Membranes. Annu Rev Biochem. 1981;50:317-48.
294. Waterhouse AM, Procter JB, Martin DMA, Clamp M, Barton GJ. Jalview Version 2-a multiple sequence alignment editor and analysis workbench. Bioinformatics. 2009;25(9):1189-91.
295. Reading CL, Penhoet EE, Ballou CE. Carbohydrate structure of vesicular stomatitis virus glycoprotein. J Biol Chem. 1978;253(16):5600-12.
296. Whitt MA, Chong L, Rose JK. Glycoprotein cytoplasmic domain sequences required for rescue of a vesicular stomatitis virus glycoprotein mutant. J Virol. 1989;63(9):3569-78.

297. Roche S, Bressanelli S, Rey FA, Gaudin Y. Crystal structure of the low-pH form of the vesicular stomatitis virus glycoprotein G. Science. 2006;313(5784):187-91.
298. Li Y, Drone C, Sat E, Ghosh HP. Mutational Analysis of the Vesicular Stomatitis-Virus Glycoprotein-G for Membrane-Fusion Domains. J Virol. 1993;67(7):4070-7.
299. Zhang L, Ghosh HP. Characterization of the Putative Fusogenic Domain in Vesicular Stomatitis-Virus Glycoprotein-G. J Virol. 1994;68(4):2186-93.
300. Durrer P, Gaudin Y, Ruigrok RWH, Graf R, Brunner J. Photolabeling Identifies a Putative Fusion Domain in the Envelope Glycoprotein of Rabies and Vesicular Stomatitis Viruses. J Biol Chem. 1995;270(29):17575-81.
301. Fredericksen BL, Whitt MA. Vesicular Stomatitis-Virus Glycoprotein Mutations That Affect Membrane-Fusion Activity and Abolish Virus Infectivity. J Virol. 1995;69(3):1435-43.
302. Shokralla S, He Y, Wanas E, Ghosh HP. Mutations in a carboxy-terminal region of vesicular stomatitis virus glycoprotein G that affect membrane fusion activity. Virology. 1998;242(1):39-50.
303. Gaudin Y, Tuffereau C, Segretain D, Knossow M, Flamand A. Reversible Conformational-Changes and Fusion Activity of Rabies Virus Glycoprotein. J Virol. 1991;65(9):4853-9.
304. Doms RW, Keller DS, Helenius A, Balch WE. Role for adenosine triphosphate in regulating the assembly and transport of vesicular stomatitis virus G protein trimers. J Cell Biol. 1987;105(5):1957-69.
305. Carneiro FA, Stauffer F, Lima CS, Juliano MA, Juliano L, Da Poian AT. Membrane fusion induced by vesicular stomatitis virus depends on histidine protonation. J Biol Chem. 2003;278(16):13789-94.
306. Gaudin Y, Tuffereau C, Durrer P, Flamand A, Ruigrok RWH. Biological Function of the Low-Ph, Fusion Inactive Conformation of Rabies Virus Glycoprotein-(G) - G Is Transported in a Fusion Inactive State-Like Conformation. J Virol. 1995;69(9):5528-34.
307. Roche S, Gaudin Y. Characterization of the equilibrium between the native and fusion-inactive conformation of rabies virus glycoprotein indicates that the fusion complex is made of several trimers. Virology. 2002;297(1):128-35.
308. Backovic M, Jardetzky TS. Class III viral membrane fusion proteins. Curr Opin Struc Biol. 2009;19(2):189-96.
309. Carr CM, Chaudhry C, Kim PS. Influenza hemagglutinin is spring-loaded by a metastable native conformation. P Natl Acad Sci USA. 1997;94(26):14306-13.
310. Chothia C, Lesk AM. The Relation between the Divergence of Sequence and Structure in Proteins. Embo J. 1986;5(4):823-6.
311. Wood TC, Pearson WR. Evolution of protein sequences and structures. J Mol Biol. 1999;291(4):977-95.
312. Vandepol SB, Lefrancois L, Holland JJ. Sequences of the major antibody binding epitopes of the Indiana serotype of vesicular stomatitis virus. Virology. 1986;148(2):312-25.
313. Grove J, Marsh M. The cell biology of receptor-mediated virus entry. J Cell Biol. 2011;195(7):1071-82.

314. de Haan CA, Li Z, te Lintelo E, Bosch BJ, Haijema BJ, Rottier PJ. Murine coronavirus with an extended host range uses heparan sulfate as an entry receptor. J Virol. 2005;79(22):14451-6.
315. Vlasak M, Goester I, Blaas D. Human rhinovirus type 89 variants use heparan sulfate proteoglycan for cell attachment. J Virol. 2005;79(10):5963-70.
316. Mercer J, Schelhaas M, Helenius A. Virus Entry by Endocytosis. Annual Review of Biochemistry, Vol 79. 2010;79:803-33.
317. Kielian M, Rey FA. Virus membrane-fusion proteins: more than one way to make a hairpin. Nat Rev Microbiol. 2006;4(1):67-76.
318. Moyer CL, Nemerow GR. Viral weapons of membrane destruction: variable modes of membrane penetration by non-enveloped viruses. Curr Opin Virol. 2011;1(1):44-9.
319. Papadopulos A, Tomatis VM, Kasula R, Meunier FA. The cortical acto-Myosin network: from diffusion barrier to functional gateway in the transport of neurosecretory vesicles to the plasma membrane. Front Endocrinol (Lausanne). 2013;4:153.
320. Marsh M. Endosomes-Key Components in Viral Entry and Replication. In: Dikic I, editor. Endosomes. Georgetown Landes Bioscince / Eurekah.com; 2006. p. 132-44.
321. Finkelshtein D, Werman A, Novick D, Barak S, Rubinstein M. LDL receptor and its family members serve as the cellular receptors for vesicular stomatitis virus. P Natl Acad Sci USA. 2013;110(18):7306-11.
322. Brown MS, Herz J, Goldstein JL. LDL-receptor structure. Calcium cages, acid baths and recycling receptors. Nature. 1997;388(6643):629-30.
323. Nikolic J, Belot L, Raux H, Legrand P, Gaudin Y, A AA. Structural basis for the recognition of LDL-receptor family members by VSV glycoprotein. Nat Commun. 2018;9(1):1029.
324. Fisher C, Beglova N, Blacklow SC. Structure of an LDLR-RAP complex reveals a general mode for ligand recognition by lipoprotein receptors. Mol Cell. 2006;22(2):277-83.
325. Jeon H, Meng W, Takagi J, Eck MJ, Springer TA, Blacklow SC. Implications for familial hypercholesterolemia from the structure of the LDL receptor YWTD-EGF domain pair. Nat Struct Biol. 2001;8(6):499-504.
326. Atkins AR, Brereton IM, Kroon PA, Lee HT, Smith R. Calcium is essential for the structural integrity of the cysteine-rich, ligand-binding repeat of the low-density lipoprotein receptor. Biochemistry-Us. 1998;37(6):1662-70.
327. Huang S, Henry L, Ho YK, Pownall HJ, Rudenko G. Mechanism of LDL binding and release probed by structure-based mutagenesis of the LDL receptor. J Lipid Res. 2010;51(2):297-308.
328. Rudenko G, Henry L, Henderson K, Ichtchenko K, Brown MS, Goldstein JL, et al. Structure of the LDL receptor extracellular domain at endosomal pH. Science. 2002;298(5602):2353-8.
329. Beglov D, Lee CJ, De Biasio A, Kozakov D, Brenke R, Vajda S, et al. Structural insights into recognition of beta 2-glycoprotein I by the lipoprotein receptors. Proteins. 2009;77(4):940-9.

330. Ferlin A, Raux H, Baquero E, Lepault J, Gaudin Y. Characterization of pH-sensitive molecular switches that trigger the structural transition of vesicular stomatitis virus glycoprotein from the postfusion state toward the prefusion state. J Virol. 2014;88(22):13396-409.
331. Baquero E, Albertini AA, Raux H, Abou-Hamdan A, Boeri-Erba E, Ouldali M, et al. Structural intermediates in the fusion-associated transition of vesiculovirus glycoprotein. Embo J. 2017;36(5):679-92.
332. Baquero E, Albertini AA, Vachette P, Lepault J, Bressanelli S, Gaudin Y. Intermediate conformations during viral fusion glycoprotein structural transition. Curr Opin Virol. 2013;3(2):143-50.
333. Smith AE, Helenius A. How viruses enter animal cells. Science. 2004;304(5668):237-42.
334. Weissenhorn W, Hinz A, Gaudin Y. Virus membrane fusion. Febs Lett. 2007;581(11):2150-5.
335. Jeetendra E, Robison CS, Albritton LM, Whitt MA. The membrane-proximal domain of vesicular stomatitis virus G protein functions as a membrane fusion potentiator and can induce hemifusion. J Virol. 2002;76(23):12300-11.
336. Baquero E, Albertini AA, Raux H, Abou-Hamdan A, Boeri-Erba E, Ouldali M, et al. Structural intermediates in the fusion-associated transition of vesiculovirus glycoprotein. Embo J. 2017;36(5):679-92.
337. Lichty BD, Power AT, Stojdl DF, Bell JC. Vesicular stomatitis virus: re-inventing the bullet. Trends Mol Med. 2004;10(5):210-6.
338. Bell J, Parato K, Atkins H. Vesicular Stomatitis Virus In: Harrington K, Vile R, Pandha H, editors. Viral Therapy of Cancer: John WIley & Sons, Ltd.; 2008. p. 187-203.
339. Ikeda H, Old LJ, Schreiber RD. The roles of IFN gamma in protection against tumor development and cancer immunoediting. Cytokine Growth Factor Rev. 2002;13(2):95-109.
340. Dunn GP, Bruce AT, Sheehan KC, Shankaran V, Uppaluri R, Bui JD, et al. A critical function for type I interferons in cancer immunoediting. Nat Immunol. 2005;6(7):722-9.
341. Stojdl DF, Lichty B, Knowles S, Marius R, Atkins H, Sonenberg N, et al. Exploiting tumor-specific defects in the interferon pathway with a previously unknown oncolytic virus. Nat Med. 2000;6(7):821-5.
342. Stojdl DF, Lichty BD, tenOever BR, Paterson JM, Power AT, Knowles S, et al. VSV strains with defects in their ability to shutdown innate immunity are potent systemic anti-cancer agents. Cancer Cell. 2003;4(4):263-75.
343. Balachandran S, Barber GN. Vesicular stomatitis virus (VSV) therapy of tumors. IUBMB Life. 2000;50(2):135-8.
344. Balachandran S, Porosnicu M, Barber GN. Oncolytic activity of vesicular stomatitis virus is effective against tumors exhibiting aberrant p53, Ras, or myc function and involves the induction of apoptosis. J Virol. 2001;75(7):3474-9.
345. Stojdl DF, Abraham N, Knowles S, Marius R, Brasey A, Lichty BD, et al. The murine double-stranded RNA-dependent protein kinase PKR is required for resistance to vesicular stomatitis virus. J Virol. 2000;74(20):9580-5.

346. Stojdl DF, Lichty B, Knowles S, Marius R, Atkins H, Sonenberg N, et al. Exploiting tumor-specific defects in the interferon pathway with a previously unknown oncolytic virus. Nature Medicine. 2000;6(7):821-5.
347. Bell JC, Lichty B, Stojdl D. Getting oncolytic virus therapies off the ground. Cancer Cell. 2003;4(1):7-11.
348. Wollmann G, Tattersall P, van den Pol AN. Targeting human glioblastoma cells: comparison of nine viruses with oncolytic potential. J Virol. 2005;79(10):6005-22.
349. Huang TG, Ebert O, Shinozaki K, Garcia-Sastre A, Woo SL. Oncolysis of hepatic metastasis of colorectal cancer by recombinant vesicular stomatitis virus in immune-competent mice. Mol Ther. 2003;8(3):434-40.
350. Cesaire R, Oliere S, Sharif-Askari E, Loignon M, Lezin A, Olindo S, et al. Oncolytic activity of vesicular stomatitis virus in primary adult T-cell leukemia. Oncogene. 2006;25(3):349-58.
351. Lichty BD, Stojdl DF, Taylor RA, Miller L, Frenkel I, Atkins H, et al. Vesicular stomatitis virus: a potential therapeutic virus for the treatment of hematologic malignancy. Hum Gene Ther. 2004;15(9):821-31.
352. Lawson ND, Stillman EA, Whitt MA, Rose JK. Recombinant vesicular stomatitis viruses from DNA. Proc Natl Acad Sci U S A. 1995;92(10):4477-81.
353. Bergman I, Griffin JA, Gao YH, Whitaker-Dowling P. Treatment of implanted mammary tumors with recombinant vesicular stomatitis virus targeted to Her2/neu. International Journal of Cancer. 2007;121(2):425-30.
354. Bergman I, Whitaker-Dowling P, Gao Y, Griffin JA. Preferential targeting of vesicular stomatitis virus to breast cancer cells. Virology. 2004;330(1):24-33.
355. Bergman I, Whitaker-Dowling P, Gao Y, Griffin JA, Watkins SC. Vesicular stomatitis virus expressing a chimeric Sindbis glycoprotein containing an Fc antibody binding domain targets to Her2/neu overexpressing breast cancer cells. Virology. 2003;316(2):337-47.
356. Stojdl DF, Lichty BD, tenOever BR, Paterson JM, Power AT, Knowles S, et al. VSV strains with defects in their ability to shutdown innate immunity are potent systemic anti-cancer agents. Cancer Cell. 2003;4(4):263-75.
357. Lichty BD, Power AT, Stojdl DF, Bell JC. Vesicular stomatitis virus: re-inventing the bullet. Trends in Molecular Medicine. 2004;10(5):210-6.
358. Roberts A, Buonocore L, Price R, Forman J, Rose JK. Attenuated vesicular stomatitis viruses as vaccine vectors. J Virol. 1999;73(5):3723-32.
359. Roberts A, Kretzschmar E, Perkins AS, Forman J, Price R, Buonocore L, et al. Vaccination with a recombinant vesicular stomatitis virus expressing an influenza virus hemagglutinin provides complete protection from influenza virus challenge. J Virol. 1998;72(6):4704-11.
360. Schlereth B, Rose JK, Buonocore L, ter Meulen V, Niewiesk S. Successful vaccine-induced seroconversion by single-dose immunization in the presence of measles virus-specific maternal antibodies. J Virol. 2000;74(10):4652-7.

361. Medaglini D, Siegrist CA. Immunomonitoring of human responses to the rVSV-ZEBOV Ebola vaccine. Curr Opin Virol. 2017;23:88-94.
362. Metzger WG, Vivas-Martinez S. Questionable efficacy of the rVSV-ZEBOV Ebola vaccine. Lancet. 2018;391(10125):1021-.
363. Pavot V. Ebola virus vaccines: Where do we stand? Clin Immunol. 2016;173:44-9.
364. Trad MA, Naughton W, Yeung A, Mazlin L, O'sullivan M, Gilroy N, et al. Ebola virus disease: An update on current prevention and management strategies. Journal of Clinical Virology. 2017;86:5-13.
365. Kahn JS, Roberts A, Weibel C, Buonocore L, Rose JK. Replication-competent or attenuated, nonpropagating vesicular stomatitis viruses expressing respiratory syncytial virus (RSV) antigens protect mice against RSV challenge. J Virol. 2001;75(22):11079-87.
366. Kahn JS, Schnell MJ, Buonocore L, Rose JK. Recombinant vesicular stomatitis virus expressing respiratory syncytial virus (RSV) glycoproteins: RSV fusion protein can mediate infection and cell fusion. Virology. 1999;254(1):81-91.
367. Ezelle HJ, Markovic D, Barber GN. Generation of hepatitis C virus-like particles by use of a recombinant vesicular stomatitis virus vector. J Virol. 2002;76(23):12325-34.
368. Rose NF, Marx PA, Luckay A, Nixon DF, Moretto WJ, Donahoe SM, et al. An effective AIDS vaccine based on live attenuated vesicular stomatitis virus recombinants. Cell. 2001;106(5):539-49.
369. Gale M, Katze MG. Molecular mechanisms of interferon resistance mediated by viral-directed inhibition of PKR, the interferon-induced protein kinase. Pharmacol Therapeut. 1998;78(1):29-46.
370. Samuel CE. Antiviral actions of interferons. Clin Microbiol Rev. 2001;14(4):778-809.
371. Hertzog PJ, O'Nei LA, Hamilton JA. The interferon in TLR signaling: more than just antiviral. Trends Immunol. 2003;24(10):534-9.
372. Kaempfer R. RNA sensors: novel regulators of gene expression. Embo Rep. 2003;4(11):1043-7.
373. Bowie AG, Haga IR. The role of Toll-like receptors in the host response to viruses. Mol Immunol. 2005;42(8):859-67.
374. Goldenberg DM. New Developments in Monoclonal-Antibodies for Cancer-Detection and Therapy. Ca-Cancer J Clin. 1994;44(1):43-64.
375. Vatti A, Monsalve DM, Pacheco Y, Chang C, Anaya JM, Gershwin ME. Original antigenic sin: A comprehensive review. J Autoimmun. 2017.
376. Kennel SJ, Flynn K, Foote L, Lankford T. Monoclonal-Antibodies in Cancer-Detection and Therapy. Bioscience. 1984;34(3):150-6.
377. Maul RW, Gearhart PJ. Controlling somatic hypermutation in immunoglobulin variable and switch regions. Immunol Res. 2010;47(1-3):113-22.
378. Muramatsu M, Kinoshita K, Fagarasan S, Yamada S, Shinkai Y, Honjo T. Class switch recombination and hypermutation require activation-induced cytidine deaminase (AID), a potential RNA editing enzyme. Cell. 2000;102(5):553-63.

379. Hartley SB, Cooke MP, Fulcher DA, Harris AW, Cory S, Basten A, et al. Elimination of Self-Reactive Lymphocytes-B Proceeds in 2 Stages - Arrested Development and Cell-Death. Cell. 1993;72(3):325-35.
380. Schroeder HW, Cavacini L. Structure and function of immunoglobulins. J Allergy Clin Immun. 2010;125(2):S41-S52.
381. Kohler G, Milstein C. Continuous cultures of fused cells secreting antibody of predefined specificity. Nature. 1975;256(5517):495-7.
382. Waldmann TA. Monoclonal antibodies in diagnosis and therapy. Science. 1991;252(5013):1657-62.
383. Padlan EA, Kabat EA. Modeling of Antibody Combining Sites. Method Enzymol. 1991;203:3-21.
384. Cobb BA, Wang Q, Tzianabos AO, Kasper DL. Polysaccharide processing and presentation by the MHCII pathway. Cell. 2004;117(5):677-87.
385. Foy TM, Laman JD, Ledbetter JA, Aruffo A, Claassen E, Noelle RJ. gp39-CD40 interactions are essential for germinal center formation and the development of B cell memory. J Exp Med. 1994;180(1):157-63.
386. Wu Y, Xu J, Shinde S, Grewal I, Henderson T, Flavell RA, et al. Rapid induction of a novel costimulatory activity on B cells by CD40 ligand. Curr Biol. 1995;5(11):1303-11.
387. Midgley CM, Bajwa-Joseph M, Vasanawathana S, Limpitikul W, Wills B, Flanagan A, et al. An in-depth analysis of original antigenic sin in dengue virus infection. J Virol. 2011;85(1):410-21.
388. Taylor A, Foo SS, Bruzzone R, Dinh LV, King NJ, Mahalingam S. Fc receptors in antibody-dependent enhancement of viral infections. Immunol Rev. 2015;268(1):340-64.
389. Klasse PJ. Neutralization of Virus Infectivity by Antibodies: Old Problems in New Perspectives. Adv Biol. 2014;2014.
390. Klasse PJ, Sattentau QJ. Occupancy and mechanism in anti body-mediated neutralization of animal viruses. J Gen Virol. 2002;83:2091-108.
391. Bachmann MF, Kalinke U, Althage A, Freer G, Burkhart C, Roost H, et al. The role of antibody concentration and avidity in antiviral protection. Science. 1997;276(5321):2024-7.
392. Bachmann MF, Kundig TM, Kalberer CP, Hengartner H, Zinkernagel RM. How Many Specific B-Cells Are Needed to Protect against a Virus. Journal of Immunology. 1994;152(9):4235-41.
393. Burton DR, Parren PW. Vaccines and the induction of functional antibodies: time to look beyond the molecules of natural infection? Nat Med. 2000;6(2):123-5.
394. Burton DR, Saphire EO, Parren PW. A model for neutralization of viruses based on antibody coating of the virion surface. Curr Top Microbiol Immunol. 2001;260:109-43.
395. Burton DR, Williamson RA, Parren PW. Antibody and virus: binding and neutralization. Virology. 2000;270(1):1-3.
396. Parren PW, Burton DR. The antiviral activity of antibodies in vitro and in vivo. Adv Immunol. 2001;77:195-262.
397. Che Z, Olson NH, Leippe D, Lee WM, Mosser AG, Rueckert RR, et al. Antibody-mediated neutralization of human rhinovirus 14 explored by

means of cryoelectron microscopy and X-ray crystallography of virus-Fab complexes. J Virol. 1998;72(6):4610-22.
398. Smith TJ, Chase ES, Schmidt TJ, Olson NH, Baker TS. Neutralizing antibody to human rhinovirus 14 penetrates the receptor-binding canyon. Nature. 1996;383(6598):350-4.
399. Hewat E, Blaas D. Structural studies on antibody interacting with viruses. Curr Top Microbiol Immunol. 2001;260:29-44.
400. Brioen P, Rombaut B, Boeye A. Hit-and-run neutralization of poliovirus. J Gen Virol. 1985;66 (Pt 11):2495-9.
401. Klasse PJ, Sattentau QJ. Mechanisms of virus neutralization by antibody. Curr Top Microbiol Immunol. 2001;260:87-108.
402. Massey RJ, Schochetman G. Topographical analysis of viral epitopes using monoclonal antibodies: mechanism of virus neutralization. Virology. 1981;115(1):20-32.
403. Massey RJ, Schochetman G. Viral epitopes and monoclonal antibodies: isolation of blocking antibodies that inhibit virus neutralization. Science. 1981;213(4506):447-9.
404. Dimmock NJ. Mechanisms of neutralization of animal viruses. J Gen Virol. 1984;65 (Pt 6):1015-22.
405. Emini EA, Ostapchuk P, Wimmer E. Bivalent attachment of antibody onto poliovirus leads to conformational alteration and neutralization. J Virol. 1983;48(2):547-50.
406. Icenogle J, Shiwen H, Duke G, Gilbert S, Rueckert R, Anderegg J. Neutralization of poliovirus by a monoclonal antibody: kinetics and stoichiometry. Virology. 1983;127(2):412-25.
407. Dietzschold B, Tollis M, Lafon M, Wunner WH, Koprowski H. Mechanisms of rabies virus neutralization by glycoprotein-specific monoclonal antibodies. Virology. 1987;161(1):29-36.
408. Possee RD, Schild GC, Dimmock NJ. Studies on the mechanism of neutralization of influenza virus by antibody: evidence that neutralizing antibody (anti-haemagglutinin) inactivates influenza virus in vivo by inhibiting virion transcriptase activity. J Gen Virol. 1982;58(Pt 2):373-86.
409. Marsh M. The entry of enveloped viruses into cells by endocytosis. Biochem J. 1984;218(1):1-10.
410. Armstrong SJ, Dimmock NJ. Neutralization of influenza virus by low concentrations of hemagglutinin-specific polymeric immunoglobulin A inhibits viral fusion activity, but activation of the ribonucleoprotein is also inhibited. J Virol. 1992;66(6):3823-32.
411. Armstrong SJ, McInerney TL, McLain L, Wahren B, Hinkula J, Levi M, et al. Two neutralizing anti-V3 monoclonal antibodies act by affecting different functions of human immunodeficiency virus type 1. J Gen Virol. 1996;77 (Pt 12):2931-41.
412. McInerney TL, McLain L, Armstrong SJ, Dimmock NJ. A human IgG1 (b12) specific for the CD4 binding site of HIV-1 neutralizes by inhibiting the virus fusion entry process, but b12 Fab neutralizes by inhibiting a postfusion event. Virology. 1997;233(2):313-26.
413. White J, Kielian M, Helenius A. Membrane fusion proteins of enveloped animal viruses. Q Rev Biophys. 1983;16(2):151-95.

414. Gollins SW, Porterfield JS. A new mechanism for the neutralization of enveloped viruses by antiviral antibody. Nature. 1986;321(6067):244-6.
415. Janeway CA. Immunobiology. 6 ed: Garland Science Publishing; 2005.
416. Klimpel GR. Immune Defenses. In: Baron S, editor. Medical Microbiology. 4th ed. Galveston, Texas: University of Texas Medical Branch; 1996.
417. Kumar BV, Connors TJ, Farber DL. Human T Cell Development, Localization, and Function throughout Life. Immunity. 2018;48(2):202-13.
418. Zhang N, Bevan MJ. CD8(+) T cells: foot soldiers of the immune system. Immunity. 2011;35(2):161-8.
419. Wong P, Pamer EG. CD8 T cell responses to infectious pathogens. Annu Rev Immunol. 2003;21:29-70.
420. Brehm MA, Selin LK, Welsh RM. CD8 T cell responses to viral infections in sequence. Cell Microbiol. 2004;6(5):411-21.
421. Khanolkar A, Fuller MJ, Zajac AJ. T cell responses to viral infections: lessons from lymphocytic choriomeningitis virus. Immunol Res. 2002;26(1-3):309-21.
422. La Gruta NL, Turner SJ. T cell mediated immunity to influenza: mechanisms of viral control. Trends Immunol. 2014;35(8):396-402.
423. Strutt TM, McKinstry KK, Marshall NB, Vong AM, Dutton RW, Swain SL. Multipronged CD4(+) T-cell effector and memory responses cooperate to provide potent immunity against respiratory virus. Immunol Rev. 2013;255(1):149-64.
424. Doherty PC, Christensen JP. Accessing complexity: the dynamics of virus-specific T cell responses. Annu Rev Immunol. 2000;18:561-92.
425. Gourley TS, Wherry EJ, Masopust D, Ahmed R. Generation and maintenance of immunological memory. Semin Immunol. 2004;16(5):323-33.
426. Kaech SM, Wherry EJ. Heterogeneity and cell-fate decisions in effector and memory CD8+ T cell differentiation during viral infection. Immunity. 2007;27(3):393-405.
427. Thomas PG, Keating R, Hulse-Post DJ, Doherty PC. Cell-mediated protection in influenza infection. Emerg Infect Dis. 2006;12(1):48-54.
428. Kawai T, Akira S. Innate immune recognition of viral infection. Nat Immunol. 2006;7(2):131-7.
429. Kumar H, Kawai T, Akira S. Pathogen recognition by the innate immune system. Int Rev Immunol. 2011;30(1):16-34.
430. Kumar H, Kawai T, Akira S. Pathogen recognition in the innate immune response. Biochem J. 2009;420(1):1-16.
431. Akira S, Takeda K, Kaisho T. Toll-like receptors: critical proteins linking innate and acquired immunity. Nat Immunol. 2001;2(8):675-80.
432. Takeda K, Akira S. Toll-like receptors in innate immunity. Int Immunol. 2005;17(1):1-14.
433. Takeda K, Akira S. Toll receptors and pathogen resistance. Cell Microbiol. 2003;5(3):143-53.
434. Takeda K, Kaisho T, Akira S. Toll-like receptors. Annu Rev Immunol. 2003;21:335-76.

435. Akira S, Uematsu S, Takeuchi O. Pathogen recognition and innate immunity. Cell. 2006;124(4):783-801.
436. Bowie A, O'Neill LA. The interleukin-1 receptor/Toll-like receptor superfamily: signal generators for pro-inflammatory interleukins and microbial products. J Leukoc Biol. 2000;67(4):508-14.
437. Akira S, Takeda K. Toll-like receptor signalling. Nat Rev Immunol. 2004;4(7):499-511.
438. Kurt-Jones EA, Chan M, Zhou S, Wang J, Reed G, Bronson R, et al. Herpes simplex virus 1 interaction with Toll-like receptor 2 contributes to lethal encephalitis. Proc Natl Acad Sci U S A. 2004;101(5):1315-20.
439. Iwasaki A, Medzhitov R. Toll-like receptor control of the adaptive immune responses. Nat Immunol. 2004;5(10):987-95.
440. Medzhitov R, Janeway CA, Jr. Innate immunity: the virtues of a nonclonal system of recognition. Cell. 1997;91(3):295-8.
441. Janeway CA, Jr., Medzhitov R. Innate immune recognition. Annu Rev Immunol. 2002;20:197-216.
442. Theofilopoulos AN, Baccala R, Beutler B, Kono DH. Type I interferons (alpha/beta) in immunity and autoimmunity. Annu Rev Immunol. 2005;23:307-36.
443. Clark R, Kupper T. Old meets new: The interaction between innate and adaptive immunity. Journal of Investigative Dermatology. 2005;125(4):629-37.
444. Bowie A, Kiss-Toth E, Symons JA, Smith GL, Dower SK, O'Neill LA. A46R and A52R from vaccinia virus are antagonists of host IL-1 and toll-like receptor signaling. Proc Natl Acad Sci U S A. 2000;97(18):10162-7.
445. DiPerna G, Stack J, Bowie AG, Boyd A, Kotwal G, Zhang Z, et al. Poxvirus protein N1L targets the I-kappaB kinase complex, inhibits signaling to NF-kappaB by the tumor necrosis factor superfamily of receptors, and inhibits NF-kappaB and IRF3 signaling by toll-like receptors. J Biol Chem. 2004;279(35):36570-8.
446. Stack J, Haga IR, Schroder M, Bartlett NW, Maloney G, Reading PC, et al. Vaccinia virus protein A46R targets multiple Toll-like-interleukin-1 receptor adaptors and contributes to virulence. J Exp Med. 2005;201(6):1007-18.
447. Li K, Foy E, Ferreon JC, Nakamura M, Ferreon AC, Ikeda M, et al. Immune evasion by hepatitis C virus NS3/4A protease-mediated cleavage of the Toll-like receptor 3 adaptor protein TRIF. Proc Natl Acad Sci U S A. 2005;102(8):2992-7.
448. Andrejeva J, Childs KS, Young DF, Carlos TS, Stock N, Goodbourn S, et al. The V proteins of paramyxoviruses bind the IFN-inducible RNA helicase, mda-5, and inhibit its activation of the IFN-beta promoter. Proc Natl Acad Sci U S A. 2004;101(49):17264-9.
449. Meylan E, Burns K, Hofmann K, Blancheteau V, Martinon F, Kelliher M, et al. RIP1 is an essential mediator of Toll-like receptor 3-induced NF-kappa B activation. Nat Immunol. 2004;5(5):503-7.
450. Meylan E, Curran J, Hofmann K, Moradpour D, Binder M, Bartenschlager R, et al. Cardif is an adaptor protein in the RIG-I antiviral pathway and is targeted by hepatitis C virus. Nature. 2005;437(7062):1167-72.

451. Lambris JD, Ricklin D, Geisbrecht BV. Complement evasion by human pathogens. Nat Rev Microbiol. 2008;6(2):132-42.
452. Walport MJ. Complement. Second of two parts. N Engl J Med. 2001;344(15):1140-4.
453. Walport MJ. Complement. First of two parts. N Engl J Med. 2001;344(14):1058-66.
454. Kinoshita T. Biology of complement: the overture. Immunol Today. 1991;12(9):291-5.
455. Janeway CA, Travers P, Walport M. Immunobiology: The Immune System in Health and Disease. New York: Garland Science; 2001.
456. Rosbjerg A, Genster N, Pilely K, Garred P. Evasion Mechanisms Used by Pathogens to Escape the Lectin Complement Pathway. Front Microbiol. 2017;8.
457. Morgan BP, Boyd C, Bubeck D. Molecular cell biology of complement membrane attack. Semin Cell Dev Biol. 2017.
458. Lu JH, Kishore U. C1 Complex: An Adaptable Proteolytic Module for Complement and Non-Complement Functions. Front Immunol. 2017;8.
459. Lichty BD, Stojdl DF, Taylor RA, Miller L, Frenkel I, Atkins H, et al. Vesicular stomatitis virus: A potential therapeutic virus for the treatment of hematologic malignancy. Human Gene Therapy. 2004;15(9):821-31.
460. Liu CS, Russell SJ, Peng KW. Systemic Therapy of Disseminated Myeloma in Passively Immunized Mice Using Measles Virus-infected Cell Carriers. Molecular Therapy. 2010;18(6):1155-64.
461. Liu TC, Galanis E, Kirn D. Clinical trial results with oncolytic virotherapy: a century of promise, a decade of progress. Nat Clin Pract Oncol. 2007;4(2):101-17.
462. Russell SJ. RNA viruses as virotherapy agents. Cancer Gene Ther. 2002;9(12):961-6.
463. Russell SJ, Peng KW, Bell JC. Oncolytic virotherapy. Nat Biotechnol. 2012;30(7):658-70.
464. Vaha-Koskela MJ, Heikkila JE, Hinkkanen AE. Oncolytic viruses in cancer therapy. Cancer Lett. 2007;254(2):178-216.
465. Wagner RR, Rose JK. Rhabdoviridae: the viruses and their replication. In: Fields BN, Knipe DM, Howley PM, editors. Fields Virology. 3 ed. Philadelphia, PA: Lippincott-Raven Publishers; 1996. p. 1121-35.
466. Croyle MA, Callahan SM, Auricchio A, Schumer G, Linse KD, Wilson JM, et al. PEGylation of a vesicular stomatitis virus G pseudotyped lentivirus vector prevents inactivation in serum. J Virol. 2004;78(2):912-21.
467. Tesfay MZ, Ammayappan A, Federspiel MJ, Barber GN, Stojdl D, Peng KW, et al. Vesiculovirus neutralization by natural IgM and complement. J Virol. 2014;88(11):6148-57.
468. Tesfay MZ, Kirk AC, Hadac EM, Griesmann GE, Federspiel MJ, Barber GN, et al. PEGylation of Vesicular Stomatitis Virus Extends Virus Persistence in Blood Circulation of Passively Immunized Mice. J Virol. 2013;87(7):3752-9.
469. Beebe DP, Cooper NR. Neutralization of Vesicular Stomatitis-Virus (Vsv) by Human-Complement Requires a Natural Igm Antibody

Present in Human-Serum. Journal of Immunology. 1981;126(4):1562-8.
470. Takeuchi Y, Liong SH, Bieniasz PD, Jager U, Porter CD, Friedman T, et al. Sensitization of rhabdo-, lenti-, and spumaviruses to human serum by galactosyl(alpha1-3)galactosylation. J Virol. 1997;71(8):6174-8.
471. Hu S, Mohan Kumar D, Sax C, Schuler C, Akkina R. Pseudotyping of lentiviral vector with novel vesiculovirus envelope glycoproteins derived from Chandipura and Piry viruses. Virology. 2016;488:162-8.
472. Evgin L, Ilkow CS, Bourgeois-Daigneault MC, de Souza CT, Stubbert L, Huh MS, et al. Complement inhibition enables tumor delivery of LCMV glycoprotein pseudotyped viruses in the presence of antiviral antibodies. Mol Ther Oncolytics. 2016;3:16027.
473. Brun J, McManus D, Lefebvre C, Hu K, Falls T, Atkins H, et al. Identification of genetically modified Maraba virus as an oncolytic rhabdovirus. Mol Ther. 2010;18(8):1440-9.
474. Kottke T, Errington F, Pulido J, Galivo F, Thompson J, Wongthida P, et al. Broad antigenic coverage induced by vaccination with virus-based cDNA libraries cures established tumors. Nat Med. 2011;17(7):854-9.
475. Miest TS, Cattaneo R. New viruses for cancer therapy: meeting clinical needs. Nat Rev Microbiol. 2014;12(1):23-34.
476. Pol JG, Zhang L, Bridle BW, Stephenson KB, Resseguier J, Hanson S, et al. Maraba virus as a potent oncolytic vaccine vector. Mol Ther. 2014;22(2):420-9.
477. Belkowski LS, Sen GC. Inhibition of Vesicular Stomatitis Viral Messenger-Rna Synthesis by Interferons. J Virol. 1987;61(3):653-60.
478. Carey BL, Ahmed M, Puckett S, Lyles DS. Early Steps of the Virus Replication Cycle Are Inhibited in Prostate Cancer Cells Resistant to Oncolytic Vesicular Stomatitis Virus. J Virol. 2008;82(24):12104-15.
479. Moerdyk-Schauwecker M, Shah NR, Murphy AM, Hastie E, Mukherjee P, Grdzelishvili VZ. Resistance of pancreatic cancer cells to oncolytic vesicular stomatitis virus: Role of type I interferon signaling. Virology. 2013;436(1):221-34.
480. Obuchi M, Fernandez M, Barber GN. Development of recombinant vesicular stomatitis viruses that exploit defects in host defense to augment specific oncolytic activity. J Virol. 2003;77(16):8843-56.
481. Saloura V, Wang LCS, Fridlender ZG, Sun J, Cheng GJ, Kapoor V, et al. Evaluation of an Attenuated Vesicular Stomatitis Virus Vector Expressing Interferon-beta for Use in Malignant Pleural Mesothelioma: Heterogeneity in Interferon Responsiveness Defines Potential Efficacy. Human Gene Therapy. 2010;21(1):51-64.
482. Critchley-Thorne RJ, Simons DL, Yan N, Miyahira AK, Dirbas FM, Johnson DL, et al. Impaired interferon signaling is a common immune defect in human cancer. P Natl Acad Sci USA. 2009;106(22):9010-5.
483. Power AT, Wang JH, Falls TJ, Paterson JM, Parato KA, Lichty BD, et al. Carrier cell-based delivery of an oncolytic virus circumvents antiviral immunity. Molecular Therapy. 2007;15(1):123-30.

484. Hangartner L, Zinkernagel RM, Hengartner H. Antiviral antibody responses: the two extremes of a wide spectrum. Nat Rev Immunol. 2006;6(3):231-43.
485. Ricklin D, Hajishengallis G, Yang K, Lambris JD. Complement: a key system for immune surveillance and homeostasis. Nat Immunol. 2010;11(9):785-97.
486. Kaever T, Meng XZ, Matho MH, Schlossman A, Li S, Sela-Culang I, et al. Potent Neutralization of Vaccinia Virus by Divergent Murine Antibodies Targeting a Common Site of Vulnerability in L1 Protein. J Virol. 2014;88(19):11339-55.
487. Benhnia MREI, McCausland MM, Moyron J, Laudenslager J, Granger S, Rickert S, et al. Vaccinia Virus Extracellular Enveloped Virion Neutralization In Vitro and Protection In Vivo Depend on Complement. J Virol. 2009;83(3):1201-15.
488. Nayak S, Herzog RW. Progress and prospects: immune responses to viral vectors. Gene Therapy. 2010;17(3):295-304.
489. Annoni A, Goudy K, Akbarpour M, Naldini L, Roncarolo MG. Immune responses in liver-directed lentiviral gene therapy. Transl Res. 2013;161(4):230-40.
490. Brown BD, Sitia G, Annoni A, Hauben E, Sergi LS, Zingale A, et al. In vivo administration of lentiviral vectors triggers a type I interferon response that restricts hepatocyte gene transfer and promotes vector clearance. Blood. 2007;109(7):2797-805.
491. Limberis MP, Bell CL, Heath J, Wilson JM. Activation of transgene-specific T cells following lentivirus-mediated gene delivery to mouse lung. Mol Ther. 2010;18(1):143-50.
492. Gromme M, Neefjes J. Antigen degradation or presentation by MHC class I molecules via classical and non-classical pathways. Mol Immunol. 2002;39(3-4):181-202.
493. Lopes L, Fletcher K, Ikeda Y, Collins M. Lentiviral vector expression of tumour antigens in dendritic cells as an immunotherapeutic strategy. Cancer Immunol Immunother. 2006;55(8):1011-6.
494. Zarei S, Abraham S, Arrighi JF, Haller O, Calzascia T, Walker PR, et al. Lentiviral transduction of dendritic cells confers protective antiviral immunity in vivo. J Virol. 2004;78(14):7843-5.
495. Zarei S, Leuba F, Arrighi JF, Hauser C, Piguet V. Transduction of dendritic cells by antigen-encoding lentiviral vectors permits antigen processing and MHC class I-dependent presentation. J Allergy Clin Immunol. 2002;109(6):988-94.
496. Annoni A, Battaglia M, Follenzi A, Lombardo A, Sergi-Sergi L, Naldini L, et al. The immune response to lentiviral-delivered transgene is modulated in vivo by transgene-expressing antigen-presenting cells but not by CD4+CD25+ regulatory T cells. Blood. 2007;110(6):1788-96.
497. Abordo-Adesida E, Follenzi A, Barcia C, Sciascia S, Castro MG, Naldini L, et al. Stability of lentiviral vector-mediated transgene expression in the brain in the presence of systemic antivector immune responses. Human Gene Therapy. 2005;16(6):741-51.
498. Follenzi A, Battaglia M, Lombardo A, Annoni A, Roncarolo MG, Naldini L. Targeting lentiviral vector expression to hepatocytes limits

transgene-specific immune response and establishes long-term expression of human antihemophilic factor IX in mice. Blood. 2004;103(10):3700-9.
499. Stein CS, Kang Y, Sauter SL, Townsend K, Staber P, Derksen TA, et al. In vivo treatment of hemophilia A and mucopolysaccharidosis type VII using nonprimate lentiviral vectors. Mol Ther. 2001;3(6):850-6.
500. Matsui H, Hegadorn C, Ozelo M, Burnett E, Tuttle A, Labelle A, et al. A microRNA-regulated and GP64-pseudotyped lentiviral vector mediates stable expression of FVIII in a murine model of Hemophilia A. Mol Ther. 2011;19(4):723-30.
501. Di Domenico C, Di Napoli D, Gonzalez YRE, Lombardo A, Naldini L, Di Natale P. Limited transgene immune response and long-term expression of human alpha-L-iduronidase in young adult mice with mucopolysaccharidosis type I by liver-directed gene therapy. Hum Gene Ther. 2006;17(11):1112-21.
502. Annoni A, Gregori S, Naldini L, Cantore A. Modulation of immune responses in lentiviral vector-mediated gene transfer. Cell Immunol. 2018.
503. Lin YC, Boone M, Meuris L, Lemmens I, Van Roy N, Soete A, et al. Genome dynamics of the human embryonic kidney 293 lineage in response to cell biology manipulations. Nat Commun. 2014;5:4767.
504. DuBridge RB, Tang P, Hsia HC, Leong PM, Miller JH, Calos MP. Analysis of mutation in human cells by using an Epstein-Barr virus shuttle system. Mol Cell Biol. 1987;7(1):379-87.
505. Oka Y, Nakajima K, Nagao K, Miura K, Ishii N, Kobayashi H. 293FT cells transduced with four transcription factors (OCT4, SOX2, NANOG, and LIN28) generate aberrant ES-like cells. J Stem Cells Regen Med. 2010;6(3):149-56.
506. Knight S, Sanber K, Stephen S, Ferraresso M, Baley R, Escors D, et al. A clinical-grade constitutive packaging cell line for the production of self-inactivating lentiviral vectors. Human Gene Therapy. 2014;25(11):A101-A2.
507. Vink CA, Counsell JR, Perocheau DP, Karda R, Buckley SMK, Brugman MH, et al. Eliminating HIV-1 Packaging Sequences from Lentiviral Vector Proviruses Enhances Safety and Expedites Gene Transfer for Gene Therapy. Mol Ther. 2017;25(8):1790-804.
508. Zufferey R, Nagy D, Mandel RJ, Naldini L, Trono D. Multiply attenuated lentiviral vector achieves efficient gene delivery in vivo. Nat Biotechnol. 1997;15(9):871-5.
509. Hoshino H, Nakamura T, Tanaka Y, Miyoshi I, Yanagihara R. Functional conservation of the neutralizing domains on the external envelope glycoprotein of cosmopolitan and melanesian strains of human T cell leukemia/lymphoma virus type I. J Infect Dis. 1993;168(6):1368-73.
510. Tamura K, Oue A, Tanaka A, Shimizu N, Takagi H, Kato N, et al. Efficient formation of vesicular stomatitis virus pseudotypes bearing the native forms of hepatitis C virus envelope proteins detected after sonication. Microbes Infect. 2005;7(1):29-40.
511. Lefrancois L, Lyles DS. The interaction of antibody with the major surface glycoprotein of vesicular stomatitis virus. I. Analysis of

neutralizing epitopes with monoclonal antibodies. Virology. 1982;121(1):157-67.
512. Keil W, Wagner RR. Epitope mapping by deletion mutants and chimeras of two vesicular stomatitis virus glycoprotein genes expressed by a vaccinia virus vector. Virology. 1989;170(2):392-407.
513. Wagner RR. Rhabdovirus biology and infection: An overview. In: Wagner RR, editor. The Rhabdoviruses. New York: Plenum; 1987. p. 9-74.
514. Hastie E, Grdzelishvili VZ. Vesicular stomatitis virus as a flexible platform for oncolytic virotherapy against cancer. J Gen Virol. 2012;93:2529-45.
515. Cosset FL, Takeuchi Y, Battini JL, Weiss RA, Collins MKL. High-Titer Packaging Cells Producing Recombinant Retroviruses Resistant to Human Serum. J Virol. 1995;69(12):7430-6.
516. Takeuchi Y, Porter CD, Strahan KM, Preece AF, Gustafsson K, Cosset FL, et al. Sensitization of cells and retroviruses to human serum by (alpha 1-3) galactosyltransferase. Nature. 1996;379(6560):85-8.
517. Sandrin V, Boson B, Salmon P, Gay W, Negre D, Le Grand R, et al. Lentiviral vectors pseudotyped with a modified RD114 envelope glycoprotein show increased stability in sera and augmented transduction of primary lymphocytes and CD34(+) cells derived from human and nonhuman primates. Blood. 2002;100(3):823-32.
518. Cronin J, Zhang XY, Reiser J. Altering the tropism of lentiviral vectors through pseudotyping. Curr Gene Ther. 2005;5(4):387-98.
519. Yee JK, Miyanohara A, Laporte P, Bouic K, Burns JC, Friedmann T. A General-Method for the Generation of High-Titer, Pantropic Retroviral Vectors - Highly Efficient Infection of Primary Hepatocytes. P Natl Acad Sci USA. 1994;91(20):9564-8.
520. Stewart HJ, Fong-Wong L, Strickland I, Chipchase D, Kelleher M, Stevenson L, et al. A stable producer cell line for the manufacture of a lentiviral vector for gene therapy of Parkinson's disease. Hum Gene Ther. 2011;22(3):357-69.
521. Yang YP, Vanin EF, Whitt MA, Fornerod M, Zwart R, Schneiderman RD, et al. Inducible, High-Level Production of Infectious Murine Leukemia Retroviral Vector Particles Pseudotyped with Vesicular Stomatitis-Virus-G Envelope Protein. Human Gene Therapy. 1995;6(9):1203-13.
522. Benmansour A, Leblois H, Coulon P, Tuffereau C, Gaudin Y, Flamand A, et al. Antigenicity of Rabies Virus Glycoprotein. J Virol. 1991;65(8):4198-203.
523. Lubeck MD, Gerhard W. Topological mapping antigenic sites on the influenza A/PR/8/34 virus hemagglutinin using monoclonal antibodies. Virology. 1981;113(1):64-72.
524. Webster RG, Laver WG. Determination of the number of nonoverlapping antigenic areas on Hong Kong (H3N2) influenza virus hemagglutinin with monoclonal antibodies and the selection of variants with potential epidemiological significance. Virology. 1980;104(1):139-48.

525. Stone MR, Nowinski RC. Topological mapping of murine leukemia virus proteins by competition-binding assays with monoclonal antibodies. Virology. 1980;100(2):370-81.
526. Seif I, Coulon P, Rollin PE, Flamand A. Rabies virulence: effect on pathogenicity and sequence characterization of rabies virus mutations affecting antigenic site III of the glycoprotein. J Virol. 1985;53(3):926-34.
527. Wiley DC, Wilson IA, Skehel JJ. Structural identification of the antibody-binding sites of Hong Kong influenza haemagglutinin and their involvement in antigenic variation. Nature. 1981;289(5796):373-8.
528. Hovanec DL, Air GM. Antigenic structure of the hemagglutinin of influenza virus B/Hong Kong/8/73 as determined from gene sequence analysis of variants selected with monoclonal antibodies. Virology. 1984;139(2):384-92.
529. Dietzschold B, Wunner WH, Wiktor TJ, Lopes AD, Lafon M, Smith CL, et al. Characterization of an antigenic determinant of the glycoprotein that correlates with pathogenicity of rabies virus. Proc Natl Acad Sci U S A. 1983;80(1):70-4.
530. Spriggs DR, Fields BN. Attenuated reovirus type 3 strains generated by selection of haemagglutinin antigenic variants. Nature. 1982;297(5861):68-70.
531. Zondag GCM, Postma FR, Van Etten I, Verlaan I, Moolenaar WH. Sphingosine 1-phosphate signalling through the G-protein-coupled receptor Edg-1. Biochemical Journal. 1998;330:605-9.
532. Lefrancois L, Lyles DS. The interaction of antibody with the major surface glycoprotein of vesicular stomatitis virus. II. Monoclonal antibodies of nonneutralizing and cross-reactive epitopes of Indiana and New Jersey serotypes. Virology. 1982;121(1):168-74.
533. Lefrancois L, Lyles DS. Antigenic determinants of vesicular stomatitis virus: analysis with antigenic variants. J Immunol. 1983;130(1):394-8.
534. Bishop DH, Repik P, Obijeski JF, Moore NF, Wagner RR. Restitution of infectivity to spikeless vesicular stomatitis virus by solubilized viral components. J Virol. 1975;16(1):75-84.
535. Matlin KS, Reggio H, Helenius A, Simons K. Pathway of vesicular stomatitis virus entry leading to infection. J Mol Biol. 1982;156(3):609-31.
536. Beglova N, North CL, Blacklow SC. Backbone dynamics of a module pair from the ligand-binding domain of the LDL receptor. Biochemistry-Us. 2001;40(9):2808-15.
537. Rasko JE, Battini JL, Gottschalk RJ, Mazo I, Miller AD. The RD114/simian type D retrovirus receptor is a neutral amino acid transporter. Proc Natl Acad Sci U S A. 1999;96(5):2129-34.
538. Tailor CS, Nouri A, Zhao Y, Takeuchi Y, Kabat D. A sodium-dependent neutral-amino-acid transporter mediates infections of feline and baboon endogenous retroviruses and simian type D retroviruses. J Virol. 1999;73(5):4470-4.
539. Kumar SR, Markusic DM, Biswas M, High KA, Herzog RW. Clinical development of gene therapy: results and lessons from recent successes. Mol Ther Methods Clin Dev. 2016;3:16034.

540. Baquero E, Albertini AA, Gaudin Y. Recent mechanistic and structural insights on class III viral fusion glycoproteins. Curr Opin Struct Biol. 2015;33:52-60.
541. Strang BL, Ikeda Y, Cosset FL, Collins MK, Takeuchi Y. Characterization of HIV-1 vectors with gammaretrovirus envelope glycoproteins produced from stable packaging cells. Gene Ther. 2004;11(7):591-8.
542. Stornaiuolo A, Piovani BM, Bossi S, Zucchelli E, Corna S, Salvatori F, et al. RD2-MolPack-Chim3, a packaging cell line for stable production of lentiviral vectors for anti-HIV gene therapy. Hum Gene Ther Methods. 2013;24(4):228-40.
543. Tijani M, Munis AM, Perry C, Sanber K, Ferraresso M, Mukhopadhyay T, et al. Lentivector producer cell lines with stably expressed vesiculovirus envelopes. Molecular Therapy: Methods & Clinical Development. 2018.
544. Sahu A, Kozel TR, Pangburn MK. Specificity of the thioester-containing reactive site of human C3 and its significance to complement activation. Biochem J. 1994;302 (Pt 2):429-36.
545. Merle NS, Noe R, Halbwachs-Mecarelli L, Fremeaux-Bacchi V, Roumenina LT. Complement System Part II: Role in Immunity. Front Immunol. 2015;6:257.
546. Merle NS, Church SE, Fremeaux-Bacchi V, Roumenina LT. Complement System Part I - Molecular Mechanisms of Activation and Regulation. Front Immunol. 2015;6:262.
547. Kishore U, Ghai R, Greenhough TJ, Shrive AK, Bonifati DM, Gadjeva MG, et al. Structural and functional anatomy of the globular domain of complement protein C1q. Immunol Lett. 2004;95(2):113-28.
548. Alberti S, Marques G, Hernandez-Alles S, Rubires X, Tomas JM, Vivanco F, et al. Interaction between complement subcomponent C1q and the Klebsiella pneumoniae porin OmpK36. Infect Immun. 1996;64(11):4719-25.
549. Stoermer KA, Morrison TE. Complement and viral pathogenesis. Virology. 2011;411(2):362-73.
550. Montefiori DC, Cornell RJ, Zhou JY, Zhou JT, Hirsch VM, Johnson PR. Complement control proteins, CD46, CD55, and CD59, as common surface constituents of human and simian immunodeficiency viruses and possible targets for vaccine protection. Virology. 1994;205(1):82-92.
551. Saifuddin M, Parker CJ, Peeples ME, Gorny MK, Zolla-Pazner S, Ghassemi M, et al. Role of virion-associated glycosylphosphatidylinositol-linked proteins CD55 and CD59 in complement resistance of cell line-derived and primary isolates of HIV-1. J Exp Med. 1995;182(2):501-9.
552. Spear GT, Lurain NS, Parker CJ, Ghassemi M, Payne GH, Saifuddin M. Host cell-derived complement control proteins CD55 and CD59 are incorporated into the virions of two unrelated enveloped viruses. Human T cell leukemia/lymphoma virus type I (HTLV-I) and human cytomegalovirus (HCMV). J Immunol. 1995;155(9):4376-81.
553. Saifuddin M, Hedayati T, Atkinson JP, Holguin MH, Parker CJ, Spear GT. Human immunodeficiency virus type 1 incorporates both glycosyl

phosphatidylinositol-anchored CD55 and CD59 and integral membrane CD46 at levels that protect from complement-mediated destruction. J Gen Virol. 1997;78 (Pt 8):1907-11.
554. Spitzer D, Hauser H, Wirth D. Complement-protected amphotropic retroviruses from murine packaging cells. Hum Gene Ther. 1999;10(11):1893-902.
555. Fujita T. Evolution of the lectin-complement pathway and its role in innate immunity. Nat Rev Immunol. 2002;2(5):346-53.
556. Ezekowitz RA, Kuhlman M, Groopman JE, Byrn RA. A human serum mannose-binding protein inhibits in vitro infection by the human immunodeficiency virus. J Exp Med. 1989;169(1):185-96.
557. Saifuddin M, Hart ML, Gewurz H, Zhang Y, Spear GT. Interaction of mannose-binding lectin with primary isolates of human immunodeficiency virus type 1. J Gen Virol. 2000;81(Pt 4):949-55.
558. Ying H, Ji X, Hart ML, Gupta K, Saifuddin M, Zariffard MR, et al. Interaction of mannose-binding lectin with HIV type 1 is sufficient for virus opsonization but not neutralization. AIDS Res Hum Retroviruses. 2004;20(3):327-35.
559. Ip WK, Chan KH, Law HK, Tso GH, Kong EK, Wong WH, et al. Mannose-binding lectin in severe acute respiratory syndrome coronavirus infection. J Infect Dis. 2005;191(10):1697-704.
560. Ji X, Olinger GG, Aris S, Chen Y, Gewurz H, Spear GT. Mannose-binding lectin binds to Ebola and Marburg envelope glycoproteins, resulting in blocking of virus interaction with DC-SIGN and complement-mediated virus neutralization. J Gen Virol. 2005;86(Pt 9):2535-42.
561. Cantore A, Nair N, Della Valle P, Di Matteo M, Matrai J, Sanvito F, et al. Hyperfunctional coagulation factor IX improves the efficacy of gene therapy in hemophilic mice. Blood. 2012;120(23):4517-20.
562. Milani M, Annoni A, Bartolaccini S, Biffi M, Russo F, Di Tomaso T, et al. Genome editing for scalable production of alloantigen-free lentiviral vectors for in vivo gene therapy. Embo Mol Med. 2017;9(11):1558-73.
563. Schauber-Plewa C, Simmons A, Tuerk MJ, Pacheco CD, Veres G. Complement regulatory proteins are incorporated into lentiviral vectors and protect particles against complement inactivation. Gene Therapy. 2005;12(3):238-45.
564. Hwang BY, Schaffer DV. Engineering a serum-resistant and thermostable vesicular stomatitis virus G glycoprotein for pseudotyping retroviral and lentiviral vectors. Gene Ther. 2013;20(8):807-15.
565. Brown BD, Lillicrap D. Dangerous liaisons: the role of "danger" signals in the immune response to gene therapy. Blood. 2002;100(4):1133-40.
566. Agudo J, Ruzo A, Kitur K, Sachidanandam R, Blander JM, Brown BD. A TLR and non-TLR mediated innate response to lentiviruses restricts hepatocyte entry and can be ameliorated by pharmacological blockade. Mol Ther. 2012;20(12):2257-67.
567. Rossetti M, Gregori S, Hauben E, Brown BD, Sergi LS, Naldini L, et al. HIV-1-Derived Lentiviral Vectors Directly Activate Plasmacytoid Dendritic Cells, Which in Turn Induce the Maturation of Myeloid Dendritic Cells. Human Gene Therapy. 2011;22(2):177-88.

568. Gopinath C, Nathar TJ, Ghosh A, Hickstein DD, Nelson EJR. Contemporary Animal Models For Human Gene Therapy Applications. Curr Gene Ther. 2015;15(6):531-40.
569. Simmonds P. SSE: a nucleotide and amino acid sequence analysis platform. BMC Res Notes. 2012;5:50.
570. Kimura M, Ota T. On the stochastic model for estimation of mutational distance between homologous proteins. J Mol Evol. 1972;2(1):87-90.
571. Kimura M. A simple method for estimating evolutionary rates of base substitutions through comparative studies of nucleotide sequences. J Mol Evol. 1980;16(2):111-20.
572. Van de Peer Y, De Wachter R. Evolutionary relationships among the eukaryotic crown taxa taking into account site-to-site rate variation in 18S rRNA. J Mol Evol. 1997;45(6):619-30.
573. Ikeda K, Ichikawa T, Wakimoto H, Silver JS, Deisboeck TS, Finkelstein D, et al. Oncolytic virus therapy of multiple tumors in the brain requires suppression of innate and elicited antiviral responses. Nat Med. 1999;5(8):881-7.
574. Munguia A, Ota T, Miest T, Russell SJ. Cell carriers to deliver oncolytic viruses to sites of myeloma tumor growth. Gene Ther. 2008;15(10):797-806.
575. Willmon C, Harrington K, Kottke T, Prestwich R, Melcher A, Vile R. Cell carriers for oncolytic viruses: Fed Ex for cancer therapy. Mol Ther. 2009;17(10):1667-76.
576. Power AT, Wang J, Falls TJ, Paterson JM, Parato KA, Lichty BD, et al. Carrier cell-based delivery of an oncolytic virus circumvents antiviral immunity. Mol Ther. 2007;15(1):123-30.
577. Power AT, Bell JC. Taming the Trojan horse: optimizing dynamic carrier cell/oncolytic virus systems for cancer biotherapy. Gene Ther. 2008;15(10):772-9.
578. Gatlin J, Melkus MW, Padgett A, Petroll WM, Cavanagh HD, Garcia JV, et al. In vivo fluorescent labeling of corneal wound healing fibroblasts. Exp Eye Res. 2003;76(3):361-71.
579. Ting-De Ravin SS, Kennedy DR, Naumann N, Kennedy JS, Choi U, Hartnett BJ, et al. Correction of canine X-linked severe combined immunodeficiency by in vivo retroviral gene therapy. Blood. 2006;107(8):3091-7.
580. Ahmed M, Cramer SD, Lyles DS. Sensitivity of prostate tumors to wild type and M protein mutant vesicular stomatitis viruses. Virology. 2004;330(1):34-49.
581. Diaz RM, Galivo F, Kottke T, Wongthida P, Qiao J, Thompson J, et al. Oncolytic immunovirotherapy for melanoma using vesicular stomatitis virus. Cancer Research. 2007;67(6):2840-8.
582. Ebert O, Harbaran S, Shinozaki K, Woo SLC. Systemic therapy of experimental breast cancer metastases by mutant vesicular stomatitis virus in immune-competent mice. Cancer Gene Therapy. 2005;12(4):350-8.
583. Ebert O, Shinozaki K, Huang TG, Savontaus MJ, Garcia-Sastre A, Woo SLC. Oncolytic vesicular stomatitis virus for treatment of orthotopic hepatocellular carcinoma in immune-competent rats. Cancer Research. 2003;63(13):3605-11.

584. Huang TG, Ebert O, Shinozaki K, Garcia-Sastre A, Woo SLC. Oncolysis of hepatic metastasis of colorectal cancer by recombinant vesicular stomatitis virus in immune-competent mice. Molecular Therapy. 2003;8(3):434-40.
585. Lun X, Senger DL, Alain T, Oprea A, Parato K, Stojdl D, et al. Effects of intravenously administered recombinant vesicular stomatitis virus (VSV Delta M51) on Multifocal and invasive gliomas. J Natl Cancer I. 2006;98(21):1546-57.
586. Shinozaki K, Ebert O, Kournioti C, Tai YS, Woo SLC. Oncolysis of multifocal hepatocellular carcinoma in the rat liver by hepatic artery infusion of vesicular stomatitis virus. Molecular Therapy. 2004;9(3):368-76.
587. Sung CK, Choi B, Wanna G, Genden EM, Woo SLC, Shin EJ. Combined VSV Oncolytic Virus and Chemotherapy for Squamous Cell Carcinoma. Laryngoscope. 2008;118(2):237-42.
588. Arce F, Rowe HM, Chain B, Lopes L, Collins MK. Lentiviral vectors transduce proliferating dendritic cell precursors leading to persistent antigen presentation and immunization. Mol Ther. 2009;17(9):1643-50.
589. Breckpot K, Corthals J, Bonehill A, Michiels A, Tuyaerts S, Aerts C, et al. Dendritic cells differentiated in the presence of IFN-{beta} and IL-3 are potent inducers of an antigen-specific CD8+ T cell response. J Leukoc Biol. 2005;78(4):898-908.
590. Breckpot K, Escors D, Arce F, Lopes L, Karwacz K, Van Lint S, et al. HIV-1 lentiviral vector immunogenicity is mediated by Toll-like receptor 3 (TLR3) and TLR7. J Virol. 2010;84(11):5627-36.
591. Dai B, Yang L, Yang H, Hu B, Baltimore D, Wang P. HIV-1 Gag-specific immunity induced by a lentivector-based vaccine directed to dendritic cells. Proc Natl Acad Sci U S A. 2009;106(48):20382-7.
592. Esslinger C, Romero P, MacDonald HR. Efficient transduction of dendritic cells and induction of a T-cell response by third-generation lentivectors. Hum Gene Ther. 2002;13(9):1091-100.
593. Palmowski MJ, Lopes L, Ikeda Y, Salio M, Cerundolo V, Collins MK. Intravenous injection of a lentiviral vector encoding NY-ESO-1 induces an effective CTL response. J Immunol. 2004;172(3):1582-7.
594. Tjomsland V, Ellegard R, Che K, Hinkula J, Lifson JD, Larsson M. Complement opsonization of HIV-1 enhances the uptake by dendritic cells and involves the endocytic lectin and integrin receptor families. Plos One. 2011;6(8):e23542.
595. Tjomsland V, Ellegard R, Burgener A, Mogk K, Che KF, Westmacott G, et al. Complement opsonization of HIV-1 results in a different intracellular processing pattern and enhanced MHC class I presentation by dendritic cells. Eur J Immunol. 2013;43(6):1470-83.
596. Bhattacharya A, Hegazy AN, Deigendesch N, Kosack L, Cupovic J, Kandasamy RK, et al. Superoxide Dismutase 1 Protects Hepatocytes from Type I Interferon-Driven Oxidative Damage. Immunity. 2015;43(5):974-86.
597. Teijaro JR, Ng C, Lee AM, Sullivan BM, Sheehan KC, Welch M, et al. Persistent LCMV infection is controlled by blockade of type I interferon signaling. Science. 2013;340(6129):207-11.

598. Wilson EB, Yamada DH, Elsaesser H, Herskovitz J, Deng J, Cheng G, et al. Blockade of chronic type I interferon signaling to control persistent LCMV infection. Science. 2013;340(6129):202-7.
599. Jones SA, Scheller J, Rose-John S. Therapeutic strategies for the clinical blockade of IL-6/gp130 signaling. J Clin Invest. 2011;121(9):3375-83.
600. Genovese MC, Fleischmann R, Furst D, Janssen N, Carter J, Dasgupta B, et al. Efficacy and safety of olokizumab in patients with rheumatoid arthritis with an inadequate response to TNF inhibitor therapy: outcomes of a randomised Phase IIb study. Ann Rheum Dis. 2014;73(9):1607-15.
601. Dinarello CA. Interleukin-1 in the pathogenesis and treatment of inflammatory diseases. Blood. 2011;117(14):3720-32.
602. Zhu RZ, Xiang D, Xie C, Li JJ, Hu JJ, He HL, et al. Protective effect of recombinant human IL-1Ra on CCl4-induced acute liver injury in mice. World J Gastroentero. 2010;16(22):2771-9.
603. Seregin SS, Appledorn DM, McBride AJ, Schuldt NJ, Aldhamen YA, Voss T, et al. Transient Pretreatment With Glucocorticoid Ablates Innate Toxicity of Systemically Delivered Adenoviral Vectors Without Reducing Efficacy. Molecular Therapy. 2009;17(4):685-96.
604. Edelstein M. Vectors Used in Gene Therapy Clinical Trials: John Wiley and Sons Ltd; 2017 [updated 2017. Available from: http://www.abedia.com/wiley/vectors.php.
605. Meneghini V, Lattanzi A, Tiradani L, Bravo G, Morena F, Sanvito F, et al. Pervasive supply of therapeutic lysosomal enzymes in the CNS of normal and Krabbe-affected non-human primates by intracerebral lentiviral gene therapy. Embo Mol Med. 2016;8(5):489-510.
606. Alton EW, Beekman JM, Boyd AC, Brand J, Carlon MS, Connolly MM, et al. Preparation for a first-in-man lentivirus trial in patients with cystic fibrosis. Thorax. 2017;72(2):137-47.
607. Cavazzana-Calvo M, Payen E, Negre O, Wang G, Hehir K, Fusil F, et al. Transfusion independence and HMGA2 activation after gene therapy of human beta-thalassaemia. Nature. 2010;467(7313):318-U94.
608. Aiuti A, Biasco L, Scaramuzza S, Ferrua F, Cicalese MP, Baricordi C, et al. Lentiviral hematopoietic stem cell gene therapy in patients with Wiskott-Aldrich syndrome. Science. 2013;341(6148):1233151.
609. Sessa M, Lorioli L, Fumagalli F, Acquati S, Redaelli D, Baldoli C, et al. Lentiviral haemopoietic stem-cell gene therapy in early-onset metachromatic leukodystrophy: an ad-hoc analysis of a non-randomised, open-label, phase 1/2 trial. Lancet. 2016;388(10043):476-87.
610. Ribeil JA, Hacein-Bey-Abina S, Payen E, Magnani A, Semeraro M, Magrin E, et al. Gene Therapy in a Patient with Sickle Cell Disease. N Engl J Med. 2017;376(9):848-55.
611. Herzog RW. Complexity of immune responses to AAV transgene products - example of factor IX. Cell Immunology. 2017.
612. Shiina T, Hosomichi K, Inoko H, Kulski JK. The HLA genomic loci map: expression, interaction, diversity and disease. J Hum Genet. 2009;54(1):15-39.

613. Mingozzi F, Liu YL, Dobrzynski E, Kaufhold A, Liu JH, Wang Y, et al. Induction of immune tolerance to coagulation factor IX antigen by in vivo hepatic gene transfer. J Clin Invest. 2003;111(9):1347-56.
614. Brown BD, Venneri MA, Zingale A, Sergi Sergi L, Naldini L. Endogenous microRNA regulation suppresses transgene expression in hematopoietic lineages and enables stable gene transfer. Nat Med. 2006;12(5):585-91.
615. Vandendriessche T, Thorrez L, Acosta-Sanchez A, Petrus I, Wang L, Ma L, et al. Efficacy and safety of adeno-associated viral vectors based on serotype 8 and 9 vs. lentiviral vectors for hemophilia B gene therapy. J Thromb Haemost. 2007;5(1):16-24.
616. Brunetti-Pierri N, Liou A, Patel P, Palmer D, Grove N, Finegold M, et al. Balloon Catheter Delivery of Helper-dependent Adenoviral Vector Results in Sustained, Therapeutic hFIX Expression in Rhesus Macaques. Molecular Therapy. 2012;20(10):1863-70.
617. Richards SM. Immunologic considerations for enzyme replacement therapy in the treatment of lysosomal storage disorders. Clinical and Applied Immunology Reviews. 2002;2(4-5):241-53.
618. Rowe HM, Lopes L, Ikeda Y, Bailey R, Barde I, Zenke M, et al. Immunization with a lentiviral vector stimulates both CD4 and CD8 T cell responses to an ovalbumin transgene. Mol Ther. 2006;13(2):310-9.
619. Maguire C, Ramirez S, Merkel S, Sena-Esteves M, Breakefield X. Gene Therapy for the Nervous System: Challenges and New Strategies. Neurotherapeutics. 2014;11(4):817-39.
620. Tardieu M, Zerah M, Husson B, de Bournonville S, Deiva K, Adamsbaum C, et al. Intracerebral Administration of Adeno-Associated Viral Vector Serotype rh.10 Carrying Human SGSH and SUMF1 cDNAs in Children with Mucopolysaccharidosis Type IIIA Disease: Results of a Phase I/II Trial. Human Gene Therapy. 2014;25(6):506-16.
621. Sigal LJ, Rock KL. Bone marrow-derived antigen-presenting cells are required for the generation of cytotoxic T lymphocyte responses to viruses and use transporter associated with antigen presentation (TAP)-dependent and -independent pathways of antigen presentation. J Exp Med. 2000;192(8):1143-50.
622. Brown BD, Cantore A, Annoni A, Sergi LS, Lombardo A, Della Valle P, et al. A microRNA-regulated lentiviral vector mediates stable correction of hemophilia B mice. Blood. 2007;110(13):4144-52.
623. Annoni A, Brown BD, Cantore A, Sergi LS, Naldini L, Roncarolo MG. In vivo delivery of a microRNA-regulated transgene induces antigen-specific regulatory T cells and promotes immunologic tolerance. Blood. 2009;114(25):5152-61.
624. Follenzi A, Santambrogio L, Annoni A. Immune responses to lentiviral vectors. Curr Gene Ther. 2007;7(5):306-15.
625. Mattiuzzo G, Page M. Personal communication. National Institute for Biological Standards and Control (NIBSC), Potters Bar, UK2018.
626. Kay MA, Glorioso JC, Naldini L. Viral vectors for gene therapy: the art of turning infectious agents into vehicles of therapeutics. Nature Medicine. 2001;7(1):33-40.

627. Thomas CE, Abordo-Adesida E, Maleniak TC, Stone D, Gerdes G, Lowenstein PR. Gene transfer into rat brain using adenoviral vectors. In: Gerfen JN, McKay R, Rogawski MA, Sibley DR, Skolnick P, editors. Current Protocols in Neuroscience. New York: John Wiley & Sons; 2000.
628. Thomas CE, Storm TA, Huang Z, Kay MA. Rapid uncoating of vector genomes is the key to efficient liver transduction with pseudotyped adeno-associated virus vectors. J Virol. 2004;78(6):3110-22.
629. Lowenstein PR. Input virion proteins: cryptic targets of antivector immune responses in preimmunized subjects. Mol Ther. 2004;9(6):771-4.
630. Kordower JH, Emborg ME, Bloch J, Ma SY, Chu Y, Leventhal L, et al. Neurodegeneration prevented by lentiviral vector delivery of GDNF in primate models of Parkinson's disease. Science. 2000;290(5492):767-73.
631. Consiglio A, Quattrini A, Martino S, Bensadoun JC, Dolcetta D, Trojani A, et al. In vivo gene therapy of metachromatic leukodystrophy by lentiviral vectors: correction of neuropathology and protection against learning impairments in affected mice. Nat Med. 2001;7(3):310-6.
632. Azzouz M, Ralph GS, Storkebaum E, Walmsley LE, Mitrophanous KA, Kingsman SM, et al. VEGF delivery with retrogradely transported lentivector prolongs survival in a mouse ALS model. Nature. 2004;429(6990):413-7.
633. Biffi A, De Palma M, Quattrini A, Del Carro U, Amadio S, Visigalli I, et al. Correction of metachromatic leukodystrophy in the mouse model by transplantation of genetically modified hematopoietic stem cells. J Clin Invest. 2004;113(8):1118-29.
634. Wong LF, Ralph GS, Walmsley LE, Bienemann AS, Parham S, Kingsman SM, et al. Lentiviral-mediated delivery of Bcl-2 or GDNF protects against excitotoxicity in the rat hippocampus. Mol Ther. 2005;11(1):89-95.
635. Kopecky SA, Willingham MC, Lyles DS. Matrix protein and another viral component contribute to induction of apoptosis in cells infected with vesicular stomatitis virus. J Virol. 2001;75(24):12169-81.
636. Power AT, Bell JC. Cell-based delivery of oncolytic viruses: a new strategic alliance for a biological strike against cancer. Mol Ther. 2007;15(4):660-5.
637. Wu L, Huang TG, Meseck M, Altomonte J, Ebert O, Shinozaki K, et al. rVSV(M Delta 51)-M3 is an effective and safe oncolytic virus for cancer therapy. Human Gene Therapy. 2008;19(6):635-47.
638. Hoffmann M, Wu YJ, Gerber M, Berger-Rentsch M, Heimrich B, Schwemmle M, et al. Fusion-active glycoprotein G mediates the cytotoxicity of vesicular stomatitis virus M mutants lacking host shut-off activity. J Gen Virol. 2010;91:2782-93.
639. Heiber JF, Ahn J, Barber GN. Vesicular stomatitis virus (VSV) expressing tumor suppressor p53 is a highly attenuated, potent oncolytic agent. Cytokine. 2011;56(1):83-.
640. Janelle V, Brassard F, Lapierre P, Lamarre A, Poliquin L. Mutations in the Glycoprotein of Vesicular Stomatitis Virus Affect

Cytopathogenicity: Potential for Oncolytic Virotherapy. J Virol. 2011;85(13):6513-20.
641. Ozduman K, Wollmann G, Ahmadi SA, van den Pol AN. Peripheral Immunization Blocks Lethal Actions of Vesicular Stomatitis Virus within the Brain. J Virol. 2009;83(22):11540-9.
642. Wollmann G, Rogulin V, Simon I, Rose JK, van den Pol AN. Some Attenuated Variants of Vesicular Stomatitis Virus Show Enhanced Oncolytic Activity against Human Glioblastoma Cells relative to Normal Brain Cells. J Virol. 2010;84(3):1563-73.
643. Leveille S, Goulet ML, Lichty BD, Hiscott J. Vesicular Stomatitis Virus Oncolytic Treatment Interferes with Tumor-Associated Dendritic Cell Functions and Abrogates Tumor Antigen Presentation. J Virol. 2011;85(23):12160-9.
644. Altomonte J, Wu L, Meseck M, Chen L, Ebert O, Garcia-Sastre A, et al. Enhanced oncolytic potency of vesicular stomatitis virus through vector-mediated inhibition of NK and NKT cells. Cancer Gene Therapy. 2009;16(3):266-78.
645. Heiber JF, Barber GN. Vesicular Stomatitis Virus Expressing Tumor Suppressor p53 Is a Highly Attenuated, Potent Oncolytic Agent. J Virol. 2011;85(20):10440-50.
646. Ebert O, Shinozaki K, Kournioti C, Park MS, Garcia-Sastre A, Woo SLC. Syncytia induction enhances the oncolytic potential of vesicular stomatitis virus in virotherapy for cancer. Molecular Therapy. 2004;9:S397-S.
647. Chang GM, Xu SP, Watanabe M, Jayakar HR, Whitt MA, Gingrich JR. Enhanced Oncolytic Activity of Vesicular Stomatitis Virus Encoding SV5-F Protein Against Prostate Cancer. J Urology. 2010;183(4):1611-8.
648. Brown CW, Stephenson KB, Hanson S, Kucharczyk M, Duncan R, Bell JC, et al. The p14 FAST Protein of Reptilian Reovirus Increases Vesicular Stomatitis Virus Neuropathogenesis. J Virol. 2009;83(2):552-61.
649. Muik A, Kneiske I, Werbizki M, Wilflingseder D, Giroglou T, Ebert O, et al. Pseudotyping Vesicular Stomatitis Virus with Lymphocytic Choriomeningitis Virus Glycoproteins Enhances Infectivity for Glioma Cells and Minimizes Neurotropism. J Virol. 2011;85(11):5679-84.
650. Ayala-Breton C, Barber GN, Russell SJ, Peng KW. Retargeting Vesicular Stomatitis Virus Using Measles Virus Envelope Glycoproteins. Human Gene Therapy. 2012;23(5):484-91.
651. Ayala-Breton C, Russell SJ, Peng KW. Oncolytic Properties of a Vesicular Stomatitis/Measles Virus Hybrid. Molecular Therapy. 2012;20:S208-S9.
652. Nakashima H, Kaur B, Chiocca EA. Directing systemic oncolytic viral delivery to tumors via carrier cells. Cytokine Growth F R. 2010;21(2-3):119-26.
653. Kottke T, Diaz RM, Kaluza K, Pulido J, Galivo F, Wongthida P, et al. Use of Biological Therapy to Enhance Both Virotherapy and Adoptive T-Cell Therapy for Cancer. Molecular Therapy. 2008;16(12):1910-8.

654. Labib M, Zamay AS, Muharemagic D, Chechik A, Bell JC, Berezovski MV. Electrochemical Sensing of Aptamer-Facilitated Virus Immunoshielding. Anal Chem. 2012;84(3):1677-86.
655. Altomonte J, Wu L, Chen L, Meseck M, Ebert O, Garcia-Sastre A, et al. Exponential enhancement of oncolytic vesicular stomatitis virus potency by vector-mediated suppression of inflammatory responses in vivo. Molecular Therapy. 2008;16(1):146-53.
656. Ikeda K, Wakimoto H, Ichikawa T, Jhung S, Hochberg FH, Louis DN, et al. Complement depletion facilitates the infection of multiple brain tumors by an intravascular, replication-conditional herpes simplex virus mutant. J Virol. 2000;74(10):4765-75.
657. Qiao J, Wang HX, Kottke T, White C, Twigger K, Diaz RM, et al. Cyclophosphamide facilitates antitumor efficacy against subcutaneous tumors following intravenous delivery of reovirus. Clinical Cancer Research. 2008;14(1):259-69.
658. Kottke T, Galivo F, Wongthida P, Diaz RM, Thompson J, Jevremovic D, et al. Treg depletion-enhanced IL-2 treatment facilitates therapy of established tumors using systemically delivered oncolytic virus. Molecular Therapy. 2008;16(7):1217-26.
659. Ghiringhelli F, Menard C, Puig PE, Ladoire S, Roux S, Martin F, et al. Metronomic cyclophosphamide regimen selectively depletes CD4(+) CD25(+) regulatory T cells and restores T and NK effector functions in end stage cancer patients. Cancer Immunol Immun. 2007;56(5):641-8.
660. Freer G, Burkhart C, Ciernik I, Bachmann MF, Hengartner H, Zinkernagel RM. Vesicular stomatitis virus Indiana glycoprotein as a T-cell-dependent and -independent antigen. J Virol. 1994;68(6):3650-5.
661. Gaiotto T, Hufton SE. Cross-Neutralising Nanobodies Bind to a Conserved Pocket in the Hemagglutinin Stem Region Identified Using Yeast Display and Deep Mutational Scanning. Plos One. 2016;11(10):e0164296.
662. Chaisri U, Chaicumpa W. Evolution of Therapeutic Antibodies, Influenza Virus Biology, Influenza, and Influenza Immunotherapy. Biomed Res Int. 2018;2018:9747549.t